Faculty of Medicine and Health Sciences
School of Medicine

Interrogating the genetic profile of sporadic colorectal cancer

Wakkas Mohammed Fadhil
MBChB, MSc

Thesis submitted to the University of Nottingham for the Degree of Doctor of Philosophy

March 2019

Declaration

This thesis entitled as “Interrogating the genetic profile of sporadic colorectal cancer” is the result of my own investigations and observations unless stated otherwise.

Wakkas Fadhil

Acknowledgment

I am very grateful for the help and dedication of my main supervisor Professor Mohammad Ilyas, who has given superb advice and guidance throughout the whole process. I am entirely indebted to him for his support and encouragement along the way, far more than he knows. He is a fantastic supervisor and has provided me with invaluable experiences.

I would also like to thank Dr. Rashmi Seth for her advice, excellent and crucial contributions to the process. Dr. Seth is a true scientist, with great passion and endless ideas, which in turn has made her constant support very valuable. I am grateful in every possible way and hope to continue our collaborations in the future.

I would like to give a special thanks to the members of the VICTOR study; Megan McGregor, Rose Wharton, Yoko Yanagisawa, Michael Presz, Alison Pritchard, Chris Womack, Susan Dutton, Rachel Kerr1, David Kerr, and Elaine Johnstone.

Moreover, I would like to thank Kirsten Mckay, Fiona MacDonald, Jenny Bell, Brendan O'Sulliva, and Phillipe Taniere for their collaboration in the MSI study.

The assistance and guidance provided by Dr Des Powe, Dr Andrew Green, and Mr Chris Nolan has been invaluable.

I would like to express my very great appreciation to Anne Wilson, Keith Ashford, Carol Rogers, Claire Hawks and all the members of the histopathology department, Nottingham University hospitals NUH NHS for their kind help, advice and assistance.

I am grateful for the assistance given by Dr Paddy Tighe and Dr Sally Chappell, who taught me the essential concepts of Genomics and Bioinformatics when I started my study. They have given constant support during my PhD study.

I would like to give a very special thanks to my friends Dr Omar Jasim, Dr Mohammed Aleskandarany, Dr Abdulkader Albasri, Dr Saleh Al Ghamdi, Dr Ahmed Benhasouna, Dr Mohamed Ahmed, Dr Tarek Ahmed, Dr Salih Ibrahem, Dr Omar Ahmad, Mr Hussain Al-masmoum, and Mr Mohammad Albanghali for their relentless effort to support me by all means throughout my study.

I would like to greatly thank all my colleagues in the Pathology Research Group especially Dr Henry Ebili, Dr William Dalleywater, Mr James Hassall and Mr Declan Sculthorpe for their sincere support.

I would also like to thank everybody who was important to the successful realisation of my thesis, as well as expressing my apology that I could not mention personally one by one.

This study was 50/50 funded by the International Office, University of Nottingham, UK and the Ministry of Higher Education, Iraq, respectively.

I am deeply appreciative for the four-year scholarship the International Office, University of Nottingham granted me for 50% tuition fees.

I thank the Ministry of Higher Education, Iraq who gave me the opportunity to pursue my PhD study and sponsored me toward 50% of the tuition fees.

Dedication

First of all, I give all my sincere thanks and gratitude to my almighty lord, Allah (May He be glorified and exalted). I dedicate my thesis to my mother and father (Allah rest their souls), and to my beloved wife and children (Allah bless them).

Wakkas Fadhil

Abstract

Background and aims: Colorectal cancer (CRC) is one of the most common types of cancers. Prognosis for CRC is dependent on the stage of the disease at diagnosis and a variety of molecular features including expression of biomarkers and gene mutation. This study sought to (i) develop molecular tests for use in molecular profiling of formalin-fixed paraffin embedded tissue (FFPE) and (ii) interrogate the molecular profile and biomarker expression in multiple cohorts of sporadic CRC.

Materials and methods:
Firstly, we developed the Quick Multiplexed Consensus (QMC) PCR protocol – a method used in conjunction with High Resolution Melting (HRM) analysis for screening of multiple mutational hotspots (10 hotspots in this study were screened) in the CRC candidate genes using DNA from FFPE tissue. The performance of the assay for the detection of single nucleotide variants (SNV) and small insertion-deletions (indels) was compared with Sanger sequencing, pyrosequencing and real-time PCR. In addition, a PCR/HRM assay was developed for testing microsatellite instability (MSI) using a panel of six quasi-monomorphic mononucleotide markers (five of which have been previously described: BAT25, BAT26, NR21, NR22, and NR24; the sixth marker, B-CAT25, is a novel in-house developed marker) and this assay was validated against the Bethesda commercial MSI PCR kit and against immunohistochemistry (IHC).

Once QMC-PCR was optimised, we sought to ascertain whether diagnostic biopsies yield sufficient information for clinical decision making. The mutation profiles of CRC candidate genes (KRAS, BRAF, PIK3CA and TP53) and MSI status were evaluated in the diagnostic biopsy specimen of 30 cases and compared with the profile in matched blocks from the resection specimen.

The classification of CRC into tumours with MSI and chromosomal instability (CIN) is well described. However tumours which show neither MSI nor CIN have been described and are known as microsatellite and chromosomal stable CRCs (MACS). We sought to evaluate the frequency of CIN and MACS in a series of 89 sporadic microsatellite-stable CRCs. PCR/HRM was used to exclude MSI tumous, while CIN tumours was discriminated from MACS tumours using flow cytometry. These tumours were also compared for mutations in KRAS/BRAF/TP53/PIK3CA by QMC-PCR. Some rectal tumours may receive neoadjuvant chemoradiotherapy (CRT) and we tested whether the CIN or MACS ploidy status could predict response in a group of 62 rectal cancers treated with neoadjuvant CRT.

We next evaluated the clinical utility of deficient Mismatch Repair (dMMR) protein and aberrant P53 protein expression, both individually and in combination, as prognostic and predictive of response to therapy biomarkers in CRC. A total of 884 tumours from the VICTOR trial (a large phase III trial of rofecoxib in stage II and III CRC) were tested for expression of four mismatch repair (MMR) proteins (MLH1, PMS2, MSH2, MSH6) and p53 by IHC. The expression was correlated with outcome.

Results:
QMC-PCR worked on DNA from FFPE tissue. Spiking experiments showed the protocol could detect a minimum of 2.5% of mutant alleles compared to 20% detectable for Sanger sequencing. Precision tests showed that there was little intra-assay and inter-assay variation. Forty-three FFPE colorectal tumours were initially sequenced for hotspots in KRAS and PIK3CA and then screened by QMC-PCR. In these tests, QMC-PCR showed a sensitivity of 100%, specificity of 71%, PPV of 76% and NPV of 100%. All 43 samples were then screened for mutations in all 10 hotspots. Of 430 tests, 43 (10%) showed aberrant melting and 36 were confirmed mutant (PPV 84%). Since our technique is more sensitive than direct sequencing, the remaining 7 tests are probably sequencing false negatives.

HRM analysis of KRAS (codon12/13) and BRAF (V600E) showed that 3% and 1.5% mutant alleles respectively could be reliably detected whilst pyrosequencing reliably detected 6% mutant alleles in each case. Of 110 tests performed on 22 DNA samples, in 109 cases HRM and pyrosequencing gave identical results.

The results of KRAS (codon12/13) screening from the comparative study of 468 cases with a real-time PCR test (DxS), showed 89.9% concordance with the DxS test. In comparison with real-time PCR, the analysis by HRM showed 87.2% sensitivity, 91.6% specificity, 86.7% positive predictive value, 91.9% negative predictive value. After refinement of the protocol, re-testing of 100 randomly selected cases showed 99% concordance between QMC-PCR/HRM and the real-time PCR test.

The performance of the HRM based MSI assay showed 100% accuracy on both cell lines and FFPE tissue in comparison to PCR and IHC.

Pertaining to the results from the paired biopsy and resection specimens work, a total of 570 paired PCR tests were performed and identical results were obtained in both biopsy and resection specimens in 569 tests (>99% concordance). Four cases (13%) showed microsatellite instability, and, in all four cases, instability was seen at identical mononucleotide markers in both biopsy and matched resection specimens. Regarding the immunostaining of MMR proteins, the staining was more intense and easier to interpret in biopsies and that it faithfully replicates the diagnosis in the resection specimen.

The results from the DNA ploidy study showed, in addition to the two classical forms of genetic instability (MSI, CIN), a significant third group of colorectal cancers (CRC) without either MSI or CIN i.e. Microsatellite and Chromosome Stable (MACS) CRCs. Fifty-one of 89 CRCs (57%) were aneuploid and 38 (43%) were diploid. There was no significant association seen between mutations in TP53/KRAS/BRAF/PIK3CA with ploidy. Testing of association between mutations revealed only mutual exclusivity of KRAS/BRAF mutation ($p<0.001$). Of the 62 rectal cancers treated with neoadjuvant chemoradiotherapy, 22 had responded (Mandard Tumour Regression Grade 1/2) and 40 failed to respond (Grade 3-5). Twenty-five of 62 (40%) tumours were diploid but there was no association between ploidy and response to the neoadjuvant CRT therapy.

Evaluation of TP53 and MMR protein expression in the VICTOR trial, showed that there was dMMR in 12% (87/735) of patients. It was associated with female gender (p=0.001), proximal location of tumour (p<0.001), poor differentiation (p<0.001) and stage II disease (p<0.001). dMMR was not associated with either disease free survival (DFS) or overall survival (OS) in the group overall or when stratified by stage. However, unexpectedly, proficient MMR (pMMR) was associated with significantly improved OS (hazard ratio 0.28 (0.11, 0.68), p=0.005) and DFS (hazard ratio 0.47 (0.22, 0.99), p=0.047) in patients who did not receive chemotherapy. Aberrant p53 expression was found in 65% (482/740) of patients. It was associated with distal location (p<0.001) and stage III disease (p<0.001) and it was negatively associated with dMMR (p<0.001). No effect was observed on DFS or OS and there was no interaction with chemotherapy or radiotherapy. When assessed in combination, dMMR and aberrant p53 expression had no effect on DFS, OS or responsiveness to adjuvant therapy.

Conclusions:
The following conclusions can be drawn from this research work:

1) QMC-PCR with HRM is a simple, robust and inexpensive technique which had greater sensitivity than Sanger sequencing. It allows multiple mutation hotspots to be rapidly screened and is thus highly suited to mutation detection in DNA derived from FFPE tissues. Both HRM and pyrosequencing can detect small numbers of mutant alleles although HRM has a lower limit of detection. Both are suitable for use in mutation detection and are both more sensitive than Sanger sequencing. QMC-PCR with HRM performs very well against real-time PCR based tests for detection of KRAS mutation. Although the real-time PCR has a lower limit of detection, HRM has greater flexibility overall. Both tests are suitable for KRAS codon 12/13 mutation detection in patients being considered for anti-epidermal growth factor receptor (EGFR) biological therapy.

2) PCR-HRM/MSI assay is simple, straightforward and highly sensitive technique for MSI testing which can be easily incorporated in a single closed-tube panel whether to screen for Lynch syndrome, or to test sporadic CRC for tumour MSI status in order to inform the decision maker to administer 5-fluorouracil-based chemotherapy to the patient or not.

2) This was the first study to show that diagnostic biopsy specimens, even though they are a tiny sample of the tumour, are sufficiently representative for use in predictive testing for early driver mutations in colorectal cancer, especially important when neoadjuvant therapy is being considered.

3) MACS-CRCs form a significant proportion of microsatellite-stable CRCs with a mutation profile overlapping that of CRCs with CIN. A diploid genotype does not however predict the responsiveness to radiotherapy in rectal cancers. This finding leads us to conclude that there are other factors in addition to ploidy that define response to radiation therapy.

4) Analysis of MMR status and p53 expression in the patients recruited to the VICTOR trial confirmed that dMMR and p53 expression are associated with site and stage of CRC. Neither biomarker has prognostic or predictive utility in this

cohort of patients overall although in sub-group analysis dMMR was indicative of poor outcome in chemo-naive patients.

Thesis related publications

1- Targeted Next-Generation Sequencing Validates the Use of Diagnostic Biopsies as a Suitable Alternative to Resection Material for Mutation Screening in Colorectal Cancer. HAM-KARIM, H.A., EBILI, H.O., MANGER, K., **FADHIL, W**., AHMAD, N.S., RICHMAN, S.D. & ILYAS, M. 2019. Mol Diagn Ther. (**W Fadhil's contribution:** Preparation of test samples, Data collection, Data analysis and interpretation, Drafting the article, Approval of the version to be published (all authors))

2- Positive association of PIK3CA mutation with KRAS mutation but not BRAF mutation in colorectal cancer suggests co-selection is gene specific but not pathway specific. Susanti S, **Fadhil W**, Murtaza S, Hassall JC, Ebili HO, Oniscu A, Ilyas M. 2019. J Clin Pathol (**W Fadhil's contribution:** Conception or design of the work, Preparation of test samples, Data collection, Data analysis and interpretation, Drafting the article, Approval of the version to be published (all authors))

3- CD10 inhibits cell motility but expression is associated with advanced stage disease in colorectal cancer. Raposo TP, Comes MS, Idowu A, Agit B, Hassall J, **Fadhil W**, Nica R, Ecker R, Yao T, Ilyas M. 2018. Exp Mol Patho (**W Fadhil's contribution:** Preparation of TMA and linked clinicopathological data, Data analysis and interpretation, Drafting the article, Approval of the version to be published (all authors))

4- N_LyST: a simple and rapid screening test for Lynch syndrome. Susanti S, **Fadhil W**, Ebili HO, Asiri A, Nestarenkaite A, Hadjimichael E, Ham-Karim HA, Field J, Stafford K, Matharoo-Ball B, Hassall JC, Sharif A, Oniscu A, Ilyas M. 2018. J Clin Pathol (**W Fadhil's contribution:** Conception or design of the work, Preparation of test samples, Data collection, Data analysis and interpretation, Drafting the article, Approval of the version to be published (all authors))

5- "Squirrel" Primer-Based PCR Assay for Direct and Targeted Sanger Sequencing of Short Genomic Segments. Ebili HO, Hassall JC, **Fadhil W**, Ham-Karim H, Asiri A, Raposo TP, Agboola AJ, Ilyas M. 2017, J Biomol Tech (**W Fadhil's contribution:** Preparation of test samples, Drafting the article, Approval of the version to be published (all authors))

6- QMC-PCRx: a novel method for rapid mutation detection. Ebili HO, Hassall J, Asiri A, Ham-Karim H, **Fadhil W**, Agboola AJ, Ilyas M. 2017. J Clin Pathol (**W Fadhil's contribution:** Conception or design of the work, preparation of test samples, Data analysis and interpretation, Drafting the article, Approval of the version to be published (all authors))

7- COLD-HRM: a combination of methods to infer the nature of somatic mutations. Ham-Karim HA, Ebili HO, Fadhil W, Asiri A, Hassall J, Ilyas M. 2017. Adv Cytol Pathol (W Fadhil's contribution: Conception or design of the work, preparation of test samples, Data analysis and interpretation, Drafting the article, Approval of the version to be published (all authors)

8- Aberrant P53 expression lacks prognostic or predictive significance in colorectal cancer: results from the VICTOR trial. McGregor MJ, Fadhil W, Wharton R, Yanagisawa Y, Presz M, Pritchard A, Womack C, Dutton S, Kerr RS, Kerr DJ, Johnstone EC, Ilyas M. 2015. Anticancer Res (**W Fadhil's contribution:** Conception or design of the work, Preparation of TMA slide images, Arraying images, scoring immunostain, Data collection, Data analysis and interpretation, Drafting the article, Approval of the version to be published (all authors)

9- STAT3 paradoxically stimulates β-catenin expression but inhibits β-catenin function. Ibrahem S, Al-Ghamdi S, Baloch K, Muhammad B, **Fadhil W**, Jackson D, Nateri AS, Ilyas M. 2014. Int J Exp Pathol. 95(6):392-400. (**W Fadhil's contribution:** Preparation of TMA and linked clinicopathological data, Data analysis and interpretation, Drafting the article, Approval of the version to be published (all authors))

10- Nuclear expression of phosphorylated focal adhesion kinase is associated with poor prognosis in human colorectal cancer. Albasri A, **Fadhil W**, Scholefield JH, Durrant LG, Ilyas M. 2014. Anticancer Res. 34(8):3969-74. (**W Fadhil's contribution:** Preparation of TMA and linked clinicopathological data, Data analysis and interpretation, Drafting the article, Approval of the version to be published (all authors))

11- DNA content analysis of colorectal cancer defines a distinct 'microsatellite and chromosome stable' group but does not predict response to radiotherapy. **Fadhil W**, Kindle K, Jackson D, Zaitoun A, Lane N, Robins A, Ilyas M. Int J Exp Pathol. 2014 Feb;95(1):16-23. (**W Fadhil's contribution:** Conception or design of the work, Preparation of test samples, Data collection, Data analysis and interpretation, Drafting the article, Approval of the version to be published (all authors))

12- Loss of expression of the double strand break repair protein ATM is associated with worse prognosis in colorectal cancer and loss of Ku70 expression is associated with CIN. Beggs AD, Domingo E, McGregor M, Presz M, Johnstone E, Midgley R, Kerr D, Oukrif D, Novelli M, Abulafi M, Hodgson SV, **Fadhil W**, Ilyas M, Tomlinson IP. 2012. Oncotarget. 3(11):1348-55. (**W Fadhil's contribution:** Preparation of TMA slide images, Arraying images, Data analysis and interpretation, Drafting the article, Approval of the version to be published (all authors))

13- The utility of diagnostic biopsy specimens for predictive molecular testing in colorectal cancer. **Fadhil W**, Ibrahem S, Seth R, AbuAli G, Ragunath K, Kaye P, Ilyas M. 2012. Histopathology. 61(6):1117-24. (**W Fadhil's contribution:** Conception or design of the work, Preparation of test samples, Data collection, Data analysis and interpretation, Drafting the article, Approval of the version to be published (all authors))

14- Embryonic NANOG activity defines colorectal cancer stem cells and modulates through AP1- and TCF-dependent mechanisms. Ibrahim EE, Babaei-Jadidi R, Saadeddin A, Spencer-Dene B, Hossaini S, Abuzinadah M, Li N, **Fadhil W**, Ilyas M, Bonnet D, Nateri AS. 2012. Stem Cells. 30(10):2076-87. (**W Fadhil's contribution:** Preparation of TMA and linked

clinicopathological data, Data analysis and interpretation, Drafting the article, Approval of the version to be published (all authors))

15- Immunostaining in the context of loss mismatch repair function: interpretive confounders and cautionary tales! **Fadhil W**, Field J, Cross G, Kaye P, Ilyas M. 2012. Histopathology. 61(3):522-5. (**W Fadhil's contribution:** Conception or design of the work, Preparation of test samples, Data collection, Data analysis and interpretation, Drafting the article, Approval of the version to be published (all authors))

16- Immunostaining for mismatch repair (MMR) protein expression in colorectal cancer is better and easier to interpret when performed on diagnostic biopsies. **Fadhil W**, Ilyas M. 2012. Histopathology. 60(4):653-5. (**W Fadhil's contribution:** Conception or design of the work, Preparation of test samples, Data collection, Data analysis and interpretation, Drafting the article, Approval of the version to be published (all authors))

17- Cten signals through integrin-linked kinase (ILK) and may promote metastasis in colorectal cancer. Albasri A, Al-Ghamdi S, **Fadhil W**, Aleskandarany M, Liao YC, Jackson D, Lobo DN, Lo SH, Kumari R, Durrant L, Watson S, Kindle KB, Ilyas M. 2011. Oncogene. 30(26):2997-3002. (**W Fadhil's contribution:** Preparation of TMA and linked clinicopathological data, Data analysis and interpretation, Drafting the article, Approval of the version to be published (all authors))

18- Comparative analysis of pyrosequencing and QMC-PCR in conjunction with high resolution melting for KRAS/BRAF mutation detection. Ibrahem S, Seth R, O'Sullivan B, **Fadhil W**, Taniere P, Ilyas M. 2010. Int J Exp Pathol. 91(6):500-5. (**W Fadhil's contribution:** Conception or design of the work, Preparation of test samples, Data collection, Data analysis and interpretation, Drafting the article, Approval of the version to be published (all authors))

19- Quick-multiplex-consensus (QMC)-PCR followed by high-resolution melting: a simple and robust method for mutation detection in formalin-fixed paraffin-embedded tissue. **Fadhil W**, Ibrahem S, Seth R, Ilyas M. 2010. J Clin Pathol. 63(2):134-40. (**W Fadhil's contribution:** Conception or design of the work, Preparation of test samples, Data collection, Data analysis and interpretation, Drafting the article, Approval of the version to be published (all authors))

20- Concomitant mutations and splice variants in KRAS and BRAF demonstrate complex perturbation of the Ras/Raf signalling pathway in advanced colorectal cancer. Seth R, Crook S, Ibrahem S, **Fadhil W**, Jackson D, Ilyas M. Gut. 2009 Sep;58(9):1234-41. (**W Fadhil's contribution:** Preparation of test samples, Data collection, Data analysis and interpretation, Drafting the article, Approval of the version to be published (all authors))

Presentations and conference communications

1- Testing for PIK3CA and BRAF Mutations in Colorectal Cancer with Microsatellite Instability. Murtaza, S.; **Fadhil, W.M**.; Hassall, J.; Ebili, H.O.; Ilyas, M. Poster presentation at Maastricht Pathology 2018. 11th Joint Meeting of the British Division of the International Academy of Pathology and the Pathological Society of Great Britain & Ireland, 19-22 June 2018 J Pathol. 2018 Sep;246 Suppl 1: S1-S46. doi: 10.1002/path.5165. (**W Fadhil's contribution:** Conception or design of the work, Preparation of test samples, Data collection, Data analysis and interpretation, Preparation of the presentation)

2- N_LyST: a simple and rapid screening test for Lynch syndrome. Susanti S; **Fadhil W**; Ebili HO; Asiri A; Nestarenkaite A; Hadjimichael E; Ham-Karim HA; Field J; Stafford K; Matharoo-Ball B; Hassall JC; Sharif A; Oniscu A; Ilyas. M. Poster presentation at Maastricht Pathology 2018. 11th Joint Meeting of the British Division of the International Academy of Pathology and the Pathological Society of Great Brit-ain & Ireland, 19-22 June 2018 J Pathol. 2018 Sep;246 Suppl 1: S1-S46. doi: 10.1002/path.5165. (**W Fadhil's contribution:** Conception or design of the work, Preparation of test samples, Data collection, Data analysis and interpretation, Preparation of the presentation)

3- Introducing a New Panel of Markers for Microsatellite Instability (MSI) Detection in Colorectal Cancer by High Resolution Melting Analysis. **W Fadhil**; S Susanti; HO Ebili; J Field; K Stafford; H Hadjimichael; M Ilyas. Oral presentation at Belfast Pathology 2017. 10th Joint Meeting of the British Division of the International Academy of Pathology and the Pathological Society of Great Britain & Ireland, 20–23 June 2017. Volume 243, Issue Supplement S1 September 2017 Pages S.13. (**W Fadhil's contribution:** Conception or design of the work, Preparation of test samples, Data collection, Data analysis and interpretation, Preparation of the presentation, and presenting the work)

4- Detection of Mutant Circulating Free DNA as a biomarker of Colorectal Cancer. Abutaleb Asiri; James Hassall; Ham-Karim; Henry Ebili; **Wakkas Fadhil**; Oliver Ng; PF Fardouly; Austin Acheson; Mohammad Ilyas. Poster presentation at Belfast Pathology 2017. 10th Joint Meeting of the British Division of the International Academy of Pathology and the Pathological Society of Great Britain & Ireland, 20–23 June 2017. Volume 243, Issue Supplement S1 September 2017 Pages S.25. (**W Fadhil's contribution:** Conception or design of the work, Data collection, Data analysis and interpretation, Preparation of the presentation)

5- Mutation and Expression Profile of Primary Colorectal Cancer and Related Liver Metastasis. **W Fadhil**; S Ibrahim; M Ilyas, The Journal of Pathology, Supplement: Summer Meeting 2012. Abstracts of the 202nd Scientific Meeting of the Pathological Society of Great Britain & Ireland, 3–5 July, Volume 228, Issue S1, Pages S1–S41. (**W Fadhil's contribution:** Conception or design of

the work, Preparation of test samples, Data collection, Data analysis and interpretation, Preparation of the presentation and presenting the work)

6- The Utility of Diagnostic Biopsies for Predictive Mutation Detection in Colorectal Cancer. **W Fadhil**; S Ibrahim; R Seth; G AbuAli; K Ragunath; P Kaye; M Ilyas , The Journal of Pathology, Supplement: Volume 224, Issue S2, Pages S1–S39. (**W Fadhil's contribution:** Conception or design of the work, Preparation of test samples, Data collection, Data analysis and interpretation, Preparation of the presentation and presenting the work)

7- High Resolution Melting Analysis (HRM) is a Novel and Robust Method for Detection of Microsatellite Instability in Colorectal Cancer. **W Fadhil**; S Ibrahim; R Seth; G AbuAli; K Ragunath; P Kaye; M Ilyas. The Journal of Pathology, Supplement: Volume 224, Issue S2, Pages S1–S39. (**W Fadhil's contribution:** Conception or design of the work, Preparation of test samples, Data collection, Data analysis and interpretation, Preparation of the presentation and presenting the work)

8- Loss of FOXA2 Expression Occurs in Advanced Colorectal Cancers Despite Gene Amplification. **W Fadhil**; M Ilyas. The Journal of Pathology, Supplement: Winter Meeting 2013. Joint Meeting of the Pathological Society of Great Britain & Ireland and the Dutch Pathological Society (NVVP), 8–9 January, Volume 229, Issue s1, pages 1–31, April 2013. (**W Fadhil's contribution:** Conception or design of the work, Preparation of test samples, Data collection, Data analysis and interpretation, Preparation of the presentation and presenting the work)

9- Tumour Ploidy Analysis of Microsatellite Stable Colorectal Cancers Identifies a Significant Subset of Diploid Tumours but does not Predict Responsiveness to Radiotherapy. **W Fadhil**; M Ilyas. The Journal of Pathology, Supplement: Winter Meeting 2013. Joint Meeting of the Pathological Society of Great Britain & Ireland and the Dutch Pathological Society (NVVP), 8–9 January, Volume 229, Issue s1, pages 1–31, April 2013. (**W Fadhil's contribution:** Conception or design of the work, Preparation of test samples, Data collection, Data analysis and interpretation, Preparation of the presentation and presenting the work)

10- Testing for Allelic Loss in Colorectal Cancer by High Resolution Melting (HRM) Analysis. **W Fadhil**; E Gosal; H Lee, M Ilyas. The Journal of Pathology, Supplement: Summer Meeting 2012. Abstracts of the 202nd Scientific Meeting of the Pathological Society of Great Britain & Ireland, 3–5 July, Volume 228, Issue S1, Pages S1–S41. (**W Fadhil's contribution:** Conception or design of the work, Preparation of test samples, Data collection, Data analysis and interpretation, Preparation of the presentation and presenting the work)

11- Revisiting Ploidy Status of Sporadic Colorectal Cancer. **W Fadhil**; K Kindle; S Hukkeri; S Ibrahem; M Ilyas. The Journal of Pathology, Supplement: Winter Meeting 2012. 201st Scientific Meeting of the Pathological Society of Great Britain & Ireland, 5–6 January, Volume 226, Issue S1, Pages S1–S34. (**W Fadhil's contribution:** Conception or design of the work, Preparation of

test samples, Data collection, Data analysis and interpretation, Preparation of the presentation and presenting the work)

Table of Contents

Index of Tables

Index of Figures

List of abbreviations

AI	Allelic imbalance
ANGEL2	Angel homolog 2
APC	Adenomatous Polyposis Coli
ARMS	Amplification Refractory Mutation Systems
ASR	Age-Standardized Rates
AURKA	Aurora kinase A
AXIN2	axis inhibitor 2
BAT25	Big Adenine Tract-25
BAT26	Big Adenine Tract-26
BAX	Bcl-2–Associated X protein
BRAF	B-Raf proto-oncogene
CCND1	Cyclin D1
CCND2	Cyclin D2
CDK4	Cyclin dependent kinase 4
CE	Capillary electrophoresis
CIMP	CpG island mutator phenotype
CIN	Chromosomal instability
CMS1	Consensus molecular subtype1
CMS2	Consensus molecular subtype2
CMS2	Consensus molecular subtype3
CMS2	Consensus molecular subtype4
CRC	Colorectal cancer
CRT	Chemoradiotherapy
Ct	Threshold cycle
DAB	3,3’-Diaminobenzidine
dHPLC	Denaturing high performance liquid chromatography
DI	DNA index
dMMR	Deficient mismatch repair
dsDNA	Double stranded DNA
ER1	Epitope Retrieval solution 1
ER2	Epitope Retrieval solution 2
ERK	Extracellular regulated MAP kinase
EWSR1	EWS RNA binding protein 1
FAP	Familial adenomatous polyposis
FBXW7	F-box and WD repeat domain containing 7
FOLFIRI	Folinic acid, fluorouracil and irinotecan
FOLFOX	Folinic acid, fluorouracil and oxaliplatin
H&E	Haematoxylin and Eosin
HNF4A	Hepatocyte nuclear factor 4 alpha
HNPCC	Hereditary non-polyposis colorectal cancer
HRM or HRMA	High Resolution Melting Analysis
HRR	Homologous recombination repair
IARC	International Agency for Research on Cancer
IGFRII	Insulin growth factor receptor 2

IHC	Immunohistochemistry
indels	Insetions/deletions
KRAS	Kirsten rat sarcoma viral oncogene homolog
LOD	Limit od detection
LOH	Loss of heterozygosity
LS	Lynch syndrome
MACS	Microsatellite And Chromosome Stable
MAP	MYH-associated polyposis
MAPK	Mitogen-activated protein kinase
MEK	MAP kinse-ERK kinase
MLH1	mutL homolog 1
MMR	Mismatch repair
MSH2	mutS homolog 2
MSH6	mutS homolog 2
MSI	Microsatelite instabe
MSS	Microsatelite stable
MYB	MYB proto-oncogene
MYC	MYC proto-oncogene
NABP1	nucleic acid binding protein 1
NCCN	National Comprehensive Cancer Network
NHEJ	Non-Homologous End Joining
NICE	National Institute of Clinical and Healthcare Excellence
N-LyST	Nottingham Lynch Syndrome Test
NotIS	Nottingham Information System
PBA	Protein blocking agent
PCR	Polymerase chain reaction
PD1	Programmed death 1
PDM	Pre-Diagnostic Multiplex
PIK3CA	phosphatidylinositol-4,5-bisphosphate 3-kinase catalytic subunit alpha
pMMR	Proficient mismatch repair
PMS2	PMS1 homolog 2
PMT	Photomultiplier Tube
SCNA	Somatic copy number alterations
SMAD2	SMAD family member 2
SMAD4	SMAD family member 4
SNPs	Single Nucleotide Polymorphisms
SNV	Single nucleotide variant
ssDNA	Single stranded DNA
SSD	Single Specific Diagnostic
Tc	Denaturation temperature
TGFB	Transforming growth factor beta 1
TGFBRII	Transforming growth factor beta receptor 2
TIL	Tumour infiltrating lymphocyte
Tm	Melting temperature
TMAs	Tissue microarrays
TP53	Tumour protein p53

TRG	Tumour Regression Grade
WNT	Wingless- type mouse mammary tumour virus integration
XELOX	Capecitabine and oxaliplatin

Chapter 1. **General Introduction**

1.1 Epidemiology of CRC

Colorectal cancer (CRC) is the commonest malignancy of the gastrointestinal tract. It is the fourth most common cancer worldwide with 1,849,519 new cases reported in 2018 and the third most common cause of cancer deaths after cancers of the lung and breast with 880,792 deaths in the same year (Ferlay et al., 2018, Ferlay et al., 2019). In the male gender CRC constitutes the third commonest cancer and the fourth commonest cause of cancer deaths after cancers of the lung, liver and stomach, whereas in the female gender CRC is the second most common cancer and the third commonest cause of cancer deaths after cancers of the breast and lung (Ferlay et al., 2018, Ferlay et al., 2019). However, the incidences of CRC vary markedly from one geographical region to another. For example, the highest incidences of CRC in 2018 are found in Australia and New Zealand, Europe, Eastern Asia and North America, where its Age-Standardized Rates (ASR) range from 36.7 to 26.2 per 100,000 population; whilst the lowest incidences are found in Africa and South-Central Asia with ASRs ranging from 9.2 to 4.9 per 100,000 population (Ferlay et al., 2018, Ferlay et al., 2019). Similarly, the mortality rates of CRC generally follow the same pattern of incidences, being highest in Australia and New Zealand, Europe and Eastern Asia, and lowest in Africa and South-Central Asia per 100,000 population. However, the mortality-to-incidence ratios are much higher in the regions with comparatively low incidences (Ferlay et al., 2018, Ferlay et al., 2019). In the United Kingdom, CRC is the fourth commonest cancer after breast, prostate and lung cancers in 2018 at an ASR of 32.1 cases per 100,000 population, as well as the fourth commonest cause of cancer deaths at a rate of 11.1 per 100,000 population (CR-UK, 2018).

Several risk factors have been established for CRC. Whereas some of these are modifiable, others are genetic/hereditary. The modifiable risk factors for CRC include obesity, sedentary lifestyle, and consumption of diets high in red and

processed meat, high calorie diet, fat-rich diet, fiber-deficient diet, high alcohol intake and tobacco smoking (Marley and Nan, 2016, Chan and Giovannucci, 2010, Turner, 2015). Others are extremely high temperature meat-cooking methods (boiling, charcoal broiling and frying), high blood insulin levels and inflammatory bowel diseases (ulcerative colitis and Crohn disease) (Marley and Nan, 2016, Chan and Giovannucci, 2010). Conversely, the protective risk factors against CRC include consumption of fish and fish oil, high intake of fiber diet, high intake of vitamin D and calcium, habitual exercise, and regular use of aspirin (Marley and Nan, 2016, Chan and Giovannucci, 2010, Turner, 2015). The genetic/hereditary risk factors of CRC will be discussed under the molecular basis of CRC.

CRC is a disease of predominantly the elderly. Online analysis of the International Agency for Research on Cancer (IARC) data showed that in high incidence regions such as Australia and New Zealand, Europe and North America the peak age incidence of CRC is in the 70 years-and-above age group (Ferlay et al., 2018, Ferlay et al., 2019). Whereas, in the Western African sub-region the peak age incidence is in the 60-69 years age group (Ferlay et al., 2018, Ferlay et al., 2019). The peak age incidence of CRC in the UK follows that of high incidence regions. In line with the IARC data, the 2013-2015 Cancer Research UK statistics shows that the highest rates of CRC are seen in the 70-79 years group (CR-UK, 2018).

There is a slight male predominance in the incidence of CRC from most regions of the world in 2018 except in Eastern and Middle Africa where slight female preponderances exist. The 2018 report for the UK puts the CRC incidence male: female ratio at 1.24 (Ferlay et al., 2018).

1.2 Clinical features of CRC

There are three patterns of clinical presentation of CRC: (i) asymptomatic patients

whose cancers are discovered only on routine screening and examination (ii) presentation with classic CRC symptoms and/or signs (iii) presentation with emergency symptoms/signs such as intestinal obstruction, peritonitis or acute gastrointestinal bleeding (Turner, 2015, Moreno et al., 2016, Moiel and Thompson, 2011).

The establishment of screening programmes for CRC – using endoscopy and faecal occult blood testing - has enabled the detection of asymptomatic CRC, which would otherwise have escaped clinical attention for a long period as CRC develops insidiously. However, the preponderance of CRC patients – about 70% to 90% - present with classic CRC symptoms and signs (Moreno et al., 2016, Moiel and Thompson, 2011, Turner, 2015). The most common clinical presenting features of CRC include haematochezia, melena, abdominal pain, iron-deficiency anaemia, and change in bowel habit. CRC patients also commonly present with rectal or abdominal mass (Elzouki et al., 2014, Hsiang et al., 2013, Labianca et al., 2013, Holch et al., 2017, Thompson et al., 2017, Mukherji et al., 2011). The combination of presenting symptoms and signs are often suggestive of the tumour site. For example, patients with caecal and right-sided colon cancer present with fatigue, weakness and iron-deficiency anaemia, whereas left-sided tumours cause occult bleeding, changes in bowel habits, cramping and left quadrant discomfort (Turner, 2015). Up to 50% of CRC patients may present with metastatic disease (Holch et al., 2017). CRC commonly metastasizes via the lymphatic, haematogenous and transperitoneal routes as well as contiguously to regional lymph nodes, liver, lungs and the peritoneum (Holch et al., 2017, Mukherji et al., 2011). Metastatic disease frequently presents as right upper quadrant pain, abdominal distention, early satiety, and supraclavicular lymphadenopathy and peri-umbilical nodules (Pratap Singh et al., 2018, Mukherji et al., 2011, Chan et al., 2014, Girijala et al., 2018, Iscan et al., 2016). Less commonly CRC patients can present with fistula formation between the colon (sigmoid carcinoma) and the urinary bladder or small bowel;

fever of unknown origin due to a perforated colon cancer causing intra-abdominal, retroperitoneal, abdominal wall or intrahepatic abscesses (Tsai et al., 2007, Alvarez et al., 2004).

1.3 Molecular pathogenesis of CRC

CRC is a heterogeneous group of diseases resulting from genetic and epigenetic mutations in cancer-related genes (Grady and Markowitz, 2015). The pathogenesis of CRC involve the stepwise accumulation of genetic and epigenetic abnormalities in cancer-related genes either in the germline or somatically (Turner, 2015, Grady and Markowitz, 2015, Yamagishi et al., 2016, Chung and Fleshman, 2004, Goel and Boland, 2012). The molecular pathogenesis generally follows three patterns of presentation: (i) inherited CRC syndromes which account for less than 10% of all CRCs, (ii) non-syndromic or "familial" CRC which accounts for 25-30% of all CRCs, and (iii) sporadic CRC which accounts for about 70% of all CRCs (Jasperson et al., 2010, Yamagishi et al., 2016, Chung and Fleshman, 2004).

Inherited CRC syndromes include the familial adenomatous polyposis (FAP), hereditary non-polyposis colorectal cancer (HNPCC, also known as Lynch syndrome, (LS)), MYH-associated polyposis (MAP). Other syndromes include the variants of FAP such as the hereditary flat adenoma (or attenuated FAP) syndrome. Less common hereditary colorectal cancer syndromes include the Peutz-Jeghers, Juvenile polyposis, Cowden, Bannayan-Ruvalcaba, Li-Fraumeni and Bloom syndromes (Jasperson et al., 2010, Turner, 2015).

The familial adenomatous polyposis syndrome is an autosomal dominant syndrome which presents as multiple (up to thousands) colorectal adenomas in the teenage. It is caused by germline mutations in the adenomatous polyposis coli gene, APC, with loci on chromosome 5q21. APC is a negative regulator of the WNT signalling

pathway. Up to 75% of these mutations are inherited whereas the remaining 25% occur de novo. In the classic FAP patients CRC invariably develops from the adenomatous polyps in the absence of prophylactic colectomy. In spite of colectomy, however, adenomas may develop elsewhere such as in the stomach or ampulla of Vater (Jasperson et al., 2010, Turner, 2015). FAP patients may also develop extra-intestinal manifestations of the syndrome, including, congenital hypertrophy of the retinal epithelium, and features of Gardner and Turcot syndromes. In about 30% of cases, polyposis develops without APC loss. These cases are caused by bi-allelic mutations of the base excision repair gene, MYH (or MUTYH), a DNA glycosylase which repairs oxidative DNA damages. MUYTH-associated polyposis (MAP) is an autosomal recessive disorder with colonic phenotype similar to attenuated FAP. Clinical presentation occurs at a later age than FAP, often at 50 years of age or later. The polyps are usually serrated and show KRAS mutations (Jasperson et al., 2010, Turner, 2015).

Hereditary non-polyposis colon cancer, Lynch syndrome, is an autosomal dominant disease caused by inherited mutations in the genes that encode DNA mismatch repair proteins, most commonly MLH1, MSH2, PMS2, PMS6, etc (Lynch and de la Chapelle, 2003, Peltomaki, 2003). These proteins are involved in the detection, excision and repair of errors that occur during DNA replication. The loss of DNA mismatch repair confers a 1000-fold higher mutation rates in the tumours of LS patients, mostly in microsatellite regions present in gene exons and introns and in extragenic sites genome-wide. Mutations in microsatellites commonly cause frameshift mutations in essential genes (Peltomaki, 2003, Boland and Goel, 2010). Lynch syndrome constitutes 2-4% of all CRCs, making it the most common form of syndromic CRC (Kastrinos and Syngal, 2011, Hampel, 2009). It is characterised by familial clustering of cancers at several sites, including colorectum, endometrium, stomach, ovary, ureters, brain, small bowel, the hepatobiliary tract, pancreas and skin. Lynch syndrome patients with CRC present

at a younger age than do patients with sporadic CRC (Jasperson et al., 2010, Turner, 2015, Boland and Goel, 2010, Cottrell et al., 1992, Ilyas et al., 1999). Numerous studies have shown that, due to the high risk of multiple cancers and its relatively high prevalence, there is a clinical and economic benefit to be gained by screening CRCs for LS. Guidance from the National Institute of Clinical and Healthcare Excellence (NICE) recommends that all CRCs should be screened for the possibility of LS (NICE, 2017b).

Familial, or non-syndromic, CRC constitutes about 25-30% of CRCs. It is characterised by the clustering of CRC with unrecognised syndromes and sporadic CRC-like features in families. As a group, familial CRCs have no established molecular mechanisms (Armelao and de Pretis, 2014, Jasperson et al., 2010). However, a few genome-wide association studies have identified common genetic risk loci for the disease group. Example of such loci are single nucleotide polymorphisms in chromosomes 8q24, 9p24, SMAD7, CRAC1 (HMPS) at 15q13.3, 11q23, 18q21, 10p14, 8q23.3, 8q24.21, 16q22, 2q32 (NABP1), 1q25.3, 12p13.32 (CCND2), 12q24.21 (T-box 3) (Zanke et al., 2007, Tomlinson et al., 2007, Haiman et al., 2007, Broderick et al., 2007, Jaeger et al., 2008, Tenesa et al., 2008, Tomlinson et al., 2008, Abuli et al., 2010, Peters et al., 2013).

The molecular pathogenesis of sporadic CRC involves three pathways (Figure 1-1) (i) classic adenoma-carcinoma sequence, which involves mutations or epigenetic silencing of the APC/β-catenin pathway, (ii) the DNA mismatch repair (MMR)-deficient or microsatellite instability (MSI) pathway, (iii) the CpG island mutator phenotype (CIMP) pathway (Yamagishi et al., 2016, Chung and Fleshman, 2004, Grady and Markowitz, 2015, Pino and Chung, 2010, Boland and Goel, 2010, Goel and Boland, 2012, Turner, 2015).

About 70-85% of sporadic CRC develop via the classic adenoma-carcinoma

sequence of CRC pathogenesis (Fearon, 2011, Ilyas et al., 1999, Pritchard and Grady, 2011). This pathway typically involves sequential accumulation of mutations starting with genetic alterations in the APC/β-catenin pathway. APC functions to bind and promote degradation of β-catenin. However, with loss of APC function, β-catenin translocates to the nucleus, where it activates TCF, a transcription factor that activates the transcription of cell proliferation genes such as MYC and CCND1. In the absence of APC loss, many CRC harbour β-catenin mutations that make them resistant to APC binding and degradation, thereby giving the same functional impact as APC loss. During tumour progression in the adenoma-carcinoma sequence, additional mutations in KRAS, SMAD2, SMAD4, and TP53 occur. It is recognised that in this pathway normal colonic epithelium usually transforms into tubular adenoma, which in turn, undergoes malignant changes to adenocarcinoma (Yamagishi et al., 2016, Chung and Fleshman, 2004, Grady and Markowitz, 2015, Pino and Chung, 2010, Turner, 2015).

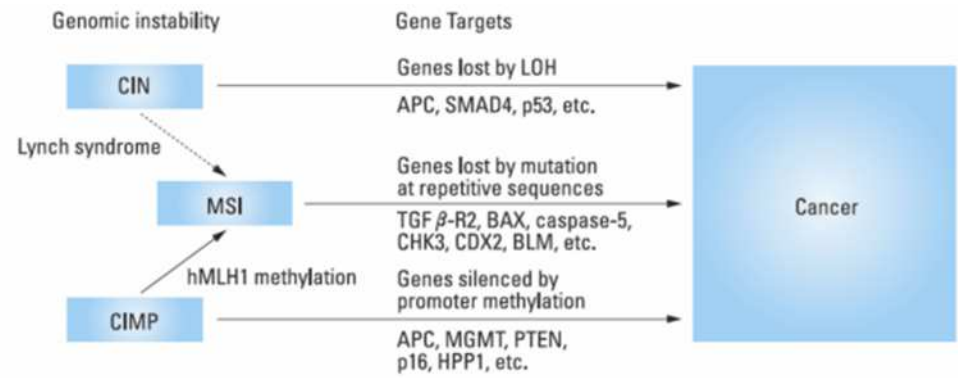

Figure 1-1 Molecular pathways in CRC

An integrated model for different forms of genetic and epigenetic instability in CRC (CIN; Chromosomal Instability, MSI; Microsatellite Instability, CIMP; CpG Island Mutator Phenotype, LOH; Loss Of Heterozygosity). *Adopted from* (Boland et al., 2009)

KRAS is a classic proto-oncogene involved in signal transduction. Activating point mutations in KRAS promotes growth and prevents apoptosis, and are among the commonest mutations found in CRCs (Turner, 2015).

The tumour suppressors SMAD2 and SMAD4 are effectors of the TGF-β signalling pathway, which normally inhibits cell growth. The disruption of this pathway via SMAD2 and SMAD4 mutations removes this inhibition and enhances uncontrolled cell growth (Turner, 2015).

TP53 is a master regulator of cell growth and proliferation. The p53 protein is a transcription factor normally regulates cell cycle progression, DNA damage repair, cellular senescence and apoptosis via binding to p53-binding elements in the promoter regions present in hundreds of genes. When cells incur DNA damage from hypoxic stress, for example, the upstream DNA-damage response signalling activates p53 accumulation. p53 upregulates p21, which in turn, inhibits CDK4/cyclin D complexes thereby blocking the progression through the cell cycle. This blockade is essential for cellular repair mechanisms to effect repair of the DNA damage. When repair is successful, the cell cycle progression blockade is relieved via downregulation of p21. When, on the other hand, DNA repair is unsuccessful p53 triggers either cellular senescence or apoptosis via activation of the pro-apoptosis gene BAX. Therefore, TP53 mutation, which commonly occurs by inactivating point mutations and chromosomal deletions, allows mutations in several other genes to go unrepaired and become established in cells. TP53 mutations occur in more than 50% of all cancers and in up to 70% of CRC (Turner, 2015).

A hallmark of the CRCs that arise through the adenoma-carcinoma sequence is chromosomal instability (CIN). CIN is characterised by numerical and structural aberrations such as aneuploidy, polyploidy, interstitial chromosomal re-arrangements including chromosomal amplification and deletions, whole arm deletions and translocations, etc. It is caused by a combination of deregulation of mitotic spindle checkpoint regulators, centrosome amplification, deregulation of dsDNA break repair, telomere erosion, etc. CIN is a cause of intratumoural

heterogeneity or clonal diversity, chemotherapy resistance, and a mechanism of tumour progression (Yamagishi et al., 2016, Chung and Fleshman, 2004, Grady and Markowitz, 2015, Pino and Chung, 2010, Turner, 2015).

DNA MMR-deficient/MSI CRC constitute about 10-15% of sporadic CRC. Sporadic CRC with MSI usually transform from serrated adenoma, in contrast to Lynch syndrome CRC that arises in a background of tubular adenoma (Abdel-Rahman et al., 2006). It is caused by somatic inactivation of the MMR genes, most commonly MLH1, MSH2 and PMS2, by aberrant DNA methylation or somatic point mutations. Inactivation of DNA MMR genes in colonic epithelial cells provides a favorable background for accumulation of mutations in several other genes, as well as genome-wide instability in microsatellite regions. Genes commonly mutated in sporadic MSI CRC include BRAF (V600E), TGFBRII, IGFRII and the pro-apoptosis gene BAX (Abdel-Rahman et al., 2006, Ilyas et al., 1999, Jass, 2007, Bae et al., 2016).

MSI CRC have a mutually exclusive occurrence with CIN. Relative to CIN tumours, patients with stages I to III sporadic MSI CRC have a better prognosis but poorer response to 5-fluorouracil-based chemotherapy (Boland and Goel, 2010, Yamagishi et al., 2016, Chung and Fleshman, 2004, Grady and Markowitz, 2015, Turner, 2015).

Less than 5% of sporadic CRCs display the CpG island mutator phenotype (CIMP) without MSI. This group show increased rates of genome-wide hypermethylation of promoter GpG islands in tumour suppressor genes, and consequently, gene repression. Many of these tumours harbour KRAS mutations but TP53 and BRAF mutations are uncommon. Like the sporadic MSI tumours, they arise in a background of serrated adenoma (Bae et al., 2016).

A subset of MSI CRC also display the CIMP with hypermethylation of MLH1. This group show significant rates of BRAF activating point mutations. TP53 and KRAS mutation are, however, uncommon (Goel and Boland, 2012, Yamagishi et al., 2016, Chung and Fleshman, 2004, Grady and Markowitz, 2015, Pino and Chung, 2010, Turner, 2015).

1.4 Why study the molecular genetics of CRC

The study of these molecular alterations that accompany tumour progression has not only deepened the knowledge of cellular biology but has enhanced the understanding of carcinogenesis and cancer progression. Much more important, perhaps, is the clinical utility of studying the molecular genetics of cancer. The genomic profiling of many cancer types has enabled the stratification of patients into prognostic and treatment subgroups (Wang et al., 2019, Linnekamp et al., 2018).

In CRC, many molecular subtyping schemes exist, but none of these has enjoyed actual clinical applications in full. For example, CRC has been subtyped according to the classic pathogenetic pathways into CIN, MSI and CIMP subtypes, as described in the preceding section. The prognostic implication of this subtyping scheme was also discussed in the preceding section.

Furthermore, CRC has been classified into the CIN, MSI and microsatellite and chromosomal stable (MACS) subgroups based on the genomic instability status. Whereas the CIN subtype or subclass of CRC shows aneuploidy, the MSI and MACS tumours are diploid or near-diploid. The MACS (and CIN) tumours by definition lack the genome-wide microsatellite instability that characterises the MSI tumours. However, beyond the prognostic advantage of MSI status in this classification schemes, the clinicopathological and prognostic significance of the

MACS status is currently unknown due to conflicting data from different reports (Linnebacher et al., 2013, Ostwald et al., 2009, Kakar et al., 2008, Cai et al., 2008, Silver et al., 2011, Hawkins et al., 2001).

More recently, the consensus molecular subtypes (CMS) of CRC were produced (Figure 1-2). In this subtyping scheme, four subgroups of CRC – consensus molecular subtypes 1 (CMS1) to consensus molecular subtypes 4 (CMS4) – are recognized (Guinney et al., 2015). CMS1 tumours comprise 14% of the consensus molecular types of CRC and are essentially hypermutated MSI tumours with immune activation and low somatic copy number alterations (SCNA). consensus molecular subtypes 2 (CMS2) tumours show high SCNA with copy number gains and losses. They comprise 37% of CRCs and have chromosomal instability with marked WNT and MYC activation. consensus molecular subtypes 3 (CMS3) tumours, comprising 15% of CRCs, are described as metabolic and epithelial since they show molecular features of metabolic dysregulation. They have few SCNA and higher CIMP-low cluster. About 30% of them are hypermutated. CMS4 tumours (23% of CRCs) are described as mesenchymal since they show prominent TGFB activation, stromal invasion and angiogenesis. Furthermore, whilst CMS1 tumours show significant BRAF mutations, receptor tyrosine kinase, the CMS2 cases show consistent enrichment only in HNF4A amplification, and not in other genetic loci. CMS3 tumours have significant rates of KRAS mutations and MAPK pathway activation. From the clinicopathological standpoint, CMS1 tumours are more frequently found in females, are right-sided and have higher histological grades. CMS2 tumours, on the other hand, are left-sided lesions, whilst CMS4 tumours are significantly diagnosed at the advanced stages (stages III and IV). Furthermore, whilst the patients with the CMS4 tumours show worse overall survival and relapse-free survival, the CMS2 patients show superior survival indices after relapse. The CMS1 patients are characterised by poor survival after relapse (Guinney et al., 2015).

CMS1 MSI immune	CMS2 Canonical	CMS3 Metabolic	CMS4 Mesenchymal
14%	37%	13%	23%
MSI, CIMP high, hypermutation	SCNA high	Mixed MSI status, SCNA low, CIMP low	SCNA high
BRAF mutations		*KRAS* mutations	
Immune infiltration and activation	WNT and MYC activation	Metabolic deregulation	Stromal infiltration, TGF-β activation, angiogenesis
Worse survival after relapse			Worse relapse-free and overall survival

Figure 1-2 Consensus molecular subtype of colorectal cancer (CMS)

The proposed molecular classification of CRC based on gene expression studies. MSI, microsatellite instability; CIMP, CpG island methylator phenotype; SCNA, somatic copy number alteration, TGF- β (Transforming Growth Factor-β). Adopted from (Guinney et al., 2015).

From the foregoing, two molecular subgroups – CIN and MSI – have consistently appeared in the different molecular subtyping schemes which have been produced using different molecular technology platforms, evidence that both subgroups are authentic patho-biological groups. Furthermore, both molecular subtypes have been given therapeutic significance clinically. For example, MSI testing is routinely performed for stage II CRC in order to inform the decision maker whether to administer 5-fluorouracil-based chemotherapy to the patient or not. Patients whose tumours test negative for MSI –presumed CIN – are offered chemotherapy in addition to surgery, whilst MSI-positive cases receive surgery treatment alone (de la Chapelle and Hampel, 2010, Des Guetz et al., 2009, NCCN, 2017).

Going further, molecular testing enables the identification of targets for therapy. Current CRC management guidelines recommend the use of targeted therapies in patients with (i) unresectable metastatic tumours, (ii) advance or metastatic disease who are not fit for intensive chemotherapy, (iii) chemo-resistant, biomarker-positive tumours (i.e. second line therapy) (NCCN, 2017). In most of these settings,

the administration of targeted therapy requires genetic testing. For example, prescription of anti-EGFR inhibitors – such as panitumumab and cetuximab - for metastatic CRC must be accompanied by testing the patients' tumours to exclude KRAS, NRAS and BRAF V600E mutations, which confer resistance to the drugs. Also, programmed death 1 (PD1) inhibitors, nivolumab and pembrolizumab are only administered to patients with MSI-positive or MMR-deficient tumours (NCCN, 2017, Ohhara et al., 2016) (NICE, 2011, NICE, 2017a).

Related to the study of molecular genetics of CRC is the subject of research and diagnostic methodologies that enable the identification and detection of molecular/genetic alterations in CRC. The study of the molecular genetics is served by (i) the availability of novel and improved methods in molecular diagnostics, methods that allow comprehensive molecular characterisation of tumours, (ii) the identification of reliable and reproducible biomarkers of response or resistance to targeted therapies and chemotherapeutic agents. In the light of the foregoing, there is a need for the continuous improvement of molecular assays in order to enhance early detection of cancer, prediction of prognosis and therapeutic response, monitoring of therapeutic response, as well as follow-up of CRC patients.

1.5 Treatment of CRC

The TNM (Tumour Node Metastasis) staging system is now the standard model used for staging CRC as it is more detailed than the historical Dukes staging system (Edge and Compton, 2010). This system has classified CRC into 4 main stages (with several substages), which determine the disease prognosis and patient treatment. Based on the National Institute for Health and Care Excellence (NICE) guideline (NICE, 2011), the main treatment for CRC patients with primary CRC at all stages (stage 0-III) is surgery. The subsequent management of patients with local CRC is dependent on the staging of the resected tumour by a pathologist. Patients

with early-stage CRC (i.e. Stage 0, I, and low-risk stage II) have a good prognosis and will not receive adjuvant therapy. While, in cases with more advanced-stage disease (i.e. high-risk stage II and III) the prognosis is more variable and consequently the management is more complex and can be followed by adjuvant therapy with chemotherapeutic agents such as the combination of oxaliplatin and 5-Fluorouracil/folinic acid (FOLFOX) or Capecitabine and oxaliplatin (XELOX) for the high-risk patients (NICE, 2011).

The recommendation for advanced and metastatic CRC patients (stage IV) included the use of standard chemotherapy combinations as well as addition of biological agents (NICE, 2011, NICE, 2017a). The patients may be offered FOLFOX as first-line treatment then single-agent irinotecan as second-line treatment, FOLFOX as the first-line treatment then FOLFIRI as second-line treatment, or XELOX, as first line-line treatment then FOLFIRI as second line-line treatment, or Raltitrexed only for patients with advanced CRC patients who are intolerant to 5-Fluorouracil and folinic acid, or Capecitabine oral therapy as an option for first-line treatment (NICE, 2011). Regarding the biological agents (NICE, 2017a), Cetuximab is available as an option for previously untreated EGFR-expressing, RAS wild-type metastatic CRC in combination with either FOLFOX or FOLFIRI. Panitumumab is available as an option for previously untreated RAS wild-type metastatic CRC in combination with either FOLFOX or FOLFIRI. Bevacizumab in combination with oxaliplatin and either fluorouracil plus folinic acid or capecitabine is not recommended for the treatment of metastatic colorectal cancer. A schematic illustration of the treatment pathways in CRC is presented in Figure 1-3.

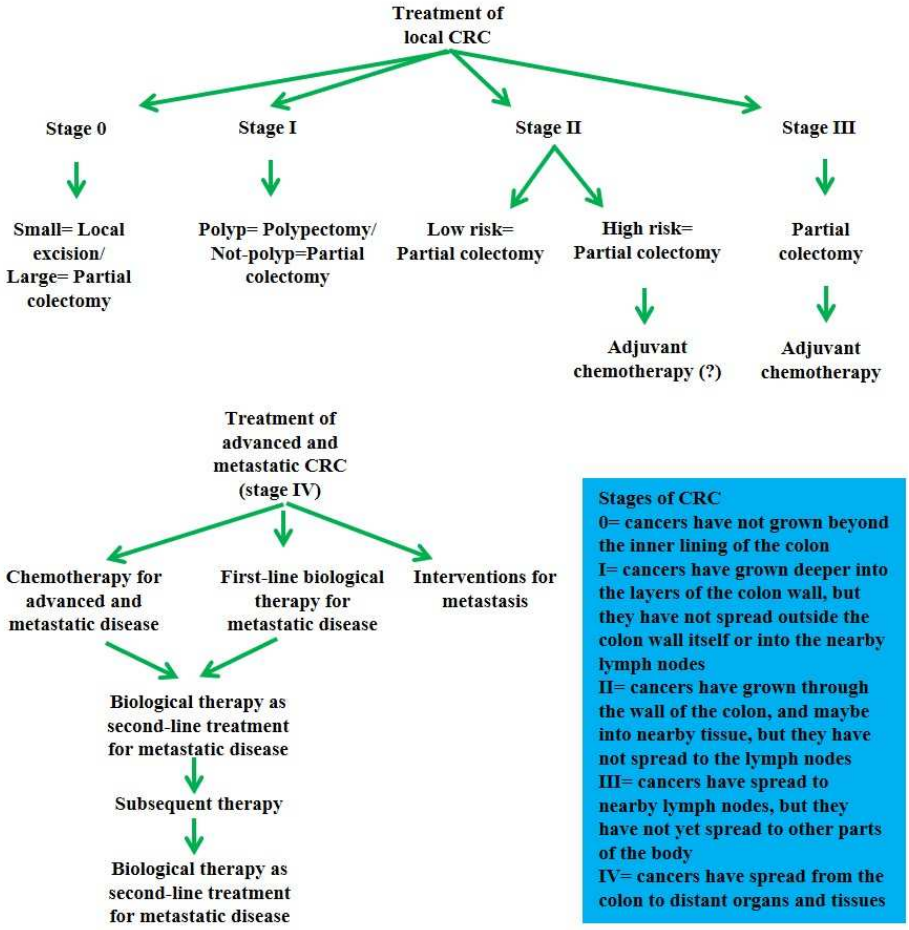

Figure 1-3 Treatment pathways in CRC

This flowchart illustrate the treatment pathways in local and advanced CRC (NICE, 2011, NICE, 2017a). It can be seen from this chart that local CRCs (0-III) are mainly treated by surgery. Subsequent adjuvant chemotherapy is offered for high risk stage II disease. Adjuvant chemotherapy is routinely prescribed for Stage III disease. While in the category of advanced disease, the initial treatment is neoadjuvant (chemotherapy or biological therapy). The blue insert (bottom right) describes the anatomical extent of CRC in each the different stages.

1.6 Mutation screening techniques

Currently, the most widely used method for mutation detection is direct sequencing which is generally regarded as the 'gold standard'. However, it is expensive, laborious and gives false negative results when a large number of normal cells are admixed with tumour cells (Tsao et al., 2005, Victor Cohen, 2006, Janne et al., 2006, Do et al., 2008). Since mutations can occur in multiple sites in a gene (usually known as "hotspots"), detection by direct sequencing would be prohibitively expensive. Screening of hotspots for mutation prior to sequencing could reduce

this cost by excluding wild type samples from further analysis.

All these limitations of direct sequencing have prompted the development of new mutation scanning techniques such as single strand conformation polymorphism (SSCP) (Gupta et al., 2005), temperature gradient gel electrophoresis (Langerod et al., 2007), denaturing high performance liquid chromatography (Rossetti et al., 2007), and MALDI-TOF (Koren-Michowitz et al., 2008, van den Boom and Ehrich, 2007) have been developed for the purposes of mutation detection. The goal of these screening techniques is to reduce the use of DNA sequencing and control costs while maintaining sensitivity and specificity. However, these techniques are complicated, expensive and tend to be available only in research institutions.

High resolution melt curve analysis (HRM) is a recently developed simple and cost-effective post PCR technique which can be used for high throughput mutation scanning and genotyping. The technique requires the use of standard PCR reagents only and the dsDNA binding dye LC Green® Plus. This closed tube pre-screening method has advantages over current mutation scanning techniques since it requires no post PCR handling (minimising the risk of PCR contamination) and no separation step, which improves analysis time (Reed et al., 2007, Wittwer et al., 2003). Many recent publications have documented the successful use of HRM on several platform (Herrmann et al., 2006) for mutation scanning / genotyping (Wittwer et al., 2003, Liew et al., 2004, Reed and Wittwer, 2004, Graham et al., 2005, Willmore-Payne et al., 2005, Dufresne et al., 2006, Margraf et al., 2006, Krypuy et al., 2007, Willmore et al., 2004) , simultaneous mutation scanning and genotyping (Zhou et al., 2005), methylation profiling (Worm et al., 2001), and genotyping with unlabeled probes (Zhou et al., 2004).

1.7 The hypothesis and aims of the study

Genetic profiling of a tumour is required for more consistent classification / staging of tumours and to allow bespoke tailoring of therapies based on tumour biology. A variety of molecular techniques can be used for mutation analysis and each has its strength and weakness. Formalin fixed and paraffin embedded (FFPE) tumour tissue is the most commonly available source of materials for research and diagnostic purposes. However, FFPE tissues tend to suffer DNA degradation and the utility of sophisticated screening techniques on this type of template remains to be proven. In addition, investigating multiple mutational hotspots in a gene or multiple genes within a specific pathway by sequencing would be prohibitively expensive. Thus, pre-sequencing mutation screening of hotspots could reduce this cost by excluding wild type samples from further analysis. Considering the forgoing, we believe that the study of molecular genetics is best served by the availability of simple, cost-effective, sensitive and versatile methods. We sought in this study to refine the High Resolution Melting (HRM) analysis technique to make it sufficiently robust for diagnostic use in FFPE tissue, and to perform in a comparable efficiency to other sensitive techniques.

This study was driven by the following hypothesis

1) Studies of tumour biology show that CRC develops as a result of waves of clonal expansion (or clonal sweeps or clonal heterogeneity) driven by mutations that give a selective advantage. As the new clone expands and becomes predominant in the tumour, the driver mutation responsible for this will eventually be present throughout the tumour. **One can hypothesise that the driver mutations responsible for the early clonal sweeps (such as KRAS gene mutation) during the adenoma–carcinoma sequence should be present in most of the tumour cells, and thus would be present in the biopsy samples.** In order to investigate whether diagnostic biopsy specimens are suitable for predictive testing, we first

performed paired evaluation of matched diagnostic biopsies and their subsequent resection specimens for the presence of mutations that are thought to occur during the pre-invasive phase of colorectal tumour growth. Second, **we hypothesised that problems in interpretation of mismatch (MMR) proteins expression could be obviated by evaluation of immunohistochemistry (IHC) for MMR proteins in biopsy samples rather than resection specimens since the former will tend to have more thorough and uniform fixation.** So, we evaluated the immunostaining of the MMR proteins expression on tumour sections from 30 consecutive cases of CRC and their corresponding pre-surgical diagnostic biopsies.

2) The diverse natural history of CRC translates the heterogeneous nature of the disease, and might be attributed to complex underlying genetic backgrounds. Several old studies reported a group of microsatellites stable (MSS) and chromosomes stable (diploid/ near-diploid chromosomes) tumours (MACS). Despite of this, a dogma has emerged that CRCs must have one or other form of genomic instability; either microsatellite instability (MSI) or chromosomal instability (CIN). Around 10-15% of sporadic CRCs show MSI, whilst the remainder are microsatellite stable (MSS) and they have been considered synonymous to CIN tumours, which are more or less mutually exclusive with MSI tumours. MACS subtype is relatively poorly described, and their clinico-pathological correlates are also poorly described, therefore, **we hypothesised that the MACS tumours form a third group which is genetically and biologically distinct from CIN CRC**, and we sought to evaluate whether there are any clinico-pathological or molecular differences between MACS-CRCs and CIN-CRCs, in an unselected series of CRCs which were shown to be microsatellite stable.

3) Chromosome aberrations are considered as primary radiation induced lethal lesion in tumour cells, as it was found that a single chromosome aberration is enough to kill a diploid cell. While in aneuploid tumour cells, perhaps higher levels

of chromosome aberrations may be required to kill the cells. Thus, if DNA ploidy influences radiation sensitivity, then the relationship between aberration frequency and cell survival will change as ploidy changes. Around 15-25% of rectal CRCs show a dramatic response to neoadjuvant chemoradiation therapy (CRT) and identification of the features predicting responsiveness would be a major step forward in the management of patients with rectal cancer. As rectal cancers are usually MSS, so, they could serve as a feasible model to study the influence of ploidy status on response to radiation, therefore **we hypothesised that MACS-CRCs (diploid/ near diploid tumours) may respond differently to radiation than CIN-CRCs (aneuploid tumours).** If so, tumour ploidy could be used as a predictive test for radiation responsiveness. Therefore, pre-radiotherapy diagnostic rectal biopsies from cases of responsive and non-responsive tumours were tested.

4) There is a need for robust predictive and prognostic biomarkers which can add to the current management approach of patients with CRC, which is mostly dependent on the staging of the resected tumour by a pathologist. Furthermore, pathological staging does not provide any information on tumour biology. Therefore, in making the choice of which biomarkers to test, then choosing those that reflect tumour biology would be a reasonable starting point. Tumour protein 53 (Tp53) is mutated in 60% of CRCs, deficient mismatch repair protein is present in up to 15% of CRCs, both markers are significantly linked to specific clinic-pathological features and their role in CRC carcinogenesis is known. Therefore, **we hypothesised that p53 and MMR should have influence on disease prognosis and response to therapy.** To test our hypothesis, we investigated the clinical utility of dMMR and aberrant p53 expression by IHC as prognostic and predictive biomarkers in a large study population which was drawn only from the VICTOR trial.

1.8 Statement of contribution to the study

The researcher (author of this PhD thesis) would like to confirm that he is the producer of this work and his contribution was as follows:

1- Conception or design of the work (all chapters)

2- Preparation of test samples (for the entire study unless stated otherwise)

3- Data collection (for the entire study unless stated otherwise)

4- Data analysis and interpretation (for the entire study unless stated otherwise)

5- Drafting and finalising the production of this thesis

Chapter 2. **Materials and Methods**

2.1 Materials

2.1.1 Cell lines

Twenty-nine-well established CRC cell lines were kindly donated by Sir Walter Bodmer and Professor Ian Tomlinson (Molecular and Population Genetics Laboratory, London Research Institute, Cancer Research UK, London), and maintained as previously described (Seth et al., 2009b, Seth et al., 2009a). In Brief: the cell lines were cultured in Dulbecco's modified Eagle's medium (DMEM; Invitrogen, Paisley, UK) supplemented with 10% fetal Bovine serum (FBS) (Sigma, UK) and penicillin/streptomycin (Invitrogen) in 5% CO2 in a humidified atmosphere. Cells were grown to 90% confluence before extraction of nucleic acid. These cell lines were screened for mutation in the CRC candidate genes and for microsatellite instability.

2.1.2 Clinical samples

Four series of sporadic CRCs were used during this study, their details are described in the subsequent sections and their main characteristics are shown in Figure 2-1. To interrogate the genetic instability pathways and mutational signatures of the candidate oncogenes/ tumour suppressor genes in sporadic CRC, we required molecular tests that could work efficiently on formalin fixed paraffin embedded tissue (FFPE), which is the commonly available tissue format for both research and diagnostic laboratories, but on the other hand it is considered the most challengeable template for molecular testing. The experimental work flow through out this study is presented in Figure 2-2, and it is outline briefly in this section. The initial optimisation process was conducted on a high-quality DNA from CRC cell lines. The molecular profiles of these CRC cell lines are very well known and so they served as an optimal model to fully optimise the proposed assays. We then further developed these assays to work robustly on FFPE tissue using a set of CRC

FFPE samples randomly collected from the histopathology archive of Nottingham University Hospitals (this set was called Nottingham series/ set-1). We compared the performance of the mutation screening assay to direct Sanger sequencing and pyrosequencing and that of the MSI testing assay to immunohistochemistry (IHC) for the mismatch repair (MMR) proteins.

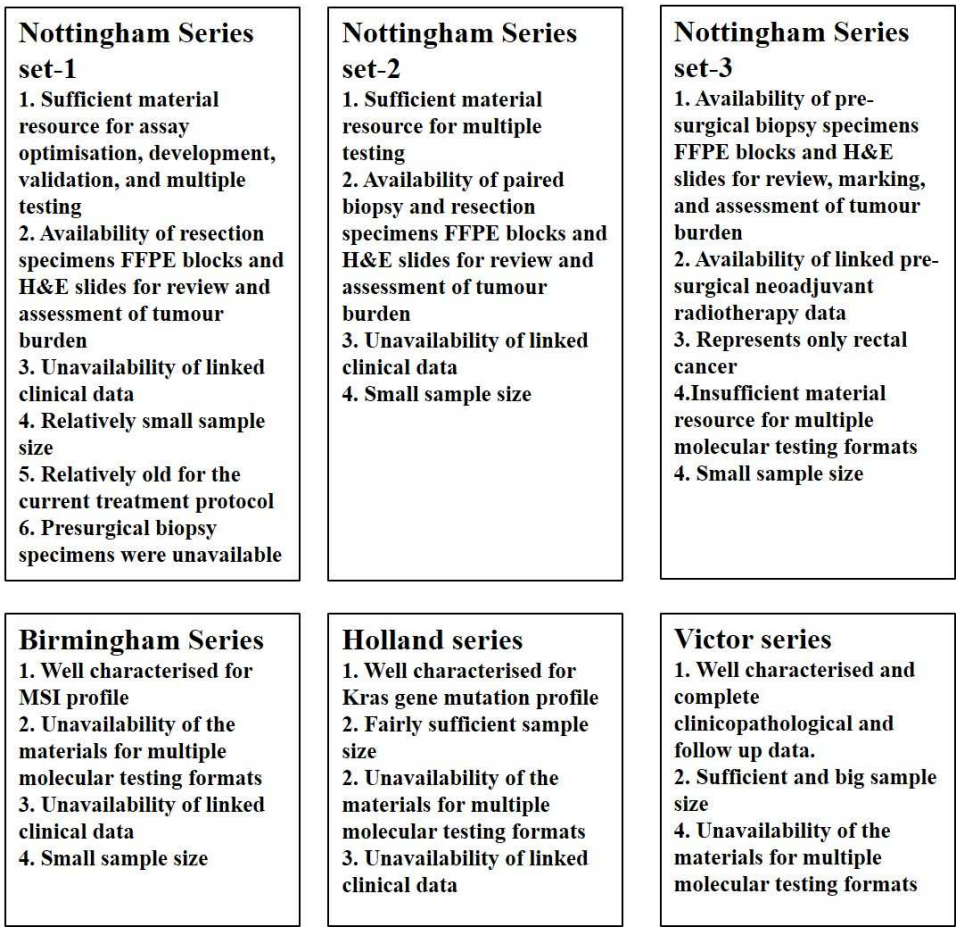

Figure 2-1 characteristics of CRC series

A diagram showing the main characteristics of the different CRC series used in this study in term of strength and weakness points of each series. (FFPE; formalin fixed paraffin embedded tissue, H&E; haematoxylin and eosin, MSI; micro-satellite instability).

Having these tests successfully worked on FFPE materials, we moved forward to test the feasibility of these assays for the diagnostic work. To achieve the requirement of this stage, we established collaborative works with external laboratories to provide us with anonymised FFPE DNA samples, which were

previously genetically fingerprinted using clinically approved tests. Hence to validate the mutation screening assay, FFPE DNA samples were received from the Dutch Colorectal Cancer Group (DCCG) (this series was called Holland series). Those clinical samples were obtained from patients with advance primary CRC recruited to the CAIRO2 trial and previously fingerprinted genotyped for the Kras exon 2 mutations using two clinically approved tests. While, for the MSI testing assay, we received DNA samples from the West Midlands Regional Genetics Laboratory (WMRGL), Birmingham Women's Hospital, and Birmingham, UK (this series was called Birmingham series). Those clinical samples were previously tested at the WMRGL for MSI status using the Bethesda Panel of MSI markers and IHC for the MMR proteins.

Then we screened a series of matched pre-surgical biopsies and subsequent resection specimens of FFPE CRC samples (this was called Nottingham series set-2) for mutations in the CRC candidate genes and for MSI status characterisation. The purpose of this part was to explore whether our assays could work on a tiny piece of tumour without having their limit of detection being confounded by low mutant allele frequency and tumour heterogeneity or not? This work also aimed to test the utility of using pre-surgical biopsy for predictive molecular testing in the era of neo-adjuvant therapy. Subsequent to mutation and MSI profiling of set-1 and 2, we investigated the tumour DNA ploidy status (CIN signature) of those cases in set-1 and 2. Then, the significance of ploidy status as predictive of response to neo-adjuvant radiotherapy in rectal cancer was investigated using a set of pre-surgical rectal biopsies (this series was called Nottingham series set-3). Finally, we looked into the prognostic and predictive significance of TP53 and MMR proteins expression by IHC in a big series of stage II-III sporadic CRC tissues obtained from patients who were recruited to the VICTOR trial. This series was used because of its big sample size and the availability of a robust linked clinicopathological and follow up data, which was not available from the other series in this study.

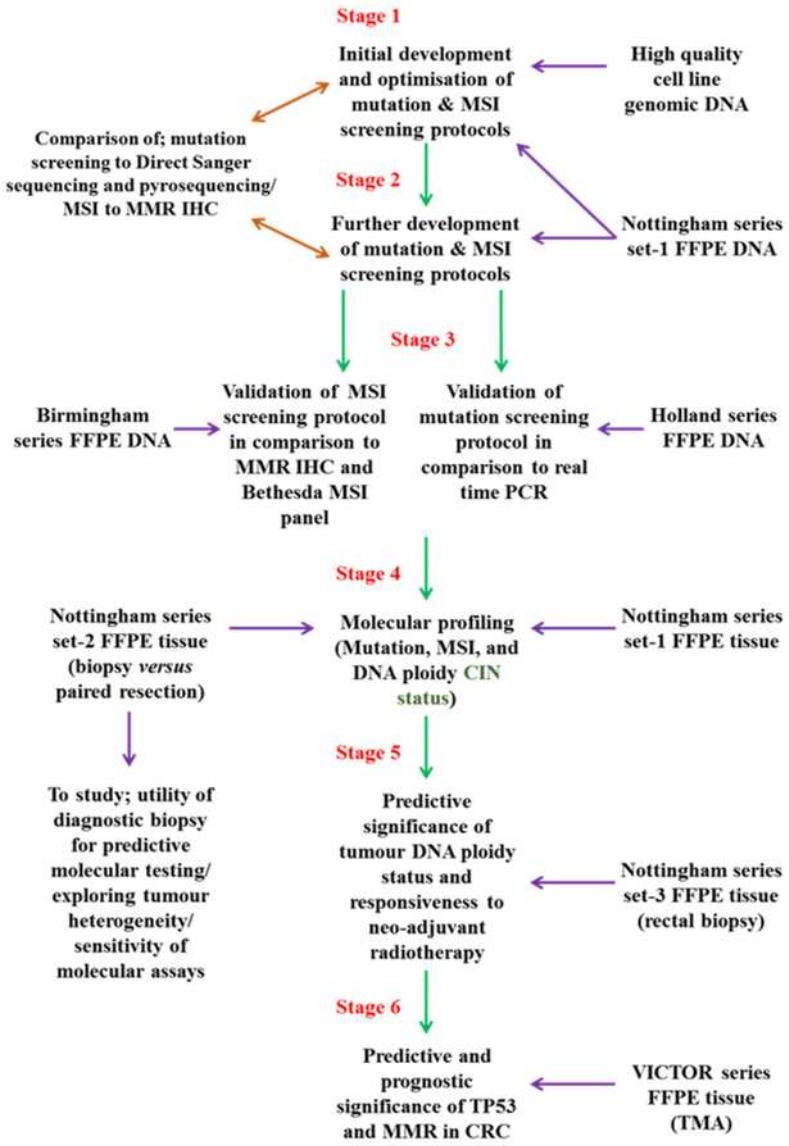

Figure 2-2 Schematic presentation of the experimental work flow

This diagram illustrates schematically the experimental stages that were followed to develop the research work in this study. It also refers to the different cohorts of samples which were used and at which specific stage.. Additionally, it shows the type of methodologies which were used for comparison and validation purposes. (MSI; micro-satellite instability, FFPE; formalin fixed paraffin embedded tissue, CIN; chromosomal instability).

.

2.1.2.1 Nottingham series

This series comprised of three sets of FFPE CRC samples which were randomly selected from the archives of the pathology department of the Nottingham

University Hospitals NHS Trust. Each sample was given a unique anonymous ID number to protect patient privacy. The project was completed with ethical approval in accordance with Research Ethics Committee, and all experimental work was undertaken with local institutional approval.

Cases in Nottingham series were identified from Nottingham University Hospitals pathology database using the relevant pathology codes (cases identification was done by Anne Wilson, in the Histopathology surgical laboratory, QMC, Nottingham University Hospitals NHS Trust). The pathology data were collected using Nottingham Information System NotIS. For Nottingham series set-1, tissue samples were collected for a total of fifty-eight sporadic CRC cases. These tumours were surgically removed at Queen's Medical Centre, Nottingham, UK, over the period 1993-2008 and the ethical approval was obtained for the use of patient materials (Research Ethics Committee reference 05/Q2402/72; a study of cancer cell death and survival in human tissue). The patients' age range was between 43-88 years, of which 24 females and 34 males with mean age ± SD of 69.6 ± 11.7 years and 68.5 ± 10 years, respectively. The H&E stained slides were reviewed to confirm the presence of tumour and to avoid sampling error and to estimate the tumour proportion. Only samples with proficient (≥ 50%) tumour tissue available were selected. This sample set was initially used as a pilot group to develop the screening protocols (mutation and MSI screening) on FFPE tissue. Materials from these tumour samples were also used to study tumour DNA content. The extracted molecular data from this series was used to study the molecular profiles of CRCs in combination with the data from Nottingham series set-2, which is described in the next paragraph.

The list of CRC cases for Nottingham series set-2 (also referred to in this study as biopsy versus resection) were kindly provided by professor Mohammad Ilyas (professor to pathology, School of Medicine, University of Nottingham, Division

of pathology, QMC, Nottingham University Hospitals NHS Trust). This set consisted of 42 cases of primary CRC removed at the QMC, Nottingham University Hospitals NHS Trust over the period 2009-2010. The patients' age range in this set was between 47-87 years, of which 19 females and 23 males with mean age ± SD of 70.5 ± 10.5 years and 71.8 ± 11.7 years, respectively. Only thirty cases from this set-2 had matched diagnostic biopsy specimen and the final resection specimen available, while from the remaining twelve cases only the biopsy specimens were available. The biopsy specimens were typically 2–3 mm in size, and the number of tissue fragments in each case ranged from two to 10. An inclusion criterion was the presence of at least 50% tumour tissue in the biopsy specimens. Blocks from the corresponding resection specimens were chosen to contain at least 50% tumour tissue, and ethical approval was obtained for the use of patient materials (Research Ethics Committee reference 05 / Q1605 / 66). This series was initially used to evaluate the utility of diagnostic biopsy specimens for predictive molecular testing in CRC. However DNA materials isolated from forty two samples were also used to study the DNA content, MSI testing, and mutation profiles of CRCs.

The third set (Nottingham series set-3) was used to evaluate the association between tumour DNA content and regression following neoadjuvant chemoradiotherapy (CRT). The pre-CRT rectal biopsies were available for 22 cases of rectal cancer that were selected from a previously reported series (Dhadda et al., 2011). Of these, 10 cases had shown a marked response (i.e. Mandard grade 1 or 2) whilst 12 cases had shown little or no response (Mandard grade 3 – 5). As we were looking for an effect of 100% (i.e. a diploid karyotype was associated with a marked response in all cases), this sample size would give us 95% power to detect this at significance level of <0.1%.

2.1.2.2 **Birmingham series**

A set of 24 anonymised FFPE tumour samples were obtained from West Midlands Regional Genetics Laboratory (WMRGL), Birmingham Women's Hospital, and Birmingham, UK. These tumours were previously tested at the WMRGL for MSI status using the Bethesda Panel (Boland et al., 1998) of MSI markers (BAT 25, BAT 26, BAT 40, D8S255, D5S346, D2S123 and D17S250) and IHC for MMR proteins. Fourteen tumours were classified as MSI-high and ten as MSS. These samples were used as a validation set to validate the utility of HRM assay as a screening tool for MSI status characterisation. DNA quality assessment of these samples was done in our laboratory as described below and one sample deemed to have low quality DNA and was omitted from analysis.

2.1.2.3 **Holland series**

Tumour DNA materials in this series were obtained from patients with advance primary CRC recruited to the CAIRO2 trial (CKTO 2005-02) and conducted by the Dutch Colorectal Cancer Group (DCCG) (Tol et al., 2009b). Genomic DNA were isolated from FFPE tumour samples and previously fingerprinted for the 7 most common mutation variants in Kras exon 2 (codon 12/13) using a real-time PCR-based assay (DXS; Manchester, UK) in a comparative analysis with direct Sanger sequencing by the DCCG (Tol et al., 2010). A total of 501 anonymised tumour DNA samples were available for use in this study. DNA quality assessment of these samples was done in our laboratory as described below and 26 samples deemed to have low quality DNA and were omitted from further analysis. These samples were primarily used to run a comparative analysis of Kras exon 2 mutation screening data, which were generated by QMC-PCR/HRM protocol, between the recently introduced high throughput HRM platform (AB 7500 fast PCR machine) and the DXS assay (data of DXS assay were originally generated by the DCCG). Subsequently, these tumours were screened for mutations in Kras (exons 3 and 4),

TP53 (exons 5-8), PIK3CA (exons 1, 9 and 20) and Braf (exons 11 and 15). Kras and Braf mutation screening of 236 samples have been done by Dr. Salih Ibrahem (Ibrahem, 2012).

2.1.2.4 VICTOR series

The VICTOR trial was a phase III randomised, placebo-controlled double-blind trial of rofecoxib (VIOXX®) in patients with stage II or III colorectal cancer who had undergone potentially curative surgery and completion of adjuvant therapy (if it was given). The trial was terminated prematurely in 2004 but up to that point it had recruited 2434 patients from 151 hospitals in the UK. The rofecoxib treated population comprised 1167 patients and there were 1160 placebo control patients. The trial showed no survival benefit of rofecoxib in the overall population and a lack of prognostic or predictive significance of COX-2 expression (Midgley et al., 2010). This series was used to study MMR, and TP53 proteins expressions by IHC in CRC.

2.2 Methods

2.2.1 DNA isolation procedures

2.2.1.1 Cell lines

CRC cell lines were cultured and maintained in the pathology research group laboratory by our laboratory manager Mr. Darryl Jackson and as previously described (Seth et al., 2009a, Seth et al., 2009b). Preparation of cell pellets was performed under his direct supervision. Cell lines cultured in T75 flask (Costar®, Corning, USA) were washed twice with Dulbecco's Phosphate Buffered Saline (DPBS) (Gibco® Invitrogen Cell Culture, Paisley, UK) after aspiration of culture medium to remove any debris and residual medium. Then they were trypsinised for 5 minutes at 37°C with 2.5ml of 1X Trypsin-EDTA (Ethylene Diamine Tetra Acetic acid) (Sigma, Cat# T4174) to detach the cells. Inactivation of trypsin was

done by addition of 10 ml DMEM/10% FBS. Cell suspension was then transferred to 20ml tube and centrifuged at 1000rpm for 5min. Supernatant was discarded, and the cells were re-suspended again in 10 ml DPBS then centrifuged again for 5min at 1000rpm and the supernatant was discarded. From this end, the subsequent extraction steps were done using a commercially available kit (QIAamp® DNA Mini Kit, Catalogue No. 51304, QIAGEN, GmbH) according to the manufacturer's recommendation. Briefly, the remaining cell pellet was reconstituted with 200µl DPBS and mixed by gentle vortexing and the whole suspension was then transferred into a 1.5ml Eppendorf tube which has already loaded with 20µl QIAGEN proteinase K (20mg/ml; >600mAU/ml). Then 200µl of AL lysis buffer was added and the whole mixture mixed by pulse-vortexing for 15seconds. It is important to increase the volume of AL buffer and proteinase K proportionally if the sample volume is larger than 200µl to ensure optimal salt and PH conditions in the lysate for efficient lysis and binding to the membrane. Suboptimal conditions may affect proteinase K activity and also retain protein and other contaminants adsorbed to the membrane which may inhibit PCR and other downstream procedures. The suspension was incubated at 56°C for 10min. (Proteinase K is particularly suitable for short digestion times and its specific activity remains stable over a wide range of temperatures and PH values which substantially increases at higher temperature). The tubes were briefly centrifuged to remove drops from the inside of the lid and 200µl of absolute ethanol was added to the suspension and mixed again by pulse-vortexing for 15seconds and followed by centrifugation to remove drop from the inside of the lid. Again, it is important to adjust the volume of ethanol proportionally to the sample volume. The whole lysate was then transferred and applied to the QIAamp Mini spin column (in 2ml collection tube) without wetting the rim. This was followed by spinning of the column for 1min at 8000rpm and the filtrate with the collecting tube was discarded and the column placed into a new collecting tube. At this stage if the lysate has not pass completely through the membrane, centrifugation at higher speed and for longer duration is

necessary until the spin column is empty. Then 500µl of washing buffer AW1 was added and the tube was centrifuged for 1min at 8000rpm. Sometimes centrifugation at higher speed and for longer duration may be required to completely dry the membrane. After discarding the collecting tube and replacing the column into new tube, 500µl of washing buffer AW2 was applied to it and spun at full speed (13000rpm) for 3min. This final spinning round can be repeated using new collection tube once more to completely dry the membrane and prevent AW2 carry-over. Then the spin column was placed into 1.5ml Eppendorf tube and 200µl of the elution buffer AE (or water) were added to the middle of the membrane and incubated for 1min at room temperature followed by centrifugation at 8000rpm for 1min. However, it has been found that incubating the spin column with the elution buffer for 5min would generally increase the DNA yield. In general, it is preferable to elute using AE buffer and storage at -20°C if the sample will be stored for long period. Elution with water is also possible if the sample is to be used immediately or to be stored for short period, but it is important to ensure that its PH is at least 7.0 to avoid degradation of DNA by acidic hydrolysis.

2.2.1.2 Clinical samples

Genomic DNA was extracted from CRC FFPE tissues using a commercially available kit (QIAamp® DNA FFPE Tissue Kit Catalogue No. 56404, QIAGEN, GmbH) with slight modifications. This procedure started with freshly cut full face sections (3-6x10µm) of FFPE tissue with immediate transfer to 1.5ml Eppendorf tube. The amount of the starting tissue was dependent on the surface area of the embedded tissue; with larger tissue (resection samples) 3x10µm sections were enough, while smaller tissues (biopsy samples) required up to 6x10µm sections to ensure enough DNA yield. To de-wax the tissue, 1ml of xylene was added and vortexed vigorously for 10seconds. Then the tubes were centrifuged at full speed (13000rpm) for 5 minutes. Supernatant was then removed by pipetting without

removing any tissue. Depending on the amount of wax, the xylene step was repeated at certain occasions until the supernatant was clear. Then to remove the xylene, 1ml of absolute ethanol was added and mixed by vortexing for 10seconds and then spun at full speed for 2minutes. The supernatant was aspirated by careful pipetting without removing any tissue. Then the tubes were left open at room temperature or at 37ºC until all residual ethanol was evaporated. Next 180µl of lysis buffer ATL and 20µl of QIAGEN proteinase K were added to the pellet and mixed by vortexing. It is important to adjust the volume of ATL to the sample volume to maintain optimal lysis condition. The tubes were then sealed with Para-film and placed into the incubator at 56ºC for 2 hours with continuous agitation. Qiagen recommended 1-hour incubation at 56ºC; however, this was not enough to completely digest the tissue, especially with fibrous tumours. Undigested tissues caused clogging to the membrane and eventually reduced the DNA yield. Therefore, we decided to modify this step by performing a second digestion. After the initial 2 hours digestion, the tubes were taken off the incubator and vortexed briefly to remove the drops from the inside of the lid and another 20µl of proteinase K was added to each tube. The tubes were then sealed and briefly vortexed and placed back into the incubator for overnight digestion at 56ºC with continuous agitation. This additional step of digestion gave almost complete digestion as indicated by homogenous suspension without clots. After the incubation step, the tubes were placed onto heating block (preheated to 90ºC) for 60min to reverse formaldehyde modification of the DNA. However, it was reported that even with heating it is not possible to completely reverse this modification (cross-linking) completely and there is length limit on amplification products from DNA isolated from FFPE tissue in the range of 450 to 650 bp (Wright and Manos, 1990). The samples were then allowed to cool to room temperature before proceeding to the subsequent steps. Next, the tubes were briefly spun to remove the drops from the inside of the lid and 400µl of a premixed AL lysis buffer and absolute ethanol (1:1 ratio) was applied and mixed thoroughly by vortexing for 15 seconds followed by

brief spinning to remove drops from the inside of the lid. The whole lysate was then transferred to the MinElute spin column (in a 2ml collection tube) and centrifuged for 1min at 8000rpm. After discarding of the collection tubes containing the flow-through, the columns were replaced into new collection tubes. The two washing steps were followed as described in the previous section (2.2.1.1 above). Finally, the spin column were placed into a clean Eppendorf tube and 50µl of elution buffer ATE were applied to the centre of the membrane and incubated at room temperature for 5 minutes then centrifuged at 8000rpm for 1 minutes. A second elution round with 20µl ATE buffer was usually performed using a new collection tube because it was found that it enhanced the purity of the yield (as indicated by the spectrophotometer) with subsequent better performance at PCR experiments.

2.2.2 DNA quality assessment

2.2.2.1 Measurement of DNA concentration and purity

The extracted genomic DNA yields were measured spectrophotometrically using NanoDrop ND-1000 UV-Vis Spectrophotometer (LabTech International Ltd, Ringmer, UK) to determine concentration and Purity of DNA. The concentration of DNA in the eluate was measured by absorbance at 260 nm. Purity was determined by calculating the ratio of absorbance at 260 nm (DNA) to absorbance at 280 nm (protein). However, scanning absorbance from 220–320 nm would show if there were other factors affecting absorbance at 260 nm. In general, pure DNA absorbance readings at 260 nm should lie between 0.1 and 1.0 to be accurate, and the A260/A280 ratio between 1.7-1.9 (Wright and Manos, 1990). It was also important to use the same elution buffer to calibrate the spectrophotometer. High quality genomic DNA was successfully extracted from most of samples used in this study as shown in Figure 2-3.

However, few FFPE samples showed unacceptable results that was mostly

indicated by low purity. In these cases, a second elution round was performed using 20µl of elution buffer ATE and re-assessed by Nanodrop. The re-elution process successfully enhanced the purity of the yield but resulted in relative reduction of the overall concentration. The second round of elution helped to reduce the amount of contaminants that could cause PCR inhibition. DNA materials were diluted to 20ng/µl with PCR grade water as working concentration and stored at 4ºC, while the rest of DNA yields were stocked in the freezer at -20ºC.

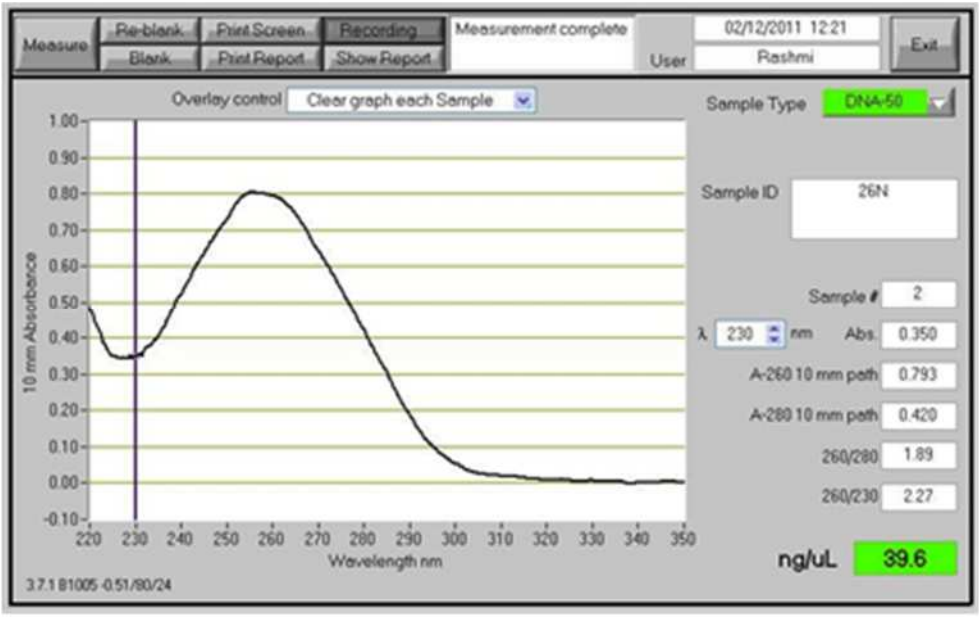

Figure 2-3 Measurement of DNA quantity and purity by Nanodrop.

DNA materials isolated from FFPE sample showed an A260/A280 absorption ratio of 1.89 indicating pure DNA with a concentration of 39.6 ng/µl.

2.2.2.2 **DNA integrity assessment**

Assessing DNA integrity was basically performed using a multiplex-based PCR assay. Two approaches were adopted to visualise the performance of multiplex PCR; first, by HRM analysis where a DNA staining dye was added to the multiplex reaction. The products melting curves were used to qualitatively assess the length by analysing the number of melting peaks on the derivative plot, the number of melting peaks corresponded the number of amplified target amplicons. The second

approach to assess the length of intact DNA molecule was by separation of PCR products electrophoretically on agarose gel and visulising them under ultraviolet trans- illuminator. While the HRM method was the primary method used in every DNA quality multiplex PCR reaction because of its simplicity (close tube method without post-PCR processing) and cost effectiveness, separation on agarose gel was used to validate the HRM results.

The DNA quality assessment multiplex PCR was basically a modification to the method previously developed by Van Beers et al to test DNA quality for array Comparative Genomic Hybridisation assay (aCGH) (van Beers et al., 2006). This assay consisted of four primer pairs amplifying across the reference gene Glyceraldehyde 3 Phosphate Dehydrogenase (GAPDH) in a single multiplex PCR to give products of 100, 200, 300 and 400 bp (GAPDH primer details are shown in Table 2-1). The initial optimisation of multiplex PCR was performed over a range of annealing temperature using Primus96 advanced® Gradient Thermal Cycler (PeQLab Biotechnology, UK) as follows: (95°C/5min) X1; [(95°C/30sec) / (62±8°C/1min) / (72°C/1min)] X45; (72ºC/10min) X1. The multiplex PCR reaction consisted of 5µl (microliter) of 2X HotShot^{TM} master mix (Cadama Medical Ltd, UK), 1µl of 10X LC Green®$^{PLUS+}$ (Idaho Technology, USA) as a DNA binding dye, 0.4µl of each primer at 6.25µM (MicroMolar) to give final concentration of 250nM (nanomolar/tube) and 1µl (20 nanogram/µl) template DNA all made up to a final volume of 10µl with PCR grade water (Nuclease Free Water, Cat. No. 129115, QIAGEN, GmbH). Each reaction tube was overlaid with 10µl molecular grade mineral oil (Mineral oil, Cat No. M5904-500ML, Sigma-Aldrich, USA).

Although LC Green has been proved not to inhibit the PCR in a concentration-dependent manner, the idea beyond the addition of LC Green dye to the PCR premixes is that the addition of LC Green has been confirmed to increase double stranded DNA melting temperature (Tm) by about 1 – 3 °C due to its effect on the

stability of DNA duplexes, which may require adjustment of cycling parameters if the optimisation was performed without LC Green. (Ririe et al., 1997, Giglio et al., 2003). While, the addition of the mineral oil to the reaction was performed to assure consistent amplification across the reaction tubes because the oil works as a barrier which prevents evaporation during thermal cycling and hence maintains consistent salt concentration, which is essential for efficient PCR.

Then, the multiplex PCR products (10µl) were mixed with 2µl of the 6x loading buffer (0.25% bromophenol blue 0.25% xylene and cyanol FF 40% (w/v) sucrose in water). Then the mixture were loaded into a freshly prepared 2% Agarose gel (1.6 gram of Agarose powder [Gibco-BR Life Technologies, USA], 80ml of 1% Tris Borate EDTA (TBE) buffer [Sigma, USA], and 8µl of 10,000X Sybrsafe dye [Invitrogen, USA]). The agarose gel preloaded with the samples were then immersed into 1X TBE solution and subjected to an electric current at 90 volts and left to run for 60min. Visualization of the PCR products was done using an ultraviolet (UV) light system (UVP Inc., USA). DNA size was estimated by concomitant separation of low molecular DNA marker (HyperLadder™ IV, Bioline). The optimal annealing temperature was determined by analysing the specificity (positional alignment of the bands in comparison to the DNA ladder)

Table 2-1 GAPDH primers sequences

L is left primer (forward), R is right primer (reverse).

Gene	Product length (bp)	Sequences
GAPDH, NG_007073.2	100	L GTTCCAATATGATTCCACCC R CTCCTGGAAGATGGTGATGG
	200	L AGGTGGAGCGAGGCTAGC R TTTTGCGGTGGAAATGTCCT
	300	L AGGTGAGACATTCTTGCTGG R TCCACTAACCAGTCAGCGTC
	400	L ACAGTCCATGCCATCACTGC R GCTTGACAAAGTGGTCGTTG

and thickness of the PCR bands, which is reflective of the reaction efficiency and products amount. The optimal annealing temperature was 62°C because it showed the brightest (thickest) bands at the predicted positions and therefore selected as the optimal temperature at the annealing hold for the multiplex DNA quality PCR (Figure 2-4).

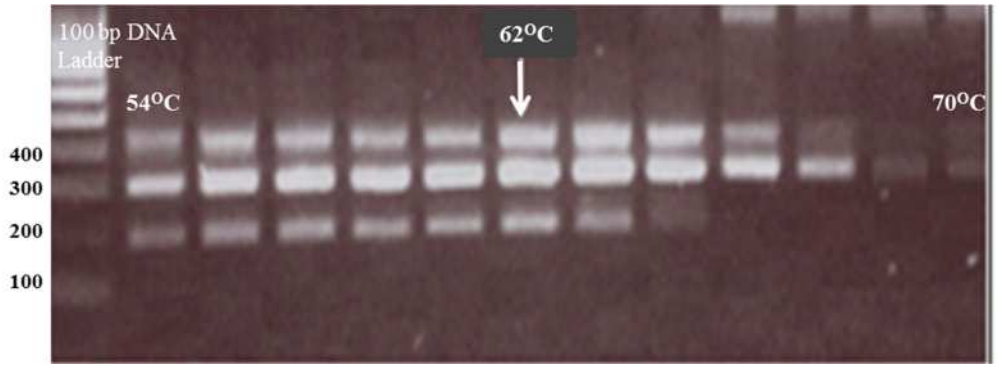

Figure 2-4 Optimisation of the multiplex PCR using a series of annealing temperatures.

Gel electrophoresis of the DNA quality multiplex PCR optimisation, 62°C was the highest annealing temperature which gave specific and most intense bands. Multiple bands can be seen (100, 200, 300, 400bp), which represent the intended amplified multiplexed PCR products and correlate to the integrity of the template DNA

Following the achievement of optimisation, the routine performance of the quality assessment assay was to transfer the PCR products first to Roche Light Cycler® capillaries (20µl) (Roche Applied Science, UK) and melt them on the HR-1 thermo-optical analyser (Idaho technology Inc, USA) as per the manufacturer's instructions (detailed description of HRM analysis is presented in the subsequent section). Then the same PCR products were resolved on a 2% agarose gel (w/v) and visualised under UV light in order to confirm the HRM results (Figure 2-5). The optimised protocol was applied for quality testing of DNA materials isolated from various sources (cell lines and FFPE samples).

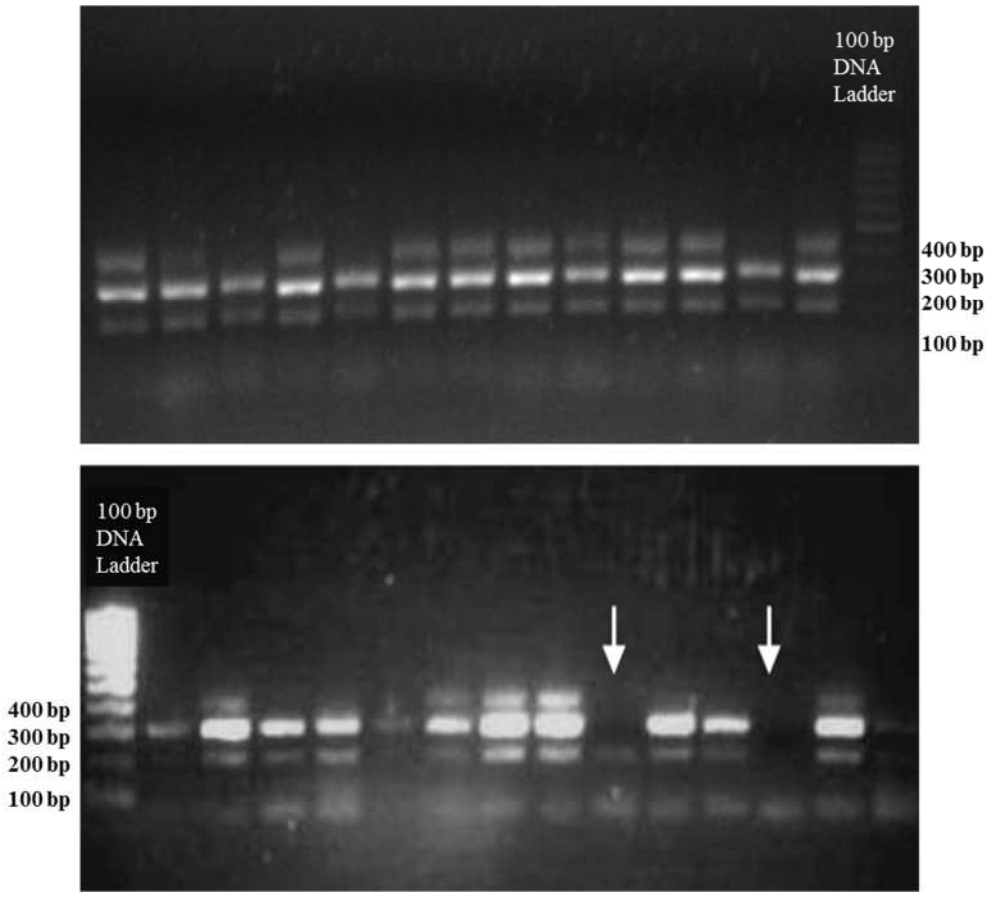

Figure 2-5 DNA quality assessment of FFPE samples using multiplex PCR.

Gel electrophoresis of the DNA quality multiplex PCR. Good quality FFPE samples tested using the optimised protocol produced bands of 100, 200, 300, 400bp (Top). Samples with variable quality produced variable number of bands, while bad quality samples (arrowed) produced single band of 100bp (Bottom).

Basically, our interpretation was to deem samples that showed at least the 200bp band as good quality samples and suitable for downstream PCR procedures. While those samples which failed to show any amplification were considered unsuitable and were omitted from any further analysis because the minimum amplicon length to be detected in our PCR assays was in the range of 100 - 240bp.

2.2.3 Mutation screening protocols

High quality DNA from some CRC cell lines was used initially for the development and optimisation of the PCR/HRM protocols. Then, the genetic fingerprinting of 29 CRC cell lines (section 2.1.1), with regard to mutations in KRAS, BRAF,

PIK3CA, TP53, FBXW7, and PTEN, were performed to confirm their genetic identity for the purpose of protocol validation. Cell lines were tested directly by a standard single-step PCR/HRM approach and validated by the two-step nested protocol and confirmed by Sanger direct sequencing. Thermal cycling was performed on a Primus96 advanced® Gradient Thermal Cycler (PeQLab Biotechnology). HRM analysis for cell line mutation screening was performed using the HR1 high resolution melting instrument (Idaho technology Inc, USA) as per the manufacturer's instructions.

The optimised PCR/HRM protocol was then used to screen the clinical samples in Nottingham series set-1 &2 (2.1.2.1) for mutations in KRAS, BRAF, PIK3CA, TP53, FBXW7, and PTEN, and in Holland series for KRAS, BRAF, PIK3CA, and TP53 (full description of this series can be found in sections 2.1.2.3 and HRM protocol details in section 2.2.3.3.10). Screening of samples in the Holland series (KRAS and BRAf only) was performed in our laboratory in collaboration with Dr. Ibrahem (Ibrahem, 2012). Mutation screening of DNA materials obtained from the archived clinical samples required an extended two-step nested protocol, as it is generally agreed that the integrity of DNA molecules are usually compromised by formalin fixation which subsequently may affect the success of any down-stream procedure (van Beers et al., 2005, Wessels et al., 2002).

We published details of the two-step nested protocol (section 2.2.3.3.3), which we called Quick-Multiplex-Consensus (QMC)-PCR (Fadhil et al., 2010). It was a nested protocol consisting of an initial Pre-Diagnostic Multiplex (PDM) reaction in which up to 10 outer primers pairs (for 10 different mutation hotspots) could be used in a single reaction. This was followed by a Single Specific Diagnostic (SSD) PCR in which a single pair of inner (nested) primers (for each of the hotspots) was used with diluted multiplexed PCR products from the PDM reaction as a template. PCR amplification for DNA materials from Nottingham series (2.1.2.1) was done

using the Primus96 advanced® Gradient Thermal Cycler (PeQLab Biotechnology) and followed by HRM SSD mutation screening of the diluted PDM PCR products using the HR1 high resolution melting instrument (Idaho technology Inc, USA) as per the manufacturer's instructions. While for the Holland samples (2.1.2.3), mutation screening using the QMC-PCR/ HRM protocol1 (2.2.3.3.10.4) was amplification was performed on the Applied Biosystems® 7500 fast Real-Time PCR System and HRM analysis was done using the Applied Biosystems High Resolution Melting software v2.0. For development purposes, 100 randomly selected cases from this series were re-tested using QMC-PCR/HRM protocol2 (2.2.3.3.10.5) on Applied Biosystems® 7500 fast Real-Time PCR System

2.2.3.1 Targets selection and primers design

2.2.3.1.1 Selection of target PCR templates

Primers amplifying across genomic areas encode for mutational hotspots in KRAS, BRAF (Ibrahem, 2012), PIK3CA, FBXW7, and PTEN were designed in house. With respect to TP53, primers previously designed in our laboratory were used (Seth et al., 2009a), apart from exon 5 primers which were redesigned into a single pair to reduce the costs and efforts of high-throughput mutation screening of CRC FFPE samples from series 2.1.2.3. So, one set of outer primers were designed for each target to screen CRC cell lines directly (standard protocol) and also to be used for multiplexing the FFPE product samples at PDM-PCR step. While for the nested SSD protocol that was used to specifically screen each individual target in the FFPE samples, an additional set of nested (inner) primers were designed.

Primarily, a basic review of the published scientific literatures, focused on mutations in sporadic CRC, was implemented in order to identify the genomic areas that showed frequent DNA sequence alterations in the candidate CRC genes, which are listed in section 2.2.3. Supplementary information about the frequency and

distribution of the somatic mutations in CRC was collected from the Wellcome Trust Sanger Institute Catalogue of Somatic Mutations in Cancer (COSMIC) database, which is designed to supply information on publications, samples and mutations relating to human cancers (Bamford et al., 2004, Forbes et al., 2008, Forbes et al., 2011). An example of mutation data collected from the COSMIC database is displayed in Figure 2-6.

Selecting suitable primers is perhaps the single most vital factor determining the specificity of the polymerase chain reaction (PCR). Precise amplification of the target DNA sequence necessitates that primers must only amplify the intended targets and does not result in non-specific amplifications. The procedure that was followed to design specific primers in this study included two stages. Initially, details of human genomic DNA reference sequences of the target genes, which were used as PCR template, were retrieved from the database of National Center for Biotechnology Information (NCBI), namely the RefSeqGene database. The RefSeqGene records have been created as a subset of NCBI's Reference Sequence (RefSeq) project. RefSeq database is a taxonomically diverse database (more than 12000 organisms as of RefSeq-release47) which incorporates a comprehensive set of separated non-redundant highly curated sequence data (genomic, transcript and protein sequence) but explicitly cross-linked nucleic acid and protein records with bibliographic information (Pruitt et al., 2002).

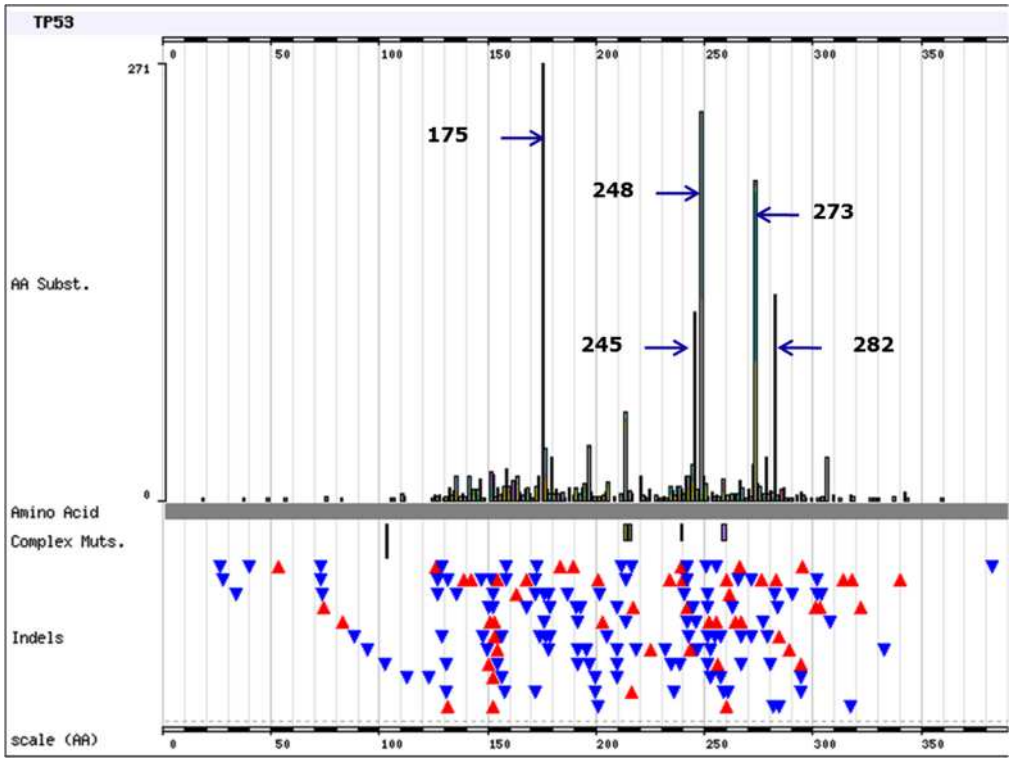

Figure 2-6 TP53 somatic mutation in CRC obtained from COSMIC database.

Histogram illustrating the frequency and distribution of TP53 somatic mutation in CRC. These data were collected from the cosmic database. Total of 10192 samples were tested for TP53 and entered to the database. 44% were mutants and 21% of the mutations were clustered in 5 mutational hotspots (arrowed). Blue arrow heads indicate short insertions; red arrow heads indicate short deletions.

The RefSeqGene project is part of the Locus Reference Genomic (LRG) project and it is used to provide more coordinated and stable genomic sequence features for individual genes as reference standards. The rationale behind using RefSeqGene database is that it provides explicit coordinates for non-coding and flanking genomic sequences in addition to the unique numbering system for exons and introns, transcripts and proteins (Dalgleish et al., 2010).

2.2.3.1.2 **Primers design**

Subsequently, after defining the regions of interest from the first step as described in the previous section 2.2.3.1.1, they were used as target PCR templates to run primer design using the publicly available web-based version of Primer3 program,

Primer3web to generate candidate primer pairs. Primer3 program search returns information about the primer size, flanking position, orientation, distance between primers, amplicon size, and virtual thermodynamic features of the primer and amplicon. It is fairly flexible tool which allows manual setting of many essential parameters; such as inclusion or exclusion of certain bases, overlapping certain positions, defining the thermodynamic properties to predict propensity of the primer oligos to form dimers and hair-pins and the tendency of the primer to anneal to undesired sites, and also to determine the primer Gs and Cs content and GC clamps (consecutive GC) location with respect to primer 3´ end (Koressaar and Remm, 2007, Untergasser et al.). However, because it does not perform target analysis against nucleotide sequence databases to examine potential targets, it was not possible to use this tool by its own to check primer specificity stringency to potential targets with certain number of mismatches. In addition, because Primer3 program does not provide information about the number and positions of mismatched bases between primers and targets, it became difficult to interrogate single nucleotide polymorphisms (SNP) in the critical primer binding sites which may significantly compromise PCR efficiency.

In order to determine the specificity of the candidate primer pairs to the intended PCR template (specificity check), each primer pairs was tested using the UCSC In-Silico PCR web-tool (Hinrichs et al., 2006). It performs a very fast alignment analysis to pick up potential targets to the input (query) primer pairs (the primer only case based search) because it is based on the Blast-Like Alignment Tool (BLAT, which is 500 times faster than other mRNA/DNA alignments tools). BLAT uses a linear alignment against a pre-processed indexed database to detect perfect match between primers and DNA template in the up to date genome assembly (Kent, 2002). In-Silico PCR also delivers theoretical thermodynamic PCR statistics based on simulation procedures using the same code of Primer3 program (Hinrichs et al., 2006). Although it is considered a quick primer designing tool in comparison

to other publicly available tools, it is not sensitive enough to pick up some amplifiable targets with minimum mismatches to primer because its indexed nature makes this job limited by the availability of database. So it may miss significant numbers of targets that have minimum mismatches to primers where they are still amplifiable. In addition, it requires going through many candidate primer pairs manually, which makes primer design a time consuming process (Untergasser et al., 2012).

The ultimate validation of the primer oligos obtained from Primer3web and In-Silico PCR tools was done by subjecting them to batch testing by means of the primer designing tool (NCBI/Primer-BLAST) to score similarity of the query input sequence (primer and target) against large nucleotide sequence databases (Untergasser et al., 2012). It is an integrated tool which basically incorporates two modules to design new primers for the submitted PCR template "template only case" and to check specificity of pre-designed primers "primer only case" in one go Ref. Primer design module is based on Primer3 program, while specificity check module is based on implementing the Needleman-Wunsch (NW) global alignment algorithms (Needleman and Wunsch, 1970) and the NCBI BLAST tool (Altschul et al., 1990) to look for matches between the primers and targets. The flexibility of NCBI/Primer-Blast allows allocating primers to specific regions or between specified bases because it is implemented with the NCBI C++ toolkit and the Primer3 C programming interface. In addition, NCBI/Primer-BLAST has the ability to detect areas on unintended template which have nearly exact matches to the intended PCR template by aid of Mega-Blast engine which is 10 time faster than the standard nucleotide BLAST (Zhang et al., 2000), to enable positioning one primer outside this region to ensure high specificity. Likewise, it is considered a highly sensitive tool because the stringent specificity testing modules ensure that a product with up to 35% sequence similarity to the intended PCR template can be detected. Finally, NCBI/Primer BLAT can also test each primer for possibility of

generating amplicons by its own. Therefore, all PCR primers combinations (forward-reverse primer pair, forward-forward as well as reverse-reverse pairs) were tested using NCBI/Primer-BLAST to ensure that no interactions between and within primers in the multiplex reaction would happen and to avoid primer pairs that can cause non-specific amplifications, hence only non-cross-reacting primers were designated (Ye, Coulouris et al. 2012).

2.2.3.1.3 SNP check

Each target gene was explored for short genetic variations (SNVs) mapped to and flanking the target genomic region using the NCBI Sequence Viewer section from the full RefSeqGene report of individual gene. This section represents a customisable integrative graphical display of nucleotide and protein sequences with explicit navigation features and extensive built-in cross links to other NCBI resources; such as NCBI's dpSNP database (Brown et al., 2006). This tool was used to generate summary of the target sequences with respect to exon/intron numbering, coding /Upstream/downstream flanking sequences, transcript isoforms, and genetic variation contained within a specified genomic sequence (Figure 2-7).

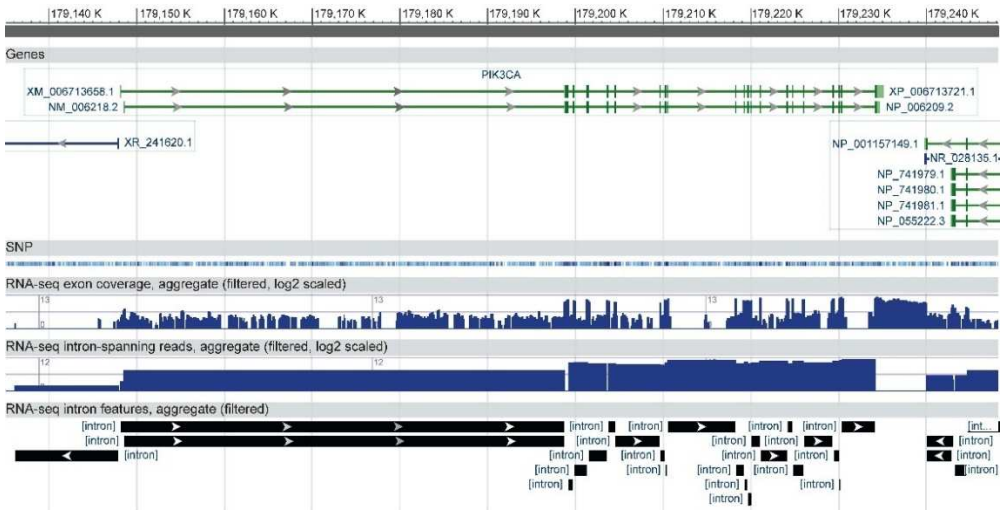

Figure 2-7 NCBI's Sequence Viewer.

A snapshot extracted from RefSeqGene full report displaying the Sequence Viewer summary of genome, transcript, and protein information of PIK3CA gene.

Single nucleotide polymorphisms (SNPs) are the most common variations in the

human sequence, with occurrence frequency distribution of one SNP every 500-1000 bases. Some of SNPs are common and represent true polymorphisms, while others are rare and may represent true somatic events and have disease association (Sherry et al., 1999, Kitts. A and Sherry. S, 2002). Common single nucleotide variations represent an important source of base pairing mismatches at the primer binding site which may adversely affect PCR efficiency. Although, there is no general agreement about the exact effect of mismatches on PCR amplification when these mismatches are located in the middle or toward the 5' end, the consensus is that mismatches in the 3' end are detrimental and two of them in this area generally prevent amplification (Ayyadevara et al., 2000, Waterfall et al., 2002, Sipos et al., 2007, Wu et al., 2009, Ghedira et al., 2009). In addition, the presence of a single base mismatch anywhere along the PCR product will change the stability and melting behavior of DNA duplex and eventually affects HRM analysis. So, the presence of a heterozygote SNP among otherwise perfectly matched bases represents a source of false positive results to the HRM assay if is designed to scan for unknown mutations because this SNP will generate heteroduplexes which melt aberrantly. Therefore, all candidate PCR primer pairs were submitted for diagnostic SNP batch checks to identify and locate SNPs in the target PCR amplicon (between and include the primer pair) to minimise the chance of having common polymorphisms included at the final designed sequences. The diagnostic SNP check was done using the free online SNPCheck bioinformatic program which searches for SNPs in the predicted PCR template using the updated build of the human genome. Each submitted oligonucleotide sequence will subjected to sequence alignment against the human reference genome using standard Local alignment NCBI's BLAST search tool. Once the primers binding sites have been identified, a search will then follow to identify and locate any known SNPs in and between primer binding sites using the contents of the current release of NCBI's dbSNP database. The output of diagnostic SNP search is presented as an annotated table listing the detected SNPs and as diagram displaying the position of SNPs

along the whole amplicon length (in and between primer binding sites) with annotation and cross-linking to the source (dbSNP database) as shown in Figure 2-8 (National Genetics Reference Laboratory Manchester, 2005).

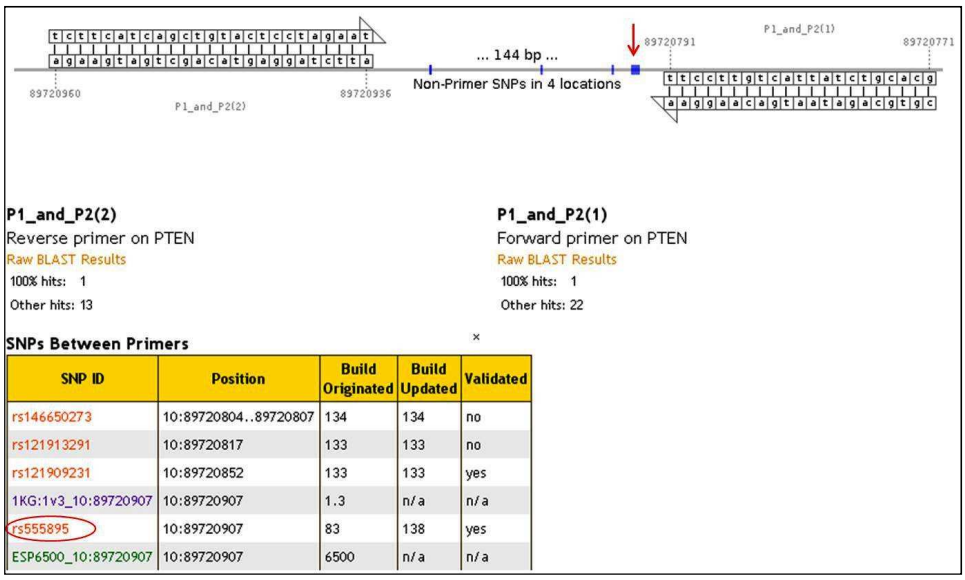

SNP ID	Position	Build Originated	Build Updated	Validated
rs146650273	10:89720804..89720807	134	134	no
rs121913291	10:89720817	133	133	no
rs121909231	10:89720852	133	133	yes
1KG:1v3_10:89720907	10:89720907	1.3	n/a	n/a
rs555895	10:89720907	83	138	yes
ESP6500_10:89720907	10:89720907	6500	n/a	n/a

Figure 2-8 Primer diagnostic SNP check.

A snapshot of results of SNP check generated by SNP Check program. The top diagram overviewing the locations of SNPs along the entire predicted amplicon for PTEN exon8 primer pair. No SNP detected at the primer binging site. Four SNPs detected between primers, however only one SNP rs555895 (red arrow) has genotype (G/T) and population data with minor allele frequency of 0.386 in the European population. The tabular display (bottom) lists the SNPs between primers, with SNP rs555895 shown inside red circle.

Details of single nucleotide polymorphisms were collected from the NCBI/dpSNP database for short genetic variations. This Entrez database provides flexible options to search variations in multiple categories. In addition, the fully integrated and extensively linked Entrez databases at NCBI allow access to SNP data from other NCBI databases if such data are available. The dbSNP Entrez provides a comprehensive report, presented as integrated graphical and tabulated displays, detailing the specific location within a molecular Sequence (nucleotide and protein sequences), variation type, summary of allele, protein coding changes, and the clinical association when available (Figure 2-9). It also provides genotypes and allele frequencies information for various populations, genotyping assay method,

and validation history of the submitted SNP (Kitts. A and Sherry. S, 2002). In this study each SNP detected by SNPCheck program or extracted from the sequence Viewer were looked up for genotype details, allele frequencies reports for European populations, and validation history. Basically, SNPs with relatively high minor allele frequencies in the European population were highlighted, and only those genomic sequences which do not contain such SNPs were selected.

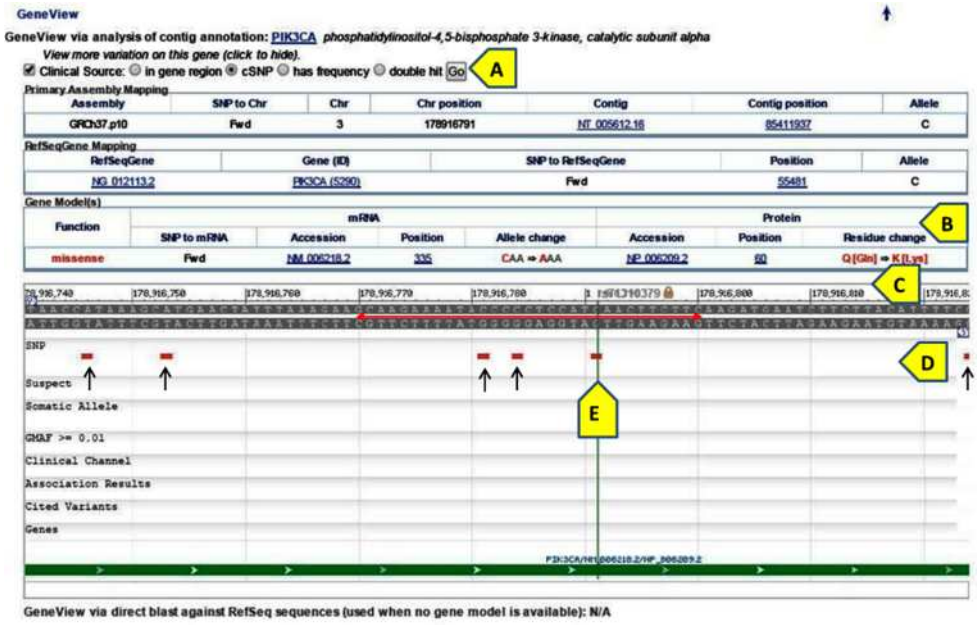

Figure 2-9 PIK3CA GeneView analysis of contig annotation.

GeneView is a separate display built-in the reference SNP (rfSNP) cluster report to highlight gene-centric listing. This section contains the following details: In the SNP: GeneView (A), listing the variations mapped to the gene. Summary table of the SNP location and the protein coding changes (B). Sequence Viewer displays the variation on the genome assembly (C). GeneVeiw displays the query SNP and its contig variations. For example ; in this snapshot the neighbouring SNPs (arrowed) of rs71310379 variation (E) are shown in (D).

2.2.3.1.4 In-Silico analysis of primers' thermodynamic properties

In-silico analysis was used to examine the primers' physical characteristics which can affect their performance and alter the efficiency of the PCR assay. These properties were tested by the web bioinformatics Oligo Analyzer (version 3.1) program provided in the Integrated DNA Technologies (IDT) SciTools server, which implements the up-to-date, most precise thermodynamic algorithms and models for Comprehensive oligonucleotide analysis (Owczarzy et al., 2008). This

tool allows predicting the physical properties of the primer oligo such as its length, complementary sequence, GC content, molecular weight, and the extinction coefficient at 260nm. It also estimates oligonucleotide's melting temperature when it hybridises to its complementary sequence using the nearest-neighbor two-state model, which is applicable to short DNA duplexes.

In addition, Oligo-Analyzer implements mFold algorithm (Zuker, 2003) for predicting hairpin secondary structures in uni-molecular interactions (fig). The other function that Oligo Analyzer can execute is the prediction of duplex formation in bi-molecular interactions when primer anneals to itself (homo-dimer) or to another oligonucleotide (hetero-dimer) in the reaction. The assessment of thermodynamic stability of hairpin structures and the potential for oligos to participate in off-target interactions is essential for PCR assay because they can compromise the efficiency of the reaction and produce non-specific products. The Scitools analyzer uses two widely applied thermodynamic parameters to qualitatively evaluate the thermodynamic propensity for the hairpin structure or primer-dimer formations and the potential of primer oligos to participate in off-target hybridisation under specified experimental conditions. These parameters are the delta G (ΔG) and melting temperature (Tm). Delta G (ΔG) is the change in Gibbs free energy (kcal/mole) and it is temperature dependent. It represents the temperature range (degrees Celsius) required for the transition of an oligo population from a 100% duplexed or structured state to a 100% random coil state. In the PCR reaction ΔG reflects the temperature functional effectiveness as a narrower transition rate (small temperature range) means few degrees higher will dramatically dissociate duplexed structure and nothing will bind, whereas few degrees lower and off-target hybridisation happens.

In general, a positive ΔG value indicates a nonspontaneous reaction to produce single stranded oligos (non-stable), while negative value indicates a spontaneous

reaction to produce duplexes or secondary structures (stable double stranded structures). In-silico analysis results of the candidate primers from this study confirmed that these primers perform within the acceptable limited as defined by IDT SciTools (tables). The results showed that the melting temperature difference (ΔTm) between oligos of each pair is within the defined limits of less than 5°C (ΔTm°C mean ± SD; 1.99°C ± 1.33°C: ΔTm°C range; 0°C - 4.5°C).

2.2.3.1.5 Prediction of amplicon melting profile

It has been recommended to avoid primer pair which give PCR amplicon longer than 400bp for three reasons. First, archival DNA samples are usually compromised by fixation and there is length limit on amplification products from DNA isolated from FFPE tissue in the range of 450 to 650 bp (Wright and Manos, 1990). Second, the chance of having single nucleotide polymorphism (SNP) inclusion is higher with longer sequences, and finally, long amplicons usually produce multiple melting domains in the HRM (Liew et al., 2004).

Therefore, primers that produce shorter amplicons (>100-< 200bp) were chosen. In order uMelt SM is a web-based application created to predict fluorescent high-resolution DNA melting curves of PCR products, each amplicon was analysed using the uMelt^{SM} melting curve predictions software, a freely available web-based computer application (Dwight, n.d.). Melting curve prediction analysis can also help to determine the melting profile and detect which part would have the main influence on major transition of the melting curve, and hence design primers which most suite HRM analysis. Melt curve predictions analysis, which is presented in Figure 2-10, illustrates examples of preferable (single domain) and non-preferable (multiple domains) melt curves. Multiple domain melt curve is not preferred in HRM because it can hide the actual change and make the analysis inconclusive. In addition, the second domain is usually mixed up by some interpreters as being generated by non-specific product. Details of primers pairs used for the mutation

screening protocols in CRC samples are listed in Table 2-2, and Table 2-3.

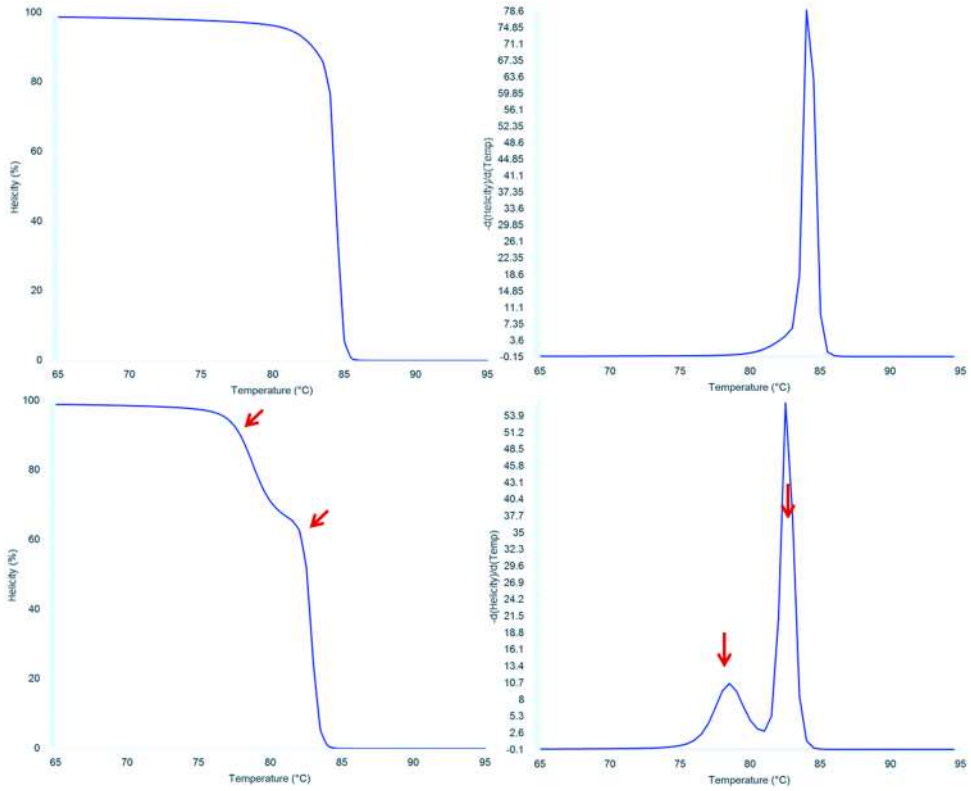

Figure 2-10 Melt curve predictions.

Melt curve predictions graphs generated using uMELT software. Top panel represents melt curve (left) and derivative plot (right) of a single transition (domain) melting. Bottom panel represents a double transitions (multiple domains) melting.

Table 2-2 The primers sequences (outer) used in the standard PCR protocol.

Gene	Ex	Primer Sequences	Tm°C	Hotspots*	size (bp)
PIK3CA** NG_012113.1	1A	F CACGACCATCATCAGGTGAA R GGAGGGGGTATTTTCTTGCT	64	38	168
	1B	F CCCCTCCATCAACTTCTTCA R TGTATCATACCAATTTCTCGATTG	64	88	194
	7	F TGGGGAAGAAAAGTGTTTTGA R ACACCAATAGGGTTCAGCAAA	64	420	201
	9	F CTGTGAATCCAGAGGGGAAA R GCACTTACCTGTGACTCCATAGAA	64	542, 545, & 546	197
	20	F TGAGCAAGAGGCTTTGGAGT R CCTATGCAATCGGTCTTTGC	68	1047	201
FBXW7 NG_029466.1	3	F CCATGTTCAGCAACACCAAC R GCAGCAATTAAGTGAGGCATT	62	224	173
	4A	F AGCTGGAGTGGACCAGAGAA R CCTCTTTAGGGAGCAATGAAA	60	278	136
	4B	F TGCAAGTGATAGAACCCCAGT R CAATTTACAGCCCTCTTTACCA	60	278, & 282	203
	7	F TGCCTTCATTTTTCTCTTCACC R CTTTGCCTGTGACTGCTGAC	64	393	196
	8	F TGGGACATACAGGTGGAGTATG R GGAAGAAGTCCCAACCATGA	64	465	202
	9A	F TTTTTCTGTTTCTCCCTCTGC R CTAACAACCCTCCTGCCATC	64	479, & 505	152
	9B	F GCAGGAGGGTTGTTAGTGGA RTGGATCAGCAATTTGACAGTG	64	545	201
	10	F GGGAATTGCATTCACACGTT R TGTCCTGTTTTGATATCCCAGA	64	582	125
KRAS NG_007524.1	2	F GCCTGCTGAAAATGACTGAA R TTGGATCATATTCGTCCACAA	62	12, & 13	114
	3	F CCAGACTGTGTTTCTCCCTTC R AAAGAAAGCCCTCCCCAGT	65	61	152
	4	F AGACACAAAACAGGCTCAGGA R CCATCTTTGCTCATCTTTTCTTT	62	146	147
BRAF NG_007873.1	11	F TGTTTGGCTTGACTTGACTTT R CTTGTCACAATGTCACCACATTACATA	62		189
	15	F ATCTACTGTTTTCCTTTACTTACTACAC R CAGCATCTCAGGGCCAA	64	600	205
TP53 NG_017013.1	5A	F CTGTCTCCTTCCTCTTCCTACAG R GCTGTGACTGCTTGTAGATGG	65	157, 158, 163, 173, 175, 176, & 179	150
	5B	F GTGCAGCTGTGGGTTGATT R AACCAGCCCTGTCGTCTCT	66		175
	6	F CCTCTGATTCCTCACTGATTGC R CTTAACCCCTCCTCCCAGAG	65	193, 196, 213, & 220	181
	7	F TTGGGCCTGTGTTATCTCCT R TGGCAAGTGGCTCCTGAC	65	234, 237, 238, 241, 242, 244, 245, 248, & 249	150
	8	F TTGCTTCTCTTTTCCTATCCTGA R GCTTCTTGTCCTGCTTGCTT	62	266, 273, 278, 280, 282, 285, & 286	186

1) Hotspot data obtained from Catalogue of Somatic Mutations in Cancer. 2) All genomic reference sequences obtained from NCBI, 3) Tm: annealing temperature, 4) All which are listed here were only used in the standard PCR protocol.

Table 2-3 The primers (inner) sequences used in the SSD PCR protocols.

Gene	Exon	Primer Sequence	Tm°C	size (bp)
PIK3CA	1A	F ATGCCCCCAAGAATCCTAGT R GAGGGGGTATTTTCTTGCTTC	55	129
	9	F AAGGGAAAATGACAAAGAACAG F CACTTACCTGTGACTCCATAGAAA	55	103
	20	F GCAAGAGGCTTTGGAGTATTTC R TTTTCAGTTCAATGCATGCTG	55	115
FBXW7	8	F CGGACACTCAAAGTGTGGAAG R GAAGTCCCAACCATGACAAGA	55	130
	9A	F TTTTCTGTTTCTCCCTCTGC R ACCCTCCTGCCATCATATTG	55	145
	10	F GGAATTGCATTCACACGTTA R TCCTGTTTTGATATCCCAGATTTT	55	122
KRAS	2	F CCTGCTGAAAATGACTGAATATAA R TGGATCATATTCGTCCACAAAA	55	112
	3	F TGTGTTTCTCCCTTCTGAGGA R AAGAAAGCCCTCCCCAGT	55	150
	4	F GACACAAAACAGGCTCAGGACT R CAGATCTGTATTTATTTCAGTGTTA	55	122
BRAF	11	F GACGGGACTCGAGTGATGAT R TGTCACAATGTCACCACATTACA	55	135
	15	F TGTTTTCCTTTACTTACTACACCTCA R CCACAAAATGGATCCAGACA	55	143
TP53	5A	F ACTCTGTCTCCTTCCTCTTCCTA R TGTGCTGTGACTGCTTGTAGA	65	156
	5B	F CCTGTGCAGCTGTGGGTTG R GGCAACCAGCCCTGTCGTC	64	176
	6	F AGGCCTCTGATTCCTCACTGAT R ACCCTTAACCCCTCCTCCCA	64	187
	7	F ATCTTGGGCCTGTGTTATCT R GGGTGGCAAGTGGCTCCT	64	156
	8	F CTCTTGCTTCTCTTTTCCTATCC R ACCGCTTCTTGTCCTGCTTG	65	192

2.2.3.2 Mutation screening using melting curve analysis

2.2.3.2.1 Principle of fluorescent melting curve analysis

DNA amplicon melting analysis has become an integral part of real time PCR since its introduction in 1997 with the LightCycler® and the asymmetric cyanine DNA specific dye SYBR® Green I. This implementation enables a real time monitoring of the entire PCR amplification and DNA melting by assessing the changes in the fluorescent intensity of double stranded DNA (dsDNA) binding dye that fluoresces only when it is incorporated into a dsDNA molecule. Thus, fluorescent melting analysis allows quantitative assessment of PCR product amplification (quantification) and qualitative confirmation of the identity and purity of PCR products after amplification (Wittwer et al., 1997b, Ririe et al., 1997, Lay and Wittwer, 1997, Wittwer et al., 1997a, Wittwer and Kusukawa, 2004). In addition, fluorescence signal monitoring is more sensitive than the traditional monitoring by ultraviolet absorbance since only nanogram amounts of DNA quantity are required to perform the fluorescence analysis. Henceforth, the smaller DNA quantity in fluorescence analysis, which requires a smaller vessel, allows precise thermal control and faster temperature transition rates (0.05-0.3ºC/s) in comparison to the ultraviolet absorbance which requires microgram amounts of DNA and transition rates of 0.1 - 1ºC/min to perform high quality melting curves (Wittwer et al., 2010).

In real time PCR, product amplification is continuously monitored using a fluorescent DNA binding dye that differentiates double stranded from single stranded DNA. Basically, during the extension phase of each cycle the fluorescence level increases because of the significant increase in dye fluorescent efficiency with its incorporation into dsDNA at lower temperatures and the duplication of DNA copies. As the fluorescence is recorded once each cycle, the speed, in term of number of cycles at which the fluorescence level surpasses the background fluorescence noise (the threshold cycle “ct”), is directly related to the initial template amount and thus quantification can be made (Ririe et al., 1997).

Monitoring of PCR product hybridisation for the quantification purpose can be well demonstrated by plotting fluorescence versus time to produce what's called the amplification plot. This approach was emerged as the first report regarding real time monitoring of PCR amplification with the nucleic acid dye ethidium bromide (Higuchi et al., 1992). However, using product amplification analysis by its own is not capable of differentiating different PCR products because the fluorescence dye will bind to the desired and undesired dsDNA and consequently confirmation of PCR specificity is not possible (Ririe et al., 1997).

From this end, and in order to outspread the dynamic limit of the fluorescence signal analysis during different stages of PCR thermal cycling, it was confirmed that monitoring the melting of DNA duplexes in the presence of dsDNA fluorescent dye during the dissociation phase could help in verification of product identity according to its thermodynamic stability (Ririe et al., 1997). Empirically, during the denaturation stage the fluorescent intensity decreases with the separation of DNA duplexes into random coils of single stranded DNA (ssDNA) and release of the intercalating dye molecule which loses its fluorescence characteristic due to conformational changes. The pattern of fluorescence signal drop during denaturation is not uniform but instead it is typically multiphasic (usually biphasic) pattern. It initially decreases quite steadily and then dramatically as the product reaches the denaturation temperature. In another word, the fluorescent dye signal gradually decreases at the beginning of heating, and then the steepest drop of fluorescence signal happens over a narrower window (melting domain or melt curve transition/ usually over 1-3 ◦C) as most of the dsDNA falls into ssDNA at this point. The entire range of melting process is usually described as the melting profile (usually encompasses 10-15 ◦C). Technically speaking, the maximum drop usually happens at the mid-point of melting domain as the heat reaches the melting temperature of PCR product (Tm). The melting temperature (Tm) is defined as the temperature at which half of the DNA is melted (single stranded) and half is double

strand (Ririe et al., 1997).

So, the continuous fluorescence monitoring of the dsDNA specific dye as the PCR product heats up during PCR denaturation segment can generate a set of data that is routinely described as DNA melting curve. DNA melting curve shape and Tm position are dependent on nucleotide sequence, amplicon length, and GC content because the thermal stability of a DNA molecule is a function of these characteristics. Hence it has become possible to differentiate different PCR products which are separated by less than 2 °C in Tms by melting curve analysis (Ririe et al., 1997). The best graphical presentation of DNA melting is by plotting fluorescence as a function of temperature to generate the amplicon melting curve. Nevertheless, the melting temperature is usually determined by plotting the negative derivative of fluorescence on the y-axis versus the temperature on the x-axis (-dF/dT against temperature) where the steepest slope is easily visualised as a melting peak. This type of graphical representation is called derivative or dissociation melting curve. Based on the fact that each DNA amplicon has a unique Tm, derivative plot is routinely used to check the specificity of PCR primers (Wittwer et al., 2010).

Furthermore, it has become a routine practice to use a final reading of the amplifications melting data which can be obtain at the end of PCR by inserting an additional 2-cycle thermal loop (rapid denaturation followed by hybridisation and then controlled slow dissociation) to perform DNA melting curve analysis (end point PCR analysis) for the purpose of product discrimination according to their Tms. So this feature has increased the adaptability of melting curve analysis as it has become possible to perform the melting analysis without the need for a real time PCR instrument (Wittwer et al., 2010). In addition, the accuracy of melting curve analysis can be enhanced if the melting profile is generated at a higher temperature by setting the machine to capture the fluorescence signal slightly below

the expected product Tm to eliminate signals generated by any non-specific product with low melting temperature such as primer dimer. Likewise, the use of dsDNA specific dye has significantly simplified and reduced the cost of quantitative real-time PCR because it enabled probe-free approach (Morrison et al., 1998).

The use of DNA melting analysis for confirming the identity of PCR products is generally considered as low-resolution melting analysis (Low-Res Melting analysis). It was described as such because the temperature resolution is limited since the melting data are collected at wide temperature increments, usually in 0.5°C/s increments, and the density of data points is not sufficient enough to interrogate small DNA sequence variations. SYBR Green I is a double-strand-specific DNA dye often used to monitor product formation and Tm in real-time PCR. Later on, DNA melting analysis was used to interrogate nucleic acid sequence alterations in limited regions encompassed by labelled hybridisation probes (Herrmann et al., 2006, Wittwer et al., 2010).

2.2.3.2.2 High Resolution Melting Curve Analysis (HRM or HRMA)

The generation of a melting profile by gradual melting of the PCR product through small increments in temperature (0.008-0.3°C/s increments) in the presence of a saturating fluorescent double stranded DNA (dsDNA) binding dye is called high resolution melting (HRM) analysis (HRMA). Recently, the high resolution melting analysis (HRMA) has been introduced as fast, simple, cost-effective, close-tube post-PCR method used for analysis of nucleic acid sequence variation and requiring only PCR and melting curve analysis software (Gundry et al., 2003, Wittwer et al., 2003). As the DNA molecule thermal stability is dependent on DNA amplicon size, GC content, and strand complementarity (heterozygosity), the dissociation behavior of DNA amplicons will vary accordingly. The saturating fluorescent dyes specifically and proficiently bind to dsDNA molecules and they have a high

fluorescence level when bound to DNA. The gradual transition of dsDNA molecule into its two strands by heating leads to the release of the intercalating dye, which loses its fluorescent characteristic due to conformational change upon release, and this is accompanied by gradual and uniform drop in the fluorescence level that can be monitored using the appropriate HRMA instrument to generate melt curve profile (Garritano et al., 2009). HRMA is highly sensitive method allows the detection of even a single nucleotide change, genotyping of entire amplicon with accurate categorisation of heterozygote and homozygote variants (Wittwer et al., 2003).

2.2.3.3 Optimisation and assay performance of PCR protocols

2.2.3.3.1 Standard PCR protocol

The standard PCR protocol was optimised for each primer pair by running PCR with a 12 temperature gradient at the annealing hold. The reaction was undertaken in a final volume of 10µl. PCR was performed using Primus96 advanced® Gradient Thermal Cycler (PeQLab Biotechnology, UK) as follows: (95°C/5min) X1; [(95°C/30sec) / (60±8°C/1min) / (72°C/1min)] X45. The total duration of the thermal cycling was 2h and 55 minutes. The PCR reaction consisted of 5µl of the 2X HotShot^{TM} master mix (Cadama Medical Ltd, UK), 1µl of the 10X LC Green ® PLUS (Idaho Technology, USA) as a DNA binding dye, each primer at 0.250µM final concentration and 1µl of the 20ng/µl template DNA all made up to a final volume of 10µl with PCR grade water (Nuclease Free Water, Cat. No. 129115, QIAGEN, GmbH). Each reaction tube was overlaid with 10µl molecular grade mineral oil (Mineral oil, Cat No. M5904-500ML, Sigma-Aldrich, USA) to prevent evaporation and ensure consistent amplification across the reaction plate. The products were melted in the HR-1 high resolution melting instrument (Idaho technology Inc, USA) as per the manufacturer's instructions and the data was analysed using the HR-1 analysis tool custom software description of HRM data

analysis is in section .. In order to validate the results of HRM, the PCR products were resolved on a 2% agarose gel (w/v) and visualised under UV light. Most of the primers showed specific amplification over the 12 temperature gradient with relatively similar efficiencies. However, few primer sets were specific only over limited temperature range as shown in Figure 2-11. Therefore, a single temperature toward the highest end (64ºC) was chosen as the optimal annealing temperature for most of those primers with wide thermal specificity in order to reduce the thermal cycling time and make the machine programming easier without the need for multiple settings.

The standard PCR protocol was used to screen cell lines using the same mixture concentrations and cycling conditions (described above) with the optimal annealing temperature specific to each primer (Table 2-2). Samples with known mutation genotype (wild type and mutant DNA samples) were included in every run for referencing. In addition, non-template controls (NTC) in duplicate (containing all the PCR reaction mixture components but not the DNA template) were included with every run to detect contamination of the reaction mixture by genomic DNA due to carry-over contamination or contamination of any of the components in the pre-mix. Because they contain no template DNA, NTC should give no amplification which indicates that the amplification in the other test tubes is genuine and results from amplification of DNA template under test.

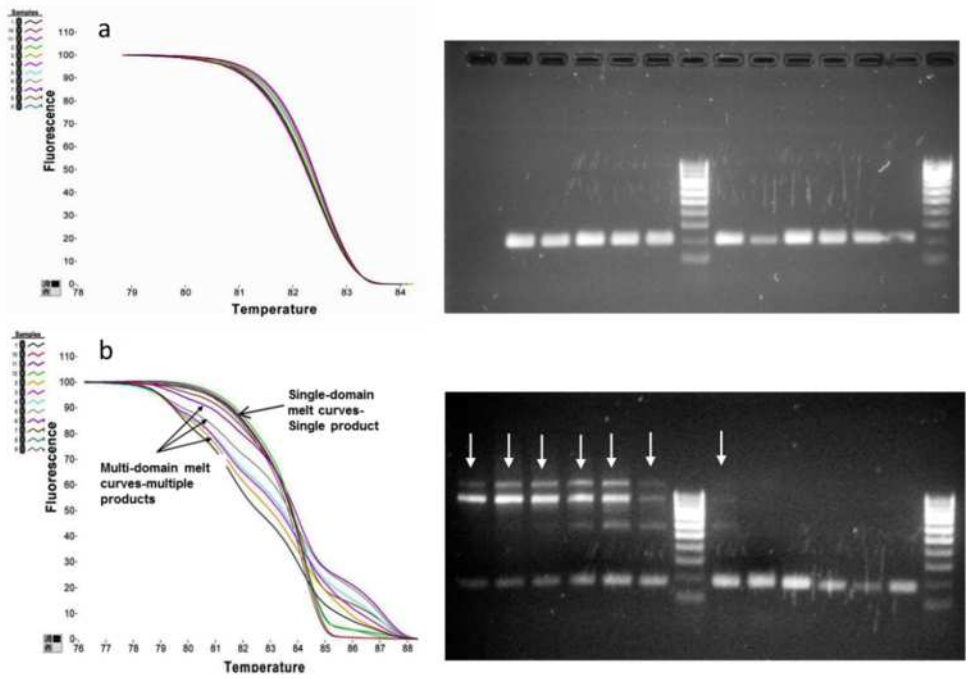

Figure 2-11 PCR primer optimisation

PCR primer optimisation. (a) Melt curves (left) illustrating an example of a primer (PIK3CA exon 9, outer primer) working over a wide temperature range as it was able to produce smooth single domain transitions representing specific products. Agarose gel (right) picture of the same PCR products showing single specific band (197 bp) over the whole wells. (b) Melting curves of a gradient PCR products for PIK3CA exon 1A (168 bp). (left) The multi-domain curves represent non-specific binding at lower temperatures set, while at a higher temperature set the melting was that of a single product (specific amplification). These results were confirmed by agarose gel (right) as there were non-specific bands at lower temperatures (arrowed).PCR primer optimisation. (a) Melt curves (left) illustrating an example of a primer (PIK3CA exon 9, outer primer) working over a wide temperature range as it was able to produce smooth single domain transitions representing specific products. Agarose gel (right) picture of the same PCR products showing single specific band (197 bp) over the whole wells. (b) Melting curves of a gradient PCR products for PIK3CA exon 1A (168 bp). (left) The multi-domain curves represent non-specific binding at lower temperatures set, while at a higher temperature set the melting was that of a single product (specific amplification). These results were confirmed by agarose gel (right) as there were non-specific bands at lower temperatures (arrowed).

2.2.3.3.2 Analysis of High resolution melting data

High Resolution Melting (HRM) analysis is a cheap in-tube (i.e. non-gel based) mutation detection technique that works on the basis that a difference in DNA sequence results in differences in the way the DNA melts. The PCR products containing the dsDNA binding dye LC Green® Plus were transferred to Roche Light Cycler® capillaries (20µl) (Roche Applied Science, UK). Then, the products were melted in the HR-1 high resolution melting instrument (Idaho technology Inc,

USA) as per the manufacturer's instructions. Briefly, each sample was denatured at a rate of 0.3°C/s, with a starting temperature of 60°C, an acquisition temperature between 70-85°C. The data was analysed using the HR-1 analysis tool custom software.

In order to compare the melting curves from different samples, they should be first normalised to bring the ends of the melting curves together. The initial analysis will be performed on the normalised melting curve as the DNA with mismatch tends to be less stable and will melt earlier (shifted to the left, Figure 2-12 a). Then, and in order to cluster the melting curves into groups according to their melting pattern and to make the difference more prominent, temperature shifting of the melting curves has to be applied. The melting data then will be displayed as derivative plots and difference plots. In the latter case, a known wild type should be used as a reference sample. Finally, visual inspection of the derivative and difference plots will help separate out the variants from the common type samples. The analysis of derivative plots basically depends on the position of the melting peaks against the temperature axis (X axis). As the mutant samples usually produce a second peak (lower melting temperature) representing the heteroduplex melting. While the wild type samples usually produce a single peak (higher melting temperature) representing the homoduplex melting (Figure 2-12 b). Analysis of the difference plots depends on the degree of fluorescence difference (Y axis) between the reference sample (x axis) and the unknown samples. A specific value of fluorescence difference should be used as cut off to separate wild from variant samples. In this work cut off value of 4 has been previously determined in our laboratory by screening samples with known genetic profile (Figure 2-12 c).

2.2.3.3.3 Quick Multiplex consensus PCR protocol

Quick Multiplexed Consensus (QMC) PCR protocol consisting of a Pre-Diagnostic Multiplex (PDM) reaction followed by a Specific Single Diagnostic (SSD) reaction

(Fadhil et al., 2010). In order to optimise the PDM protocol, a gradient PCR reaction was set up with a 12 temperature gradient at the annealing hold and two different primer concentrations (0.250µM and 0.400µM, respectively). The multiplex reaction was undertaken in a final volume of 25µl. Each reaction consisted of 1X HotShot™ master mix, 10 primer pairs (outer primers) with each primer at 0.250µM or 0.400µM final concentration per tube, 20ng template DNA and an appropriate volume of PCR grade water. Primers in PDM stage covered 10 hotspots in KRAS (exons 2, 3 and 4 encompassing codons 12/13, 61 and 146 respectively), BRAF (exons 11 and 15 (the latter encompassing codon 600)), PI3KCA (exons 1, 9 and 20), and FBXW7 (exons 8 and 10). PCR was performed using a two-step cycling program with the following cycling conditions: (95°C/5min) X1; [(95°C/1sec) / (60 ± 10°C/1sec)] X25. The total duration time was 38 minutes. The PCR products were then resolved on a 2% agarose gel (w/v) and visualised under UV light.

The SSD reaction was optimised by using different template dilutions (1:100, 1:200, and 1:500) from the PDM PCR products in order to reduce the effect of any contained PCR inhibitor. To identify a universal annealing temperature, the SSD reaction has been tested for each primer at each template dilution with a different annealing temperature (55°C and 60°C, respectively). The SSD reaction mixture contains the following reagents concentration: 1X HotShot™ master mix, 1 primer pair (inner primer) with each primer at 0.250µM final concentration per tube, 1X LC Green ® PLUS (Idaho Technology, USA), 1µl of diluted multiple PCR products and an appropriate volume of PCR grade water to make a final volume 10µl reaction. Each tube was overlaid with 10µl of the mineral oil and PCR performed using the following two step cycling protocol: (95°C/5min) X1; [(95°C/1sec) / (55°C or 60°C /1sec)] X45. The total duration time was 1 hour and 10 minutes.

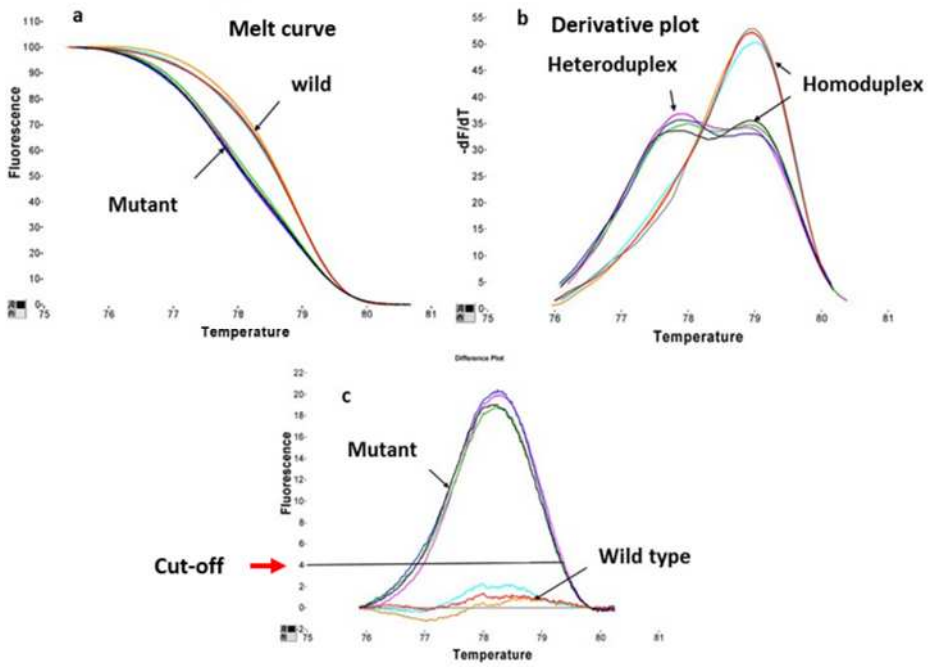

Figure 2-12 Analysis of High Resolution Melting curve

(a) Normalised melt curve showing earlier melting of mutant samples (shifted to the left). (b) A derivative plot of the normalised melt curve data showing how the mutant samples in (a) will generate a heteroduplex peak (representing the mismatched containing DNA) and a homoduplex peak (representing the DNA with no mismatch), while the wild type sample have only a single homoduplex peak. (c) Difference plot displays each sample fluorescence difference from a given wild type control reference (x axis). Each samples with a fluorescence level higher than the cut-off value regarded as variant (mutant). Cut-off of 4 flourescence was determined by direct sequencing of samples with variable fluorescence difference values. Samples with a fluorescence value of => 4 were proven mutatant by sequencing and hence a cut-off of 4 flourescence difference was adopted

2.2.3.3.4 QMC PCR evaluation in cell lines and DNA from FFPE tissue

QMC protocol was first tested on high quality DNA derived from 29 CRC cell lines with direct sequencing proven mutation status for the hotspots in KRAS, BRAF, and PIK3CA. Subsequently, 29 cell lines underwent screening for all 10 hotspots and those called as “mutant” were validated by direct sequencing. In order to test the assay in DNA derived from FFPE tissue, 43 samples from the Nottingham series set-1 (section 2.1.2.1) underwent direct sequencing analysis for the hotspots in KRAS exon 2 and PIK3CA exon 20 and were then screened by QMC-PCR. Subsequently, the 43 samples were screened for all 10 hotspots and those called as “mutant” were validated by direct sequencing. To further validate the efficiency of

this protocol, it was compared with the standard single step protocol for PIK3CA exon 20 (using neat DNA from FFPE tissues) and with the modified full cold PCR (section 2.2.3.3.8) using the same template materials used for the SSD PCR in order to eliminate any confounder effect.

2.2.3.3.5 Performance of QMC-PCR against standard PCR using DNA isolated from FFPE tissue

The QMC-PCR protocol was also compared with a standard protocol for the hotspots in PIK3CA exon 20 and BRAF exon 15 using DNA derived from FFPE tissue from Nottingham series set-1. The details of reaction mixture and cycling condition for the standard reaction are described in section (2.2.3.3.1).

2.2.3.3.6 Limit of detection of QMC-PCR

In order to assess the limit of detection of QMC-PCR, dilution experiments were performed by spiking DNA from diploid cell lines with known mutations into diploid cell lines known to be wild type at that hotspot. Thus DLD1 (containing a heterozygous E545K mutation in PIK3CA) was spiked into VACO5 (wild type at codon 545). Similarly VACO5 (heterozygous V600E mutant in BRAF) was spiked into HCT116 (wild type in BRAF). Spiking was carried out to produce 40%, 20%, 10%, 5%, 2.5% and 1.25% mutant alleles in the DNA mix.

2.2.3.3.7 Short term and long term precision of QMC-PCR in DNA derived from FFPE tissue

Intra and inter-assay variation (respectively short term and long term precision) was also assessed. For the intra-assay variation tests were conducted for exon 20 of PIK3CA and in exon 15 of BRAF. Two FFPE derived DNA samples, one wild type and one mutant, were tested as 15 replicates for each sample on two separate occasions. To test inter-assay variation, a series of 6 FFPE derived samples from Nottingham series set-1 (3 mutant and 3 wild type for exon 20 of PIK3CA) were tested on 3 consecutive days.

2.2.3.3.8 Performance of QMC-PCR against cold PCR

For the purpose of comparison with QMC-PCR, the "cold PCR" protocols (fast cold and full cold PCR) were tested. Cold PCR was described as modifications of the standard PCR protocol which can enrich for mutant alleles by inserting a step of melting at a specific critical denaturation temperature (Tc) (Li et al., 2008). The enrichment is due to the differences in denaturation temperatures between mutant DNA duplexes and wild-type DNA duplexes. The fast cold PCR protocol basically has 3 temperature holds; denaturation at Tc, annealing and extension. This protocol was found to enrich mutant alleles up to 100 folds (Table 2-4) but this is limited to "Tm reducing mutations" such as G>A or C>T substitution which makes this method less utilisable in mutation screening. The full cold PCR, which was introduced to identify different mutation types, consists of 5 temperature holds as follows: denaturation at 94°C, hybridisation at 70 °C for 2-8 min, denaturation at Tc, annealing at 55°C and extension (cold PCR protocols are schematically represented in Figure 2-13). The published full cold protocol lasts over 4 hours in our hands using PeQLab instrument. Given that the Tc needs to be highly accurate and that there will inevitably be machine to machine variation in temperature control and the Tc needs to be determined empirically for each exon and PCR machine.

In order to identify the Tc for our targets, a modified fast cold PCR was used. Two known cell lines, one wild type (SW837) and one with a known mutation (SW948) for the target sequence in PIK3CA exon 9, and additional two known cell lines, one wild type (SW837) and one mutant (HCT116) for the target sequence in PIK3CA exon 20 were selected. Initially, following the analysis of the derivative plots from our previous HRM data, it was possible to identify the melting temperatures (Tms) for those target sequences. Those Tms were subsequently used as guide to set a denaturation temperature gradient during the optimisation of cold PCR protocols.

For the modified fast cold PCR, the thermo-cycler was programmed to produce a temperature gradient of Tc ±4°C to empirically determine the Tc for each product using the following cycling conditions: (95°C/5min) X1; [(95°C/1sec) / (55°C/1sec)] X10; [(80±4°C/10sec) / (55°C/15sec) / (72°C/10sec)] X25. The same reaction mixture of the optimised SSD PCR protocol (section 2.2.3.3.3) was used. The products were analysed using HR-1 and the lower denaturation temperatures that produce efficient amplifications were chosen as the critical denaturation temperatures (Tc) for that target sequence. Subsequently, a modified full cold PCR was used to scan a group of FFPE samples (sequence proven) for the purpose of comparison with the QMC protocol. For the modified full cold protocol, the reaction mixtures were as described above for the single reaction and the cycling conditions were: (95°C/5min) X1; [(95°C/1sec) / (55°C/1sec)] X10; [(95°C/1sec) / (55°C/1sec) / (Tc/5sec) / (55°C/10sec)]

X28.

Table 2-4 Mutation prevalence for various types of somatic mutations in CRC and mutation enrichment anticipated via COLD-PCR.

Modified from (Li et al., 2008).

Mutation	Prevalence of somatic mutation in colon cancer %	Enrichment Full cold	Enrichment Fast cold
C:G> T:A	78	5-12 FOLD	10-100 FOLD
C:G> A:T	6		
T:A> A:T	2	5-8 FOLD	NONE
C:G> G:C	4		
T:A> G:C	2	3-5 FOLD	NONE
T:A> C:G	8		
Indels	~0	>50-fold one or more rounds	>100 FOLD

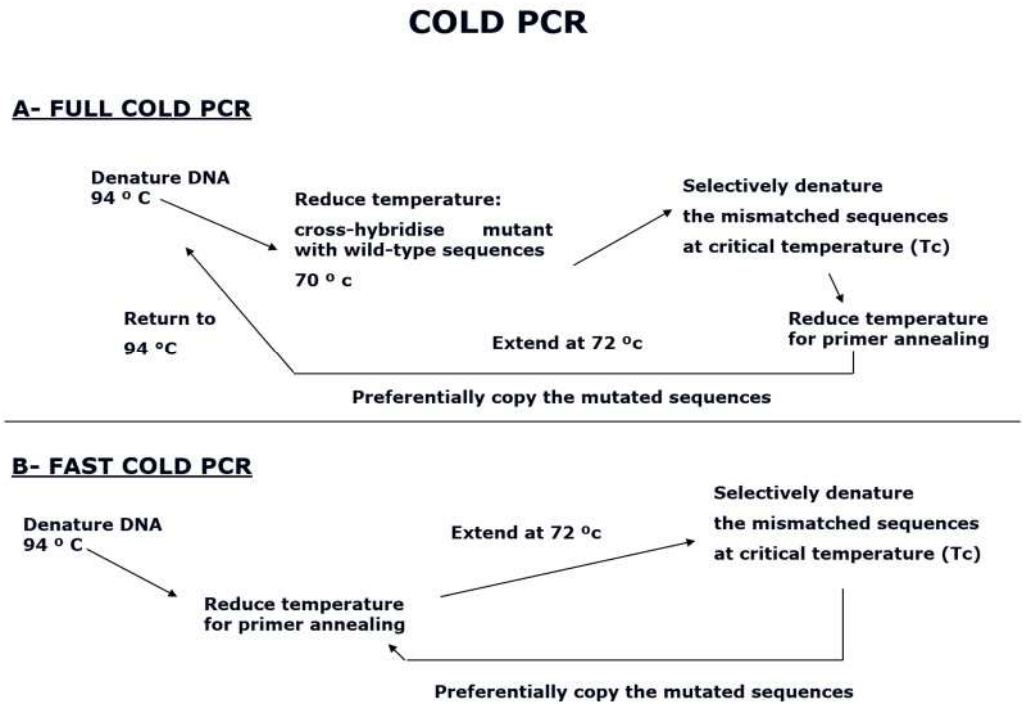

Figure 2-13 Schematic diagram representing the cold PCR protocols.

(A) Full cold PCR consists of 5 temperature holds as follows: denaturation at 94°C, hybridisation at 70 °C for 2-8 min, denaturation at Tc, annealing at 55°C and extension. (B) Fast cold PCR consists of 3 temperature holds; denaturation at Tc, annealing and extension. Modified from (Li et al., 2008).

2.2.3.3.9 Performance of QMC-PCR against pyrosequencing

This work was done in collaboration with Dr Salih Ibrahem and Dr Reshmi Seth (Ibrahem et al., 2010). In brief, both limited and frequency of mutation detection were investigated. For limit of detection (LOD), DNA spiking experiments were conducted using two diploid CRC cell lines carrying heterozygous alterations at the target region. One (HCT116) harboring heterozygous mutation at KRAS codon 13 (G13D) but wild type for BRAF, and the second cell line (VACO5) contains a heterozygous mutation at BRAF codon 600 (V600E) with wild type genotype for KRAS. Serial allele proportions (25% / 12.5% / 6.25% / 3.125% / 1.625% / 0.8%) were produced for each hotspot by admixing varying quantities of DNA from the cell lines. Subsequently, each sample underwent twice mutation analyses, once by QMC-PCR assay and a second one by pyrosequencing. For the QMC-PCR, the work was performed as described above (section 2.2.3.3.3), however, for the

purpose of this study, only 5 primer sets were mixed in the PDM reaction.

So as to investigate the frequency of mutation detection by QMC-PCR in comparison to pyrosequencing, thirteen clinical samples (from Nottingham series set-1) and 9 CRC cell lines were tested by QMC-PCR and pyrosequencing for mutations in KRAS codon 12/13 (in exon 2), KRAS codon 61(in exon 3), BRAF exon11 and BRAF V600E (exon 15). Those samples were previously tested by direct sequencing as mention in the previous sections.

For pyrosequencing analysis, which was done by Dr Reshmi Seth (Molecular Diagnostics lab, Nottingham University Hospital NHS trust), all samples underwent testing for mutation in KRAS codon 12/13 (in exon 2), KRAS codon 61(in exon 3), BRAF exon11 and BRAF V600E (in exon 15) using the commercial pyrosequencing kits Pyromark™ Q24 Kras v2.0 (Biotage) and Pyromark™ Q24 BRAF (Biotage) in accordance with the manufacturer's instruction. For KRAS codon 146 (exon 4) PCR and sequencing primers were designed de-novo (Ibrahem et al., 2010).

The pyrosequencing kits use a biotinylated reverse primer allowing isolation of single stranded templates (of the reverse strand) from the PCR products by adding Binding Buffer (Qiagen), streptavidin sepharose high-performance beads (GE Healthcare), sterile water and eluting product using the PyroMark Vacuum Prep WorkStation (Qiagen). Pyrosequencing reactions were carried out with a nested sequencing primer in the PyroMark MD machine (Qiagen) using PyroGold Reagents (Qiagen) in accordance with the manufacturer's instructions. The results were analysed using pyro Q-CpG Software (Qiagen) (Ibrahem et al., 2010).

2.2.3.3.10 Comparison of QMC-PCR with real-time PCR

A series of 475 anonymised cases from the Dutch Cairo 2 trial (see also section

2.1.2.3) which had been previously tested for KRAS codon 12/13 mutation by real-time PCR were screened using the Quick Multiplex Consensus (QMC) PCR protocol followed by HRM. Details of patient recruitment and extraction of DNA from FFPE tumour tissue have been previously published (Tol et al., 2009b).

2.2.3.3.10.1 KRAS mutation detection by real-time PCR

The commercially available real-time PCR kit (DxS, Manchester, UK) detects the 7 most common mutations in KRAS codon 12/13. The entire series of tumours were previously tested with this assay in a comparative analysis with direct Sanger sequencing (Tol et al., 2010) . These data were used for comparison with HRM in this study and the real-time assay was not repeated.

2.2.3.3.10.2 High throughput mutation detection using a modified QMC-PCR / HRM

We used the QMC-PCR protocol for high throughput mutation screening with some modifications in order to improve its performance with a high throughput as described below and in the following sections. Firstly, for the purposes of this study, the PDM reaction contained only 5 primer pairs (covering the mutation hotspots in KRAS and BRAF) and only the SSD for the KRAS codon 12/13 hotspot was analysed. The primers sequences are listed in Table 2-2 and Table 2-3, and were previously published (Fadhil et al., 2010).

2.2.3.3.10.3 The modified QMC-PCR and quality control

For each sample, a PDM reaction was carried out in a final volume of 25µl containing 1X Sensi- Mix™ HRM Kit (Bioline), 0.4µM concentration of each primer, 0.4X LC green® Plus+ dye (Idaho technology, USA) and 20ng DNA template. The samples underwent thermal cycling on an Applied Biosystems 7500 fast PCR machine (Applied Biosystem CA, USA) using the 7500 Software v2.0.1.

The cycling programme consisting of one cycle of 95°C for 10min, followed by 45 cycles of [(95°C for 1s) / (55°C for 1s)]. The presence of the LC green dye allows fluorescent data to be captured during the PCR and this can be used to assess sample quality. Samples showing late amplification (i.e. >5 cycles later than the mean Ct value) were regarded as low quality and were not tested further.

The products from the PDM-PCR were diluted 1:100 in PCR grade water and used as a template for the analytic SSD-PCR. This was done in a final volume of 10µl containing 1X SensiMix™ HRM Kit (Bioline), 0.4X LC green dye (Idaho technology,USA); 0.25µM concentration of each internal primer and 1µl of diluted PCR products. Mineral oil (10 µL) was added to each tube. The samples underwent thermal cycling on the AB 7500 fast PCR machine using a cycling programme consisting of one cycle of 95°C for 10min, followed by 45 cycles of [(95°C for 1s) / (55°C for 1s)] followed by a melt curve stage. This consisted of one cycle of [(95°C for 15 s) / (55°C for 1min) followed by slow ramping up (at 0.03 degrees/s) to 95°C for 15s. Fluorescent data were captured (25-28 points per degree) during this phase and then there was rapid cooling down (maximum ramp rate) to 60°C.

2.2.3.3.10.4 Modified QMC-PCR/ protocol 1

The fluorescence data were analysed using the Applied Biosystems High Resolution Melting software *v*2.0. This program uses the default analysis setting to automatically assign a variant call to each sample. The variant calls are determined by the melt curve characteristics (melt curve shapes and Tm values). However, the variant calls can also be determined manually. The software displays the analysed data as normalised melting curve and difference plots. In the first set of experiments, 8 wells of a 96 well plate were used for negative controls. The remaining 88 wells were used for sample testing and included a small number of known wild type cases. The samples were designated as wild type if they clustered

with the known wild type otherwise they were designated as mutant.

2.2.3.3.10.5 Modified QMC-PCR/ protocol 2

Following the initial experiments, the data and protocol were reviewed in order to identify possible sources of variation. A refined protocol was produced which differed from the original in that (a) any single experiment was limited to a maximum of 25 cases, (b) all cases were to be tested in duplicate and (c) a variation of the clustering software was used in which the known wild types samples were identified before the clustering and a class distinction algorithm was used. One hundred cases were randomly selected from the samples and these were tested using the refined protocol.

2.2.4 Introducing PCR-HRM method as a novel approach for testing Microsatellite Instability (MSI) in colorectal cancer

We were able to introduce a novel, robust, accurate, simple, and cost effective method for MSI detection by implementing the PCR-HRM approach (Fadhil et al., 2012b, Fadhil et al., 2014).

2.2.4.1 Development of the PCR-HRM MSI detection assay

DNA materials isolated from 29 CRC cell lines were used first to test the feasibility of PCR-HRM approach for testing genetic instability at microsatellite markers. A panel of six quasi-monomorphic mononucleotide markers was used, five of which have been previously described (BAT25, BAT26, NR21, NR22, and NR24) (Suraweera et al., 2002). The sixth marker, B-CAT25, is a novel in-house marker that targets an A_{25} sequence in the 3′ untranslated region of the CTNNB1 gene. New primers amplifying short amplicons were designed following the procedures

described in section 2.2.3.1 and its subsections. PCR was carried out in a final volume of 10 µl containing 1 × Sensi- Mix HRM Kit (Bioline), 0.25 µM each primer, 1 × LC green Plus+ dye (Idaho Technology), and 20 ng of DNA template. Mineral oil (10 µL) was added to each tube. Thermal cycling was as follows: 1 cycle at 95°C for 10 min; and 45 cycles of 95°C for 3s, annealing temperature for 30s, and 72°C for 10s using Primus 96 advanced®Gradient (PeQlab, Biotechnologie GmbH) PCR instrument. All primer sequences are shown in Table 2-5.

Table 2-5 MSI markers primer sequences

Marker	Gene/position	Sequence	Amplicon size (bp)
BAT25	c-kit/ Intron 16, (24 T)	5'-TCGCCTCCAAGAATGTAAGTG-3'	149
		5'-TGGTTACCACACTTCAAAATGAC-3'	
BAT26	hMSH2/ Intron 5, (26 A)	5'-TTGGATATTGCAGCAGTCAGAG-3'	140
		5'-TTTAGCTCCTTTATAAGCTTCTTC-3'	
BCAT25	Beta-catenin/3`UTR (25 T)	5'-TCTGTAATGGTACTGACTTTGCT-3'	102
		5'-AACTTAACACTACGAGAGACTTAAAA-3'	
NR21	SLC7A8/5`UTR (21 T)	5'-TCGCTGGCACAGTTCTATTTT-3'	122
		5'-CCGCATTCACACTTTCTGGT-3'	
NR22	Transmembrane Preciusor protein B5/ 3`UTR (22 T)	5'-TTCGCACTGAGCACATCAC-3'	120
		5'-CCAAGACAAAACTTCCAGACAA-3'	
NR24	Zinc finger 2/3`UTR (24 T)	5'-CCTCCTGACTCCAAAAACTCT-3'	119
		5'-AGATTGTGCCATTGCATTCC-3'	

.

2.2.4.2 Evaluation of the PCR-HRM MSI detection assay using CRC cell lines and DNA derived from FFPE

Twenty-nine CRC cell lines with known MSI status were blindly screened using PCR-HRM assay in order to validate the performance and accuracy of the assay. Additionally, the assay was used to screen the samples from the Birmingham series (section 2.1.2.2). MSI status of those cases were previously characterised by West

Midlands Regional Genetics Laboratory (WMRGL), Birmingham Women's Hospital, and Birmingham, UK, using PCR and IHC PCR method was performed with the Bethesda panel of microsatellite markers (this panel consists of three dinucleotide (D5S346, D2S123 and D17S250), and two mononucleotide markers BAT25 and BAT26 (Perucho, 1999, Boland et al., 1998)) While the IHC was performed for the four MMR proteins (MLH1, PMS2, MSH2, MSH6) However, for the purpose of this work, the researcher were blinded to these results. In this study, PCR reaction mixture, cycling condition and HRM analysis were performed as described in the previous section (2.2.4.1). Samples were only regarded as MSI if there was instability at two or more of 6 markers.

2.2.4.3 Comparative performance of the PCR-HRM MSI protocol

A total of 100 cases from the Nottingham series set1 & 2 were tested for the presence of microsatellite instability using PCR-HRM approach. Screening for MSI was performed with a singleplex PCR followed by HRM analysis. PCR was carried out in a final volume of 10 µl containing 1× Sensi- Mix HRM Kit (Bioline), 0.25 µM each primer, 1× LC green Plus+ dye (Idaho Technology), and 20 ng of DNA template. Thermal cycling was as follows: 1 cycle at 95°C for 10 min; and 45 cycles of 95°C for 3 s, 55°C for 30 s, and 72°C for 10 s. Mineral oil (10 µL) was added to each tube. Thermal cycling was performed on the ABI 7500 fast PCR machine, and HRM analysis was performed as described above (section 2.2.3.3.10.5). All these cases were later tested by IHC for expression of MMR proteins (MLH1, PMS2, MSH2, and MSH6) at the immunocytochemistry lab, division of histopathology, QMC, NUH, NHS TRUST and examined by a consultant histopathologist (MI). As mentioned in the previous section, Samples were only regarded as showing MSI if there was instability at two or more of 6 markers.

2.2.5 The utility of diagnostic biopsy for predictive molecular testing

If stratified medicine is to be applied in the neoadjuvant setting, predictive testing will have to be undertaken on preoperative diagnostic biopsy specimens. The aim of this study was to evaluate whether a diagnostic biopsy was adequately representative of the main tumour in colorectal cancer.

2.2.5.1 Study design

Full description of the cases Nottingham series set-2 which were used to conduct this work is given in section 2.1.2.1. In brief, thirty cases, from whom both the diagnostic biopsy specimen and the final matched resection specimen were available, were randomly selected from the archives of the pathology department of the Nottingham University Hospitals NHS Trust. The biopsy specimens were typically 2–3 mm in size, and the number of tissue fragments in each case ranged from two to 10. An inclusion criterion was the presence of at least 50% tumour tissue in the biopsy specimens. Blocks from the corresponding resection specimens were chosen to contain at least 50% tumour tissue, and ethical approval was obtained for the use of patient materials in this study (Research Ethics Committee reference 05/Q1605/66). Four sections, each at a thickness of 10 μm, were cut from each block and given a unique anonymous ID number. DNA was extracted as described in section 2.2.1.2.

2.2.5.2 Molecular testing

Thirty cases of paired biopsy and subsequent resection specimens were randomly selected. Samples were screened for mutation in KRAS (codons 12/13, 61, and 146), BRAF (codon 600 and exon 11), PIK3CA (exons 1, 9, and 20), TP53 (exons

5–8), and microsatellite instability using PCR-HRM based approach. For all cases the final single diagnostic reaction was performed in duplicate, and, in all cases, sequence-proven wild-type samples were run as controls alongside the experimental samples and used as reference samples for evaluation of the HRM data. However, for technical reasons related to the nature of the target sequence and the required test, three assays were used as describe in the following three subsections.

2.2.5.2.1 Mutation screening for KRAS/ BRAF/ PIK3CA

These cases were tested for mutations in KRAS exon 2 (codons 12/13), exon 3 (codon 61), and exon 4 (codon 146), BRAF exon 11 and exon 15 (codon 600), and in PIK3CA exons 1, 9, and 20. Screening for mutations in these hotspots was undertaken using Modified QMC-PCR/ protocol 2 as described in section 2.2.3.3.10.5.

2.2.5.2.2 Testing for MSI

Screening for MSI was performed with a single plex PCR followed by HRM analysis. PCR reaction mixture, thermal cycling was performed on the ABI 7500 fast PCR machine, and HRM analysis was performed as described above in section 2.2.4.3. The cases used in this study were tested for the MMR proteins expression as mentioned in section 2.2.4.3.

2.2.5.2.3 Mutation screening for TP53

Screening for TP53 mutation was performed using a refined nested PCR-HRM protocol. Basically, because the sequence of TP53 is a GC-rich one, which makes it thermodynamically more stable and higher annealing temperature is required for successful amplification. So, it was not possible to apply the universal SSD annealing temperature (55 ˚C) to this template. Instead, a unique annealing temperature were optimised and used for each of the five TP53 target sequences

(details of TP53 primers are listed in Table 2-2 and Table 2-3). For TP53 mutation, five primer pairs were used to cover the hotspot of exons 5–8. PCR Reaction mixtures for the PDM and SSD are as described above (section 2.2.3.3.10.3). The thermal cycling conditions were performed on the ABI 7500 fast PCR machine as follows: PDM was 1 cycle at 95°C for 10 min; and 45 cycles of 95°C for 3 s, 53°C for 30 s, and 72°C for 10 s, while SSD was 1 cycle at 95°C for 10 min; and 45 cycles of 95°C for 3 s, annealing temperature for 30 s, and 72°C for 10 s. HRM was performed as described above (2.2.3.3.10.5). The amplification and melting peaks from the refined TP53 PDM-PCR are shown in Figure 2-14

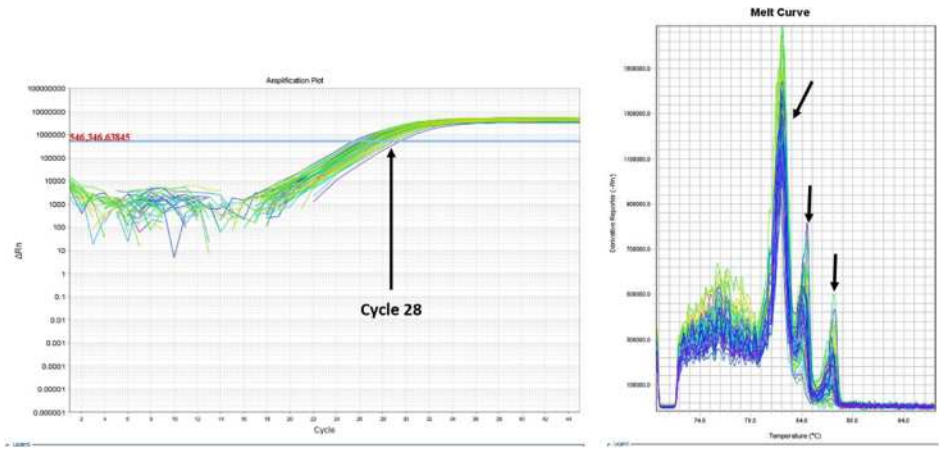

Figure 2-14 TP53 PDM-PCR

P53 multiplex PCR using the ABI 7500 fast PCR machine. **(Left)** amplification plot showing efficient and consistent amplification of all samples. All samples started to amplify simultaneously at cycle 28, which indicated good and comparable quality of the tested samples. **(Right)** dissociation curve showing multiple melting peaks (arrows) which confirmed the amplification of multiple PCR products.

2.2.5.3 Evaluation of immunostaining for mismatch repair (MMR) protein expression in diagnostic biopsies and corresponding resection specimens in CRC

Full description of the patient samples used in this study is in section 2.1.2.1, and it is referred to there as the biopsy versus resection set. Tumour sections from 30 consecutive cases of CRC and their corresponding pre-surgical diagnostic biopsies

were anonymised, stained for all 4 MMR proteins and reviewed blind. Immunostaining for mismatch repair (MMR) protein is described below in section 2.2.7.2. Initially, an assessment of each case was made in accordance with the local diagnostic reporting protocol at the department of histopathology, NUH, NHS TRUST. Only nuclear staining is assessed and scored as follows: Present (some positive tumour nuclei showing greater staining intensity of staining than stromal nuclei), absent (all tumour nuclei negative with positive adjacent stromal nuclei), Indefinite (positive tumour nuclei with intensity of staining similar or less than adjacent stromal nuclei) and Unassessable (negative tumour nuclei and negative stromal nuclei). A total of 240 sections were stained and in 239 (99%) sections the IHC could be assessed (i.e. some stromal cell staining was apparent). The section that was unassessable was from a resection specimen.

2.2.6 Chromosomal instability analysis in CRC

To study the chromosomal instability in CRC, DNA content (ploidy) was examined in 89 sporadic microsatellite-stable CRCs using flow cytometry. The tumours were also screened for mutations in KRAS/BRAF/TP53/PIK3CA by QMC-PCR. In order to examine the value of tumour ploidy in predicting response to chemoradiotherapy, DNA content was tested in a separate group of 62 rectal cancers treated with neoadjuvant chemoradiotherapy.

2.2.6.1 Sample collection

Three sample sets were tested (please see section 2.1.2.1). Nottingham series set-1 & 2 was used for the study to evaluate the DNA content and mutation profiles of CRCs. A total of 100 anonymised cases of sporadic CRC who underwent surgery between 1993 and 2008 were selected from the archives of the Nottingham University Hospitals Department of Histopathology. Only cases in which clinic-pathological data were available were selected and one tumour block (containing

at least 50% tumour) from each case was chosen for testing. Of these, 11 cases were excluded due to either the presence of microsatellite instability (see below) or PCR failure. The remaining 89 cases underwent DNA content analysis and mutation profiling.

Nottingham series set-3 was used only for the study to evaluate the association between DNA content (ploidy) and regression following neoadjuvant chemoradiotherapy (CRT). A series of 62 cases were selected from a previously reported series (Dhadda et al., 2011). Of these, 22 cases had shown a marked response (i.e. Mandard Tumour Regression Grade 1 or 2) whilst 40 cases had shown little or no response (Mandard Tumour Regression Grade 3 – 5). If ploidy is associated with responsiveness to CRT, one would expect a non-random distribution of aneuploid and diploid genotypes between the responders and non-responders. The pre-CRT biopsies from these cases were retrieved from the archives of the Nottingham University Hospitals Department of Histopathology and were tested for DNA content analysis. All experimental work was undertaken with local institutional approval.

2.2.6.2 Molecular analysis of tumour samples

2.2.6.2.1 DNA isolation

DNA was extracted from Formalin-Fixed Paraffin-Embedded (FFPE) tissue from all cases of Nottingham series set-1 & 2 as described in section 2.2.1.2.

2.2.6.2.2 Testing for Microsatellite Instability

All cases in sample set-1 & 2 were screened for the presence of microsatellite instability (MSI) which was performed by PCR followed by HRM analysis as described in section 2.2.4.3.

2.2.6.2.3 Mutation analysis

All cases in Nottingham series set-1 & 2 were screened for mutation in the hotspots of KRAS (Codons 12/13, 61 and 146), BRAF (Codon 600 and exon 11) and PIK3CA (exon 1, exon 9 and exon 20) using the modified QMC-PCR/ protocol 2 followed by high resolution melting (HRM) analysis as described in section 2.2.3.3.10.5. Also, all samples were screened for mutation in the TP53 mutation hotspot (exon 5-8) using the refined TP53 protocol as described above (section 2.2.5.2.3)

2.2.6.2.4 Ploidy analysis

2.2.6.2.4.1 Isolation of nuclei

The DNA content of tumour cells was measured by flow cytometry using FFPE tumour tissue. All tumours (Nottingham series set-1 & 2) were tested and whole nuclei were extracted using a modification of the method of Hedley et al (Hedley et al., 1983).

Following pathology review (to choose the block with the highest proportion of tumour cells), a single 30µ thick section was cut. Sections were de-waxed in xylene and rehydrated in graded alcohols. The sections were washed in distilled water (twice) and then digested at 37 °C in 1 ml of 1.5% pepsin (p-7000, Sigma Aldrich) in 0.9% NaCl (pH 1.5) for two hours with intermittent vortex mixing. Following digestion, the sections were vigorously vortexed for 60 seconds to release the nuclei. The suspended nuclei were counted using a Neubauer chamber to ensure that there were more than 106ml-1 nuclei present. The tissues were then passed through a 70µm nylon filter (Becton Dickinson) and centrifuged at 1,500rpm for 5 minutes. The supernatant was removed and the pellet was re-suspended and washed twice in PBA (0.1% BSA in PBS) to remove residual pepsin. The cell pellet then was re-suspended in the staining solution in the flow cytometer tubes.

2.2.6.2.4.2 Flow cytometry

Prior to analysis by flow cytometry, the suspended nuclei were stained by incubation for 30 minutes Propidium Iodide and RNase (both Sigma) at a respective final concentration of $1mgml^{-1}$ and $10mgml^{-1}$ in PBA. Flow cytometry was performed on a Beckman Coulter FC500 Flow Cytometer and experiments were performed following the guidelines of Ormerod et al (Ormerod et al., 1998), using doublet discrimination on a DNA fluorescence area vs peak plot. Fluorescence from a minimum of 30,000 events per sample was captured over 1024 channels and samples were deemed unacceptable if background aggregates and debris (i.e. sub-G1 fraction and clumps) comprised >20% of the total events.

Each tumour sample consists of tumour cells together with stromal cells and lymphocytes. The non-tumour cells are diploid and were used to set internal parameters and as internal controls. The Photomultiplier Tube (PMT) voltage of the flow cytometer was adjusted so that the G0/G1 peak of the non-tumour cells was captured at a channel number >200. The G0/G1(2c) and G2/M (4c) peaks of the internal controls were assigned to the channel with the maximum fluorescence for each and a sample was acceptable if there was linearity between the G0/G1 and G2/M peaks (i.e. the ratio was between 1.95 and 2.05), the G2/M peak did not exceed 10% of the total events, the proportion of events at >6c (i.e. clumps) was not greater than 1% and the co-efficient of variation of the G0/G1peak for the internal controls was <6%.

2.2.6.2.4.3 Data analysis

Data analysis was performed using the Weasel v2.7 software (www.wehi.edu.au). Every single sample had easily identifiable 2c and 4c peaks for the internal non-tumour cells. The DNA index (DI) for additional peaks was calculated as the ratio of the channel position of the tumour G0/G1 peak to the control G0/G1 peak.

Tumour samples were considered diploid / near-diploid when the DI was between 0.9 and 1.1 and aneuploid when the DI was outside these ranges. If the G2/M (4c) peak of the controls comprised more than 10% of the total and there was a corresponding 8c peak, the tumour was deemed as tetraploid.

2.2.7 Immunostaining for MMR and TP53 proteins in the VICTOR series

2.2.7.1 Tissue microarrays (TMA)

Formalin-fixed paraffin-embedded (FFPE) tumour samples was collected (with full consent for research use) from 1006 patients. Of these, 884 were suitable for use in tissue microarrays (TMAs) and the characteristics of this population were typical of the whole VICTOR population (Table 2-6). Three cores of tumour (plus, if available, one core from adjacent normal tissue) were taken from each block and a total of 29 TMAs were assembled at the Astra-Zeneca Oncology Molecular Pathology laboratory (Alderley Park, Cheshire, UK) and Oxford University Oxford Radcliffe Bio-bank using standard techniques.

Table 2-6 Comparison of basic summary of patient characteristics in all VICTOR patients versus tested groups

This table shows that the characteristics of the tested population were typical of the whole VICTOR population and was an extremely good outcome in the VICTOR trial patients IHC: Immunohistochemistry; MMR: mismatch repair.

		No of patients			
		All VICTOR Patients	**IHC MMR (n=735)**	**IHC P53 (n=740)**	**MMR/P53 (n= 677)**
Sex n (%)	M	1560 (64)	468 (64)	474 (64)	432 (64)
	F	874 (36)	267 (36)	266 (36)	245 (36)
Age Mean (SD)		64 (10)	64 (10)	64 (10)	64 (10)
Stage n (%)	II	1159 (47)	337 (46)	334 (45)	308 (45)
	III	1275 (52)	398 (54)	406 (55)	369 (55)
Chemotherapy n (%)	Yes	1580 (65)	467 (64)	482 (65)	434 (64)
	None	854 (35)	268 (36)	258 (35)	243 (36)
Radiotherapy n (%)	Yes	299 (12)	75 (10)	77 (10)	72 (10)
	None	2135 (88)	660 (90)	663 (90)	605 (89)
Recurrence (%)		704 (29)	201 (27)	208 (28)	190 (28)
Deaths (%)		487 (20)	145 (20)	146 (20)	135 (20)
Disease Free Survival					
All					
3yr [95% CI]		74.6 [72.7, 76.3]	76.5 [73.2, 79.5]	75.8 [72.5,78.8]	76.0 [72.5, 79.1]
5yr [95% CI]		66.5 [64.3, 68.7]	67.8 [63.4, 71.7]	67.0 [62.7,71.0]	66.8 [62.3, 70.9]
Stage II					
3yr [95% CI]		83.9 [81.5, 86.0]	86.1 [81.8, 89.5]	86.6 [82.2, 89.9]	86.2 [81.7, 89.7]
5yr [95% CI]		76.4 [73.3, 79.2]	78.0 [71.6, 83.2]	78.1 [71.6, 83.3]	77.9 [71.0, 83.3]
Stage III					
3yr [95% CI]		66.2 [63.4, 68.8]	68.1 [63.1, 72.5]	67.2 [62.2, 71.6]	67.6 [62.4, 72.2]
5yr [95% CI]		57.7 [54.4, 60.8]	59.0 [53.1, 64.5]	58.2 [52.4, 63.6]	58.0 [51.8, 63.6]
Overall Survival					
All					
3yr [95% CI]		87.3 [85.8, 88.6]	88.1 [85.5, 90.3]	87.8 [85.2,90.0]	88.0 [85.3, 90.3]
5yr [95% CI]		78.2 [76.3, 78.0]	78.6 [75.2, 81.7]	78.8 [75.3, 81.8]	78.5 [74.9, 81.7]
Stage II					
3yr [95% CI]		93.3 [91.6, 94.6]	93.8 [90.6, 96.0]	94.4 [91.2, 96.4]	93.9 [90.6, 96.2]
5yr [95% CI]		86.6 [84.2, 88.7]	87.2 [82.6, 90.7]	88.9 [84.4, 92.1]	88.0 [3.2, 91.5]
Stage III					
3yr [95% CI]		81.9 [79.6, 83.9]	83.3 [79.2, 86.6]	82.4 [78.3, 85.8]	83.2 [78.9, 86.6]
5yr [95% CI]		70.7 [67.9, 73.4]	71.6 [66.6, 76.0]	70.8 [65.8, 75.2]	71.0 [65.7, 75.6]

2.2.7.2 **Immunohistochemistry (IHC)**

All immunohistochemistry (IHC) was performed using compact polymer technology on an automated Bond-Max (Leica Microsystems, Germany) in the fully accredited IHC division of the Diagnostic Histopathology Department of the Nottingham University Hospitals NHS Trust (Nottingham, UK). The MMR panel comprises four antibodies - MLH1 (clone ES05; Leica, cat. no.NCL-L-MLH1),

MSH2 (clone 25D12, Novocastra, cat. no.NCL-MSH2), MSH6 (clone 44/MSH6, BD Transduction Labs, cat. no.610918), and PMS2 (clone A16-4, BD Pharmingen, cat. no.556415). The primary antibody against P53 was the D07 clone (Leica Microsystems, NCL-L-p53-D07).

2.2.7.2.1 Protocol for immunohistochemistry

MLH1 was stained optimally at a dilution of 1:100 with antigen retrieval performed using Epitope Retrieval solution 1 (ER1) for 30 min; MSH2 at 1:50 with Epitope Retrieval solution 2 (ER2) for 30 min; MSH6 at 1:100 with ER1 for 20 min; and PMS2 at 1:100 with ER2 for 30 min; and P53 at 1:100 with ER1 for 30 mins. ER1 (AR9961) is a ready-to-use citrate-based pH 6.0 solution; ER2 (AR9640) is a ready-to-use EDTA based pH 9.0 solution. Positive control sections were colorectal tumour expressing p53, and appendix for the MMR panel.

Sections were cut at 3 µm, dried at room temperature for 20 min, then, incubated at 60°C for 20 min prior to loading onto the automated Bond strainers. The staining machines perform all steps in the procedure from dewaxing to counterstaining.

The Bond staining protocol is briefly as follows: Dewax using Leica Dewax solution (AR9222) for 30 s at 72°C, followed by the appropriate antigen retrieval step. After washing in Leica Bond wash solution (AR9590) sections were immersed in peroxide block solution (Kit DS9800) to block endogenous peroxidase for 5 min at RT. Primary antibody incubation was for 15 min at RT, post primary and polymer detection system were incubated each for 8 min at RT, before DAB for 10 min at RT followed by the DAB enhancer (AR9432) for 5 min at RT. The sections were counterstained with haematoxylin for 5 min at RT. All wash steps were performed using Leica Bond Wash solution (AR9590) between each step. Peroxidase block, post primary, polymer, DAB and Haematoxylin are all supplied in Leica Bond Refine Detection kit (DS9800). Finally, sections were then removed

from the Bond staining machine, dehydrated in three baths of 100% Industrial methylated spirits (Genta Medical), cleared in Xylene (Genta Medical) and permanently mounted under glass coverslips using Pertex (Histolab).

2.2.7.3 Criteria for the scoring of the IHC

The stained TMA sections were scanned (at X40 magnification) using the NanoZoomer Digital slide scanner (Hamamatsu, Japan) and the digital images were uploaded into the slidePath digital pathology system (Leica microsystems) and scored using Distiller software. Blinded scoring was performed by two independent observers for p53 (W.F and M.M) and the MMR panel (M.I and W.F).

The antibodies for the MMR proteins (MLH1, MSH2, MSH6, PMS2) are fixation-dependent and may result in difficulties in interpretation (Fadhil and Ilyas, 2012, Klarskov et al., 2010, Shia et al., 2011). In order to avoid misinterpretation, stringent scoring criteria were used. Each of the antibodies was scored individually and only the nuclei were assessed. Cores were scored as "positive" (if there was nuclear staining in the tumour cells which was stronger than the nuclear staining in the adjacent stromal cells), "negative" (if there was no nuclear staining in the tumour cells but there was positive nuclear staining in the adjacent stromal cells) or "unclassifiable" (if there was no nuclear staining in either the stromal cells or the tumour cells). Once the scoring of all the antibodies was completed, the whole panel was assessed for each core. A tumour was deemed as having deficient MMR (dMMR) if one or more of the immunostains was negative in the tumour cells of all three cores. However, it is known that loss of nuclear MLH1 expression is almost always accompanied by loss of its binding partner PMS2 (Figure 2-15) and loss of MSH2 expression is almost always accompanied by loss MSH6. A core was only scored as negative for MLH1 if it was also negative for PMS2. Similarly, negative staining for MSH2 was only accepted if there was negative MSH6

staining. In contrast, loss of PMS2 or MSH6 expression is known to occur without being accompanied by loss of the respective binding partner. Thus, individual loss of either PMS2 or MSH6 was accepted if the other criteria were fulfilled.

Three patterns of TP53 immunostain were previously described (Abdel-Fatah et al., 2010, Callagy et al., 2006, Abdel-Fatah et al., 2008, Vagunda et al., 2003, Allred et al., 1998), by analysis of these reports we found that assessment of P53 expression was based on the intensity, pattern and percentage of stained tumour nuclei and we decided, in agreement with the previous investigators, that a cut-off of 10% positive tumour nuclei with intense staining to dichtomise the expression scores into positive and negative groups. The importance of this scoring system is that it could serve as a surrogate marker for the existence of TP53 gene mutations (Lonning et al., 2007, Sjogren et al., 1996, Geisler et al., 2001, Nenutil et al., 2005, Abdel-Fatah et al., 2010). Non-neoplastic colonic mucosa, inflammatory and stromal cells adjacent to neoplastic cells show weak staining and served as positive internal controls. Using these as a reference, two patterns of aberrant p53 expression were seen.

In this study, the more common pattern was strong nuclear expression in >10% of the tumour cells and this has been shown to be indicative of misense mutations of TP53 (Baas et al., 1994). In addition, we and others have described a pattern characterised by complete loss of p53 expression in the tumour cells and this has been correlated with truncating TP53 mutations (Kaye et al., 2010, Kobel et al., 2010). Either of the aberrant patterns was classed as “p53+” whilst other patterns were classed as “p53-” (Figure 2-15). There were tumours where neither the tumour cells nor the stromal cells showed any p53 expression and these cases were considered as “unclassifiable” and omitted from further analysis.

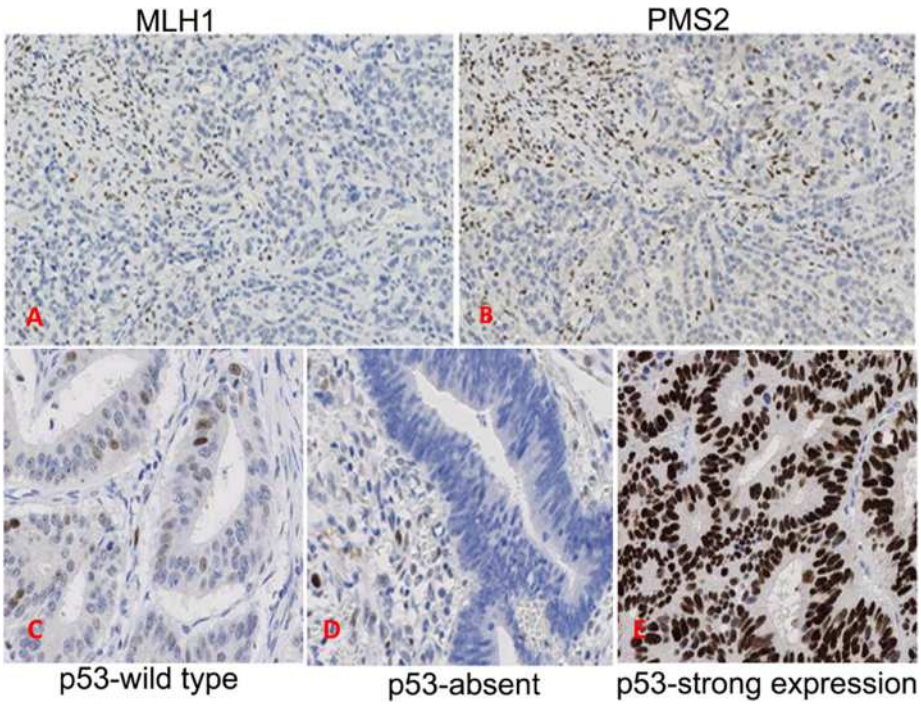

Figure 2-15 Immunohistochemical staining for mismatch repair (MMR) and p53 proteins.

The antibodies for the MMR proteins, especially MLH1 and MSH6, are prone to fixation artefact and, in order to avoid over-interpretation of this and other potential technical artefacts, evaluation of each marker was dependent on the whole panel. The top panels show immunostaining for a case which was negative for MLH1 (top left panel, Figure 1A) and PMS2 (top right panel, Figure 1B). Since MLH1 loss is always accompanied by loss of PMS2, in such cases the defect was attributed to loss of MLH1 expression. Conversely, if there was apparent loss of MLH1 but PMS2 was retained, this was regarded as a false negative MLH1 test and the tumour was scored as proficient for MMR. Figure 1c shows the aberrant patterns of p53 staining. Ordinarily tumours with wild type p53 would be expected to show weak staining in the epithelium and stroma (bottom left panel, Figure 1C). With truncating mutations, the epithelium is negative but the stroma is weakly positive (i.e. the "absent" pattern, bottom central panel, Figure 1D). With misense mutations, the epithelium is strongly positive (bottom right panel, Figure 1E). The patterns of strong expression and the absent pattern were grouped together and scored as p53+ (as this is indicative of TP53 mutation) whilst the weak expression was scored as p53-. Validation of the IHC was performed by: (a) inclusion of Positive and negative (omission of the primary and post primary antibodies) controls in each run, and (b) inclusion of known positive and negative tissue controls in each run.

2.2.8 Statistical analysis Methods

2.2.8.1 VICTOR study

For MMR status, tumours were scored as dMMR, pMMR or unclassifiable. For

p53, tumours were scored as p53+, p53- , p53 absent or unclassifiable. Absent was grouped with p53+ and the unclassifiable group were excluded from all analysis. Cases stained for both p53 and MMR were combined into 4 groups, dMMR/p53-, dMMR/p53+, pMMR/p53-ve and pMMR/p53+. Descriptive statistics of p53, MMR and p53/MMR combined are presented, including the number of samples expressed at each level.

Overall survival (OS) is defined as the time from randomisation until death from any cause. Patients not reported as dead were censored at their last known date alive. Disease free survival (DFS), a secondary endpoint, is defined as time from randomisation until recurrence or death from any cause. Patients who were alive and recurrence-free were censored at their last known recurrence-free date. OS and DFS are displayed using Kaplan Meier plots by expression category together with the associated log-rank test for both MMR and p53. Univariate and multivariate analysis was undertaken using the Cox proportional hazard model for p53 expression, MMR, and p53/MMR combined adjusting for treatment and for clinical factors including gender, tumour site (proximal – defined as proximal to the sigmoid colon; distal – defined as within the sigmoid and rectum), tumour stage, age and prior chemotherapy and radiotherapy treatment. Hazard ratios and 95% confidence intervals are presented. The proportional hazards assumption was assessed graphically and using the proportional hazards test. Analyses were repeated by stage and chemotherapy treatment. Associations between p53 and MMR with prognostic categorical clinical variables were tested using Pearson chi-square test or a Mantel Haenszel test for trend where appropriate. Analysis was carried out using STATA version 11.0.

2.2.8.2 Elsewhere statistical analysis

Statistical analysis was performed using the GraphPad Prism software package

(GraphPad Software Inc., USA). Categorical data were tested for association using a two-sided Pearson's chi-square test or Fisher's exact test, where appropriate. Non-parametric continuous data were analysed using the Mann-Whitney test. In all cases p-values <0.05 was considered as statistically significant.

Chapter 3. **Molecular pathology methodology development**

3.1 Introduction

Cancer management has traditionally depended heavily on histopathology. From morphological evaluation of the initial diagnostic biopsy to mapping of disease spread in resection specimens, the Pathologist has been central to the decision-making process in most types of tumour. Descriptive analysis of tumours is however prone to inter-observer variation and does not give any insight into tumour biology (Morris et al., 2008). As the number of treatment options increases, new criteria – in addition to those used by Pathologists – are required for more consistent classification / staging of tumours and to allow bespoke tailoring of therapies based on tumour biology. New criteria may comprise "profiling" the mutations present within a tumour. Some mutations are specific for certain types and sub-types of cancer and can therefore be used for diagnostic classification of those cancers (Lee et al., 2005). Other mutations seem to carry prognostic importance and, perhaps most importantly, some mutations are predictive of response to specific therapies (Nomoto et al., 2006, Marchetti et al., 2005, Willmore et al., 2004, van Krieken et al., 2008, Amado et al., 2008, Lièvre A, 2006, Van Cutsem et al., 2009). For example, it has been shown that the presence of KRAS mutations in colorectal cancers abrogates tumour response to anti-EGFR therapies and the National Comprehensive Cancer Network (NCCN) guidelines now recommend routine testing for KRAS mutation in all cases where such therapy is being considered (http://www.nccn.org/).

Predictive testing assumes even more importance when considering neo-adjuvant chemotherapies since significant clinical down-staging can be achieved before definitive surgery and thus correct choice of therapy is essential. A variety of techniques can be used for mutation analysis. Direct DNA sequencing is generally regarded as the 'gold standard' although it is expensive, laborious and gives false negative results when a large number of normal cells are admixed with tumour

cells. Since mutations can occur in multiple sites in a gene (usually known as "hotspots") and multiple genes may be mutated within a specific pathway, detection of pathway disruption by direct sequencing would be prohibitively expensive. Screening of hotspots for mutation prior to sequencing could reduce this cost by excluding wild type samples from further analysis. Techniques such as single strand conformation polymorphism (SSCP) (Gupta et al., 2005), temperature gradient gel electrophoresis (Langerod et al., 2007), denaturing high performance liquid chromatography (Rossetti et al., 2007) and MALDI-TOF (Koren-Michowitz et al., 2008, van den Boom and Ehrich, 2007) have been developed for the purposes of mutation detection. However, these techniques are complicated, expensive and tend to be available only in research institutions. Furthermore, even in research institutes, routine practice is for tumour tissue to be formalin fixed and paraffin embedded to allow histological analysis. Tissues thus processed tend to suffer DNA degradation and the utility of sophisticated screening techniques on this type of template remains to be proven.

High Resolution Melting analysis and pyrosequencing are probably the most versatile and easy to interpret techniques. High Resolution Melting analysis is a cheap in-tube (i.e. non-gel based) mutation detection technique that works on the basis that a difference in DNA sequence results in differences in the way the DNA melts (Wittwer et al., 2003). This is particularly pronounced when mutant and wild allele are mixed since the formation of heteroduplexes results in a unique melting pattern. Unlike the other techniques it requires no post-PCR processing, expensive fluorescently labelled oligonucleotides or allele-specific PCR and interpretation of the data is very simple. HRM was initially developed for detection of Single Nucleotide Polymorphisms (SNPs) but it is suitable for mutation analysis (Reed and Wittwer, 2004). HRM technique has been used to identify somatic mutations in a variety of genes (Wittwer et al., 2003) and recently, it has been used for quantitative methylation detection (Wojdacz and Dobrovic, 2007). Pyrosequencing

is an alternative method to Sanger sequencing which is quick, gel-free and reportedly has a lower limit of detection that Sanger sequencing.

Real-time PCR is a quantitative assay which uses fluorescent reporters and is therefore exquisitely sensitive for detection of small quantities of nucleic acid. The commercially available DxS test is a real-time PCR assay which has been recently developed for the detection KRAS mutation in FFPE tissue. This assay uses amplification refractory mutation specific (ARMS) PCR to enrich for mutant alleles and scorpion probes as reporters (Thelwell et al., 2000). It has been designed to detect the seven most common sequence changes seen in KRAS mutation in CRC. This method has been shown to compare very well with Sanger sequencing and, since it uses real-time technology and mutant allele enrichment, it will pick up a few as 1% of mutant alleles in a DNA sample (Thelwell et al., 2000, Whitcombe et al., 1999, Board et al., 2008).

As with all the screening techniques, HRM is dependent on quality of DNA template. Our experience hitherto and that of others is that HRM on FFPE tissue is prone to false positive artefacts (Do et al., 2008). This study sought to refine the HRM technique to make it sufficiently robust for diagnostic use in FFPE tissue, and to perform in a comparable efficiency to two other sensitive techniques, pyrosequencing and real-time PCR assay for KRAS mutation detection, respectively. Herein we describe a simple, standardised and rapid methodology which allows multiple genes to be screened and analysed in an automated fashion. Using this technique, a mutation profile of a tumour can be rapidly produced. Furthermore, it is sufficiently cheap and simple to be implemented in Pathology laboratories in both teaching hospitals and non-teaching hospitals.

3.2 Development of the QMC-PCR

3.2.1 Quality Control and single step PCR/HRM

Template quality control consisted of multiplex PCR for four different sized fragments (100, 200, 300, and 400bp) in the reference gene, GAPDH. As expected, when high quality DNA extracted from cell lines was tested, all four bands were present indicating minimal fragmentations. These are seen as specific peaks in the derivative plot produced by HRM analysis (Figure 3-1). However, the FFPE samples produced variable numbers of band reflecting variable DNA integrity. However, 7/50 (14%) of the samples (predominantly the older samples) did not show any amplification and were deemed unsuitable for PCR and not further analysed.

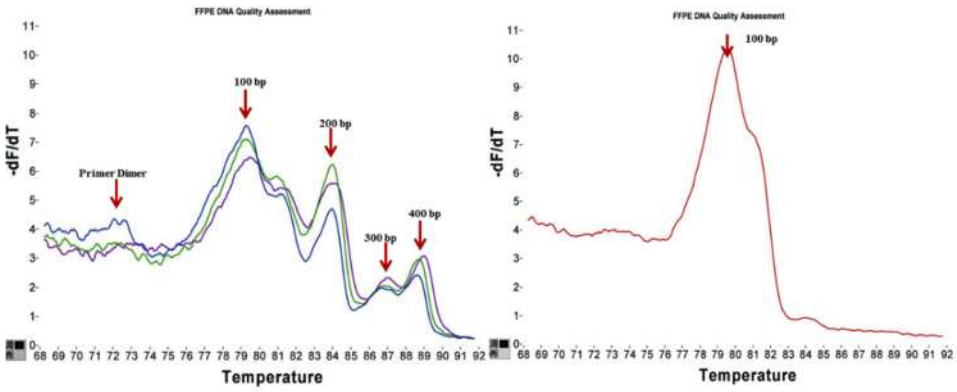

Figure 3-1 HRM testing of DNA quality.

A multiplex PCR was performed using four primer pairs intended to give 4 different sizes of PCR products, The PCR products analysed using high-resolution melting after addition of LC green. (Left) High quality DNA produced fragments of 100, 200, 300 and 400 bp, which are seen as four peaks on the derivative plot (arrowed). (Right) Sample producing just a single peak of 100 bp. If there was no evidence of PCR amplification, the DNA was deemed too poor for PCR analysis. A small peak is also seen after the 100bp peak, this could be a result of a multiple transition melting curve due the presence of short runs of similar nucleotides which melt differently. The melting temperature (a unique characteristic of PCR product and indicator of specificity of amplification) is usually determined by plotting the negative derivative of fluorescence (-dF/dT) on the y-axis versus the temperature on the x-axis (-dF/dT against temperature) where the steepest slope is easily visualised as a melting peak.

3.2.2 QMC-PCR on DNA from cell lines

Twenty-nine cell lines underwent direct sequencing analysis of the hotspots in KRAS and BRAF and were then screened by QMC-PCR. The results showed 100% sensitivity and specificity together with 100% positive predictive value (PPV) and 100% negative predictive value (NPV) (Figure 3-2, Figure 3-3, Table 3-1 and Table 3-2). Cell lines were then screened for somatic mutations in 10 hotspots in KRAS, BRAF, PIK3CA, and FBXW7 using the QMC-PCR protocol and, of the 40 mutations detected, every single one was confirmed by sequencing (100% PPV). Thus, even though the PDM reaction contained 10 primer pairs the QMC-PCR protocol with HRM showed outstanding performance when compared to direct sequencing.

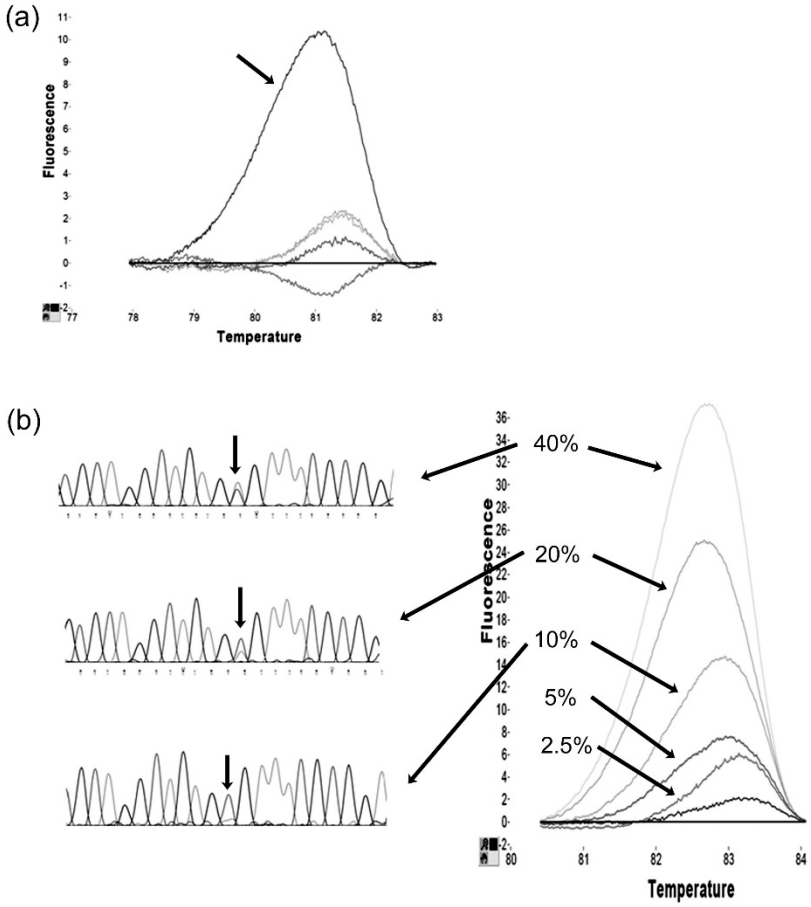

Figure 3-2 Optimisation and testing QMC-PCR. High-quality DNA from fingerprinted cell lines was used to optimise the QMC-PCR protocol

(a) is the difference plot of BRAF exon 15 conducted on 6 cell lines and shows how one of the cell lines containing a heterozygous mutation (HT29, arrowed) melts differently to the five wild type alleles due to the formation of heteroduplexes. (b) shows spiking experiments to test the limit of detection of QMC-PCR in comparison with direct sequencing. Pure genomic DNA from known mutant diploid cell lines (50% mutant allele) was spiked into pure genomic DNA of known diploid wild types (0% mutant allele) to produce mixtures containing 40%, 20%, 10%, 5%, 2.5% and 1.25% mutant alleles. The difference plot (for BRAF exon 15, on the right side) shows that as few as 2.5% mutant alleles can be detected by HRM. In contrast, the chromatograms (on the left side) show that the mutant allele cannot be detected below the 20% level by direct sequencing. The reference sample (baseline x-axis) in the difference plot is the wild type sample (0% mutant allele).

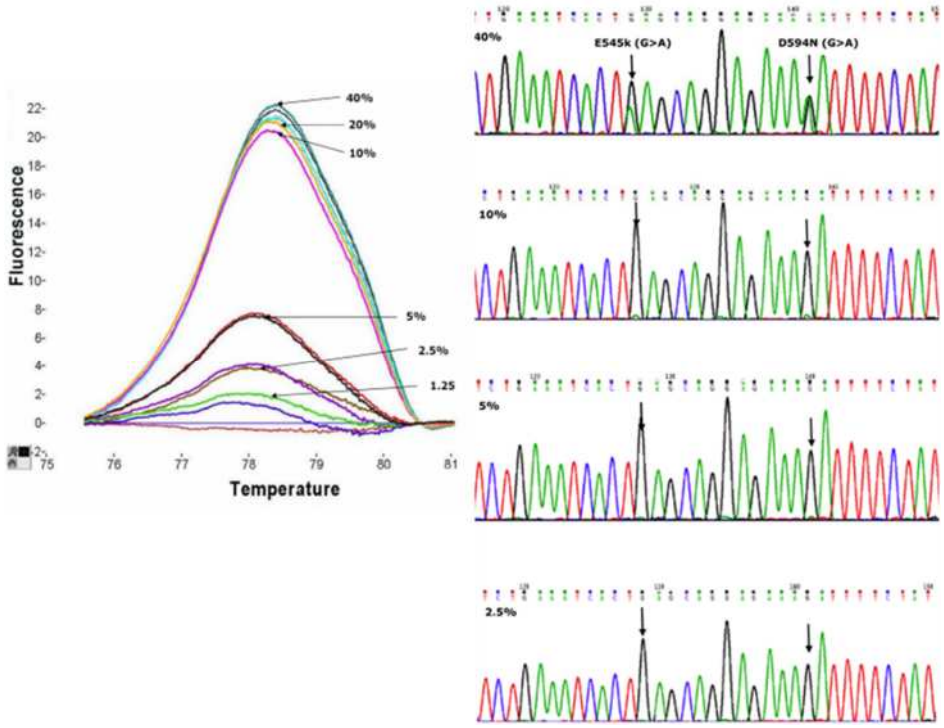

Figure 3-3 The limit of detection of QMC-PCR in comparison with direct sequencing using pure genomic DNA from cell lines

Spiking experiments using pure genomic DNA from diploid cell lines to test the limit of detection of QMC-PCR in comparison with direct sequencing. DNA from known mutant cell lines was spiked into DNA of known wild types to produce mixtures containing 40%, 20%, 10%, 5%, 2.5% and 1.25% mutant alleles. (Left) The difference plot (PIK3CA exon 9) shows that as few as 2.5% mutant alleles can be detected by HRM. In contrast, the chromatograms (on the left side) show that the mutant allele cannot be detected below the 20% level by direct sequencing as no double peaks can be visualised in the chromatograms for the 10% sample run, while is very obvious on the 40% run above it. .

Table 3-1 Comparison between mutation detection in cell lines by HRM and Direct sequencing

Comparison of QMC-PCR/HRM performance with direct sequencing in cell lines. NPV cannot be calculated for the 10 hotspot tests (lower cell) as only the mutant samples were sequenced. (PPV: positive predictive value; NPV: negative predictive value)

			Sequencing analysis of hotspots		
			Mutant	**Wild Type**	
QMC-PCR & HRM analysis of hotspots	***KRAS* & *BRAF* only**	**Mutant**	23	0	(PPV 100%)
		Wild type	0	122	(NPV 100%)
	All hotspots	**Mutant**	40	0	(PPV 100%)
		Wild type	(250 – not validated by sequencing)		

Table 3-2 Mutation profile of CRC cell lines

CRC cell line genetic fingerprinting by PCR/HRM and direct sequencing

Cell line	*BRAF*	*KRAS*	*PIK3CA*	*CDC4*
C125	WT	K117N	WT	WT
C32	WT	WT	WT	R278*
C80	WT	A146V	WT	WT
C84	WT	G12A^	WT	WT
Caco2	WT	WT	WT	WT
COLO201	V600E	WT	WT	WT
COLO205	V600E	WT	WT	WT
COLO320DM	WT	WT	WT	WT
DLD1	WT	G13D	E545K D549N	WT
GP2D	T529A	G12D	H1047L	H580R
HCA7	WT	WT	WT	R479*
HCA46	WT	WT	E542K	WT
HCT116	WT	G13D	H1047R	WT
HRA-19	WT	WT	E542K	WT
HT29	V600E	WT	P449T	WT
HT55	N581Y	WT	WT	WT
HuTu80	WT	WT	WT	WT
LoVo	WT	G13D	WT	R505C
LS1034	V600E	WT	H1047R	WT
RKO	V600E	WT	H1047R	WT
SKCO-1	WT	G12V^	WT	WT
SW1116	WT	G12A	WT	WT
SW1222	WT	A146V^	WT	WT
SW480	WT	G12V	WT	WT
SW620	WT	G12V	WT	WT
SW837	WT	G12C	WT	L403fs*
SW948	WT	Q61L	E542K	WT
VACO10MS	WT	Q61L	WT	R505H
VACO5	V600E	WT	R38S H1047R	WT

3.2.3 QMC-PCR on DNA from FFPE tissues

3.2.3.1 Comparison with standard PCR-HRM

In order to be utilisable in the routine diagnostic setting, QMC-PCR must work with DNA derived from FFPE tissue. For any PCR based technique, template quality is probably the most important factors and thus we excluded 7 low quality DNA samples from further analysis. In the remaining 43 samples, a PCR product of at least 200bp could be amplified. We firstly compared QMC-PCR and HRM with standard PCR and HRM since it is possible that QMC-PCR – especially with its multiplexed reaction – may result in poorer performance of the HRM technique. We tested samples for mutation in the BRAF exon 15 hotspot and PIK3CA exon 20 and found a much higher frequency of aberrant melting using the standard

protocol than the QMC-PCR protocol. In a total of 43 tests, 7 samples were positive by standard analysis (Figure 3-4) but negative by QMC-PCR. However, the melting curve was frequently shifted to the right indicating that melting was delayed – an unexpected finding since the melting of heteroduplexes should occur earlier and the curve should be shifted to the left. All samples were sequenced, and it was shown that the 7 samples identified to be "mutant" by standard analysis but identified as wild type by QMC-PCR, were in fact all wild type. Similar figure was obtained with PIK3CA exon 20. As 9 samples showed aberrant melting in standard PCR in comparison to only 3 aberrant samples by QMC-PCR. The QMC-PCR results were confirmed by sequencing (Figure 3-5). These data are consistent with those in the literature which cite a false positive rate of around 16% when standard PCR and HRM are used for mutation detection in FFPE tissue derived DNA (Do et al., 2008). These data also show that the QMC-PCR protocol eliminates the false positives generated by standard techniques.

Although QMC-PCR worked superior to direct PCR and showed several advantages, there is still several drawbacks which could impact the utility of this assay. The main disadvantages of QMC-PCR are as follow: extra considerations are required when designing primers to match HRM requirement; inclusion of multiple primer pairs means higher possibility primer-primer hybridization with possibility of producing non-specific peaks which makes the analysis of HRM difficult; the two step nature of the process increases the potential of carry-over PCR contamination.

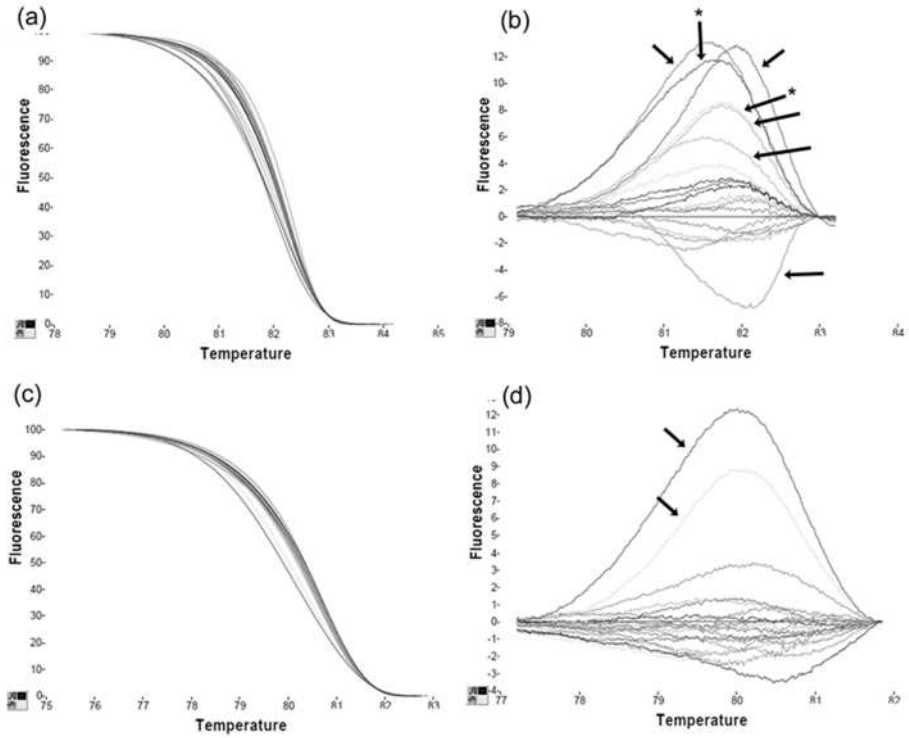

Figure 3-4 QMC-PCR eliminates false positive artefacts generated with standard PCR when using DNA from FFPE tissue.

(a) shows that with standard PCR, some samples show right shifted melting curves and (b) shows marked changes on the difference plot suggesting, in this group of samples, at least seven samples (arrowed) may contain mutations as these samples show fluorescence value higher than 4 (cut-off approved by sequencing). However, (c) shows that with QMC-PCR on these samples that there were no right shifted samples and (d) is the difference plot showing that only two were called as mutant (denoted by * in (b)). Sequencing confirmed the QMC-PCR results.

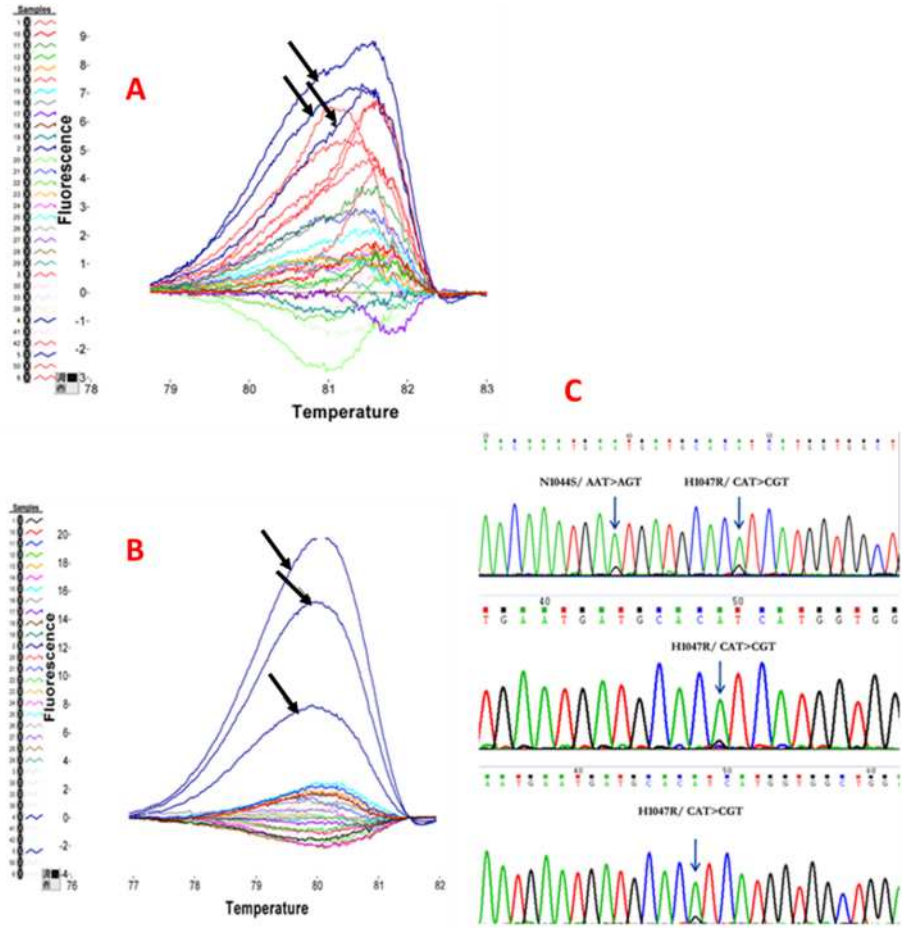

Figure 3-5 Performance of QMC-PCR versus standard PCR in FFPE tissue.

(a) shows that with standard PCR, there is marked changes on the difference plot suggesting, in this group of samples tested for PIK3CA exon 20, at least 9 samples may contain mutations. However, (b) shows that with QMC-PCR, only three samples showed aberrant melting (arrowed) and these have been confirmed by sequencing as in C (blue arrows). Top sequencing trace from sample 1 shows two mutations (N1044S, H1047R), sample 2 (middle trace) shows only 1 mutation H1047R, and the bottom trace from sample 3 shows also 1 mutation (H1047R).

3.2.3.2 **Assay precision**

In order to test the robustness of the technique, both long term and short-term precision (intra and inter-assay variation) were tested. For short term precision, one hotspot in each of PIK3CA and BRAF was tested. Two cases – one mutant and one wild type –were tested as 15 replicates and showed a very tight clustering together of the replicates (Figure 3-6 a). For long term precision analysis, a series of (sequence proven) wild type and mutant samples for a hotspot in PIK3CA were

tested on three consecutive days and yielded the same results on each occasion (Figure 3-6 b). These data show that this is a very robust and reproducible technique.

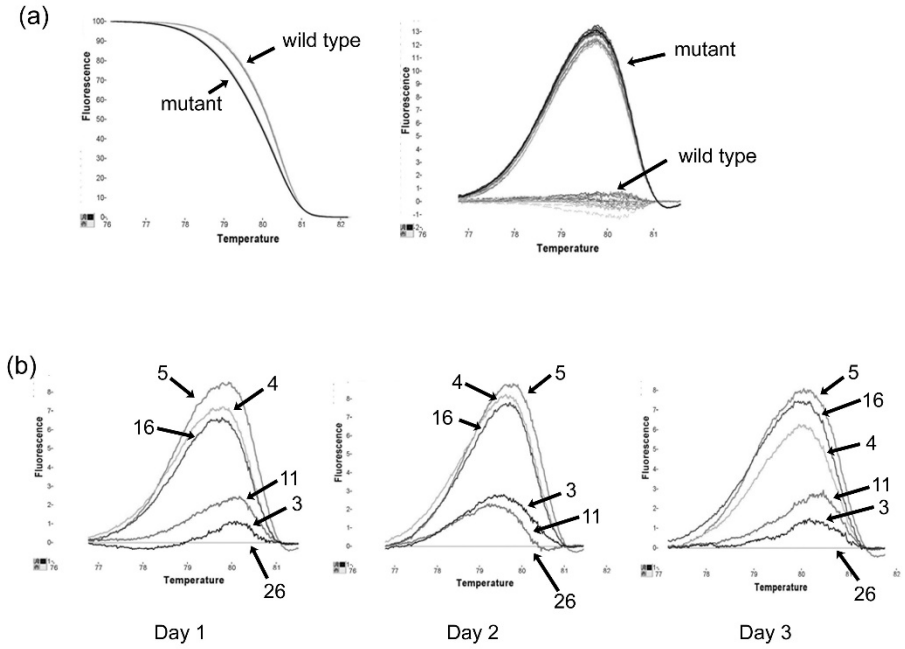

Figure 3-6 Testing reproducibility of QMC-PCR.

(a) is a difference plot showing the intra-assay variation for PIK3CA exon 20. Two FFPE samples (one mutant and one wild type) were analysed as 15 replicates and showed negligible variation. (b) Inter-assay variation for the same target sequence using 3 mutant FFPE samples (4, 5 and 16) and 3 wild types (3, 11 and 26) on three different days showing very little variation.

3.2.3.3 QMC-PCR as a screening tool in FFPE tissue

To test the utility of QMC-PCR with HRM as a screening test in DNA derived from FFPE tissue in comparison with direct sequencing, 43 samples underwent direct sequencing analysis for the hotspots in KRAS exon 2 and PIK3CA exon 20. In the KRAs test, 15/43 (35%) were called as mutant by QMC-PCR whilst in the PIK3CA test, 6/43 (14%) were called as mutant (Table 3-3). In these tests, QMC-PCR showed a sensitivity of 100%, specificity of 71%, PPV of 76% and NPV of 100%.

Table 3-3 Performance of mutation detection by QMC-PCR in FFPE tumour samples in comparison to direct sequencing

NPV cannot be calculated for the 10 hotspot tests (lower cell) as only the mutant samples were sequenced. (PPV: positive predictive value; NPV: negative predictive value)

			Sequencing analysis of hotspots		
			Mutant	Wild Type	
QMC-PCR & HRM analysis of hotspots	*KRAS* & *PIK3CA only*	Mutant	16	5	(PPV 76%)
		Wild type	0	65	(NPV 100%)
	All hotspots	Mutant	36	7	(PPV 84%)
		Wild type	(387 – not validated by sequencing)		

Following this, all cases were screened for all 10 hotspots at least twice with no change in melting pattern on repeat and in 430 screening tests, a total of 43 (10%) potential mutations were identified. All cases considered mutant underwent direct sequencing and 36/43 were thus confirmed thereby giving a PPV of 84%. However, the reproducible nature of the aberrant melting in the 7 "false positives" and the fact that we have shown that the HRM technique is much more likely to pick up small numbers of mutant alleles than direct sequencing leads us to think that these cases probably represent sequencing "false negatives" with true mutations present in a minority population of cells. Subsequently, three of those 7 cases (2 cases in KRAS exon 2 and 1 case in BRAF exon 11) were confirmed mutant by pyrosequencing, as discussed in section 3.2.5.2.

3.2.4 Cold PCR on cell lines and FFPE

The purpose of the current study was to optimize protocols for mutation detection. "Cold" PCR has recently been described as a variation on the usual protocol which can enrich for mutant alleles. Although the "cold" protocols would significantly

lengthen the mutation screening protocols, we reasoned that the time cost would be acceptable if it resulted in improved mutation detection. We empirically derived the Tc for PIK3CA exon 9 and exon 20 on our thermal cycler and tested both the "full" and the "fast" cold protocols on both spiked DNA mixtures and FFPE derived DNA. However, we found that cold PCR did not give any improvement in mutation detection over QMC-PCR.

3.2.5 Comparative analysis of Pyrosequencing and QMC-PCR

3.2.5.1 Limit of detection of HRM and pyrosequencing

All sample DNA (both cell line and FFPE-tissue derived) was of sufficient quality to allow successful PCR for all the mutation hotspots tested. HRM analysis of PCR products depends on the formation of heteroduplexes between the mutant and wild type alleles. These are more unstable than homoduplexes of either wild type or mutant sequence and thus will melt at a lower temperature. This is manifest as a "left shift" of the melting curve due to the early loss fluorescence as alleles separate to release the dye. The greater the proportion of heteroduplexes, the more pronounced the difference of the melting curves compared to pure homoduplexes. For KRAS exon 2 mutation detection, there was sufficient difference in melting characteristics for confident detection of mutation when as few as 3% mutant alleles were present in the sample (Figure 3-7a). Pyrosequencing generates sequence data by sequential addition of bases to primed template and the chemistry is such that incorporation of bases into the DNA results in light emission. There is also background "noise" even when the bases are not incorporated. Testing of the DNA mixture for KRAS exon 2 by pyrosequencing allowed confident detection of mutation when 6% mutant alleles were present in the sample. For BRAF exon 15 mutation, HRM allowed confident detection of 1.5% mutant alleles. In contrast, pyrosequencing had a lower limit of detection of 6% (Figure 3-7b).

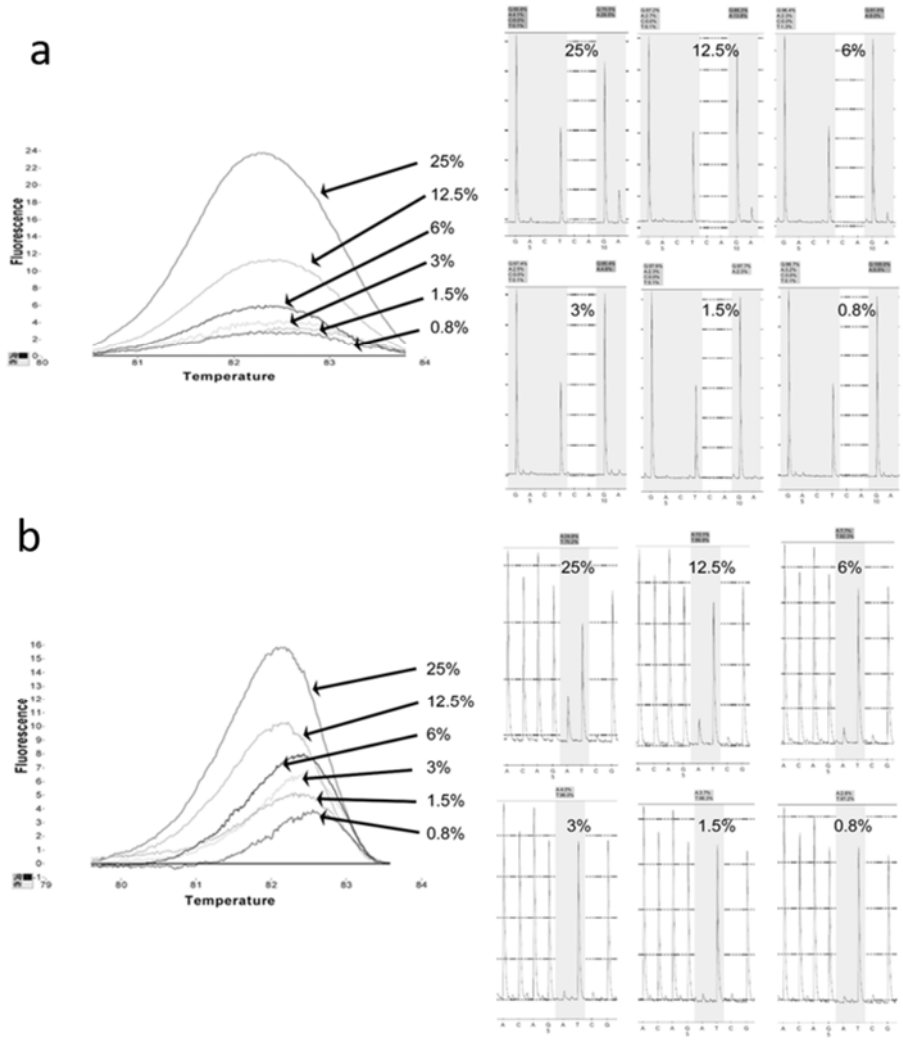

Figure 3-7 Limit of detection of HRM and pyrosequencing

Cell line DNA was admixed to produce samples containing differing proportions of mutant alleles (percentage numbers indicate calculated percentage mutant alleles present). With HRM the presence of mutant alleles can be detected due to formation of heteroduplexes which are inherently more unstable, and which melt differently when compared to homoduplexes. The difference plot shows the difference in fluorescence between each individual sample and a reference sample (usually a known wild type). Thus, greater the proportion of heteroduplexes, the more unstable is the sample and the greater the difference which can be seen on the difference plot as "peaks". With pyrosequencing, aberrant incorporation of nucleotides can be seen as novel or enhanced peaks although unincorporated nucleotides can still give background noise. HRM allows for 3% of mutant KRAS alleles (A) and 1.5% of mutant BRAF alleles (B) to be detected with confidence. By pyrosequencing, around 6% of mutant KRAS alleles and 6% of mutant BRAF alleles can be detected with confidence.

3.2.5.2 Comparative performance for mutation detection

Five different hotspots in KRAS and BRAF were tested in 22 DNA samples (9 obtained from CRC cell lines, 13 obtained from FFPE tumour tissue) by both pyrosequencing and HRM. Identical results were obtained in 109/110 tests performed (99% concordance, Chi squared test of association: $p<0.001$, Table 3-4). Of 90 cases called as wild type by pyrosequencing, all were called wild type by HRM. Of 20 samples shown to have a mutation by pyrosequencing, 19 were also called as mutant by HRM (95% specificity) with the single discrepancy seen in BRAF exon 11. So, the QMC-PCR showed 95% sensitivity, 100% specificity, 100% positive predictive value (PPV), and 99%; negative predictive value (NPV) in comparison to pyrosequencing. All of the cases have been previously tested by direct Sanger sequencing (and 3 cases, 2 in KRAS exon 2 and 1 in BRAF 11, previously called as wild type (3.2.3.3), were found to have mutations by both HRM and pyrosequencing (Figure 3-8). Demonstrating that these cases were Sanger sequencing "false negatives". In these cases, the DNA was derived from non-microdissected FFPE tumour tissue.

Table 3-4 Mutation analysis of 22 DNA samples by QMC-PCR and pyrosequencing from cell lines and FFPE

The results of the two methodologies are presented in this table as pairs: OMC-PCR/pyrosequencing (W: wild type; M: mutant). QMC-PCR gave identical results to pyrosequencing in 109/110 test (95% sensitivity, 100% specificity, positive predictive value (PPV) 100%; negative predictive value (NPV) 99%).

FFPE sample ID	KRAS 12,13	KRAS 61	BRAF exon11	Kras 146	BRAF Exon15
5	W/**W**	M/**M**	W/**W**	W/**W**	W/**W**
16	W/**W**	W/**W**	M/**M**	W/**W**	W/**W**
36	W/**W**	W/**W**	M/**M**	W/**W**	W/**W**
23	M/**M**	W/**W**	W/**W**	W/**W**	W/**W**
28	M/**M**	W/**W**	W/**W**	W/**W**	W/**W**
37	W/**W**	W/**W**	W/**M**	W/**W**	W/**W**
25	W/**W**	W/**W**	W/**W**	W/**W**	M/**M**
34	W/**W**	W/**W**	W/**W**	W/**W**	M/**M**
11	W/**W**	W/**W**	W/**W**	W/**W**	M/**M**
45	M/**M**	W/**W**	W/**W**	W/**W**	W/**W**
30	M/**M**	W/**W**	W/**W**	W/**W**	W/**W**
18	W/**W**	M/**M**	W/**W**	W/**W**	W/**W**
CRC 1notts	W/**W**	W/**W**	W/**W**	M/**M**	W/**W**
Cell lines					
HCA7	W/**W**	W/**W**	W/**W**	W/**W**	W/**W**
RKO	W/**W**	W/**W**	W/**W**	W/**W**	M/**M**
HT29	W/**W**	W/**W**	W/**W**	W/**W**	M/**M**
C32	W/**W**	W/**W**	W/**W**	W/**W**	W/**W**
LS1034	M/**M**	W/**W**	W/**W**	W/**W**	W/**W**
HCT116	M/**M**	W/**W**	W/**W**	W/**W**	W/**W**
GP2D	M/**M**	W/**W**	W/**W**	W/**W**	W/**W**
VACO5	W/**W**	W/**W**	W/**W**	W/**W**	M/**M**
C80	W/**W**	W/**W**	W/**W**	M/**M**	W/**W**

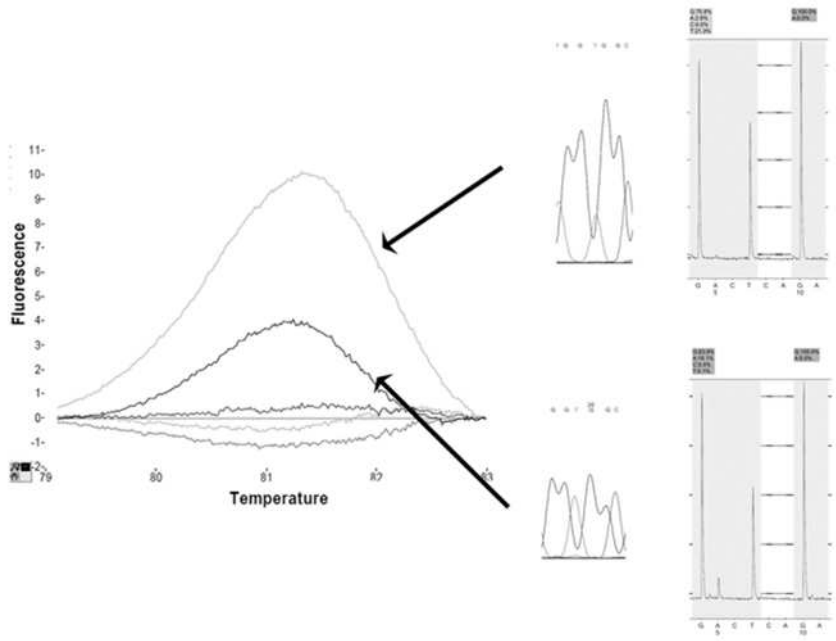

Figure 3-8 Pyrosequencing *versus* Direct Sanger sequencing

Direct Sanger sequencing failed to detect mutation in two cases of CRC (central panel). However, in both cases aberrant melting was seen by HRM for KRAS exon 2 (left panel shows the aberrant melting peaks (arrows) seen in contradistinction from the wild types which show a flat melting pattern) and these were also detected by pyrosequencing (right upper panel shows G12V, right lower panel shows G12D).

3.2.6 Comparison of real-time PCR with QMC-PCR / High resolution Melting.

3.2.6.1 Assessment of sample quality

It is a truism of PCR that poor starting template will give poor results. Although all the samples tested in this study had been previously tested by the DxS assay, it was deemed necessary to ensure that the DNA was of sufficient quality for use in the HRM assay. The PDM reaction, even though it is a multiplexed reaction still generates enough PCR product for detection by intercalating dyes and thus can be used to indicate quality of DNA template. All 475 samples underwent a PDM reaction and evaluation of the amplification plot identified 7 samples as being of low quality since they had a high Ct value which was >5 cycles away from the mean value of all the samples (Figure 3-9). These samples were excluded from

further analysis.

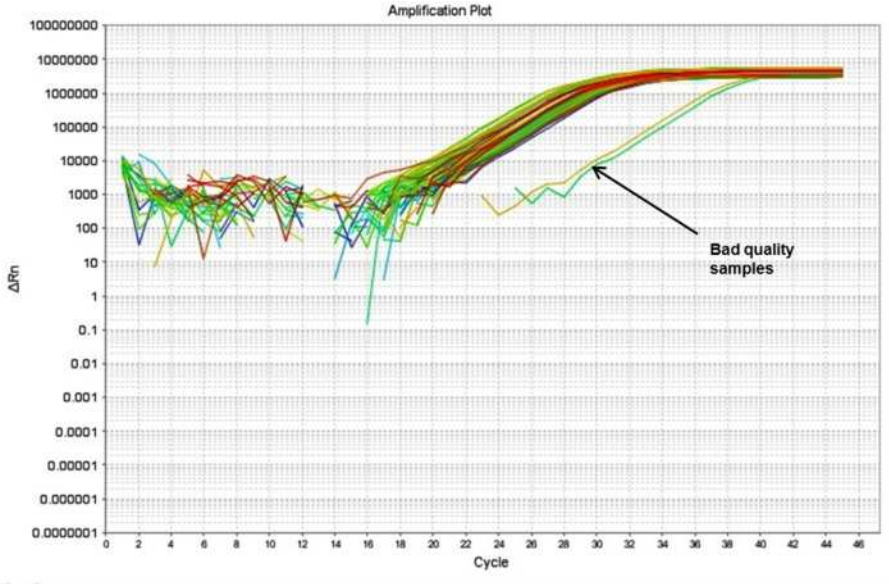

Figure 3-9 Amplification plot of the pre-diagnostic multiplex PCR

The amplification plot of the pre-diagnostic multiplex reaction can be used to assess quality of DNA samples. Even though only a limited number of cycles are performed, there is sufficient PCR product produced for detection. The image shows an amplification with the good samples tend to give a relatively early signal whilst the poor-quality sample (arrowed) gives a late signal.

3.2.6.2 Comparison of real-time PCR with HRM protocol 1

All cases included in this study have previously been used in a study to compare mutation detection by Sanger sequencing and the real-time PCR assay (Tol et al., 2009a). There was high concordance between these two methods and thus the data generated by the real-time PCR assay were regarded as the standard against which HRM analysis was to be compared. The HRM protocol 1 was a high throughput single test of each sample and Table 3-5 shows the comparative analysis of the real-time PCR with this protocol. Of 468 samples tested, identical results were generated in 421 samples (89.9% concordance) by HRM protocol 1. A total of 180 (38.5%) samples were called as mutant by the real-time PCR whilst 181 (38.6%) were called as mutant by HRM protocol 1. One hundred and fifty-seven cases were common to both tests whilst 23 mutant cases were missed by HRM (giving a sensitivity of 89.2%) and 24 wild type cases were overcalled as mutant (86.7%

positive predictive value). A total of 288 (61.5%) samples were called as wild type by the real-time PCR whilst 287 (61.4%) were called as wild type by HRM protocol 1. Two hundred and sixty-four cases were common to both tests and, considering the false positives and false negatives, this gave a specificity of 91.6% and a negative predictive value of 91.9%.

Table 3-5 Comparison of mutation analysis for codon 12/13 of KRAS between the real-time DxS PCR based assay and the modified QMC-PCR/HRM1 protocol

Sensitivity 89.2%, positive predictive value (PPV) 86.7%, specificity 91.6%, negative predictive value 91.9%

		DxS		
		Mutant	**Wild Type**	**Total**
QMC-PCR/HRM1	**Mutant**	157	24	181
	Wild Type	23	264	287
	Total	180	288	468

3.2.6.3 Comparison of real-time PCR with HRM protocol 2

Evaluation of the data derived from screening the tumour samples with the HRM protocol 1 showed that statistically the performance against the real-time PCR was good and it was a suitable tool for research purposes. However, it was felt that the test was not sufficiently robust at a clinical level. Particularly worrying was the relatively poor sensitivity which would potentially result in 1 in 10 patients receiving inappropriate therapy. Also, rather perplexing was the observation that the proportion of false positives was lower than the false negatives as from our experience hitherto we would have expected the reverse.

The data from all the discrepant cases were re-examined including the amplification plots, the melt curves and the derivative plots. From this it seemed that miscalling

of samples could be attributed to a number of factors including sub-optimal PCR efficiency in occasional samples, greater background "noise" in the wild type as a consequence of large numbers of cases tested in each run and the inability of the program to temperature-shift the data. In order to avoid these pitfalls, HRM protocol 2 was developed and 100 cases were randomly selected and re-tested using HRM protocol 2. In these cases, 99% of the calls made by the automated analysis were the same as real-time PCR (Figure 3-10).

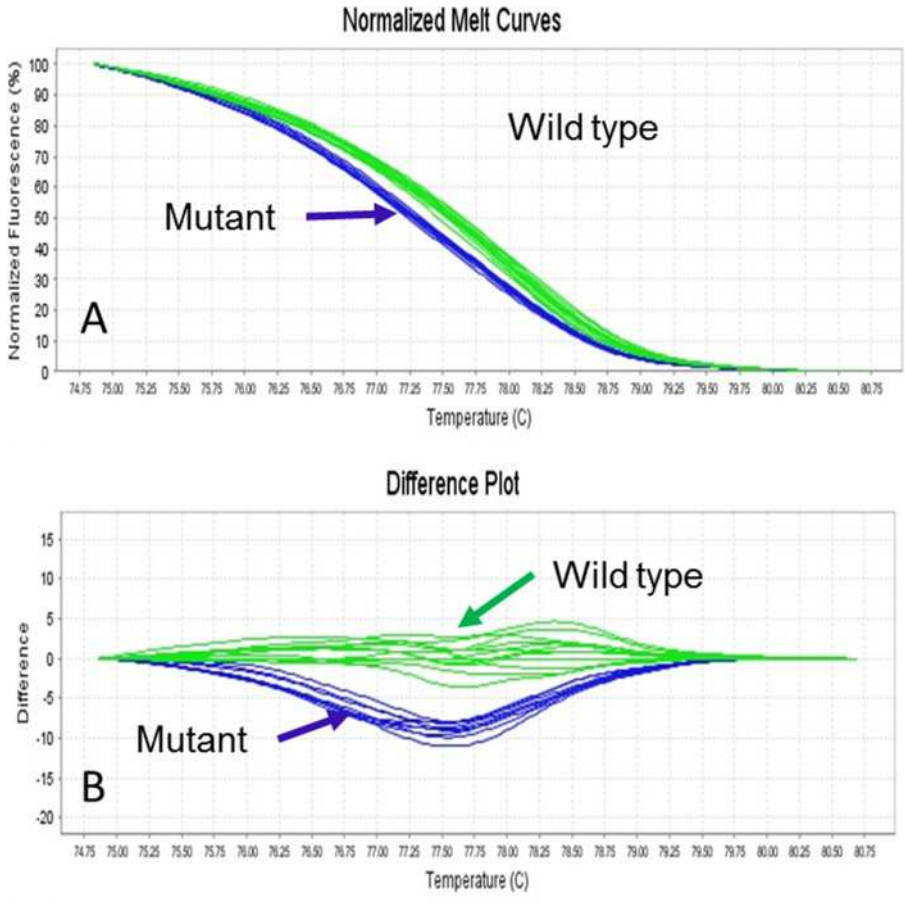

Figure 3-10 The modified QMC-PCR HRM protocol 2

The HRM Protocol 2 was refined allowing comparable identification of KRAS mutation in comparison to real time KRAS DxS PCR assay. (a) is the normalised melt curve generated by ABI 7500 fast real PCR shows clear discrimination of the mutant samples (blue) from the wild type (green). (b) is the difference plot from the same run showing tight clustering of the samples into two groups. Wild type=Green (clustering with wild type controls included in the protocol); Mutants=Blue (clustering separately from the wild types).

This included one case in which a mutation could not be found on Sanger sequencing but both HRM and real-time PCR had called as mutant thereby

indicating that this was probably a false negative by sequencing. The one case that was discrepant on repeat analysis, was called as positive by HRM protocol 2 but negative by real-time PCR. This case contained a sequence verified mutation but this specific sequence is not included amongst the seven mutations which are tested by this real-time DxS PCR assay.

3.2.7 Introducing a PCR/HRM assay for MSI testing

3.2.7.1 Performance in DNA from cell lines

Twenty CRC cell lines were tested for MSI status using a Panel of six microsatellite markers (BAT25, BAT26, NR21, NR22, NR24, B-CAT25) by the HR1 melter. In the cell line experiments, the result was 100 % concordant (100% sensitivity and specificity) with the published data, and with ability to differentiate between monomorphic and polymorphic allelic changes depending on the shape of the melting curve before and after temperature shift. The seven cell lines which are known to be MSI showed instability for the six markers (Table 3-6), giving a 100% accuracy. Only LOVO which failed to amplify for BAT26 as it is deleted at the locus of this marker (Both alleles are deleted (1072-1350) ref (PMID: 8182040). It was important not to temperature shift during the analysis as this will mask the DNA with homozygous like mismatch. This is because the DNA from cell line is pure and those markers are quasimonomorphic mononucleotide repeats (Figure 3-11).

Table 3-6 MSI testing on CRC cell lines using PCR-HRM assay.

Seven MSI CRC cell lines were tested by HRM for instability in 6 microsatellite markers. In all cell lines instability was detected in every marker by HRM. Except Lovo failed to amplify for BAT26 because the locus is deleted in this cell line

CELL LINE	NR-21	NR-22	NR-24	B-CAT25	BAT 25	BAT 26	MSI/ MSS
DLD1	Unstable	Unstable	Unstable	Unstable	Unstable	Unstable	MSI
GP2D	Unstable	Unstable	Unstable	Unstable	Unstable	Unstable	MSI
HCA7	Unstable	Unstable	Unstable	Unstable	Unstable	Unstable	MSI
HCT116	Unstable	Unstable	Unstable	Unstable	Unstable	Unstable	MSI
LOVO	Unstable	Unstable	Unstable	Unstable	Unstable	Both alleles are deleted (1072-1350) ref (PMID: 8182040)	MSI
RKO	Unstable	Unstable	Unstable	Unstable	Unstable	Unstable	MSI
VACO5	Unstable	Unstable	Unstable	Unstable	Unstable	Unstable	MSI

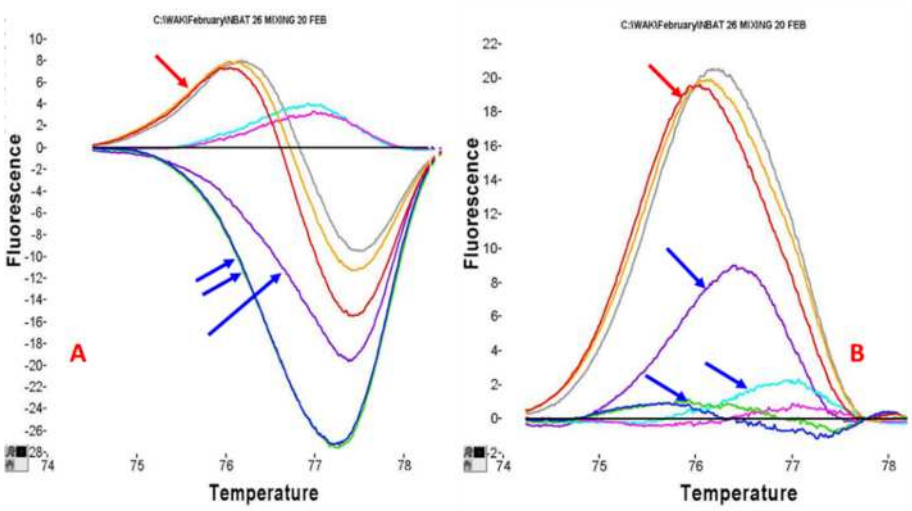

Figure 3-11 MSI testing by HRM using Pure genomic DNA from cell lines

(a) Difference plot (before temperature shifting) generated using HR1 melter for BAT26 on 9 cell line DNA. It showed 3 melting curves (red arrows) with two-domain transition in a heterozygous like pattern. The other homozygous like pattern can be seen as single domain curve (blue arrows). (b) difference plot after temperature shifting led to masking of melting curves of the two homozygous samples (blue arrows).

3.2.7.2 Performance in DNA from FFPE

Analysis of the HRM data was generally straightforward as the clinical sample DNA contains a mixture of tumour cells (MSI) and non-tumor cells (MSS) from the contaminating stroma. So, applying the temperature shifting further facilitated the discrimination. Regarding the MSI-HRM testing of the CRC tumour samples from the Birmingham series, all the MSI cases were correctly characterised as they showed aberrant melting with at least three MSI markers. PCR-HRM assay showed 100% concordance with IHC. One sample deemed unstable by Bethesda test for showing instability only at two dinucleotide markers (which are generally considered less reliable). However, this sample was called stable by HRM assay and originally reported as proficient MMR by IHC. The sensitivity and specificity on FFPE samples was 100%. Consequently, the assay was used to screen 100 FFPE samples (Nottingham series set-1&2) to validated the assay, this time also the test showed 100% concordance to MMR proteins expression by IHC (see also section 4.3).

3.3 Discussion

Demands for mutation detection in tumours will inevitably going increase as more predictive mutations are identified. Tumour mutation profiling may become a routine part of the Pathologist's workload which in turn requires technologies which work reliably on DNA derived from FFPE tissue. Furthermore, since the majority of cancer treatment is undertaken out with research institutes, the methods must be implementable in District General Hospitals. We have described QMC-PCR as a very rapid (about 100 minutes cycling time) and simple method which works robustly in FFPE tissue sections. It is a two-step nested procedure in which the first reaction is a Pre-Diagnostic Multiplexed (PDM) PCR reaction containing up to ten primer pairs. This is followed by a Specific Single Diagnostic (SSD) reaction during which each of the hotspots are individually analysed. The fact that

only a single protocol is used (i.e. rapid cycling between 95°C and 55°C) means that multiple targets can be tested in a single run. If PCR machines are used which can capture high density fluorescence data sufficient for HRM analysis (such as certain Real-Time PCR machines), then multiple targets can be analysed simultaneously. The ease of data interpretation, the gel-free nature of the methodology and the fact that the tests can be done on inexpensive equipment all represent significant advantages over more traditional methods of mutation screening.

We have shown that QMC-PCR works efficiently in both fresh and archival tissue. Using high quality DNA from cell lines with known mutations in a variety of genes, we have shown that it has 100% sensitivity and 100% specificity. QMC-PCR has a limit of mutation detection which is nearly an order of magnitude better than the current "gold standard" of Sanger sequencing. This increased detection becomes important in cases where a tumour has a heavy infiltration of stromal cells which then may "veil" mutations in the less sensitive techniques. Furthermore, QMC-PCR compares very favourably with "cold" PCR since, in our hands, the cold protocols did not improve on the level of detection. Since cold PCR requires that a critical temperature (Tc) be optimised for each target and it is likely that the Tc may vary between machines, we consider our technique to be simpler.

We further tested the robustness of the QMC-PCR method by evaluating variability both between and within assays. Tests performed on a number of DNA samples derived from FFPE tissue on 3 consecutive days gave identical results showing that there was little inter-assay variation. Analysis of two samples (one wild type and one mutant for PIK3CA), each tested as 15 replicates, resulted in near identical melting curves of each of the replicates thereby showing that the technique has high precision with negligible intra-assay variation.

In archival FFPE tissue, standard PCR followed by HRM is a technique prone to false-positive artefacts thereby limiting its utility. QMC-PCR produced far fewer artefacts and led to a 16% increase in specificity. This is probably due to the nested nature of the procedure in which – in the SSD reaction – contaminants are diluted out and only specific PCR product is used as template. Compared to direct sequencing we found that QMC-PCR has 100% sensitivity and did not miss any mutations. However, our study identified a number of clinical samples in which there was aberrant melting, but no mutations were detectable. These are theoretically regarded as false positives but having demonstrated that QMC-PCR is more sensitive than direct sequencing, we think it likely that these cases contained small numbers of mutant alleles and that the sequencing data represent false-negatives. This does lead to a situation where the results of the screen cannot be validated by the current "gold standard". It is possible that more sensitive sequencing techniques such as pyrosequencing may resolve this problem. Based on our experience, we would believe the QMC-PCR data over the sequencing data. Given the sensitivity of the technique, it may possible that HRM becomes the new gold standard for mutation screening.

Subsequently we compared QMC-PCR to pyrosequencing. Initially we compared the limit of mutation detection of HRM and pyrosequencing for KRAS exon 2 and BRAF exon15 using wild type DNA spiked with varying quantities of mutant DNA. We showed that, for KRAS exon 2, HRM and pyrosequencing had similar levels of sensitivity and were able to confidently detect 3% and 6% of mutant alleles respectively. For BRAF exon15, HRM could detect around 1.5% mutant alleles whilst pyrosequencing was able to detect 6% mutant alleles with confidence. The differences between HRM assays for different hotspots is not unexpected since the stability of the heteroduplex is dependent on both the specific changes that occur and context in which they occur (the "nearest neighbour" effect (Peyret et al., 1999)). The level of 1.5% mutant alleles for the BRAF V600E mutation is

consistent with other studies of HRM analysis of this mutation (Pichler et al., 2009). The similar levels in sensitivity between pyrosequencing assays for different hotspots is as expected since single base variation in non-primer sequence should not affect PCR efficiency and the mutation does not create a mononucleotide run of repeat sequences (which may impede sequence analysis).

This is the first direct comparison of limit-of-detection (LOD) between HRM and pyrosequencing. Since we used diploid cell lines for the spiking experiments, our limit of detection tests are probably more accurate than studies using aneuploid cell lines or tumour samples (Dufort et al., 2009). Probably neither technique is as sensitive as the DxS test (quoted as being around 1% mutant alleles) but both are sufficiently sensitive for use in clinical diagnosis.

Next, we undertook a comparison of the performance of both types of mutation detection assay for 5 hotspots in two different genes. Of 110 tests performed, there was concordance in 109 showing that both tests were performing equally well. The samples had all been previously examined by Sanger sequencing and both HRM and pyrosequencing identified 3 cases which had been previously been incorrectly called negative by the Sanger method. Although both assays are more sensitive than Sanger sequencing and are suitable for clinical applications, they have complementary strengths. The HRM assay can only be used for screening and positive cases still need to be confirmed by a sequencing method in order to exclude the possibility of aberrant melting due to a single nucleotide polymorphism. Pyrosequencing is more expensive and less flexible than HRM when searching for unknown mutations. A combined strategy of screening for mutation by HRM followed by confirmation of mutation by pyrosequencing is probably the best method for mutation detection when it is necessary to test multiple hotspots in multiple genes.

The choice of mutation detection strategy is an important one since capital equipment and staff training costs will probably mean that institutes will not be able to invest in multiple different platforms. Our findings using HRM and pyrosequencing are consistent with much of published literature which has tended to test just one method (Do et al., 2008, Packham et al., 2009). A large study by Whitehall et al. evaluated seven different methodologies (including HRM and pyrosequencing) for mutation detection in both frozen and FFPE tissue (Whitehall et al., 2009). The authors found that there was around 96% concordance amongst the top five performing assays in FFPE tissue. As expected, HRM had some false positives whilst pyrosequencing had some false negatives but both assays were deemed acceptable.

Whitehall's study also found that Sanger sequencing had a sensitivity of 90% thereby re-iterating the facts that due to a low limit-of-detection, Sanger sequencing will miss some cases. At first glance it would seem that Sanger sequencing should no longer be regarded as the gold standard for mutation detection in predictive testing. However, careful selection of tumour blocks prior to testing will obviate the problem of low tumour cell population within the sample but in itself raises another question about the utilisation of such exquisitely sensitive techniques. The biological significance of a minority KRAS mutant population, within a tumour which is otherwise wild type, is uncertain. It is possible that treatment of such a tumour with anti-EGFR biologics could select for the growth of therapy resistant KRAS mutant sub-clones (Ilyas et al., 1999). Alternatively, it is equally possible that such a small population will be dealt with by standard therapies given alongside the biologics and thus an over-senstive technique will inappropriately deny this therapy to patients.

It is thus important to have a highly sensitive and versatile test for mutation detection which can work on poor quality DNA template derived from formalin-

fixed paraffin-embedded tumour tissue. Here we assumed that a real-time PCR test for KRAS mutations was the "gold standard" and sought to compare it against our QMC-PCR HRM in a series of 468 cases of colorectal cancer obtained from the Cairo 2 trial. We have previously compared the QMC-PCR protocol combined with HRM with Sanger sequencing and found that it had a lower limit of detection and that it had 100% sensitivity for detection of mutant alleles.(Fadhil et al.) In agreement with others, we found that it was more prone to Type I errors than Type II errors (Fadhil et al., Do et al., 2008). In the current study, our initial analysis showed that QMC-PCR / HRM performed adequately against the real-time PCR test with 87.2% sensitivity and 91.6% specificity. Whilst acceptable for research projects, we didn't think that this was sufficiently accurate for clinical application. In addition, we were perplexed by the switch in error type with Type II errors predominating over Type I errors.

There are a number of reasons for the discrepancy between the initial assay here in comparison with both the real-time PCR assay data and our own previous data. Firstly, in the current study, in order to create a "high throughput" mutation screening scenario (akin to the requirements of a clinical service) we performed the HRM analysis on an AB 7500 fast PCR machine rather than the HR1 machine we had previously used. The AB 7500 fast captures and analyses data in a different way and does not temperature shift the data. Furthermore, each run contained 88 samples in a single reaction thereby increasing the background "noise". In the first series of experiments, we had not taken these variations into account and had simply used our original protocol (HRM protocol 1). In order to obviate these problems, we revised the protocol (HRM protocol 2) to reduce the number of cases in each experiment, performed analyses in duplicate and indicated known wild type controls to the software. One hundred random cases were re-tested and, using the revised protocol, identical results were obtained to the real-time PCR test in 99% of the cases. This included one case which had been missed by direct sequencing

and which re-iterates the advantage that both the real-time PCR test and the HRM assay have in detecting low numbers of mutant alleles. The one discrepant case was a sequence proven Glycine to Glutamine mutation in codon 12 (G12Q) which could not have been detected by this particular real-time PCR test since this particular sequence occurs at low frequency and is therefore not included in the primer and probe set.

The choice of methodology for mutation detection in the context of routine molecular pathology needs to be driven primarily by the accuracy of the test on poor quality template derived from FFPE tissue. Other important considerations are technical demands of the test, ease of data interpretation, flexibility of the test and the financial cost. Our data show that, once optimised, HRM has a similar level of accuracy as real-time PCR for mutation detection. Since the real-time PCR test enriches for mutant alleles and uses real-time chemistries as reporters, it will inevitably have a lower limit of detection (which is usually quoted as 1% of mutant alleles) than HRM. However, in most instances this level of sensitivity is not required and careful selection of tumour blocks prior to testing should ensure that there are sufficient numbers of tumour cells in the specimen. Furthermore, the gain in sensitivity from this test is more than offset by the fact that the real-time PCR test requires 8 PCR reactions to be performed for each sample in order to screen only the codon 12/13 hotspot. The situation is further complicated by recent studies which demonstrate that mutations in KRAS codon 61/146, BRAF codon 600 and PIK3CA hotspots may also be predictive of response to anti-EGFR therapies (Di Nicolantonio et al., 2008, Loupakis et al., 2009, Sartore-Bianchi et al., 2009). If these studies are validated, then it will also be necessary to screen these hotspots prior to considering anti-EGFR therapy. Currently these hotspots cannot be screened by the real-time PCR test used in this study and inclusion of these hotspots into the assay will increase the number of PCR tests required and will inevitably make the assay more complicated. In contrast, HRM is a very flexible test and in

conjunction with the QMC-PCR protocol, many hotspots (in several different genes) can be screened with little extra effort. As other predictive tests emerge for other therapies, it will be possible to adapt HRM to screen for these too.

Although HRM is an excellent screening tool, the nature of the methodology means that any SNPs present will also cause aberrant melting (Vandersteen et al., 2007). Given this fact, we would recommend that mutations identified by HRM are confirmed by sequencing before any clinical decision is made. Thus, HRM can be used to screen several hotspots and only those most likely to contain mutations need to be sequenced. Given that HRM is more sensitive than Sanger sequencing, if a sequence change cannot be found to explain the aberrant melting we would recommend that a mutation enrichment procedure (such as "cold" PCR) is used to unmask the cause of the aberrant melting or using highly sensitive sequencing technique such as pyrosequencing.

We also tested whether HRM could be used to detect Microsatellite Instability. This is characterised by multiple sized bands arising due to insertion/deletion mutations consequent to DNA slippage during replication. It would therefore be expected that numerous heteroduplexes would form giving rise to aberrant melting. Firstly, the utility of HRM for MSI detection was tested in a series of cell lines and FFPE tumours which had been genotyped using fluorescently labelled primers for the Bethesda panel followed by electrophoresis of the PCR products. We decided to use a panel of quasimonomorphic mononucleotide markers as there seemed to be general acceptance that these are more sensitive than dinucleotide markers. In addition, we designed a new marker of our own to test alongside the previously published panel.

In the cell lines testing, our genotyping analysis was in perfect concordance with the known genotype of these cell lines. All unstable markers melted aberrantly

when compared with the stable markers and this could be easily visualised on the difference plot. The HRM data are much easier to interpret than the traditional method where stutter bands can sometimes interfere with the interpretation.

All CRC have some inherent instability and, if enough markers are tested, all tumors will have some degree of instability. Although the HRM MSI results from clinical samples showed 100 concordance with IHC, there was one case deemed MSI only by the Bethesda panel. We think that the Bethesda panel might have misclassified this samples because it only showed instability by two dinucleotide markers (D2S123 and (D8S255) which are less reliable anyway. Therefore, we have shown that HRM based MSI testing is not inferior to IHC and traditional Gel based MSI methods, instead it is simple and straightforward MSI analysis method which can identify MSI tumors with a high sensitivity and specificity. It also offers several distinct advantages in that there is no need to compare tumor with matching germline DNA. Therefore, it reduces time and costs involved in MSI testing. Furthermore, we think that MSI-HRM assay can be easily integrated in a single closed-tube test panel to screen for Lynch syndrome, or to be used on its own to test stage II CRC for MSI in order to inform the decision maker to administer 5-fluorouracil-based chemotherapy to the patient or not.

Chapter 4. The utility of diagnostic biopsy specimens for predictive molecular testing in colorectal cancer

4.1 Introduction

Testing for mutations that are associated with responsiveness to specific therapies is known as predictive testing and forms the basis of stratified medicine. For adjuvant therapy, tumour material from the resection specimen can be used for predictive testing. However, the use of neoadjuvant therapy in patients with CRC is likely to increase. Currently, neoadjuvant therapy is given to patients with rectal tumours, and a clinical trial of neoadjuvant chemotherapy for locally advanced colonic cancer (bearing the acronym Foxtrot (Dighe et al., 2012) is now underway in the UK. If this trial shows improved outcomes, then the use of neoadjuvant therapy may become routine in the management of CRC. If this were to be the case, then the only material available for predictive testing would be the diagnostic biopsy specimens taken to confirm the presence of invasive malignancy. These specimens represent only a tiny fraction of the overall tumour, and heterogeneity within tumours has been described.(Giaretti et al., 2000) The utilization of preoperative diagnostic biopsy material for predictive testing would thus seem, at first glance, to be highly prone to false-negative errors, owing to insufficient sampling. This could lead to inappropriate treatment of patients, and, given the cost (in terms of both patient morbidity and finance) of some of the treatments, could be a major cause for concern.

Studies of tumour biology show that CRC develops as a result of waves of clonal expansion (or clonal sweeps) resulting from mutations (called ‘driver mutations’) that give a selective advantage.(Greaves and Maley, 2012) As the new clone expands and becomes predominant in the tumour, the driver mutation responsible for this will eventually be present throughout the tumour. One can hypothesize that the driver mutations responsible for the early clonal sweeps during the adenoma–carcinoma sequence should be present in most of the tumour cells, and thus would be present in the biopsy samples.

One concern of biomarker analysis in biopsies is that only a tiny proportion of the tumour is sampled and may give a false negative result. On the other hand, diagnostic biopsy can represent a good alternative to the resection specimens especially when evaluating protein expression by IHC. For instance, the use of immunohistochemistry to detect loss of MMR protein expression (which implies loss of MMR function) is now standard practice in many laboratories(Shia, 2008), and the interpretation of the IHC is usually straightforward (especially when a panel of four antibodies is used) However, it has been reported that MMR proteins are fixation-dependent and may result in difficulties in interpretation even amongst specialists due to technical sources of variation (such as tissue fixation and poor antibody affinity) that can make interpretation difficult specialists (Klarskov et al., 2010, Barrow et al., 2010). In order to investigate whether diagnostic biopsy specimens are suitable for predictive testing, we first performed paired evaluation of diagnostic biopsies and their subsequent resection specimens for the presence of mutations that are thought to occur during the pre-invasive phase of colorectal tumour growth. Second, we hypothesised that problems in interpretation of MMR proteins expression could be obviated by evaluation of IHC for MMR proteins in biopsy samples rather than resection specimens since the former will tend to have more thorough and uniform fixation. So, we evaluated the immunostaining of the MMR proteins expression on tumour sections from 30 consecutive cases of CRC and their corresponding pre-surgical diagnostic biopsies.

4.2 Overall Mutation profile

A total of 30 individual cases underwent screening for mutation in four different genes and for MSI (Table 4-1). HRM following either QMC–PCR or standard PCR was used, as this is a quick and reliable method for mutation screening and for MSI testing. Evaluation of data generated by HRM is generally straightforward, as

mutation alters the sequence of the target DNA, and this change in base composition alters the melting pattern of the PCR products (Wittwer, 2009). Changes in DNA melting can be seen easily in the melting plots generated by the software (Figure 4-1).

The overall mutation profile was what would be expected for a randomly selected series of cases and is shown in Table 4-1. Thus, KRAS mutations were detected in 15 (50%) of the 30 cases, with 13 of these (87%) occurring in exon 2 (codon 12/13), and one mutation (6%) being detected in each of the hotspots in exon 3 (codon 61) and exon 4 (codon 146). PIK3CA mutations were detected in four cases (13%) and were found exclusively in exon 9. BRAF mutations were found in three (10%) of the 30 cases, and all were in exon 15 at the codon 600 hotspot. TP53 mutations were found in 14 cases (47%), and eight of these (57%) were detected in exon 5. MSI was present in four (13%) of the 30 tumours.

The combination of mutations was as expected. Three of the PIK3CA mutations co-occurred with KRAS mutations, as has been previously described (Janku et al., 2011). BRAF and KRAS mutations were mutually exclusive, and seven (23%) of the 30 tumours showed the concomitant presence of KRAS and TP53 mutations. Two (7%) had concomitant KRAS/PIK3CA/TP53 mutations, and six (20%) did not show any aberrant change (that is, they had a microsatellite stable phenotype and no mutations were detected in any of the genes tested).

Table 4-1 Comparison of mutation profiles of biopsy and resection specimens

This table shows that in all but one case, the mutations detected in the resection specimens were also detected in the biopsy specimens. Test results are presented as pairs (Bx I RX) per each sample per hotspot. Samples with mutation are reported by name of the exon carrying the mutation (i.e. Ex2, Ex4, etc…). (Bx: Biopsy; Rx: resection; Ex: exon; WT: Wild Type).

	KRAS	BRAF	PIK3CA	TP53	MSI
Case no.	Bx I Rx	Bx I Rx	Bx I Rx	Bx I Rx	Bx I Rx
1	Ex2 I Ex2	WT I WT	WT I WT	WT I WT	MSS I MSS
2	Ex2 I Ex2	WT I WT	WT I WT	WT I WT	MSI I MSI
3	WT I WT	WT I WT	WT I WT	WT I WT	MSS I MSS
4	Ex2 I Ex2	WT I WT	Ex9 I Ex9	WT I WT	MSS I MSS
5	Ex2 I Ex2	WT I WT	WT I Ex9	Ex5 I Ex5	MSS I MSS
6	WT I WT	WT I WT	WT I WT	Ex5 I Ex5	MSS I MSS
7	WT I WT	WT I WT	WT I WT	WT I WT	MSS I MSS
8	WT I WT	WT I WT	WT I WT	WT I WT	MSS I MSS
9	Ex2 I Ex2	WT I WT	WT I WT	WT I WT	MSS I MSS
10	Ex2 I Ex2	WT I WT	WT I WT	Ex5 I Ex5	MSS I MSS
11	Ex4 I Ex4	WT I WT	WT I WT	WT I WT	MSS I MSS
12	Ex2 I Ex2	WT I WT	WT I WT	Ex5 I Ex5	MSS I MSS
13	Ex2 I Ex2	WT I WT	WT I WT	Ex8 I Ex8	MSS I MSS
14	Ex2 I Ex2	WT I WT	WT I WT	WT I WT	MSS I MSS
15	Ex2 I Ex2	WT I WT	WT I WT	WT I WT	MSS I MSS
16	WT I WT	WT I WT	WT I WT	Ex6 I Ex6	MSS I MSS
17	WT I WT	Ex15 I Ex15	WT I WT	WT I WT	MSS I MSS
18	WT I WT	WT I WT	WT I WT	Ex5 I Ex5	MSS I MSS
19	Ex2 I Ex2	WT I WT	WT I WT	Ex5 I Ex5	MSS I MSS
20	WT I WT	WT I WT	WT I WT	WT I WT	MSS I MSS
21	Ex2 I Ex2	WT I WT	Ex9 I Ex9	Ex8 I Ex8	MSS I MSS
22	WT I WT	WT I WT	WT I WT	WT I WT	MSS I MSS
23	WT I WT	WT I WT	WT I WT	Ex5 I Ex5	MSS I MSS
24	WT I WT	WT I WT	WT I WT	WT I WT	MSS I MSS
25	WT I WT	WT I WT	WT I WT	Ex6 I Ex6	MSS I MSS
26	WT I WT	WT I WT	Ex9 I Ex9	WT I WT	MSI I MSI
27	Ex2 I Ex2	WT I WT	WT I WT	WT I WT	MSS I MSS
28	WT I WT	Ex15 I Ex15	WT I WT	Ex5 I Ex5	MSI I MSI
29	Ex3 I Ex3	WT I WT	WT I WT	Ex6 I Ex6	MSI I MSI
30	WT I WT	Ex15 I Ex15	WT I WT	Ex8 I Ex8	MSS I MSS

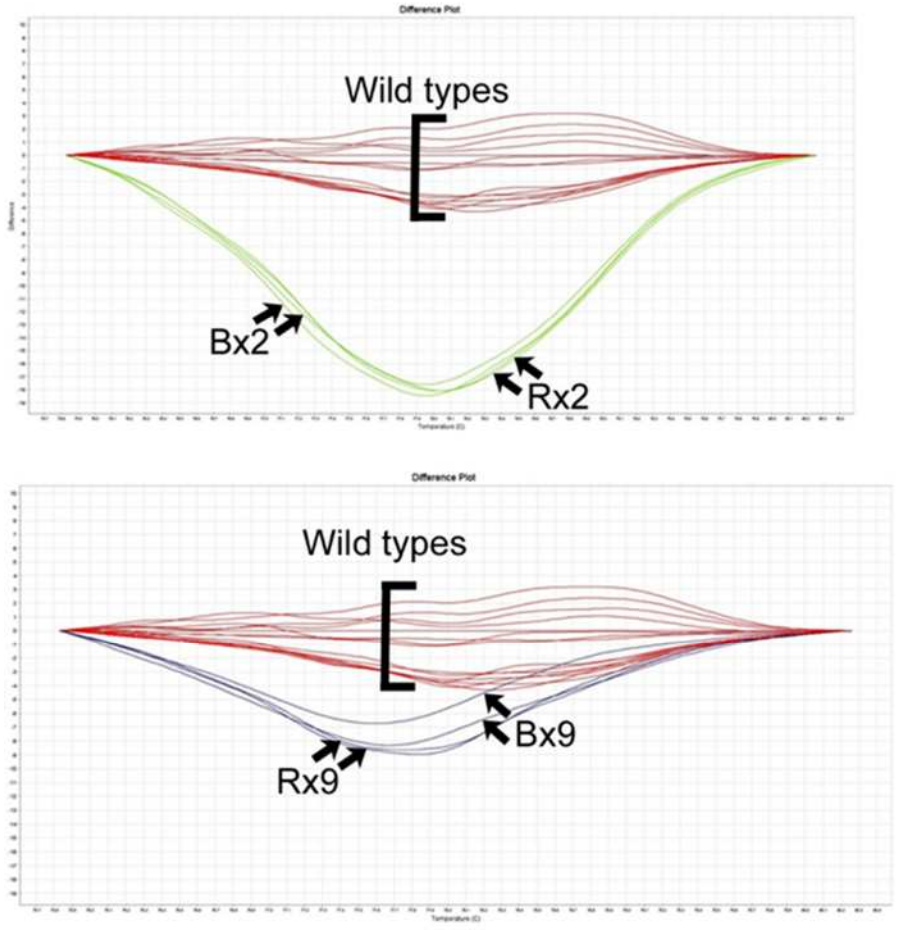

Figure 4-1 DNA melting pattern generated by ABI 7500 fast PCR machine

DNA melting is dependent on sequence, and thus different sequence changes at the same site will alter the melting pattern in different ways. The data show high-resolution melting analysis of paired samples from two separate cases (case 2 and case 9). Each sample was tested in duplicate. In each of the cases, there is a mutation in codon 12/13 of KRAS in both the biopsy (Bx) and resection (Rx) specimens. The melting pattern within each case is similar, showing that the biopsy and resection specimens contain the same mutation. However, the melting pattern between cases is different, showing that cases 2 and 9 contain different mutations. The samples labelled 'wild type' consist of sequence-proven wild-type controls and other cases showing normal melting.

4.3 Mutation detection and MSI in biopsy and resection specimens

Comparative analysis of the 30 cases of paired biopsy and resection specimens was undertaken using 13 primer pairs for mutation detection (to cover the hotspots in four different genes) and six primer pairs for MSI. A total of 570 paired tests were

performed, and identical results in each pair were obtained in 569 tests. This gives a concordance of >99%, and provides overwhelming evidence that, for these genes, the biopsy material is representative of the main tumour. Although HRM does not identify specific mutations, the DNA melting patterns tend to be sequence-specific. Generally, the melting pattern was similar in both the biopsy and the matched resection specimens, allowing us to infer that each contained the same mutation (Figure 4-1).

Four of the cases showed MSI, and, of these, three showed instability at all six mononucleotide markers in both the biopsy and the resection specimen. One case showed instability at four of the six markers (BAT25, BAT26, NR24, and BCAT25), and instability was seen at identical markers in both the biopsy and the resection specimen (Figure 4-2).

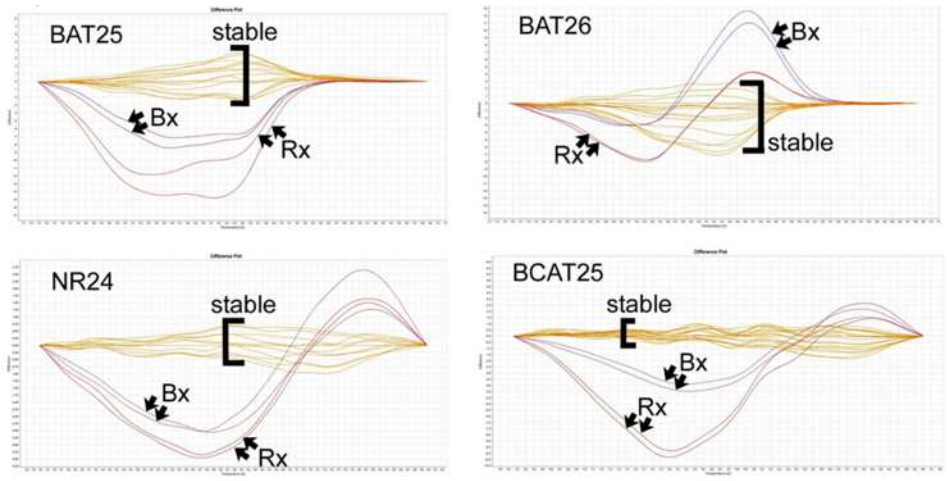

Figure 4-2 HRM melting plots for MSI markers

Four cases showed microsatellite instability in both the biopsy and the matched resection specimen. In three cases, there was instability at all six mononucleotide markers. In one case (case 28), there was instability at only four markers, although the same markers were unstable in both the biopsy (Bx) and resection (Rx) specimens. The data show the HRM melting plots for the four markers at which instability was seen, and duplicates of both the Bx and Rx specimens are shown. The samples labelled as 'stable' represents cases that do not show instability at these loci.

Discrepancy between the biopsy and resection specimens was seen only in one

case. In this case, the biopsy was shown to be wild type for PIK3CA, whereas an exon 9 mutation was detected in the resection specimen. This case also had KRAS and TP53 mutations, and these were identical in the biopsy and resection specimens (Figure 4-3).

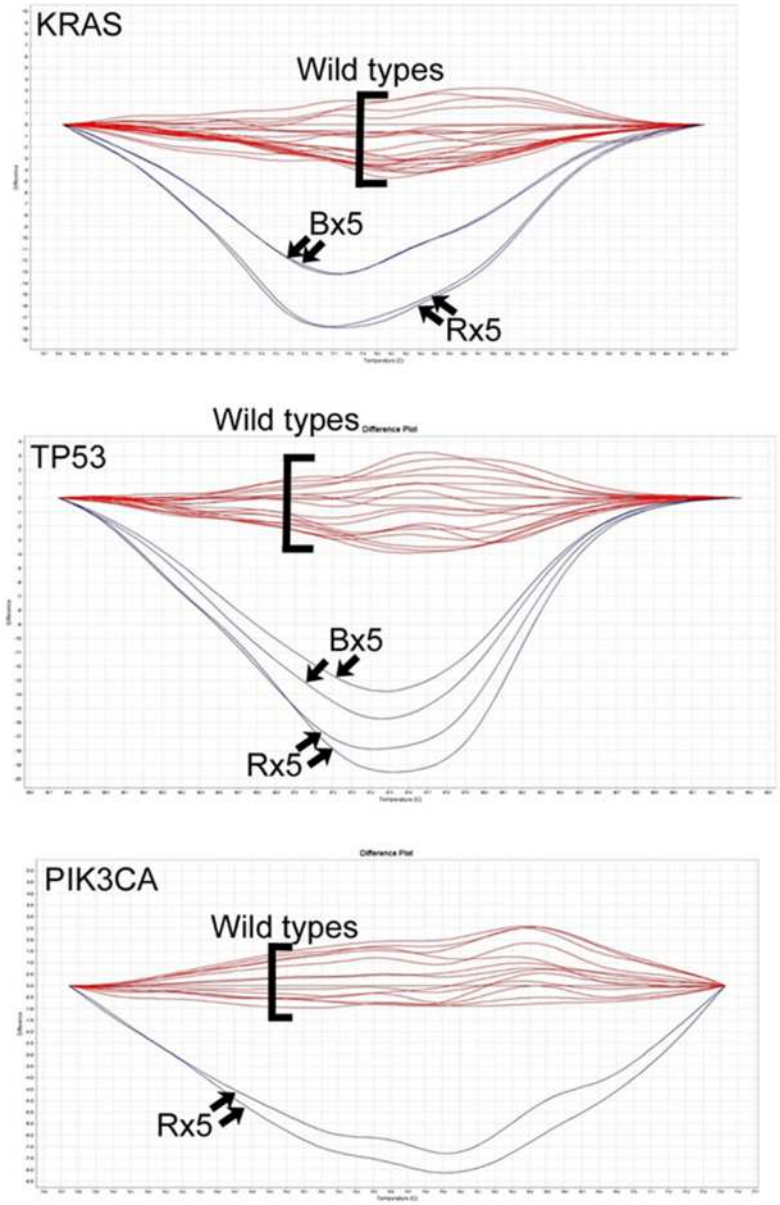

Figure 4-3 Melting plots for a discrepant case

One case only showed discrepancy between the biopsy (Bx) specimen and the resection (Rx) specimen. In this case, both the Bx and Rx specimens showed mutation in KRAS (top panel) and TP53 (middle panel). However, only the Rx specimen showed mutation in PIK3CA (bottom panel), and the Bx specimen showed the same melting pattern as the controls. We interpret this as subclonal evolution within the tumour.

4.4 Evaluation of immunostaining for mismatch repair (MMR) protein expression in biopsy and resection specimens

A total of 240 sections were stained and in 239 (99%) sections the IHC could be assessed (i.e. some stromal cell staining was apparent). The section that was unassessable was from a resection specimen. Immunostaining for all four of the MMR proteins was more intense and uniform in the biopsies than the resection specimens which tended to be more heterogeneous with areas frequently showing absence of expression in both tumour and stroma (Figure 4-4 a,b). Interpretation was much easier in the biopsy specimens than the corresponding resection specimens and this was especially so in cases where nuclear staining was score as "Absent" as the intensely stained stromal cells contrasted markedly with the unstained tumour cells (Figure 4-4 c,d).

Notwithstanding the limited nature of the biopsies, the interpretation was identical in both biopsy and the subsequent resection specimen. Three of the 30 (10%) cases were deemed as having lost MMR protein expression (and therefore presumed as MSI+) which is consistent with published literature.

In order to more formally evaluate the differences between the biopsy specimens and the resection specimens, each section was scored for the percentage of positive tumour nuclei regardless of intensity of staining or presence of staining in the stroma. Paired analysis showed that there were significantly more positively staining nuclei in the biopsies than in the resection specimens ($p<0.001$ for each protein, Wilcoxon signed rank test, Figure 4-5). This difference was particularly marked for immunostaining for MLH1 and MSH6.

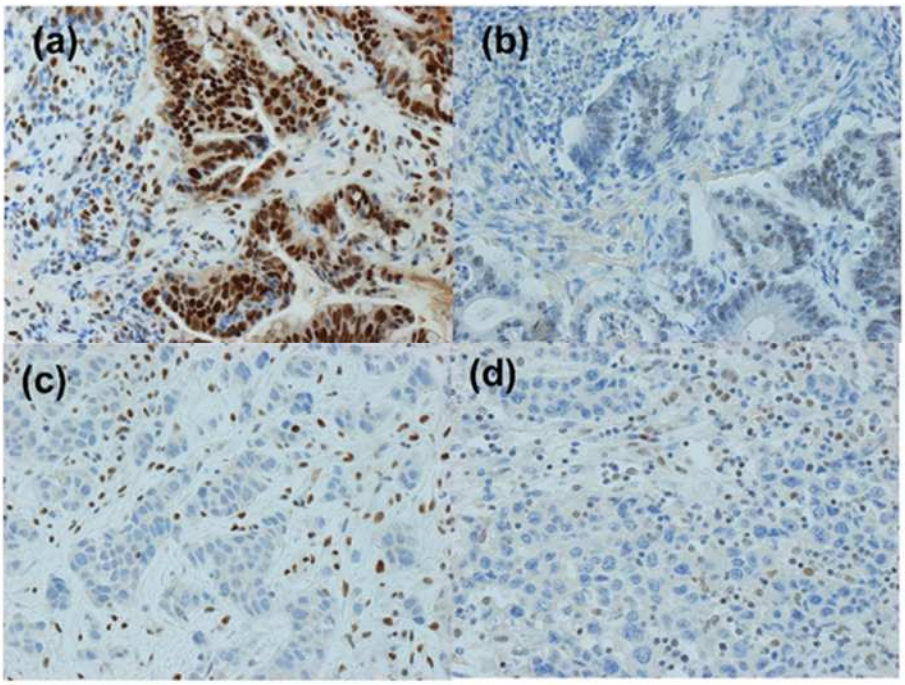

Figure 4-4 Comparative qualitative immunostaining in biopsies and resection specimens.

(a) and (b) show MLH1 staining respectively in biopsies and resection specimen from the same patient. Better fixation means the immunostaining is more intense in the biopsies thus it is easier to interpret. This is most manifest in cases where there has been loss of expression as shown in (c) and (d) which show PMS2 staining respectively in biopsies and resection specimen from the same patient. The more intense stromal staining in the biopsies contrast against the unstained tumour cells making interpretation straightforward

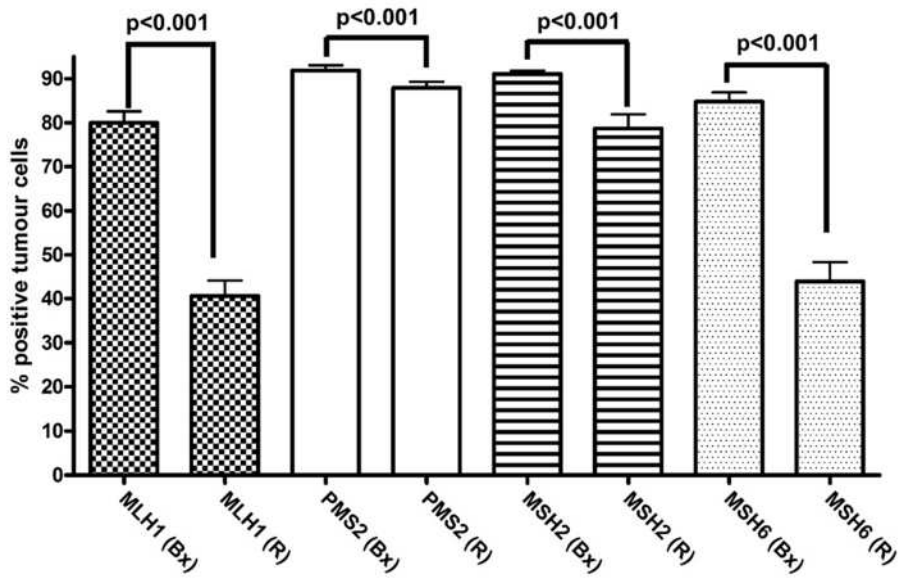

Figure 4-5 Comparative quantitative immunostaining in biopsies and resection specimens.

Positive staining tumour cells were quantified, and, in all cases, there were significantly more positive tumour cells seen in the biopsy than the resection specimen ($p<0.001$ for each). The differences were most stark in MLH1 and MSH6 which are the more fixation prone antibodies. (Bx: biopsy; R: resection)

4.5 Discussion

Whereas neoadjuvant therapy is commonly used in many types of cancer, its use in CRC is limited to rectal tumours. The results can be spectacular, with complete tumour regression seen in approximately 10–20% of patients following long-course chemoradiotherapy (Dhadda et al., 2011, Huebner et al., 2012, Tsutsumi et al., 2011). If the Foxtrot trial is successful, then neoadjuvant therapy may become routine in the management of CRC. If so, it will necessitate predictive testing on diagnostic biopsy specimens. As these represent a tiny fragment of the tumour, it is important to know whether biopsies are sufficiently representative of the tumour as a whole to allow their use in patient stratification. This is a new question arising from recent developments in oncology and is specifically addressed by our study.

Our data unequivocally show that, for certain mutations, diagnostic biopsy

specimens are suitable for predictive testing. From a total of 570 paired tests, identical results were obtained in both the biopsy and the subsequent resection specimen in 569 tests. The genes that were tested have all been linked in some way with responsiveness to certain chemotherapies. Mutations in KRAS, BRAF, PIK3CA and TP53 have all been reported to be predictive of responsiveness to therapies targeted at EGFR (De Roock et al., 2008, Van Cutsem et al., 2009, Di Fiore et al., 2007, Oden-Gangloff et al., 2009). MSI arises from mutation/epigenetic silencing of one of the mismatch repair genes, and has been linked with lack of responsiveness to 5-fluorouracil and enhanced responsiveness to irinotecan (Bertagnolli et al., 2009, Sargent et al., 2010, Sinicrope et al., 2011). Mutations in these genes and MSI are thought to occur in the early pre-invasive stages of colorectal tumour development (Fearon, 2011, Ilyas et al., 1999). In accordance with the theory of Darwinian evolution during carcinogenesis, it would be expected that 'early' driver mutations would be present in most cells in the invasive tumour. Thus, the high concordance between our biopsy and resection specimens is not surprising. Although the number of cases with MSI is small, there are two studies showing that testing for deficient mismatch repair by immunohistochemistry of biopsies reflects the pattern seen in the corresponding resection specimens (Shia et al., 2011). Coupled with the fact that the instability is seen at the same markers in biopsy and resection specimens, this allows us to confidently interpret our data (as with KRAS, BRAF, PIK3CA, and TP53) as a demonstration of clonal dominance.

There was just one discrepancy in our study: a tumour found to be wild type for PIK3CA in the biopsy was mutant in the resection specimen. This case also had mutations in KRAS and TP53 that were found in both the biopsy and the resection specimen. It is unlikely that the discrepancy resulted from technical artefact, and it is more likely to represent subclonal evolution.

Although no other study has compared tumour biopsies with the resection

specimens, others have been conducted that suggested clonal dominance. Comparisons of primary tumours with their matched metastases have shown 90–95% concordance for the mutation status of KRAS, BRAF, and PIK3CA, thereby demonstrating that metastatic deposits probably develop from dominant clones in the primary tumour (Cejas et al., 2009, Italiano et al., 2010, Knijn et al., 2011, Santini et al., 2008). Thus, mutation profiling of the primary tumour will identify many of the mutations present in metastases.

Mutation rates in humans have been calculated at 10^{-9} per nucleotide per cell division,(Bozic et al., 2010),(Jones et al., 2008) and, with the human genome comprising 3×10^9 bases, there will be three mutations every time that a cell divides. Heterogeneity within a tumour is therefore to be expected and, indeed, provides the variation required for tumours to overcome environmental constraints. However, some studies have shown intratumour heterogeneity even of the early driver mutations (Giaretti et al., 2000, Baisse et al., 2001, Baldus et al., 2010). Probably the most meticulous study was that of Goronova et al., in which multiple sites within a tumour were microdissected (by laser capture microdissection) and tested for APC, KRAS and TP53 mutations. Each microdissected site represented ~200 tumour cells, and their data showed that, although heterogeneity was undoubtedly present, there was generally a single dominant clone that occupied approximately 80–90% of the tumour volume (Goranova et al., 2011). The other studies have similarly shown dominance by a single clone, demonstrating that each clonal sweep does not necessarily lead to complete obliteration of earlier dominant clones. This may be a consequence of either there having been insufficient time for the dominant clone to take over the whole of the tumour, or the existence of micro-niches within the different parts of the tumour wherein the early clones can compete effectively with the dominant clone.

Our data suggest that, when multiple biopsies are taken during a diagnostic

procedure, there is a high probability that the dominant clone will be sampled. There are, however, two important caveats to consider when interpreting data from tumour biopsy specimens. First, Baldus et al. demonstrated 8%, 1% and 5% discrepancy in KRAS, BRAF and PIK3CA mutations, respectively, between the centre and the invasive edge of colorectal tumours (Baldus et al., 2010). In this particular study, the mutation was usually present in the central part of the tumour and absent at the invasive edge. Such a distinct topographical localization has not been reported by others, and one explanation may lie in the fact that invasive edges are probably more prone to stromal contamination than the central portions of the tumour. Failure to detect mutation in the tumour edge may thus be a technical artefact resulting from the limit of detection of the method used. We showed in Chapter 3 that our HRM methodology, is able to detect as few as 5% mutant alleles. Although the invasive tumour edge was characterised by absence of the studied mutations, if there are other genetic changes that do map consistently to this part of the tumour then these will inevitably be missed on biopsies taken from the gut lumen. The second caveat relates to the possibility that some of the early driver mutations are occasionally selected late, and may thus be present in a sub-clone that has not yet gained dominance. This has been experimentally demonstrated in vitro, where hypoglycaemic culture conditions have resulted in selection of KRAS mutations in cell lines that were originally wild type for this gene (Yun et al., 2009). This may be the explanation for our one discrepant test result, but it would suggest that it is happening at a very low frequency.

Thus, having compared pre-surgical diagnostic biopsies with resection specimens for immunostaining for MMR proteins, we conclude that the staining is usually more intense and easier to interpret in biopsies and that it faithfully replicates the diagnosis in the resection specimen. A variety of considerations (such as limited tissue in biopsies) may mean that immunostaining on resection specimens remains the preferred option.

In summary, the aim of this study was to test whether presurgical diagnostic tumour biopsy specimens are suitable for predictive testing in CRC. We conclude that, for KRAS, BRAF, PIK3CA and TP53 mutations, biopsies are adequately representative of the tumour as a whole, and that this is an acceptable strategy for mutation detection. Additionally, it can be concluded from the results of this study, in cases where poor fixation makes interpretation impossible, then immunstaining in biopsies is a robust alternative.

Chapter 5. **DNA content analysis of colorectal cancer defines a distinct group**

5.1 Introduction

The role of genomic instability in the development of cancer is a contentious issue. Some have argued that onset of genomic instability, through mutation of "caretaker" genes which are responsible for the maintenance of genomic integrity, results in an increased mutation rate and this is essential to the carcinogenetic process (Levitt and Hickson, 2002). Others, however, have argued that tumour evolution through waves of mutation-driven clonal expansion is sufficient for tumour development without the requirement of genomic instability (Sieber et al., 2003). Irrespective of its precise role in tumour development, genomic instability is very commonly seen in many different cancers and it accelerates the rate of tumour development.

Sporadic colorectal cancers (CRCs) are usually considered to have two main types of genomic instability i.e. Microsatellite Instability (MSI) or Chromosomal Instability (CIN) (Ilyas et al., 1999, Jass, 2007). Colorectal cancers acquire MSI as a result of loss of mismatch repair function arising from mutational or epigenetic inactivation of any one of four genes – MLH1, MSH2, PMS2, MSH6 (Abdel-Rahman et al., 2006, Karran, 1995, Lothe, 1997, Thibodeau et al., 1993). Loss of mismatch repair function results in a failure to repair base-pair mismatches and small-scale insertion/deletion mutations resulting in genome-wide mutations of these types. Karyotypically, however, CRCs with MSI (MSI-CRCs) have a diploid or near-diploid DNA content (Curtis et al., 2000, Frei, 1992, Kouri et al., 1990).

CIN is more or less mutually exclusive with MSI and it is characterised by large scale genomic changes including deletions, amplifications and gains/losses of whole chromosomes. The cause of CIN in CRCs is not known although a number of candidates such as APC, AXIN2, TP53, AURKA and FBXW7, have been proposed (Baba et al., 2009, Fodde et al., 2001, Hadjihannas et al., 2006,

Rajagopalan et al., 2004, Williams et al., 1997). Those CRCs with CIN (CIN-CRCs) characteristically show aneuploidy on examination of DNA content (Pino and Chung, 2010).

Around 10-15% of sporadic CRCs show MSI whilst the remainder are microsatellite-stable and are usually considered to show CIN. However, prior to the discovery of mismatch repair deficiency and MSI, tumour DNA content was commonly evaluated and a review of these published studies shows that the proportion of diploid tumours reported varied from 11–64% (Armitage et al., 1991, Flyger et al., 1999, Heimann et al., 1990, Tang et al., 1995). A recent meta-analysis of these studies estimated that, of 5,478 patients, 42% showed a diploid genotype (Araujo et al., 2007). If the cases with probable MSI are removed, then the data would suggest that a significant proportion of all CRCs have neither MSI nor CIN (henceforth referred to as Microsatellite and Chromosomal Stable, MACS). This point is reinforced in studies which have exclusively tested rectal cancers. Of the tumours located at this site, only 2 – 3% will have MSI (Hutchins et al.) but the reported frequency of diploid rectal tumours is 30–64%(Fisher et al., 1989, Heimann et al., 1990, Michelassi et al., 1992). There have been some reports of MACS-CRCs although these are relatively few (Georgiades et al., 1999, Hawkins et al., 2001, Silver et al., 2011). Despite these reports and the circumstantial evidence from earlier studies, a dogma has emerged that CRCs must have one or other form of genomic instability and recent reviews have cited the frequency of CIN as around 85% (Fearon, 2011, Pritchard and Grady, 2011).

The MACS-CRCs therefore may form a third group which is distinct from CRC with MSI and CIN. As well as having implications for cancer theory, this may have clinical implications. MSI-CRCs have distinct clinico-pathological features including, amongst others, right-sided location and a comparatively good clinical outcome. Conversely, CIN-CRCs have a left sided predominance and a generally

poorer outcome than MSI-CRCs. Since MACS-CRCs are a relatively poorly described group, their clinico-pathological correlates are also poorly described.

As well as providing prognostic information, genotypic analysis of tumours may predict responsiveness to specific therapies. For example, MSI-CRCs reportedly have poor response to 5-Fluorouracil but better response to irinotecan than their CIN counterparts (Bertagnolli et al., 2009, Ribic et al., 2003). In recent years, neoadjuvant (chemo) radiotherapy has become commonplace for rectal CRCs. Approximately 15-25% of these tumours undergo marked regression (Mandard Grade 1 or 2) although currently it is impossible to predict which tumours will respond (Dhadda et al., 2011, Dhadda et al., 2009, Suarez et al., 2008, Vecchio et al., 2005). It is known that the primary lethal lesion induced by ionizing radiation is a chromosome aberration (Bedford, 1991). It was demonstrated that a direct relationship exists between ploidy and mean lethal chromosome aberration frequency, which means that that changes in DNA ploidy are an important contributor to radiation sensitivity variations (Schwartz et al., 1999). So, if responsiveness to radiation could be predicted with certainty, it would allow a significant proportion to patients to avoid major surgery. We hypothesised that MACS-CRCs (diploid/ near diploid tumours) may respond differently to radiation than CIN-CRCs (aneuploid tumours). If so, tumour ploidy could be used as a predictive test for radiation responsiveness.

Given the relative paucity of knowledge about the MACS-CRCs we firstly evaluated the DNA content and mutation profile in an unselected series of CRCs which were shown to be microsatellite-stable. In order to test our hypothesis that MACS-CRCs and CIN-CRCs may have different responses to radiation, we then evaluated the DNA content of pre-radiotherapy biopsies from a series of rectal cancers and correlated tumour regression with ploidy status.

5.2 Screening cases for microsatellite instability

A total of 100 cases (Nottingham series set-1 & 2) were tested for the presence of microsatellite instability. Each tumour was tested using a panel of 6 mononucleotide markers. Of the tumours tested, 8 cases showed instability in over 2 of the markers (Figure 5-1 a) and were excluded from sample set 1.

5.3 Flow cytometry

Of the 92 tumours tested for flow cytometry, reliable data could not be obtained for three of these and these were excluded from further analysis. Reliable data were obtained from the remaining 89 tumours and there were three distinct patterns seen. Firstly, there were samples in which a single G0/G1 peak was seen with a smaller G2/M peak (Figure 5-1 b) and this was deemed to be a diploid tumour. A second pattern was that of two peaks at G1/G0 that lay very close to each other with a ratio of 0.9 – 1.1 seen between the two peaks.

There were also two closely associated G2/M peaks and this pattern was deemed a "near-diploid" tumour (Figure 5-1 c). The third pattern was that of an aneuploid population in which extra peaks were seen between the G0/G1 and G2/M peaks of the internal diploid controls. There was usually just one extra peak although occasionally multiple extra peaks were seen. These represented the G0/G1 peak of an aneuploid population (Figure 5-1 d). Of the 89 microsatellite-stable CRCs tested, a total of 51 (57%) were aneuploid (i.e. CIN-CRCs) whilst 38 (43%) were diploid or near-diploid (i.e. MACS-CRCs). Thus a high proportion of the tumours tested were of the MACS genotype but there were no significant clinico-pathological differences seen between CIN-CRCs and MACS-CRCs (Table 5-1).

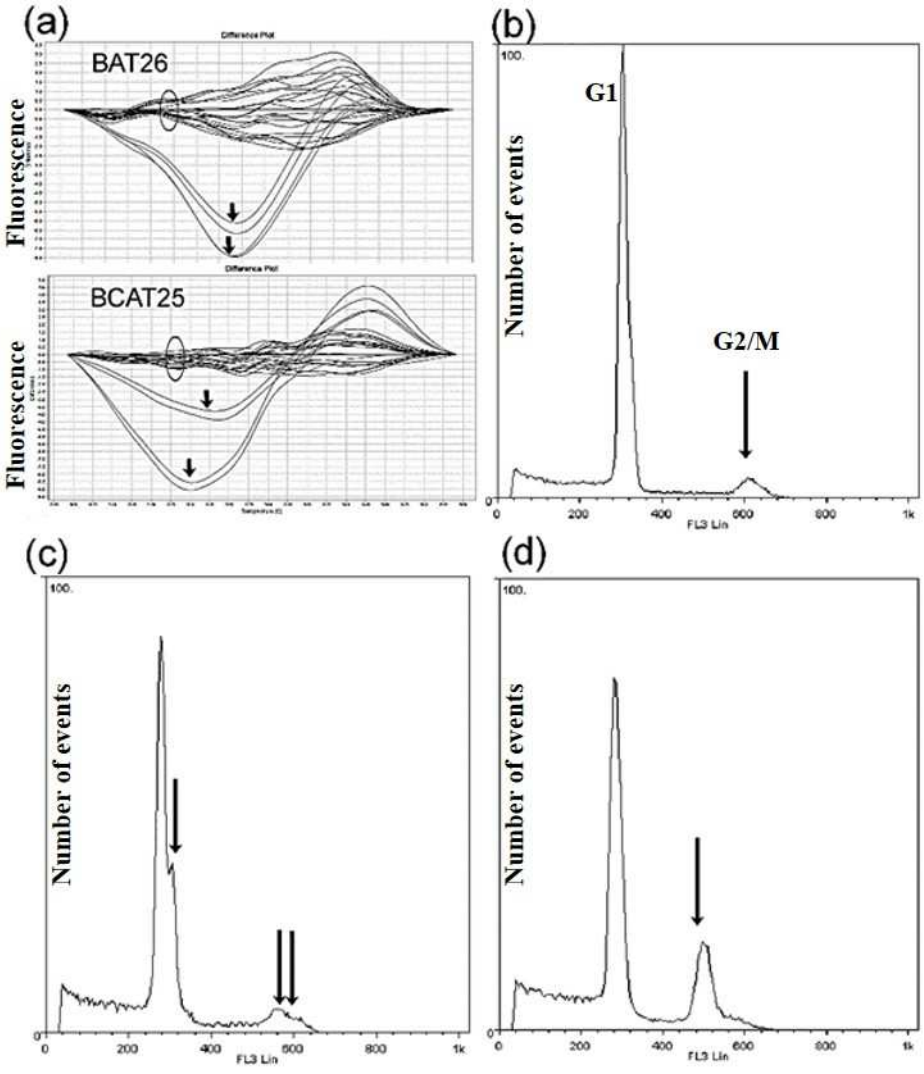

Figure 5-1 Evaluation of the DNA content of colorectal tumours.

Firstly, the tumours were screened for the presence of MSI by PCR/HRM for 6 separate mononucleotide markers. (a) shows data for BAT26 and BCAT25 markers. The microsatellite stable cases show similar patterns of melting (circled) whilst two cases are shown (each in duplicate and denoted by the arrows) in which there is instability at these markers resulting in aberrant melting. (b) – (d) show the three patterns seen when evaluating microsatellite stable cases by flow cytometery. (b) shows a diploid pattern in which the tumour cells and stromal cells lie within a single dominant diploid peak. The arrow indicates the G2/M peak (representing 4c DNA content). (c) shows a "near-diploid" pattern in which a separate peak (single arrow) is clearly discernible from the dominant G0/G1 peak but the DNA index of this is less than 1.1. The G2/M peaks are shown by the double arrow. (d) the arrow shows a clearly aneuploid peak which, in this case, has a DNA index of 1.6.

Table 5-1 Clinico-pathological features and mutation profile of CIN-CRCs and MACS-CRCs

CIN-CRCs: chromosomal instable-CRCs; MACS-CRCs: microsatellite and chromosomal stable-CRCs. EMVI: extramural vascular invasion; V0: absent; V1: present.

		CIN-CRC	MACS-CRC		Total sample
Sex	M	32 (63%)	22 (58%)	p=0.6	54 (61%)
	F	19 (37%)	16 (42%)		35 (39%)
Age	Median	66	73	p=0.06	70
	IQR	58-78	66-78.5		62-78
	Mean	67	71		69
Dukes' stage	A/B	21 (48%)	14 (44%)	p=0.8	35 (46%)
	C/D	23 (52%)	18 (56%)		41 (54%)
EMVI	V0	17 (36%)	12 (39%)	p=1.0	29 (37%)
	V1	30 (64%)	19 (61%)		49 (63%)
Location	Right sided	16 (31%)	12 (32%)	p=1.0	28 (32%)
	Left sided	35 (69%)	25 (68%)		60 (68%)
KRAS	Mutant	20 (39%)	21 (55%)	p=0.19	41 (46%)
	Wild type	31 (61%)	17 (45%)		48 (54%)
BRAF	Mutant	5 (10%)	4 (11%)	p=1.00	9 (10%)
	Wild type	46 (90%)	34 (89%)		80 (90%)
PIK3CA	Mutant	9 (18%)	4 (11%)	p=0.38	13 (15%)
	Wild type	42 (82%)	34 (89%)		76 (85%)
TP53	Mutant	35 (69%)	19 (50%)	p=0.08	54 (61%)
	Wild type	16 (31%)	19 (50%)		35 (39%)

5.4 The mutation profile of CIN-CRCs and MACS-CRCs

All 89 tumours in the first series were screened for the presence of mutation in the hotspots of KRAS, BRAF, PIK3CA and TP53 (Table 5-2). The frequency of mutations of the total sample set was as follows: KRAS: 46%, BRAF: 10%, PIK3CA: 15% and TP53: 61%. The frequency of mutation is in line with what would be expected for an unselected series of CRCs. Sub-group analysis and comparison of CIN-CRCs with MACS-CRCs showed that generally there was a

similar mutation frequency within the two groups with no significant difference emerging. Of interest, however, was that 69% of CIN-CRCs contained TP53 mutation whilst this was seen in 50% of the MACS-CRCs. This was no statistically significant (p=0.08) but raises the possibility that TP53 mutation may be permissive for the aneuploid state as has been previously suggested and consistent with its proposed role as a "caretaker" gene. Similarly, 39% of CIN-CRCs were mutant for KRAS compared to 55% of MACS-CRCs suggesting a preference of the latter for development along a KRAS-dependent pathway. Evaluation of the total mutation burden showed that 5/51 (10%) CIN tumours did not have mutation in any of these genes whilst, for the MACS group, 8/38 (27%) tumours were wild type for these genes. The difference was not statistically significant (p = 0.22). The association of mutations with each other was also tested. In the group overall, there was the expected negative association between mutation of KRAS and BRAF (p=0.001). Apart from this, there was no significant association seen in either the overall group or either of the sub-groups (Table 5-2).

Table 5-2 Association of gene mutations in CIN-CRCs and MACS-CRCs

			BRAF			PIK3CA			TP53		
			Mut*	WT**		Mut	WT		Mut	WT	
	KRAS	Mut	0	41	p=0.003	8	33	p=0.26	24	17	p=0.7
		WT	9	39		5	43		30	18	
All cases	BRAF	Mut				1	8	p=1.00	6	3	p=1.00
		WT				12	68		48	32	
	PIK3CA	Mut							6	7	p=0.36
		WT							48	28	
	KRAS	Mut	0	20	p=0.14	5	15	p=0.28	13	7	p=0.7
		WT	5	26		4	27		22	9	
CIN	BRAF	Mut				1	4	p=1.00	3	2	p=0.64
		WT				8	38		32	14	
	PIK3CA	Mut							4	5	p=0.12
		WT							31	11	
	KRAS	Mut	0	21	p=0.03	3	18	p=0.61	11	10	p=1.00
		WT	4	13		1	16		8	9	
MACS	BRAF	Mut				0	4	p=1.00	3	1	p=0.60
		WT				4	30		16	18	
	PIK3CA	Mut							2	2	p=1.00
		WT							17	17	

Mut*: Mutant/ WT**: Wild Type

5.5 The association of DNA content with radiation responsiveness

We had hypothesised that tumour responsiveness to radiation may be predicted by DNA content. To test this, we evaluated the DNA content of diagnostic biopsies from a separate series of 62 rectal cancers. Of these, 22 had responded (Mandard Tumour Regression Grade 1 & 2) and 40 had shown little response (Mandard Tumour Regression Grade 3-5) following neo-adjuvant chemoradiotherapy. Overall 35/62 (60%) cases were aneuploid whilst 25/60 (40%) cases were diploid. Of the responders, 12/22 (54%) were CIN-CRCs and 10/22 (46%) were MACS-CRCs. Of the non-responders, 25/40 (62%) were CIN-CRCs and 15/40 (38%) were MACS-CRCs. Sub-group analysis however failed to show any association between tumour DNA content and response to the radiotherapy.

5.6 Discussion

In this study we evaluated the DNA content of microsatellite stable CRCs in order to evaluate the proportion of aneuploid and diploid tumours. The aneuploid group were deemed to show chromosomal instability (CIN) and were therefore designated as CIN- CRCs. The diploid group, because of their stable karyotype, were considered to be both microsatellite and chromosomal stable (MACS) and were designated as MACS-CRCs. Two independent sets of tumours were analysed – a series of 89 colorectal tumours was tested in order to test the association between ploidy and clinicopathological / molecular features and a second series of 62 rectal cancers which had received neoadjuvant CRT was tested in order to ascertain whether ploidy could predict responsiveness to radiation.

Using flow cytometry to quantify the tumour DNA content, we found that MACS-CRCs comprised 43% of the first sample set and 45% of the second sample set.

Archival studies have reported the proportion of diploid tumours as ranging from 20 – 60% but it has always been greater than the proportion of expected MSI-CRCs. Both of our sample sets are consistent with the published literature and with each other. All of our cases were reviewed to ensure a minimum of 50% tumour cells within the samples tested. Our data strongly challenge the dogma that CRCs can all be dichotomised into tumours which progress along either the MSI or CIN pathway (Fearon, 2011, Pritchard and Grady, 2011). We have shown that a significant proportion of CRCs belong to a third group which involves neither CIN nor MSI. These tumours may not have any genomic instability or they may have a third form of genomic instability; such as that caused by POLE mutations (Muzny et al., 2012, Palles et al., 2012).

In sample set one, we sought to evaluate whether there were any clinico-pathological or molecular differences between MACS-CRCs and CIN-CRCs. Firstly, comparison of the clinico-pathological features of MACS-CRCs with the CIN-CRCs did not show any significant differences. Old studies of tumour ploidy have found a significant association of diploid tumours with the right side of the colon and with better prognosis although these would have been obviously confounded by the inclusion of tumours with MSI. Studies which have evaluated MACS-CRCs specifically have published mixed data with some reporting a left sided predominance of the MACS-CRCs or a poor prognosis whilst others have not found these features (Hawkins et al., 2001, Silver et al., 2011).

Screening for mutation in four genes commonly mutated in CRCs demonstrated no significant differences apart from a slightly greater frequency of TP53 mutation in the CIN-CRCs. This series of cases is of insufficient size to pick up small or moderate differences in mutation frequency between the two groups. Our data do show that, for the genes tested, the differences between the two groups are not stark and that whilst TP53 mutation may be permissive for aneuploidy, it is not a major

cause of aneuploidy. The similarity in the mutation profiles of the CIN-CRCs and the MACS-CRCs also suggests that the events which lead to aneuploidy probably occur late in the carcinogenetic process after these mutations are likely to have occurred. This is consistent with data showing that aneuploid clones rarely occur in early or intermediate stage adenomas but can be identified in the late stage adenomas (Goh and Jass, 1986, Quirke et al., 1986, van den Ingh et al., 1985).

We also investigated whether the MACS phenotype was associated with responsiveness to neoadjuvant radiation therapy in a separate set of rectal cancers. Around 15-25% of rectal CRCs show a dramatic response to neoadjuvant radiation therapy and identification of the features predicting responsiveness would be a major step forward in the management of patients with rectal cancer. We hypothesised that the DNA content may be associated with responsiveness and thus pre-radiotherapy diagnostic biopsies from cases of responsive and non-responsive tumours were tested. We and other investigators (West, 1994) couldn't find a relationship between DNA ploidy and response to radiation. This finding leads us to conclude that there are other factors in addition to ploidy that define response. In fact, previous studies reported that the primary factor underlying the radiosensitivity differences is alterations in DNA double-strand break rejoining kinetics. This means that DNA repair alterations define the probability of producing a chromosome aberration, while ploidy defines how many aberrations are required to kill the cell (West, 1994, Schwartz, 1998, Schwartz et al., 1999).

In summary, we have demonstrated that MACS-CRCs form a significant group in the microsatellite stable CRCs. The Fearon and Vogelstein model of colorectal tumourigenesis was postulated over 30 years ago and did not feature tumour ploidy. This should be revisited and should include three distinct groups i.e. MSI-CRC, CIN-CRC and MACS-CRC within the classification. Whilst these groupings may be associated with the biology of CRCs, they do not influence the response to

radiation therapy.

Chapter 6. The prognostic significance of TP53 and MMR expression: results from the VICTOR trial.

6.1 Introduction

In the UK, colorectal cancer is the 4th most common cancer, accounting for 12% of all new cancer cases, and the second most common cause of cancer related death (CR-UK, 2018). Management of patients with CRC is dependent on the staging of the resected tumour by a pathologist. Patients with early-stage CRC (i.e. Stage I) have a good prognosis and will not receive adjuvant therapy (Day et al., 2003). In cases with more advanced-stage disease (i.e. stage II and III) the prognosis is more variable and consequently the management is more complex. Treating all cases of stage II disease with adjuvant chemotherapy gives a net benefit of around 4% improvement in survival (Midgley and Kerr, 2005). Such parsimonious returns are most probably due to the fact that around 70% of patient with stage II CRC will be disease free 5 years later and thus will not benefit from adjuvant therapy. It would be expedient to target only the 30% of stage II cases who are at a high risk of recurrent disease. However, discriminating between the two groups is not easy – certain pathological features (such as extramural vascular invasion) are associated with poorer outcome. However pathological evaluation is operator-dependent and can be a highly variable method of gathering prognostic information (Morris et al., 2007). Furthermore, pathological staging does not provide any information on tumour biology. Almost all patients with stage III disease are given adjuvant chemotherapy as the overall prognosis is quite poor (Poston et al., 2012). However, not all tumours are the same and, with the increasing availability of targeted therapies, identification of factors which predict tumour responsiveness to specific therapies would facilitate the bespoke tailoring of therapies.

There is thus a need for robust predictive and prognostic biomarkers which can add to current standard pathological analysis (Locker et al., 2006). In making the choice of which biomarkers to test, then choosing those that reflect tumour biology would be a reasonable starting point. CRCs are thought to develop along three main

genetic pathways: the chromosomal instability (CIN) pathway, the microsatellite instability (MSI) pathway (Fearon, 2010, Ilyas et al., 1999) and the rather poorly described microsatellite and chromosomal stable (MACS) pathway (Chan et al., 2001, Georgiades et al., 1999, Silver et al., 2011). Tumours developing along the CIN pathway are characterised by gross chromosomal aneuploidy and extensive allelic gains and losses. Tumours developing along the MSI pathway are characterised by diploid chromatin content and numerous insertion/deletion mutations in DNA repeat sequences known as microsatellites. MSI arises due to deficient mismatch repair mechanism which in turn is caused by loss of expression or function of any one of 4 main MMR proteins (i.e. MLH1, PMS2, MSH2 and MSH6) (Fearon, 2010). The MMR proteins can be detected by immunohistochemistry (IHC) and thus the biologically distinct CRCs with either CIN or MSI can be distinguished by this method (Shia, 2008, Zhang, 2008).

Another potential biomarker would be expression of the tumour protein 53 (TP53). TP53 is a tumour suppressor gene and it is mutated in 60-70% of CRCs (Hollstein et al., 1991). It can be inactivated by truncating mutations or by misense mutations and these lead to aberrant p53 protein expression. In the former case there is complete loss of expression of p53 protein whilst in the latter case there is post-translational stabilisation leading to gross over-expression of the protein (Lane, 1992). These changes can also be detected by IHC thereby allowing tumours containing mutant TP53 to be distinguished from those which are wild type for TP53 (Baas et al., 1994).

We aimed to test the clinical utility of dMMR and aberrant p53 expression as prognostic and predictive markers in CRC. Although there have been previous studies investigating these biomarkers, the published data are not completely conclusive. Studies have been confounded by a variety of factors such as pooling data from multiple trials and technical variation in the laboratory methods. This

study was performed on tissue obtained from patients recruited to the VICTOR trial (a single large randomised phase III trial run in the UK) (Midgley et al., 2010) and all the IHC was performed in a single, fully accredited, diagnostic laboratory.

6.2 Profile of the overall trial population and experimental sub-groups.

VICTOR recruited a total of 2434 patients and, from this population, MMR was evaluated in 735 patients, p53 was evaluated in 740 patients and combined MMR/p53 was evaluated in 677 patients. Table 2-6 shows that clinico-pathological and demographic profile (with respect to age, sex, stage and treatment) of each of the evaluated groups was identical to that of the overall trial population. This confirms that there was no bias introduced by the processes of tissue collection, TMA construction and IHC. The overall trial population had a 5 year DFS and OS rate of 66.5% and 78.2% respectively. Analysis by stage showed 5 year DFS and OS of 76.4% and 86.6% respectively in Stage II disease and 5 year DFS and OS of 57.7% and 70.7% respectively in Stage III disease. This shows that there was an extremely good outcome in the VICTOR trial patients although, as expected, there was a significant difference in DFS (Hazard ratio (HR) 2.12 (1.70, 2.64), $p<0.001$) and OS (HR 2.38 (1.81, 3.13), $p<0.001$) for stage III disease compared to stage II disease as shown in Table 6-1. Also, there were no differences observed in OS or DFS between each of the evaluated groups and the overall trial population (Table 6-1).

Table 6-1 Comparison of stage specific 5-year survival in all patients versus tested groups

This table shows that there was a significant difference in disease free survival (DFS Hazard ratio p<0.001) and overall survival (OS Hazard ratio p<0.001) for stage III disease compared to stage II disease, but no differences observed in DFS or OS between each of the evaluated groups and the overall trial population.

stage III vs. stage II	All Patients	IHC MMR (n=735)	IHC P53 (n=740)	MMR/P53 (n= 677)
Disease Free Survival				
Unadjusted Hazard ratio	2.17	2.48	2.82	2.37
(95% CI)	(1.85, 2.54)	(1.82, 3.36)	(1.74, 3.00)	(1.72, 3.25)
P-value	<0.001	<0.001	<0.001	<0.001
Adjusted Hazard ratio	2.12	2.40	2.34	2.50
(95% CI)	(1.70, 2.64)	(1.57, 3.67)	(1.70, 3.19)	(1.75, 3.56)
P-value	<0.001	<0.001	<0.001	<0.001
Overall Survival				
Unadjusted Hazard ratio	2.47	3.11	2.76	2.82
(95% CI)	(2.02, 3.00)	(2.10, 4.60)	(1.96, 3.89)	(1.90, 4.20)
P-value	<0.001	<0.001	<0.001	<0.001
Adjusted Hazard ratio	2.38	3.27	2.82	3.19
(95% CI)	(1.81, 3.13)	(1.90, 5.62)	(1.92, 4.14)	(2.05, 4.97)
P-value	<0.001	<0.001	<0.001	<0.001

6.3 Clinico-pathological features and outcomes associated with dMMR

Loss of IHC expression of MMR proteins is indicative of deficient MMR and, from this, the presence of microsatellite instability (MSI) can be inferred with confidence. In the sporadic setting, the majority of cases of dMMR will be due to loss of MLH1 expression and this has prompted many studies to perform IHC with only two antibodies – MLH1 and MSH2.

We opted to use a panel of antibodies for all four of the MMR proteins since (i) isolated MSH6 and PMS2 loss does occur and (ii) the performance of the antibodies is variable. The antibody for MLH1, for example, is particularly sensitive to tissue fixation but, given that there is a heterodimeric association of the proteins, loss of expression of the binding partner can be used to confirm loss of expression of MLH1 and MSH2 (Figure 2-15).

A total of 735 tumours could be evaluated for all 4 of the MMR proteins. Deficient MMR was found in 11.8% (87/735) of the total patients analysed in this sub group (Table 6-2, Table 6-3). The most common deficiency was an absence of MLH1 (79%) followed by MSH2 (12%), PMS2 (5%) and MSH6 (2%). There was one case in which all 4 MMR proteins were lost (Table 6-4). The frequency of detected MSH6 deficiency may be a slight underestimate of the true frequency as the antibody used is fixation sensitive. Consequently, cases were excluded in which MSH6 deficiency was suspected but for which the IHC was not of sufficient quality for a definitive conclusion.

Compared to tumours with pMMR, the tumours with dMMR had a significant positive association with female gender ($p=0.001$), proximal location ($p<0.001$), poor differentiation ($p<0.001$), earlier clinical stage ($p<0.001$) and a higher

proportion of cases with adequate lymph node recovery (i.e. 12 or more lymph nodes retrieved) from the resection specimen (p=0.019). There was no association with age of patient at presentation, pathological T stage or vascular/lymphatic invasion. The patients with dMMR tumours were less likely to have received chemotherapy /radiotherapy (p<0.001) which probably reflects their clinical staging and their proximal location (Table 6-2).

The hazard ratio for DFS for pMMR versus dMMR was 1.01 (0.61, 1.69), p= 0.973. The 5-year DFS rates were 66.9 (62.3, 71.1) for pMMR and 72.0 (59.9, 82.3) for dMMR. The hazard ratio for OS for pMMR versus dMMR was 0.80 (0.45, 1.41), p = 0.441. The 5-year OS rates were 78.6 (75.0, 81.8) for pMMR and 78.8 (67.7, 86.4) for dMMR. When analysed in stage specific groups, the presence of dMMR was not associated with any significant difference in 5-year DFS or OS in either of the stage II or stage III disease sub-groups alone (Table 6-3).

It has been suggested that dMMR tumours may respond differently to chemotherapy to those with pMMR. We therefore compared the outcomes in the chemotherapy treated and chemotherapy naive sub-groups (Table 6-3). In the treated sub-group, there was no significant difference between dMMR and the pMMR cases. In the chemotherapy naive sub-group, however, pMMR was significantly associated with a better outcome than dMMR for both OS (hazard ratio 0.28 (0.11, 0.68), p=0.005) & DFS (hazard ratio 0.47 (0.22, 0.99), p=0.047).

Table 6-2 Clinico-pathological features and outcomes associated with dMMR

This table shows that dMMR tumours have a significant positive association with female gender, proximal location, poor differentiation and earlier clinical stage, but they don't have significant association of dMMR status with pathological T stage (T stage) and vascular invasion in comparison to pMMR tumours. It also shows that patients with dMMR tumours are less likely to have received chemotherapy /radiotherapy ($p<0.001$).

No of patients		All: n(%)	dMMR: n(%)	pMMR: n(%)	P value*
Sex n (%)	M	468 (63.7)	46 (52.9)	221 (34.1)	0.001
	F	267 (36.3)	41 (47.1)	427 (65.9)	
Age mean (SD)		64.20 (10.0)	65.93 (11.17)	64.08 (9.79)	0.105
Location	Proximal	503 (68.4)	80 (91.9)	423 (65.3)	<0.001
	Distal	332 (31.6)	7 (8.1)	225 (34.7)	
Differentiation	Well	53 (7.4)	5 (5.9)	48 (7.5)	<0.001
	Moderate	585 (81.0)	50 (58.8)	535 (84.0)	
	Poor	83 (11.5)	30 (35.3)	53 (8.3)	
	Unknown	1 (0.1)	0 (0.00)	1 (0.20)	
T stage	pT1/2	69 (9.6)	6 (7.1)	63 (9.9)	0.331
	pT3	508 (70.3)	65 (76.4)	443 (69.5)	
	pT4	142 (19.7)	13 (15.3)	129 (20.2)	
	Unknown	3 (0.4)	1 (1.2)	2 (0.3)	
Vascular invasion	Yes	136 (18.8)	15 (17.7)	121 (19.00)	0.696
	No	576 (19.8)	68 (80.0)	508 (79.7)	
	Unknown	10 (1.4)	2 (2.3)	8 (1.3)	
Lymphatic invasion	Yes	66 (9.1)	7 (8.2)	59 (9.2)	0.691
	No	646 (89.5)	76 (89.4)	570 (89.5)	
	Unknown	10 (1.4)	2 (2.4)	8 (1.3)	
Number of LN removed	Mean (SD)	13.19 (7.68)	14.42 (7.48)	13.02 (7.70)	0.1197
LN staging n (%)	<12 LN	337 (46.7)	30 (35.3)	307 (48.2)	0.019*
	≥12 LN	362 (50.1)	53 (62.3)	309 (48.5)	
	Unknown	23 (3.2)	2 (2.4)	21 (3.3)	
Clinical Stage n (%)	II	337 (45.9)	59 (67.8)	278 (42.9)	<0.001
	III	398 (54.1)	28 (32.2)	370 (57.1)	
Chemotherapy n (%)	Yes	467 (63.5)	46 (52.9)	421 (65)	0.028
	No	268 (36.5)	41 (47.1)	227 (35)	
Radiotherapy n (%)	Yes	75 (10.2)	2 (2.3)	73 (11.3)	0.009
	No	660 (89.8)	85 (97.7)	575 (89.8)	
Recurrence n (%)	Yes	201 (27.4)	20 (23)	181 (27.9)	0.331
	No	534 (72.6)	67 (77)	467 (72.1)	
Deaths n (%)	Yes	145 (19.7)	17 (19.5)	128 (19.8)	0.963
	No	590 (80.3)	70 (80.5)	520 (80.2)	

LN = lymph nodes, *Chi-squared test – dMMR vs pMMR.

Table 6-3 Effects of MMR on 5-year Disease Free Survival and Overall Survival: sub-group analysis

This table shows that there was no significant difference in disease free survival hazard ratio (DFS HR p<0.001) and overall survival hazard ration (OS HR p<0.001) between dMMR and pMMR patients. However, it can be noticed in this bottom row from this table that in the chemotherapy naive sub-group, pMMR was significantly associated with a better outcome than dMMR for both overall survival (OS) and disease free survival (DFS).

		n	DFS (95%CI)	HR (95%CI)	p value*	OS (95%CI)	HR (95%CI)	P value *
All patients	All	735	67.8 (63.4, 71.7)			78.6 (75.2, 81.7)		
	dMMR	87	72.9 (59.9, 82.3)	1.07 (0.66,	0.793	78.8 (67.7, 86.4)	0.80 (0.45,	0.441
	pMMR	648	66.9 (62.3, 71.1)	1.73)		78.6 (75.0, 81.8)	1.41)	
Stage II	All	337	78.1 (71.6, 83.3)			87.2 (82.6, 90.7)		
	dMMR	59	77.9 (58.9. 88.9)	1.18 (0.52,	0.695	85.6 (71.5, 93.1)	0.88 (0.34,	0.788
	pMMR	278	77.9 (70.8, 83.5)	2.67)		87.5 (82.4, 91.3)	2.29)	
Stage III	All	398	59.0 (53.1, 64.5)			71.6 (66.6, 76.0)		
	dMMR	28	60.8 (40.5, 76.0)	0.84 (0.44,	0.608	65.2 (44.9, 79.5)	0.70 (0.35,	0.310
	pMMR	370	58.9 (52.7, 64.6)	1.62)		72.2 (67.0, 76.8)	1.40)	
Chemothera	All	467	62.0 (56.7, 66.9)			73.7 (69.3, 77.7)		
py treated	dMMR	46	79.7 (64.5, 88.9)	1.81 (0.86,	0.117	82.1 (67.3, 90.6)	1.56 (0.70,	0.276
	pMMR	421	60.5 (54.6, 65.8)	3.81)		73.5 (68.6, 77.8)	3.49)	
Chemonaive	All	268	77.8, 70.8, 83.4)			87.2 (82.2, 90.8)		
	dMMR	41	66.5 (45.7, 80.9)	1.07 (0.75,	0.047	75.2 (57.1, 86.5)	0.28 (0.11,	0.005
	pMMR	227	79.5 (71.4, 85.6)	1.54)		88.6 (83.2, 92.3)	0.68)	

*multivariate analysis adjusted for age at randomisation, gender, radiotherapy, chemotherapy, treatment, disease site and stage.

Table 6-4 Relationship between p53 and MMR status and MMR protein pattern observed

P53 status	dMMR n	pMMR n	Total n	MMR protein pattern n (%)					Total n (%)
				MLH1	MSH2	MSH6	PMS2	ALL	
Positive	16	436	452	10 (67)	2 (13)	1 (7)	2 (13)	1	16 (100)
Negative	67	158	225	55 (82)	8 (12)	1 (2)	3 (4)		67 (100)
Total	83	594	677	65 (79)	10 (12)	2 (2.5)	5 (6)	1	83 (100)
The chi-squared test, p<0.001									

Other prognostic features were reviewed and, in the chemotherapy naive group, there were no significant differences between the dMMR and pMMR group in terms of pathological T stage of tumour, vascular invasion, lymph node recovery or Stage III tumours not given adjuvant therapy (Table 6-5, Table 6-6).

Table 6-5 Clinicopathological features of patients not treated with chemotherapy

T stage: pathological T stage;

		All	dMMR	pMMR	P value
Vascular invasion	No	230 (88.5)	33 (82.5)	197 (89.6)	0.200
	Yes	30 (11.5)	7 (17.5)	23 (10.4)	
T-stage	T0 – T2	9 (3.5)	1 (2.5)	8 (3.6)	
	T3	222 (87.7)	35 (87.5)	187 (84.2)	0.862
	T4	31 (11.8)	4 (10.0)	27 (12.2)	
Adequacy of lymph node staging	<12 removed	124 (47.3)	15 (37.5)	109 (49.1)	0.181
	≥12 removed	132 (50.4)	25 (62.5)	107 (48.2)	
	Not stated	6 (2.3)	0 (0.0)	6 (2.7)	

Table 6-6 Proportion of patients treated with chemotherapy by stage and MMR status

Chemo: chemotherapy

		All	Chemo	No Chemo	P value
Stage II	dMMR	59	21 (35.6)	38 (64.4)	0.27
	pMMR	278	77 (27.7)	201 (72.3)	
Stage III	dMMR	28	25 (89.3)	3 (10.7)	
	pMMR	370	344 (93.0)	26 (7.0)	0.44

6.4 Clinico-pathological features and outcomes associated with p53 expression

Scoring for p53 expression was dichotomised into either p53+ (including both patterns associated with TP53 mutation) or p53- (associated with wild-type TP53, Figure 2-15). Overall, 65% (482/740) of the tumours were p53+ (Table 6-7) and were negatively associated with dMMR ($p<0.001$, Table 6-4). Compared to p53- tumours, the p53+ tumours were associated with distal location ($p<0.001$) and advanced stage ($p=0.009$). There was no association with gender, age of patient at presentation, pathological T stage, vascular/lymphatic invasion or lymph node

recovery (Table 6-7).

The hazard ratio for DFS for p53+ve versus p53-ve was 1.08 (0.79, 1.47) p= 0.634. The 5-year DFS rates were 70.9 (63.6, 77.0) for p53-ve and 65.0 (59.5, 70.0) for p53+ve. The hazard ratio for OS for p53+ve versus p53-ve was 1.12 (0.77, 1.62), 0.55. The 5-year OS rates were 81.0 (752, 85.6) for p53-ve and 77.6 (73.2, 81.3) for p53+ve. The p53+ tumours were more likely to have received chemotherapy and radiotherapy than p53- tumours ($p<0.001$) which probably reflects their clinical staging and distal location (Table 6-7). However, analysis by chemotherapy sub-group (Table 6-8) did not reveal any significant difference in outcome between the p53 and the pMMR tumours in either the chemotherapy treated or chemotherapy naive groups. Removal of the dMMR tumours from the analysis did not alter any of these associations (Table 6-9).

Table 6-7 Clinico-pathological features and outcomes associated with p53 expression

This table shows that p53 mutant (p53+) tumours are significantly associated with distal location and advanced stage. There was no association with gender, age of patient at presentation, pathological T stage, vascular/lymphatic invasion or lymph node recovery. The p53+ tumours were more likely to have received chemotherapy and radiotherapy than p53- tumours ($p<0.001$). (p53-: p53 wild type)

No of patients		All	P53-ve	P53+ve	P value
Sex n (%)	M	474 (64.0)	164 (63.6)	310 (64.3)	0.840
	F	266 (36.0)	94 (36.4)	172 (35.7)	
Age Mean (SD)		64.08 (10.17)	64.58 (11.18)	64.24 (9.41)	0.327
Location	Proximal	500 (67.6)	204 (79.1)	296 (61.4)	<0.001
	Distal	240 (32.4)	54 (20.9)	186 (38.6)	
Differentiation	Well	55 (7.6)	21 (8.3)	34 (7.2)	0.561
	Moderate	589 (81.0)	200 (78.7)	389 (82.2)	
	Poor	82 (11.3)	33 (13.0)	49 (10.4)	
	Unknown	1 (0.1)	0 (0.00)	1 (0.2)	
T stage	pT1/2	66 (9.1)	16 (6.3)	50 (10.6)	0.299
	pT3	512 (70.4)	185 (72.8)	327 (69.1)	
	pT4	146 (20.1)	52 (20.5)	94 (19.9)	
	Unknown	3 (0.4)	1 (0.4)	2 (0.4)	
Vascular invasion	Yes	136 (18.7)	38 (15.0)	98 (20.7)	0.161
	No	581 (79.9)	212 (83.5)	369 (78.0)	
	Unknown	10 (1.4)	4 (1.6)	6 (1.3)	
Lymphatic invasion	Yes	68 (9.3)	23 (9.0)	45 (9.5)	0.928
	No	649 (89.3)	227 (89.4)	422 (89.2)	
	Unknown	10 (1.4)	4 (1.6)	6 (1.3)	
Clinical Stage n (%)	II	334 (45.1)	139 (53.9)	195 (40.5)	<0.001
	III	406 (54.9)	119 (46.1)	287 (59.5)	
Chemotherapy n (%)	Yes	482 (65.1)	155 (60.1)	327 (67.8)	0.035
	No	258 (34.9)	103 (39.9)	155 (32.2)	
Radiotherapy n (%)	Yes	77 (10.4)	14 (5.4)	63 (13.1)	0.001
	No	663 (89.6)	244 (94.6)	419 (86.9)	
Recurrence n (%)	Yes	208 (28.1)	64 (24.8)	144 (29.9)	0.144
	No	532 (71.9)	194 (75.2)	338 (70.1)	
Deaths n (%)	Yes	146 (19.7)	45 (17.4)	101 (20.9)	0.253
	No	594 (80.3)	213 (82.6)	381 (79.1)	

Table 6-8 Effects of p53 on Disease Free Survival and Overall Survival: sub-group analysis

This table shows that there is no significant difference in outcome between the p53 and the pMMR tumours in either the chemotherapy treated or chemotherapy naive groups. DFS: disease free survival; HR: hazard ration; OS: overall survival; P53-:p53 wild type; p53+: p53 mutant.

		n	DFS (95%CI)	HR (95%CI)	p value *	OS (95%CI)	HR (95%CI)	p value *
	All pts	740	67.0 (62.7, 71.0)			78.8 (75.3, 81)		
	P53-ve	258	70.9 (63.6, 77.0)	1.08 (0.79,	0.634	81.0 (75.2, 85.6)	1.12 (0.77,	0.555
	P53+ve	482	65.0 (59.5, 70.0)	1.47)		77.6 (73.2, 81.3)	1.62)	
						88.9 (84.4, 92.1)		
Stage II	All	334	78.1 (71.6, 83.3)					
	P53-ve	139	81.6 (71.4, 88.4)	1.31 (0.72,	0.383	91.3 (84.2, 95.3)	1.71 (0.75,	0.200
	P53+ve	195	76.0 (67.0, 82.8)	2.38)		87.1 (80.7, 91.6)	3.86)	
Stage	All	406	58.2 (52.4, 63.6)	1.04 (0.72,	0.838	70.8 (65.8, 75.2)		
III	P53-ve	119	59.3 (48.4, 68.5)	1.51)		69.6 (60.0, 77.3)	1.02 (0.67,	0.936
	P53+ve	287	57.8 (50.6, 64.2)			71.2 (65.1, 76.4)	1.55)	
Prior	All	482	61.6 (56.1, 66.6)		0.712	74.3 (70.0, 78.2)		
chemo	P53-ve	155	65.5 (55.6, 73.7)	1.07 (0.75,		78.0 (70.1, 84.1)	1.24 (0.80,	0.330
	P53+ve	327	59.8 (53.2, 65.9)	1.54)		72.5 (66.8, 77.4)	1.91)	
No								
prior	All	258	77.4 (70.1, 83.2)			87.3 (82.2, 91.1)		
chemo	P53-ve	103	79.2 (67.7, 87.0)	1.29 (0.69,	0.422	85.5 (76.1, 91.4)	1.03 (0.48,	0.931
P53-ve	P53+ve	155	76.3 (66.0, 83.9)	2.43)		88.5 (81.7, 92.9)	2.22)	
P53+ve								

*multivariate analysis adjusted for age at randomisation, gender, radiotherapy, chemotherapy, treatment, disease site and stage.

Table 6-9 Comparison of p53 negative with p53 positive for pMMR patients

Removal of the dMMR tumours from the analysis did not alter any of these associations P53-:p53 wild type; p53+: p53 mutant; T stage; pathological T stage.

No of patients		All	P53-ve	P53+ve	P value
Sex n (%)	M	393 (65.9)	109 (68.5)	258 (65.0)	0.417
	F	203 (34.1)	50 (31.5)	153 (35.0)	
Age Mean (SD)		64.03 (9.89)	64.21 (11.40)	63.96 (9.30)	0.783
Location	Proximal	384 (64.4)	119 (74.8)	265 (60.6)	0.001
	Distal	212 (35.6)	40 (25.2)	172 (39.4)	
Differentiation	Well	46 (7.9)	15 (9.55)	31 (7.2)	0.222
	Moderate	493 (84.1)	135 (86.0)	358 (83.5)	
	Poor	46 (7.8)	7 (4.5)	39 (9.1)	
	Unknown	1 (0.2)	0 (0.0)	1 (0.2)	
T stage	pT1/2	58 (9.9)	11 (7.0)	47 (10.0)	0.422
	pT3	409 (69.8)	113 (72.0)	296 (69.0)	
	pT4	117 (20.0)	33 (21.0)	84 (19.6)	
	Unknown	2 (0.3)	0 (0.00)	2 (0.4)	
Vascular invasion	Yes	109 (18.6)	133 (84.7)	336 (78.3)	0.122
	No	469 (80.0)	21 (13.4)	88 (20.5)	
	Unknown	8 (1.4)	3 (1.91)	5 (1.2)	
Lymphatic invasion	Yes	55 (9.4)	15 (9.6)	40 (9.3)	0.784
	No	523 (89.3)	139 (88.5)	384 (89.5)	
	Unknown	8 (1.3)	3 (1.9)	5 (1.2)	
Clinical Stage n (%)	II	253 (42.5)	80 (50.3)	173 (39.6)	0.019
	III	343 (57.5)	79 (46.7)	264 (60.4)	
Chemotherapy n (%)	Yes	391 (65.6)	97 (61.0)	294 (67.3)	0.154
	No	205 (34.4)	62 (39.0)	143 (32.7)	
Radiotherapy n (%)	Yes	70 (11.7)	12 (7.5)	58 (13.3)	0.055
	No	526 (88.3)	147 (92.5)	379 (86.7)	
Recurrence n (%)	Yes	172 (28.9)	39 (24.5)	133 (30.4)	0.159
	No	424 (71.1)	120 (75.5)	304 (69.6)	
Deaths n (%)	Yes	120 (20.1)	27 (17.0)	93 (21.3)	0.247
	No	476 (79.9)	132 (83.0)	344 (78.7)	

6.5 Combined evaluation of MMR status and p53 expression

Evaluation of the MMR status and p53 expression together was possible in 677 tumours. The combined evaluation produced 4 possible groups i.e. dMMR/p53-, dMMR/p53+, pMMR/p53+, pMMR/p53- (Table 6-10). There were no significant differences in OS or DFS between the groups. The numbers in the sub-groups were small and Cox multivariate analyses for the effects of dMMR and p53 expression on disease free survival and overall survival found no significant effect of combining MMR status and p53 expression either in the overall population or when stratified by stage. Similarly, and again with the caveat of small numbers, no significant effect of combining MMR status and p53 expression was seen on response to chemotherapy.

Table 6-10 Effects of combined MMR/p53 on survival

This table shows that there no significant differences in overall survival (OS) or disease free survival DFS between the 4 groups. dMMR/P53-: deficient MMR/P53 wild type; dMMR/P53+: deficient MMR/P53 mutant; pMMR/P53-: proficient MMR/P53 wild type; pMMR/P53+: proficient MMR/P53 mutant.

	n	DFS (95%CI)	HR (95%CI)	P value	OS (95%CI)	HR (95%CI)	P value
All pts	677						
dMMR/P53-	67	70.6 (54.9, 81.7)			78.0 (64.5, 86.8)		
dMMR/P53+	16	87.5 (58.6, 96.7)	0.49 (0.11, 2.14)	0.341	87.5 (58.6, 96.7)	0.72 (0.16, 3.23	0.670
pMMR/P53-	158	70.6 (61.2, 78.1)	0.84 (0.46, 1.51)	0.553	81.5 (73.9, 87.1)	0.71 (0.36, 1.39)	0.319
pMMR/P53+	436	64.1 (58.2, 69.4)	0.98 (0.57, 1.68)	0.927	77.2 (72.5, 81.1)	0.84 (0.46, 1.56)	0.593
Stage II	308						
dMMR/P53-	43	74.1 (49.3, 88.1)			84.5 (65.5, 93.5)		
dMMR/P53+	12	91.7 (53.9, 98.8)	0.34 (0.04, 2.79)	0.313	91.7 (53.9, 98.8)	0.46(0.05, 4.13)	0.491
pMMR/P53-	80	86.2 (75.9, 92.4	0.61 (0.22, 1.66)	0.330	93.1 (84.2, 97.1)	0.39(0.10, 1.44)	0.156
pMMR/P53+	173	74.0 (63.8, 81.7	1.06 (0.45, 2.46)	0.900	86.1 (78.8, 91.0)	0.92 (0.33, 2.58)	0.868
Stage III	369						
dMMR/P53-	24	61.0(38.4, 77.5)			66.2 (43.6, 81.5)		0.995
dMMR/P53+	4	0	0.62 (0.08, 5.02)	0.652	0	0.94 (0.11, 7.85)	0.554
pMMR/P53-	78	57.0(43.1, 68.7)	0.83 (0.38, 1.77)	0.623	70.6 (58.4, 80.0)	0.78 (0.34, 1.77	0.704
pMMR/P53+	263	57.7 (50.2, 64.4)	0.92 (0.45, 1.86)	0.811	71.4 (65.1, 76.8)	0.86 (0.40, 1.85)	
Prior chemo	391						
dMMR/P53-							
dMMR/P53+							
pMMR/P53-	97	61.3 (48.6, 71.7)			76.8 (66.2, 84.4)		
pMMR/P53+	294	58.6 (51.5, 65.0)			71.8 (65.7, 76.9)		
No prior chemo	205						
dMMR/P53-							
dMMR/P53+	62	87.0 (74.6, 93.6)			89.3 (77.8, 95.1)		
pMMR/P53-	143	76.1 (64.6, 84.3)			88.9 (81.6, 93.4)		
pMMR/P53+							

6.6 Discussion

This study sought to investigate the clinical utility of dMMR and aberrant p53 expression as prognostic and predictive biomarkers in CRC. We had a large study population (n= 824) which was drawn only from the VICTOR trial. We ensured technical excellence by performing the IHC in a full accredited diagnostic lab, having two reviewers for each of the immunostains and using stringent scoring criteria to avoid fixation artefacts. Under these conditions we failed to find any prognostic or predictive value for either dMMR or aberrant p53 expression (both alone and in combination).

The published data regarding the effect of dMMR in CRC are heterogeneous. There is general consensus that dMMR tumours are associated with poor differentiation, proximal location, female gender, early clinical stage and a better yield of lymph nodes from the resection specimen; our findings are wholly in agreement with this. However, we found that although overall 12% of tumours had dMMR, in the Stage II CRCs the frequency of dMMR was 18%. A recent very large study by Hutchins et al. of Stage II disease detected dMMR in 12% (Hutchins et al., 2011) whilst an even larger study by Sinicrope et al. (albeit a pooled study of several clinical trials) reported 21% of Stage II CRCs as having dMMR (Sinicrope et al., 2011). In our Stage III CRCs, 7% of tumours were scored as dMMR whilst, in contrast, the studies of Sinicrope et al. and Bertagnolli et al. (Bertagnolli et al., 2009) each reported dMMR in 13% of Stage III CRCs. The discrepancies of reported frequency of dMMR between the various studies most probably reflect technical variation and study design.

Given the variation of reported frequency of dMMR, it comes as no surprise that there is also inconsistency in the data reporting the clinical impact of dMMR. Our study found that there was no association between dMMR and DFS or OS either in the overall population or in the stage-specific analysis. This is in agreement with

the study by Kim et al. (Kim et al., 2007) but contrasts with other studies. Thus Hutchins et al. found that, in stage II disease, dMMR was associated with a better prognosis than pMMR (Hutchins et al., 2011) whilst Sinicrope et al. found that for stage II disease there was no impact for dMMR on outcome but there was improved outcome in stage III disease (Sinicrope et al., 2011). This was however restricted to those cases with a germline mutation and did not extend to sporadic cases with dMMR. Roth et al. found dMMR improved both DFS and OS in both stage II and III (Roth et al., 2009) but Bertagnolli et al. did not find any difference in either DFS or OS between dMMR and pMMR patients with stage III disease (Bertagnolli et al., 2009).

Amidst these contradictory data, the effect of dMMR on outcome in CRC is not clear. If there is an effect, then the size of the effect may be small so that it can be confounded by variations in methodology used to detect dMMR and differences in clinical practice within the study populations. Both DFS and OS in the patients recruited to the VICTOR trial are excellent with respective 5-year DFS and OS rates of 76% and 87% in Stage II CRC and 58% and 71% in Stage III. These are much better than the traditional outcome figures and probably reflect improvements in recent years in surgical and oncological care. It is possible that small benefits conferred by dMMR become inconspicuous in the context of optimal clinical care.

It has been proposed that the MMR status of CRCs may also predict response to chemotherapy. Studies by Sargent et al. and Ribic et al. have suggested that 5-FU based therapy is ineffective in tumours with dMMR and may even worsen the outcome (Ribic et al., 2003, Sargent et al., 2010). Bertagnolli et al. found dMMR was associated with improved response to irinotecan (Bertagnolli et al., 2009) whilst Elsaleh et al. found (albeit outwith the context of a clinical trial) that dMMR was associated with improved response to 5-FU based therapy (Elsaleh and Iacopetta, 2001). In contrast, studies by Kim et al. and Hutchins et al did not find

any interaction between MMR status and response to chemotherapy. We analysed chemotherapy treated and chemotherapy naive patients as distinct sub-groups. In the former, there was no difference in either 5-year DFS or OS. In the chemotherapy naive group, however, we unexpectedly found that both 5-year DFS and OS were significantly worse in the dMMR cases. This could occur if the untreated dMMR cases were enriched for poor prognostic features but evaluation of the pathological features showed no difference between the dMMR and pMMR groups (Table 6-5, Table 6-6). As yet we cannot find an explanation for our observation – it may represent a chance anomaly due to small numbers of patients in the sub group analysis or, if validated by other studies, it may be indicative of a need to change our thinking about the prognostic value of dMMR.

As with MMR status, the published data regarding the prognostic significance of aberrant p53 expression are contradictory (Bell et al., 1993, Hamelin et al., 1994, Ilyas et al., 1998, Khine et al., 1994, Morikawa et al., 2011, Morrin et al., 1994, Remvikos et al., 1992, Sun et al., 1992, Tornillo et al., 2007). In this study we defined two patterns of aberrant expression which are associated with TP53 mutation and grouped these patterns together as "p53+". Tumours with "wild-type" pattern of p53 expression were designated as "p53- ". Consistent with many studies, our data showed that 65% of the tumours were p53+ and this was associated with distal location and inversely associated with dMMR. We found that aberrant p53 expression was associated with advanced stage ($p<0.001$) and that this association was maintained even if the dMMR tumours were removed from the analysis. This finding runs contrary to the Fearon and Vogelstein model which postulates that TP53 mutation presages the acquisition of invasive tendencies within an adenoma (Fearon and Vogelstein, 1990). However, other studies have also reported this association (Kimura et al., 1996, Theodoropoulos et al., 2009, Tomoda and Kakeji, 1995) and this suggests that a diathesis for lymph node metastasis may follow TP53 mutation. However, despite this association, analysis of DFS and OS showed no

difference between the p53+ and the p53- tumours either in the group overall or in stage-specific analysis. Furthermore, there was no effect of aberrant p53 expression on response to either chemotherapy or radiotherapy. Given these data and those derived from the evaluation of the MMR proteins, it was not surprising to find that when the two sets of biomarkers were combined, there was no effect seen on either DFS or OS.

In summary, this has been a meticulous study of the prognostic and predictive value of dMMR and aberrant p53 expression conducted in the context of the VICTOR clinical trial for stage II and III CRC. Whilst many of the previously reported clinico-pathological associations were confirmed, there was no prognostic or predictive information to be derived from evaluation of these biomarkers. An interesting but unexplained observation was that dMMR conferred a worse prognosis in untreated CRCs.

Chapter 7. **Discussion**

In this research work, I designed or modified three molecular pathology assays for the detection of molecular alterations in CRC.

The QMC-PCR/HRM proved to be a robust, sensitive and cost-effective assay that is suitable for mutation detection in FFPE DNA (Fadhil et al., 2010). Whereas the sensitivity of QMC-PCR/HRM was better than that of Sanger sequencing, a similar sensitivity was found between the new assay and the commercially available DXS assay, which is an Amplification Refractory Mutation Systems (ARMS) PCR-based assay (Thelwell et al., 2000). A cost-effective strategy for mutation detection would be to subject only the samples with aberrant high-resolution melting to Sanger sequencing, rather than the entire sample set to direct sequencing. Comparatively, the QMC-PCR /HRM was by far easier to operate than the DXS assay because whilst it takes only one experiment to screen the KRAS codon 12/13 mutation hotspot per sample, the DXS assay requires eight experiments to screen the same hotspot for mutations. For this same reason, it would be safe to say that the QMC-PCR/HRM assay is also much more cost-effective than the DXS assay. Furthermore, the QMC-PCR/HRM assay has similar sensitivity levels to pyrosequencing, which however, has a higher limit of detection than QMC-PCR/HRM (Ibrahem et al., 2010). This advantage makes the QMC-PCR/HRM superior to pyrosequencing at detecting very low mutant allele frequency.

Our group has applied the QMC-PCR/HRM assay in screening for GNAS1 mutations in CRC cohorts, in the development of the Co-amplification at Lower Denaturation temperature (COLD) PCR followed by HRM (COLD HRM) assay (Ham-Karim et al., 2017), and in the validation of targeted next generation sequencing results (Ham-Karim et al., 2019). Furthermore, other groups have utilized the QMC-PCR/HRM, such as in the detection of mutations in a Saudi cohort of sporadic CRC (Naser et al., 2014), as well as in plant genetics. Furthermore, our research group has since modified the QMC-PCR/HRM to enable

the multiplexing of the SSD reactions (Ebili et al., 2017).

The COLD HRM was modified and re-purposed for the differentiation of somatic point mutations and germline SNPs in tumour DNA, and for testing allelic imbalance (AI) or loss of heterozygosity (LOH) in known SNP loci (Ham-Karim et al., 2017). The method is based on three principles, (i) both somatic mutations and AI (or loss of heterozygosity, LOH) can produce minor allele fractions which can be enriched by COLD PCR (ii) HRM is semi-quantitative (ii) HRM can detect changes in the ratios of mutant and wild type allele in a tumour DNA. An attractive feature of this assay is that it eliminates the requirement for paired normal DNA in the detection of AI/LOH or the distinguishing of SNPs from somatic mutations. This necessarily makes the assay cost-effective and easier to operate than other methods used for these purposes (Mei et al., 2000, Staaf et al., 2008, Horbinski et al., 2012, Ryland et al., 2015, Argos et al., 2008, Bertheau et al., 2001).

Using the HRM as a new platform, I developed a HRM-based assay for the detection of microsatellite instability by using the conventional biomarkers BAT25, BAT26, NR21, NR22 and NR24, in addition to a novel, highly sensitive marker – BCAT25 – found in the course of the assay development (Fadhil et al., 2012b, Fadhil et al., 2014). Compared to published data on MSI characteristics of CRC cell lines, capillary electrophoresis (CE) and immunohistochemistry (IHC), this assay showed a 100% concordance in sensitivity and specificity (Susanti et al., 2018). Moreover, it is more cost-effective than the older methods (capillary electrophoresis (CE), immunohistochemistry (IHC) and denaturing high performance liquid chromatography (dHPLC)) (Deschoolmeester et al., 2006). It is easy to use as it can be performed as a single-tube assay and the results are easily interpretable. The assay has been applied in determining the utility of diagnostic biopsies for molecular testing, as well as in the differentiation of CIN from MSI tumours (Fadhil et al., 2012b, Ham-Karim et al., 2019). Other research groups have

similarly applied HRM for the testing of MSI in CRC. For example, both Janavicius et al and Ladas et al found HRM-based methods to be highly sensitive methods for MSI detection (Janavicius et al., 2010, Ladas et al., 2018).

Furthermore, this assay has been modified by our research group to the Nottingham Lynch Syndrome Test (N_LyST) by incorporating new microsatellite markers (TP53, MYB, ANGEL2, EWSR1, etc), and MLH1 methylation that allows it to detect or infer Lynch syndrome (Susanti et al., 2018).

In line with the aims and objectives of testing the feasibility of using alternative sample types for molecular analyses, I sought to determine the utility of diagnostic biopsies in molecular testing by PCR and IHC. Analyses of mutation hotspots in KRAS, BRAF, PIK3CA and TP53 in diagnostic biopsies of CRC and matched resection samples showed a 99.82% concordance in point mutations, in addition to a 100% match in microsatellite instability status (Fadhil et al., 2012b). The findings from this study has direct clinical application in the testing of tumour samples for neoadjuvant therapies. For example, if the use of neoadjuvant therapies for colonic tumours is successfully translated into clinical practice, diagnostic biopsies may become the only material available for testing (Foxtrot Collaborative, 2012, Jakobsen et al., 2015). My findings have been replicated by other groups who have used different types of molecular testing platforms, including the one used in this research work (i.e. HRM). For example, Krol et al tested the concordance rates between diagnostic biopsies and resection samples in the mutation status of KRAS codons 12 and 13 and BRAF V600E, and found high rates of 97.4%, 98.4% and 99.2% for KRAS when using ARMS, direct Sanger sequencing and HRM respectively, and 98.4% and 99.2% for BRAF and using pyrosequencing/direct Sanger sequencing and HRM respectively (Krol et al., 2012). Furthermore, our group has recently validated the use of diagnostic biopsies of CRC tumours as suitable alternatives to resection samples for molecular testing using targeted next-

generation sequencing (Ham-Karim et al., 2019). Additionally, several others have tested the feasibility of using small biopsies for molecular testing and found test feasibilities between 87.3% and 99.4% (Ku et al., 2018, Zheng et al., 2016, Illei et al., 2017, DiBardino et al., 2017).

Going further on the objective of using diagnostic biopsies in place of resection samples for molecular testing, I evaluated the feasibility of using diagnostic biopsies for the study of expression of mismatch repair proteins wherein I compared the expression of the MMR protein between 30 pairs of diagnostic and resection samples (Fadhil and Ilyas, 2012, Fadhil et al., 2012a). My findings were interesting because whilst the interpretation of staining for the biopsy and resection samples were identical, I found that the staining for diagnostic biopsies were less heterogeneous, more intense and that the contrast between the positively staining stromal nuclei and the negatively staining tumour nuclei were sharper in the diagnostic biopsies than in the resection samples. Furthermore, the number of positively staining nuclear were more abundant in the diagnostic biopsies than in the resection samples especially with the MLH1 and MSH6 stains. The findings confirmed my hypothesis that, because diagnostic biopsies are small, they undergo more thorough and uniform fixation than resection samples and are thus more suitable for immunohistochemistry as they would enable easier interpretation of staining. The implication of these findings are far-reaching for the management of CRC patients with metastatic, unresectable tumours where the only materials available for treatment-informing molecular testing would be diagnostic biopsies (Foxtrot Collaborative, 2012, Jakobsen et al., 2015). In addition, even if resection sample are available, in the light of these evidence of superiority of the diagnostic biopsies over the resection samples in IHC interpretation, the tendency should be to shift to the use of diagnostic biopsies for clinical IHC work.

With respect to improving the diagnostic interpretation of d-MMR in tissue sections

stained with MLH1, MSH2, PMS2 and MSH6, and removing some of the challenges associated with interpretation of MMR IHC, I examined some of patterns of staining MMR proteins that confound interpretations using the support of MSI testing and drew up some rules of the thumb for interpretation of MMR staining in CRC tissue sections, (i) interpretation of MMR protein expression in the malignant epithelial cells must be done relative to the expression of MMR proteins in the stromal cells and tumour infiltrating lymphocyte (TILs) nuclei – the stromal cells and TILs must serve as positive internal controls and in the absence of positively staining stromal cells and TILs, the staining must be regarded as un-assessable; (ii) the staining patterns of the binding partners MLH1 and PMS2 must be concordant, but not necessarily so for MSH2 and MSH6; in the absence of such concordance the staining must be regarded as un-assessable; (iii) some tumours show a combination of positively staining and negatively staining tumour epithelial cells relative to the stromal cells and TILs; such tumour should be regarded as deficient in MMR (MMR-d); (iv) tumours with weak nuclear MMR protein expression relative to the stromal cells and TILs must be regarded as MMR-d (Fadhil and Ilyas, 2011, Fadhil et al., 2012a).

Beyond diagnostic interpretations of MMR expression, however, the staining patterns of the MMR proteins raises some questions regarding tumour biology and molecular classification or subtyping of individual tumours. In two of the CRC cases examined, it was found that some proportion of the malignant cells expressed the MMR proteins as strongly as the stromal cells and TILs, whilst some others show loss of expression of the proteins. Although such tumours are classified as MSI (or MMR-d) by current schemes, it would be logical to say that in such tumours there are two different clones of malignant cells: MSI and MSS (or MMR-d and MMR-proficient (MMR-p)) clones. The implication of this is three-fold (i) the current tumourigenesis models may be inadequate in elucidating molecular carcinogenesis, (ii) individual tumours may fall under more than one CRC subtype,

especially with the CIN-MSI-MACS classification scheme in which the mechanism of genomic instability in the so-called MACS tumours are currently unknown, (iii) the presence of two or more clones with differing genomic instability patterns within an individual patient's tumour will necessarily have implications for tumour biology, treatment response and patient's prognosis (Linnebacher et al., 2013, Kakar et al., 2008, Cai et al., 2008, Silver et al., 2011, Hawkins et al., 2001, Ostwald et al., 2009). It is interesting to note that one study has found that about 3% of CIN (i.e. MSS) CRC are also MSI (Domingo et al., 2013).

This research work confirmed the high rate of known KRAS mutations in CRC cell lines and clinical tumours (Bos et al., 1987). It also validated the previously reported codons 11 and 15 BRAF mutations in cell lines and clinical tumours (Davies et al., 2002, Andreadi et al., 2012). Moreover, the study confirmed the tendency to mutual exclusivity of KRAS and BRAF mutations in CRC, even though it showed that rare tumours show concomitant KRAS and BRAF mutations. Studies that are more recent have validated the concomitant presence of KRAs and BRAF mutations in rare CRC cases (Larki et al., 2017, Seth et al., 2009a, Midthun et al., 2019).

I undertook the investigation of the prognostic and predictive significance of p53 expression in a well-defined group of CRC (the VICTOR trial) using TMA and immunohistochemistry. The clinical significance of p53 expression patterns in CRC had previously not been defined.

The study found some association between p53 expression and tumour location, thereby validating the findings from other studies. It also found that p53 expression was associated with stage III CRC, a finding which refutes the Fearon and Vogelstein hypothesis of colorectal carcinogenesis but confirms the findings from other more recent studies (Fearon and Vogelstein, 1990, Kimura et al., 1996,

Theodoropoulos et al., 2009). Additionally, this research work did not find any prognostic or predictive significance of p53 expression in CRC. However, it should be noted that the different patterns of aberrant p53 expression are caused by different TP53 mutations. For example, whereas p53 overexpression is caused by missense mutations in the TP53 mutation hotspots R175H, G245S/D, R248Q/W/L, R249S, R273H/C/L, and R282W, loss of p53 expression is associated with nonsense mutations such as R213*, R196*, R306*, W146*, and E298* and loss of TP53 alleles via chromosome 7p deletion (loss of heterozygosity, LOH) (Murnyak and Hortobagyi, 2016)(Murnyak et al., 2016, Pim and Loranzo, 2018). TP53 mutations (missense, nonsense and deletions) can impart loss of functions (TP53 deletion and nonsense mutations), dominant negative effect (somatic missense mutation with a wild type allele) or gain of function mutations (missense mutations) (Zhou et al., 2014, Kang et al., 2018, Liu et al., 2016). It has been shown that TP53 mutation types differentially affect tumour cell behaviour and overall prognosis. Whilst the TP53 deletions and nonsense mutations appear to confer the classic loss-of-tumour-suppressor-gene-function phenotype, the TP53 missense mutations exert a gain-of-function effect, giving tumour cells added tumourigenic advantage. Further, this gain of function effects occurs with certain types of amino acid substitutions but not with others. For example, the overexpression of the p53 P151S, R175H, G245C and R282W mutations, but not the E336X, were shown to promote invasive cell growth (Zhou et al., 2014). Specifically, P151S overexpression leads to increased tumour growth and reduced animal survival in mouse orthotopic xenograft tumour model (Zhou et al., 2014). In addition, homozygous p53 R248Q mice displayed a reduced overall survival relative to p53-null mice. However, this shortened survival was not observed with the homozygous p53 G245S mice, indicating altered gain-of-function activities of mutant p53 proteins with R248Q compared to G245S mutations. Owing to these documented evidences of p53 expression-TP53 mutation and the TP53 mutation type-prognosis correlations, it is plausible that an actual p53 expression-prognosis correlate may

have been missed by lumping aberrant p53 expressions (loss of expression and overexpression) together in a group.

Lastly, using DNA content analysis by flow cytometry and MSI evaluation by HRM analysis, I confirmed the existence of MACS-CRC, which was previously observed by other groups (Hawkins et al., 2001, Silver et al., 2011). This refutes the dogma that colorectal carcinogenesis proceeds by either the CIN or MSI pathways. However, mutation analyses of KRAS, BRAF, PIK3CA and TP53 did not provide additional information on the potential genomic instability pattern(s) associated with MACS CRC. In addition, the study did not clarify the clinicopathological features of MACS tumours relative to the other subtypes of CRC. Furthermore, the ploidy status was not predictive of response to radiation in rectal cancers.

It should be noted that all the TP53 mutations were again lumped together in the analyses performed to differentiate CIN from MACS tumours at the molecular level. However, as have been mentioned above, different TP53 mutations confer differing biological activities to tumours (Zhou et al., 2014). Therefore, the lumping together of different TP53 mutations may have obscured any associations with tumour ploidy status. Going further, MACS CRC may be a heterogeneous group of tumours at the molecular level, and analysing them together without regards to the underlying molecular features of each possible MACS CRC subset may obscure the distinctness of each subset.

Regarding ploidy status and tumour response to chemoradiation therapy, it has been argued that loss of double-stranded DNA (dsDNA) repair either by homologous recombination repair (HRR) or Non-Homologous End Joining (NHEJ), rather than ploidy status, is a good predictor of tumour response to chemoradiation (Bakhoum et al., 2015, Zaki et al., 2014, Kennedy and D'Andrea, 2006). Whilst potentially all

aneuploidy tumours also have dsDNA repair loss, a good many diploid tumours are characterised by dsDNA loss and are responsive to chemoradiation therapy (Kennedy and D'Andrea, 2006, Bakhoum et al., 2015). Furthermore, it has been shown that graded CIN or aneuploidy levels is a better predictor of chemoradiation response than simple ploidy status determination by flow cytometry (Zaki et al., 2014, Zhang et al., 2016, Janssen et al., 2009). In graded CIN, whilst CIN-high tumours are exquisitely sensitive to chemoradiation, CIN-low tumours are resistant. Thus, the use of simple ploidy status (i.e. CIN+ve/ CIN-ve) to gauge tumour radio-response has given conflicting results. Moreover, flow cytometry may not be a good measure of ploidy status since the output is simply an averaging out of the total chromosomal deletions and amplifications present in the tumour cells aggregates.

In conclusion, my research work has focused on the development of cost-effective, yet sensitive and specific molecular assays that has enable the study of molecular alterations in CRC. It has also focused on the identification of molecular alterations which are of importance to CRC biology, as well as the confirmation, validation or replication many of the previously found molecular alterations in CRC.

Chapter 8. **References**

ABDEL-FATAH, T.M., POWE, D.G., AGBOOLA, J., ADAMOWICZ-BRICE, M., BLAMEY, R.W., LOPEZ-GARCIA, M.A., GREEN, A.R., REIS-FILHO, J.S. & ELLIS, I.O. 2010. The biological, clinical and prognostic implications of p53 transcriptional pathways in breast cancers. *J Pathol,* 220**,** 419-34.

ABDEL-FATAH, T.M., POWE, D.G., HODI, Z., REIS-FILHO, J.S., LEE, A.H. & ELLIS, I.O. 2008. Morphologic and molecular evolutionary pathways of low nuclear grade invasive breast cancers and their putative precursor lesions: further evidence to support the concept of low nuclear grade breast neoplasia family. *Am J Surg Pathol,* 32**,** 513-23.

ABDEL-RAHMAN, W.M., MECKLIN, J.P. & PELTOMAKI, P. 2006. The genetics of HNPCC: application to diagnosis and screening. *Crit Rev Oncol Hematol,* 58**,** 208-20.

ABULI, A., BESSA, X., GONZALEZ, J.R., RUIZ-PONTE, C., CACERES, A., MUNOZ, J., GONZALO, V., BALAGUER, F., FERNANDEZ-ROZADILLA, C., GONZALEZ, D., DE CASTRO, L., CLOFENT, J., BUJANDA, L., CUBIELLA, J., RENE, J.M., MORILLAS, J.D., LANAS, A., RIGAU, J., GARCIA, A.M., LATORRE, M., SALO, J., FERNANDEZ BANARES, F., ARGUELLO, L., PENA, E., VILELLA, A., RIESTRA, S., CARRENO, R., PAYA, A., ALENDA, C., XICOLA, R.M., DOYLE, B.J., JOVER, R., LLOR, X., CARRACEDO, A., CASTELLS, A., CASTELLVI-BEL, S. & ANDREU, M. 2010. Susceptibility genetic variants associated with colorectal cancer risk correlate with cancer phenotype. *Gastroenterology,* 139**,** 788-96, 796 e1-6.

ALLRED, D.C., HARVEY, J.M., BERARDO, M. & CLARK, G.M. 1998. Prognostic and predictive factors in breast cancer by immunohistochemical analysis. *Mod Pathol,* 11**,** 155-68.

ALTSCHUL, S.F., GISH, W., MILLER, W., MYERS, E.W. & LIPMAN, D.J. 1990. Basic local alignment search tool. *J Mol Biol,* 215**,** 403-10.

ALVAREZ, J.A., BALDONEDO, R.F., BEAR, I.G., ALVAREZ, P. & JORGE, J.L. 2004. Anaerobic liver abscesses as initial presentation of silent colonic cancer. *HPB (Oxford),* 6**,** 41-2.

AMADO, R.G., WOLF, M., PEETERS, M., VAN CUTSEM, E., SIENA, S., FREEMAN, D.J., JUAN, T., SIKORSKI, R., SUGGS, S., RADINSKY, R., PATTERSON, S.D. & CHANG, D.D. 2008. Wild-type KRAS is required for panitumumab efficacy in patients with metastatic colorectal cancer. *J Clin Oncol,* 26**,** 1626-34.

ANDREADI, C., NOBLE, C., PATEL, B., JIN, H., AGUILAR HERNANDEZ, M.M., BALMANNO, K., COOK, S.J. & PRITCHARD, C. 2012. Regulation of MEK/ERK pathway output by subcellular localization of B-Raf. *Biochem Soc Trans,* 40**,** 67-72.

ARAUJO, S.E., BERNARDO, W.M., HABR-GAMA, A., KISS, D.R. & CECCONELLO, I. 2007. DNA ploidy status and prognosis in colorectal cancer: a meta-analysis of published data. *Dis Colon Rectum,* 50**,** 1800-10.

ARGOS, M., KIBRIYA, M.G., JASMINE, F., OLOPADE, O.I., SU, T., HIBSHOOSH, H. & AHSAN, H. 2008. Genomewide scan for loss of heterozygosity and chromosomal amplification in breast carcinoma using

single-nucleotide polymorphism arrays. *Cancer Genet Cytogenet,* 182**,** 69-74.

ARMELAO, F. & DE PRETIS, G. 2014. Familial colorectal cancer: a review. *World J Gastroenterol,* 20**,** 9292-8.

ARMITAGE, N.C., BALLANTYNE, K.C., SHEFFIELD, J.P., CLARKE, P., EVANS, D.F. & HARDCASTLE, J.D. 1991. A prospective evaluation of the effect of tumor cell DNA content on recurrence in colorectal cancer. *Cancer,* 67**,** 2599-604.

AYYADEVARA, S., THADEN, J.J. & SHMOOKLER REIS, R.J. 2000. Discrimination of primer 3'-nucleotide mismatch by taq DNA polymerase during polymerase chain reaction. *Anal Biochem,* 284**,** 11-8.

BAAS, I.O., MULDER, J.W., OFFERHAUS, G.J., VOGELSTEIN, B. & HAMILTON, S.R. 1994. An evaluation of six antibodies for immunohistochemistry of mutant p53 gene product in archival colorectal neoplasms. *J Pathol,* 172**,** 5-12.

BABA, Y., NOSHO, K., SHIMA, K., IRAHARA, N., KURE, S., TOYODA, S., KIRKNER, G.J., GOEL, A., FUCHS, C.S. & OGINO, S. 2009. Aurora-A expression is independently associated with chromosomal instability in colorectal cancer. *Neoplasia,* 11**,** 418-25.

BAE, J.M., KIM, J.H. & KANG, G.H. 2016. Molecular Subtypes of Colorectal Cancer and Their Clinicopathologic Features, With an Emphasis on the Serrated Neoplasia Pathway. *Arch Pathol Lab Med,* 140**,** 406-12.

BAISSE, B., BOUZOURENE, H., SARAGA, E.P., BOSMAN, F.T. & BENHATTAR, J. 2001. Intratumor genetic heterogeneity in advanced human colorectal adenocarcinoma. *Int J Cancer,* 93**,** 346-52.

BAKHOUM, S.F., KABECHE, L., WOOD, M.D., LAUCIUS, C.D., QU, D., LAUGHNEY, A.M., REYNOLDS, G.E., LOUIE, R.J., PHILLIPS, J., CHAN, D.A., ZAKI, B.I., MURNANE, J.P., PETRITSCH, C. & COMPTON, D.A. 2015. Numerical chromosomal instability mediates susceptibility to radiation treatment. *Nat Commun,* 6**,** 5990.

BALDUS, S.E., SCHAEFER, K.L., ENGERS, R., HARTLEB, D., STOECKLEIN, N.H. & GABBERT, H.E. 2010. Prevalence and heterogeneity of KRAS, BRAF, and PIK3CA mutations in primary colorectal adenocarcinomas and their corresponding metastases. *Clin Cancer Res,* 16**,** 790-9.

BAMFORD, S., DAWSON, E., FORBES, S., CLEMENTS, J., PETTETT, R., DOGAN, A., FLANAGAN, A., TEAGUE, J., FUTREAL, P.A., STRATTON, M.R. & WOOSTER, R. 2004. The COSMIC (Catalogue of Somatic Mutations in Cancer) database and website. *Br J Cancer,* 91**,** 355-8.

BARROW, E., JAGGER, E., BRIERLEY, J., WALLACE, A., EVANS, G., HILL, J. & MCMAHON, R. 2010. Semiquantitative assessment of immunohistochemistry for mismatch repair proteins in Lynch syndrome. *Histopathology,* 56**,** 331-44.

BEDFORD, J.S. 1991. Sublethal damage, potentially lethal damage, and chromosomal aberrations in mammalian cells exposed to ionizing radiations. *Int J Radiat Oncol Biol Phys,* 21**,** 1457-69.

BELL, S.M., SCOTT, N., CROSS, D., SAGAR, P., LEWIS, F.A., BLAIR, G.E., TAYLOR, G.R., DIXON, M.F. & QUIRKE, P. 1993. Prognostic value of p53 overexpression and c-Ki-ras gene mutations in colorectal cancer. *Gastroenterology,* 104**,** 57-64.

BERTAGNOLLI, M.M., NIEDZWIECKI, D., COMPTON, C.C., HAHN, H.P., HALL, M., DAMAS, B., JEWELL, S.D., MAYER, R.J., GOLDBERG, R.M., SALTZ, L.B., WARREN, R.S. & REDSTON, M. 2009. Microsatellite instability predicts improved response to adjuvant therapy with irinotecan, fluorouracil, and leucovorin in stage III colon cancer: Cancer and Leukemia Group B Protocol 89803. *J Clin Oncol,* 27**,** 1814-21.

BERTHEAU, P., PLASSA, L.F., LEREBOURS, F., DE ROQUANCOURT, A., TURPIN, E., LIDEREAU, R., DE THE, H. & JANIN, A. 2001. Allelic loss detection in inflammatory breast cancer: improvement with laser microdissection. *Lab Invest,* 81**,** 1397-402.

BOARD, R.E., THELWELL, N.J., RAVETTO, P.F., LITTLE, S., RANSON, M., DIVE, C., HUGHES, A. & WHITCOMBE, D. 2008. Multiplexed assays for detection of mutations in PIK3CA. *Clin Chem,* 54**,** 757-60.

BOLAND, C.R. & GOEL, A. 2010. Microsatellite instability in colorectal cancer. *Gastroenterology,* 138**,** 2073-2087 e3.

BOLAND, C.R., SHIN, S.K. & GOEL, A. 2009. Promoter methylation in the genesis of gastrointestinal cancer. *Yonsei Med J,* 50**,** 309-21.

BOLAND, C.R., THIBODEAU, S.N., HAMILTON, S.R., SIDRANSKY, D., ESHLEMAN, J.R., BURT, R.W., MELTZER, S.J., RODRIGUEZ-BIGAS, M.A., FODDE, R., RANZANI, G.N. & SRIVASTAVA, S. 1998. A National Cancer Institute Workshop on Microsatellite Instability for cancer detection and familial predisposition: development of international criteria for the determination of microsatellite instability in colorectal cancer. *Cancer Res,* 58**,** 5248-57.

BOS, J.L., FEARON, E.R., HAMILTON, S.R., VERLAAN-DE VRIES, M., VAN BOOM, J.H., VAN DER EB, A.J. & VOGELSTEIN, B. 1987. Prevalence of ras gene mutations in human colorectal cancers. *Nature,* 327**,** 293-7.

BOZIC, I., ANTAL, T., OHTSUKI, H., CARTER, H., KIM, D., CHEN, S., KARCHIN, R., KINZLER, K.W., VOGELSTEIN, B. & NOWAK, M.A. 2010. Accumulation of driver and passenger mutations during tumor progression. *Proc Natl Acad Sci U S A,* 107**,** 18545-50.

BRODERICK, P., CARVAJAL-CARMONA, L., PITTMAN, A.M., WEBB, E., HOWARTH, K., ROWAN, A., LUBBE, S., SPAIN, S., SULLIVAN, K., FIELDING, S., JAEGER, E., VIJAYAKRISHNAN, J., KEMP, Z., GORMAN, M., CHANDLER, I., PAPAEMMANUIL, E., PENEGAR, S., WOOD, W., SELLICK, G., QURESHI, M., TEIXEIRA, A., DOMINGO, E., BARCLAY, E., MARTIN, L., SIEBER, O., KERR, D., GRAY, R., PETO, J., CAZIER, J.B., TOMLINSON, I. & HOULSTON, R.S. 2007. A genome-wide association study shows that common alleles of SMAD7 influence colorectal cancer risk. *Nat Genet,* 39**,** 1315-7.

BROWN, G., WALLIN, C., TATUSOVA, T., PRUITT, K. & MAGLOTT, D. (2006) Gene Help: Integrated Access to Genes of Genomes in the Reference Sequence Collection. *Gene Help.* Bethesda (MD), National Center for Biotechnology Information (US).

CAI, G., XU, Y., LU, H., SHI, Y., LIAN, P., PENG, J., DU, X., ZHOU, X., GUAN, Z., SHI, D. & CAI, S. 2008. Clinicopathologic and molecular features of sporadic microsatellite- and chromosomal-stable colorectal cancers. *Int J Colorectal Dis,* 23**,** 365-73.

CALLAGY, G.M., PHAROAH, P.D., PINDER, S.E., HSU, F.D., NIELSEN, T.O., RAGAZ, J., ELLIS, I.O., HUNTSMAN, D. & CALDAS, C. 2006. Bcl-2 is a prognostic marker in breast cancer independently of the Nottingham Prognostic Index. *Clin Cancer Res,* 12**,** 2468-75.

CEJAS, P., LOPEZ-GOMEZ, M., AGUAYO, C., MADERO, R., DE CASTRO CARPENO, J., BELDA-INIESTA, C., BARRIUSO, J., MORENO GARCIA, V., LARRAURI, J., LOPEZ, R., CASADO, E., GONZALEZ-BARON, M. & FELIU, J. 2009. KRAS mutations in primary colorectal cancer tumors and related metastases: a potential role in prediction of lung metastasis. *PLoS One,* 4**,** e8199.

CHAN, A.T. & GIOVANNUCCI, E.L. 2010. Primary prevention of colorectal cancer. *Gastroenterology,* 138**,** 2029-2043 e10.

CHAN, D.Y., TAY, K.V. & MANTOO, S.K. 2014. Supraclavicular lymph node metastasis as a first sign of rectal cancer without visceral metastasis. *ANZ J Surg,* 84**,** 896-7.

CHAN, T.L., CURTIS, L.C., LEUNG, S.Y., FARRINGTON, S.M., HO, J.W., CHAN, A.S., LAM, P.W., TSE, C.W., DUNLOP, M.G., WYLLIE, A.H. & YUEN, S.T. 2001. Early-onset colorectal cancer with stable microsatellite DNA and near-diploid chromosomes. *Oncogene,* 20**,** 4871-6.

CHUNG, T.P. & FLESHMAN, J.W. 2004. he Genetics of Sporadic Colon Cancer. *Seminars in Colon and Rectal Surgery,* 15**,** 128-135.

COTTRELL, S., BICKNELL, D., KAKLAMANIS, L. & BODMER, W.F. 1992. Molecular analysis of APC mutations in familial adenomatous polyposis and sporadic colon carcinomas. *Lancet,* 340**,** 626-30.

CR-UK, 2018. *Bowel cancer incidence statistics*. [online] Update Date: 24/01/2018 Available at:<https://www.cancerresearchuk.org/health-professional/cancer-statistics/statistics-by-cancer-type/bowel-cancer>[Accessed March 2019].

CURTIS, L.J., GEORGIADES, I.B., WHITE, S., BIRD, C.C., HARRISON, D.J. & WYLLIE, A.H. 2000. Specific patterns of chromosomal abnormalities are associated with RER status in sporadic colorectal cancer. *J Pathol,* 192**,** 440-5.

DALGLEISH, R., FLICEK, P., CUNNINGHAM, F., ASTASHYN, A., TULLY, R.E., PROCTOR, G., CHEN, Y., MCLAREN, W.M., LARSSON, P., VAUGHAN, B.W., BEROUD, C., DOBSON, G., LEHVASLAIHO, H., TASCHNER, P.E., DEN DUNNEN, J.T., DEVEREAU, A., BIRNEY, E., BROOKES, A.J. & MAGLOTT, D.R. 2010. Locus Reference Genomic sequences: an improved basis for describing human DNA variants. *Genome Med,* 2**,** 24.

DAVIES, H., BIGNELL, G.R., COX, C., STEPHENS, P., EDKINS, S., CLEGG, S., TEAGUE, J., WOFFENDIN, H., GARNETT, M.J., BOTTOMLEY, W., DAVIS, N., DICKS, E., EWING, R., FLOYD, Y., GRAY, K., HALL, S., HAWES, R., HUGHES, J., KOSMIDOU, V., MENZIES, A., MOULD, C., PARKER, A., STEVENS, C., WATT, S., HOOPER, S., WILSON, R., JAYATILAKE, H., GUSTERSON, B.A., COOPER, C., SHIPLEY, J., HARGRAVE, D., PRITCHARD-JONES, K., MAITLAND, N., CHENEVIX-TRENCH, G., RIGGINS, G.J., BIGNER, D.D., PALMIERI, G., COSSU, A., FLANAGAN, A., NICHOLSON, A., HO, J.W., LEUNG, S.Y., YUEN, S.T., WEBER, B.L., SEIGLER, H.F., DARROW, T.L., PATERSON, H., MARAIS, R., MARSHALL, C.J., WOOSTER, R., STRATTON, M.R. &

FUTREAL, P.A. 2002. Mutations of the BRAF gene in human cancer. *Nature,* 417**,** 949-54.

DAY, D.W., JASS, J.R., PRICE, A.B., SHEPHERD, N.A., SLOAN, J.M., TALBOT, I.C., WARREN, B.F. & WILLIAMS, G.T. 2003. *Morson and Dawson's Gastrointestinal Pathology,* Oxford, Blackwell Sciences Ltd.

DE LA CHAPELLE, A. & HAMPEL, H. 2010. Clinical relevance of microsatellite instability in colorectal cancer. *J Clin Oncol,* 28**,** 3380-7.

DE ROOCK, W., PIESSEVAUX, H., DE SCHUTTER, J., JANSSENS, M., DE HERTOGH, G., PERSONENI, N., BIESMANS, B., VAN LAETHEM, J.L., PEETERS, M., HUMBLET, Y., VAN CUTSEM, E. & TEJPAR, S. 2008. KRAS wild-type state predicts survival and is associated to early radiological response in metastatic colorectal cancer treated with cetuximab. *Ann Oncol,* 19**,** 508-15.

DES GUETZ, G., SCHISCHMANOFF, O., NICOLAS, P., PERRET, G.Y., MORERE, J.F. & UZZAN, B. 2009. Does microsatellite instability predict the efficacy of adjuvant chemotherapy in colorectal cancer? A systematic review with meta-analysis. *Eur J Cancer,* 45**,** 1890-6.

DESCHOOLMEESTER, V., BAAY, M., WUYTS, W., VAN MARCK, E., PELCKMANS, P., LARDON, F. & VERMORKEN, J.B. 2006. Comparison of three commonly used PCR-based techniques to analyze MSI status in sporadic colorectal cancer. *J Clin Lab Anal,* 20**,** 52-61.

DHADDA, A.S., DICKINSON, P., ZAITOUN, A.M., GANDHI, N. & BESSELL, E.M. 2011. Prognostic importance of Mandard tumour regression grade following pre-operative chemo/radiotherapy for locally advanced rectal cancer. *Eur J Cancer,* 47**,** 1138-45.

DHADDA, A.S., ZAITOUN, A.M. & BESSELL, E.M. 2009. Regression of rectal cancer with radiotherapy with or without concurrent capecitabine--optimising the timing of surgical resection. *Clin Oncol (R Coll Radiol),* 21**,** 23-31.

DI FIORE, F., BLANCHARD, F., CHARBONNIER, F., LE PESSOT, F., LAMY, A., GALAIS, M.P., BASTIT, L., KILLIAN, A., SESBOUE, R., TUECH, J.J., QUEUNIET, A.M., PAILLOT, B., SABOURIN, J.C., MICHOT, F., MICHEL, P. & FREBOURG, T. 2007. Clinical relevance of KRAS mutation detection in metastatic colorectal cancer treated by Cetuximab plus chemotherapy. *Br J Cancer,* 96**,** 1166-9.

DI NICOLANTONIO, F., MARTINI, M., MOLINARI, F., SARTORE-BIANCHI, A., ARENA, S., SALETTI, P., DE DOSSO, S., MAZZUCCHELLI, L., FRATTINI, M., SIENA, S. & BARDELLI, A. 2008. Wild-type BRAF is required for response to panitumumab or cetuximab in metastatic colorectal cancer. *J Clin Oncol,* 26**,** 5705-12.

DIBARDINO, D.M., RAWSON, D.W., SAQI, A., HEYMANN, J.J., PAGAN, C.A. & BULMAN, W.A. 2017. Next-generation sequencing of non-small cell lung cancer using a customized, targeted sequencing panel: Emphasis on small biopsy and cytology. *Cytojournal,* 14**,** 7.

DIGHE, S., SWIFT, I., MAGILL, L., HANDLEY, K., GRAY, R., QUIRKE, P., MORTON, D., SEYMOUR, M., WARREN, B. & BROWN, G. 2012. Accuracy of radiological staging in identifying high-risk colon cancer patients suitable for neoadjuvant chemotherapy: a multicentre experience. *Colorectal Dis,* 14**,** 438-44.

DO, H., KRYPUY, M., MITCHELL, P.L., FOX, S.B. & DOBROVIC, A. 2008. High resolution melting analysis for rapid and sensitive EGFR and

KRAS mutation detection in formalin fixed paraffin embedded biopsies. *BMC Cancer,* 8**,** 142.

DOMINGO, E., RAMAMOORTHY, R., OUKRIF, D., ROSMARIN, D., PRESZ, M., WANG, H., PULKER, H., LOCKSTONE, H., HVEEM, T., CRANSTON, T., DANIELSEN, H., NOVELLI, M., DAVIDSON, B., XU, Z.Z., MOLLOY, P., JOHNSTONE, E., HOLMES, C., MIDGLEY, R., KERR, D., SIEBER, O. & TOMLINSON, I. 2013. Use of multivariate analysis to suggest a new molecular classification of colorectal cancer. *J Pathol,* 229**,** 441-8.

DUFORT, S., RICHARD, M.J. & DE FRAIPONT, F. 2009. Pyrosequencing method to detect KRAS mutation in formalin-fixed and paraffin-embedded tumor tissues. *Anal Biochem,* 391**,** 166-8.

DUFRESNE, S.D., BELLONI, D.R., WELLS, W.A. & TSONGALIS, G.J. 2006. BRCA1 and BRCA2 mutation screening using SmartCycler II high-resolution melt curve analysis. *Arch Pathol Lab Med,* 130**,** 185-7.

DWIGHT, Z. n.d. *uMelt [SM]: Melting Curve Predictions Software*. [Web-based application] Salt Lake City, Utah: Wittwer DNA Lab: University of Utah. Available at:<www.dna.utah.edu/umelt/umelt.html>.

EBILI, H.O., HASSALL, J., ASIRI, A., HAM-KARIM, H., FADHIL, W., AGBOOLA, A.J. & ILYAS, M. 2017. QMC-PCRx: a novel method for rapid mutation detection. *J Clin Pathol,* 70**,** 702-711.

EDGE, S.B. & COMPTON, C.C. 2010. The American Joint Committee on Cancer: the 7th edition of the AJCC cancer staging manual and the future of TNM. *Ann Surg Oncol,* 17**,** 1471-4.

ELSALEH, H. & IACOPETTA, B. 2001. Microsatellite instability is a predictive marker for survival benefit from adjuvant chemotherapy in a population-based series of stage III colorectal carcinoma. *Clin Colorectal Cancer,* 1**,** 104-9.

ELZOUKI, A.N., HABEL, S., ALSOAEITI, S., ABOSEDRA, A. & KHAN, F. 2014. Epidemiology and clinical findings of colorectal carcinoma in two tertiary care hospitals in Benghazi, Libya. *Avicenna J Med,* 4**,** 94-8.

FADHIL, W., FIELD, J., CROSS, G., KAYE, P. & ILYAS, M. 2012a. Immunostaining in the context of loss mismatch repair function: interpretive confounders and cautionary tales! *Histopathology,* 61**,** 522-5.

FADHIL, W., IBRAHEM, S., SETH, R., ABUALI, G., RAGUNATH, K., KAYE, P. & ILYAS, M. 2012b. The utility of diagnostic biopsy specimens for predictive molecular testing in colorectal cancer. *Histopathology,* 61**,** 1117-24.

FADHIL, W., IBRAHEM, S., SETH, R. & ILYAS, M. 2010. Quick-multiplex-consensus (QMC)-PCR followed by high-resolution melting: a simple and robust method for mutation detection in formalin-fixed paraffin-embedded tissue. *J Clin Pathol,* 63**,** 134-40.

FADHIL, W. & ILYAS, M. 2011. Immunostaining for mismatch repair (MMR) protein expression in colorectal cancer is better and easier to interpret when performed on diagnostic biopsies. *Histopathology,* 60**,** 653-5.

FADHIL, W. & ILYAS, M. 2012. Immunostaining for mismatch repair (MMR) protein expression in colorectal cancer is better and easier to interpret when performed on diagnostic biopsies. *Histopathology,* 60**,** 653-5.

FADHIL, W., KINDLE, K., JACKSON, D., ZAITOUN, A., LANE, N., ROBINS, A. & ILYAS, M. 2014. DNA content analysis of colorectal

cancer defines a distinct 'microsatellite and chromosome stable' group but does not predict response to radiotherapy. *Int J Exp Pathol,* 95**,** 16-23.

FEARON, E.R. 2010. Molecular genetics of colorectal cancer. *Annu Rev Pathol,* 6**,** 479-507.

FEARON, E.R. 2011. Molecular genetics of colorectal cancer. *Annu Rev Pathol,* 6**,** 479-507.

FEARON, E.R. & VOGELSTEIN, B. 1990. A genetic model for colorectal tumorigenesis. *Cell,* 61**,** 759-67.

FERLAY, J., COLOMBET, M., SOERJOMATARAM, I., MATHERS, C., PARKIN, D.M., PINEROS, M., ZNAOR, A. & BRAY, F. 2019. Estimating the global cancer incidence and mortality in 2018: GLOBOCAN sources and methods. *Int J Cancer,* 144**,** 1941-1953.

FERLAY, J., ERVIK, M., LAM, F., COLOMBET, M., MERY, L., PIÑEROS, M., ZNAOR, A., SOERJOMATARAM, I. & BRAY, F. 2018. Global Cancer Observatory: Cancer Today. *A Cancer Journal for Clinicians,* 68**,** 394-424.

FISHER, E.R., SIDERITS, R.H., SASS, R. & FISHER, B. 1989. Value of assessment of ploidy in rectal cancers. *Arch Pathol Lab Med,* 113**,** 525-8.

FLYGER, H.L., LARSEN, J.K., NIELSEN, H.J. & CHRISTENSEN, I.J. 1999. DNA ploidy in colorectal cancer, heterogeneity within and between tumors and relation to survival. *Cytometry,* 38**,** 293-300.

FODDE, R., KUIPERS, J., ROSENBERG, C., SMITS, R., KIELMAN, M., GASPAR, C., VAN ES, J.H., BREUKEL, C., WIEGANT, J., GILES, R.H. & CLEVERS, H. 2001. Mutations in the APC tumour suppressor gene cause chromosomal instability. *Nat Cell Biol,* 3**,** 433-8.

FORBES, S.A., BHAMRA, G., BAMFORD, S., DAWSON, E., KOK, C., CLEMENTS, J., MENZIES, A., TEAGUE, J.W., FUTREAL, P.A. & STRATTON, M.R. 2008. The Catalogue of Somatic Mutations in Cancer (COSMIC). *Curr Protoc Hum Genet,* Chapter 10**,** Unit 10 11.

FORBES, S.A., BINDAL, N., BAMFORD, S., COLE, C., KOK, C.Y., BEARE, D., JIA, M., SHEPHERD, R., LEUNG, K., MENZIES, A., TEAGUE, J.W., CAMPBELL, P.J., STRATTON, M.R. & FUTREAL, P.A. 2011. COSMIC: mining complete cancer genomes in the Catalogue of Somatic Mutations in Cancer. *Nucleic Acids Research,* 39**,** D945-D950.

FOXTROT COLLABORATIVE, G. 2012. Feasibility of preoperative chemotherapy for locally advanced, operable colon cancer: the pilot phase of a randomised controlled trial. *Lancet Oncol,* 13**,** 1152-60.

FREI, J.V. 1992. Hereditary nonpolyposis colorectal cancer (Lynch syndrome II). Diploid malignancies with prolonged survival. *Cancer,* 69**,** 1108-11.

GARRITANO, S., GEMIGNANI, F., VOEGELE, C., NGUYEN-DUMONT, T., LE CALVEZ-KELM, F., DE SILVA, D., LESUEUR, F., LANDI, S. & TAVTIGIAN, S.V. 2009. Determining the effectiveness of High Resolution Melting analysis for SNP genotyping and mutation scanning at the TP53 locus. *BMC Genet,* 10**,** 5.

GEISLER, S., LONNING, P.E., AAS, T., JOHNSEN, H., FLUGE, O., HAUGEN, D.F., LILLEHAUG, J.R., AKSLEN, L.A. & BORRESEN-DALE, A.L. 2001. Influence of TP53 gene alterations and c-erbB-2 expression on the response to treatment with doxorubicin in locally advanced breast cancer. *Cancer Res,* 61**,** 2505-12.

GEORGIADES, I.B., CURTIS, L.J., MORRIS, R.M., BIRD, C.C. & WYLLIE, A.H. 1999. Heterogeneity studies identify a subset of sporadic

colorectal cancers without evidence for chromosomal or microsatellite instability. *Oncogene,* 18**,** 7933-40.

GHEDIRA, R., PAPAZOVA, N., VUYLSTEKE, M., RUTTINK, T., TAVERNIERS, I. & DE LOOSE, M. 2009. Assessment of primer/template mismatch effects on real-time PCR amplification of target taxa for GMO quantification. *J Agric Food Chem,* 57**,** 9370-7.

GIARETTI, W., RAPALLO, A., SCIUTTO, A., MACCIOCU, B., GEIDO, E., HERMSEN, M.A., POSTMA, C., BAAK, J.P., WILLIAMS, R.A. & MEIJER, G.A. 2000. Intratumor heterogeneity of k-ras and p53 mutations among human colorectal adenomas containing early cancer. *Anal Cell Pathol,* 21**,** 49-57.

GIGLIO, S., MONIS, P.T. & SAINT, C.P. 2003. Demonstration of preferential binding of SYBR Green I to specific DNA fragments in real-time multiplex PCR. *Nucleic Acids Res,* 31**,** e136.

GIRIJALA, R.L., RIAHI, R.R. & COHEN, P.R. 2018. Sister Mary Joseph Nodule as a Cutaneous Manifestation of Metastatic Appendiceal Adenocarcinoma: Case Report and Literature Review. *Cureus,* 10**,** e2244.

GOEL, A. & BOLAND, C.R. 2012. Epigenetics of colorectal cancer. *Gastroenterology,* 143**,** 1442-1460 e1.

GOH, H.S. & JASS, J.R. 1986. DNA content and the adenoma-carcinoma sequence in the colorectum. *J Clin Pathol,* 39**,** 387-92.

GORANOVA, T.E., OHUE, M., SHIMOHARU, Y. & KATO, K. 2011. Dynamics of cancer cell subpopulations in primary and metastatic colorectal tumors. *Clin Exp Metastasis,* 28**,** 427-35.

GRADY, W.M. & MARKOWITZ, S.D. 2015. The molecular pathogenesis of colorectal cancer and its potential application to colorectal cancer screening. *Dig Dis Sci,* 60**,** 762-72.

GRAHAM, R., LIEW, M., MEADOWS, C., LYON, E. & WITTWER, C.T. 2005. Distinguishing Different DNA Heterozygotes by High-Resolution Melting. *Clin Chem,* 51**,** 1295-1298.

GREAVES, M. & MALEY, C.C. 2012. Clonal evolution in cancer. *Nature,* 481**,** 306-13.

GUINNEY, J., DIENSTMANN, R., WANG, X., DE REYNIES, A., SCHLICKER, A., SONESON, C., MARISA, L., ROEPMAN, P., NYAMUNDANDA, G., ANGELINO, P., BOT, B.M., MORRIS, J.S., SIMON, I.M., GERSTER, S., FESSLER, E., DE SOUSA, E.M.F., MISSIAGLIA, E., RAMAY, H., BARRAS, D., HOMICSKO, K., MARU, D., MANYAM, G.C., BROOM, B., BOIGE, V., PEREZ-VILLAMIL, B., LADERAS, T., SALAZAR, R., GRAY, J.W., HANAHAN, D., TABERNERO, J., BERNARDS, R., FRIEND, S.H., LAURENT-PUIG, P., MEDEMA, J.P., SADANANDAM, A., WESSELS, L., DELORENZI, M., KOPETZ, S., VERMEULEN, L. & TEJPAR, S. 2015. The consensus molecular subtypes of colorectal cancer. *Nat Med,* 21**,** 1350-6.

GUNDRY, C.N., VANDERSTEEN, J.G., REED, G.H., PRYOR, R.J., CHEN, J. & WITTWER, C.T. 2003. Amplicon melting analysis with labeled primers: a closed-tube method for differentiating homozygotes and heterozygotes. *Clin Chem,* 49**,** 396-406.

GUPTA, V., ARORA, R., RANJAN, A., BAIRWA, N.K., MALHOTRA, D.K., UDHAYASURIYAN, P.T., SAHA, A. & BAMEZAI, R. 2005. Gel-based nonradioactive single-strand conformational polymorphism and

mutation detection: limitations and solutions. *Methods Mol Biol,* 291**,** 247-61.

HADJIHANNAS, M.V., BRUCKNER, M., JERCHOW, B., BIRCHMEIER, W., DIETMAIER, W. & BEHRENS, J. 2006. Aberrant Wnt/beta-catenin signaling can induce chromosomal instability in colon cancer. *Proc Natl Acad Sci U S A,* 103**,** 10747-52.

HAIMAN, C.A., LE MARCHAND, L., YAMAMATO, J., STRAM, D.O., SHENG, X., KOLONEL, L.N., WU, A.H., REICH, D. & HENDERSON, B.E. 2007. A common genetic risk factor for colorectal and prostate cancer. *Nat Genet,* 39**,** 954-6.

HAM-KARIM, H.A., EBILI, H., FADHIL, W., ASIRI, A., HASSALL, J. & ILYAS, M. 2017. COLD-HRM: a combination of methods to infer the nature of somatic mutations. *Adv Cytol Pathol,* 2**,** 54-61.

HAM-KARIM, H.A., EBILI, H.O., MANGER, K., FADHIL, W., AHMAD, N.S., RICHMAN, S.D. & ILYAS, M. 2019. Targeted Next-Generation Sequencing Validates the Use of Diagnostic Biopsies as a Suitable Alternative to Resection Material for Mutation Screening in Colorectal Cancer. *Mol Diagn Ther*.

HAMELIN, R., LAURENT-PUIG, P., OLSCHWANG, S., JEGO, N., ASSELAIN, B., REMVIKOS, Y., GIRODET, J., SALMON, R.J. & THOMAS, G. 1994. Association of p53 mutations with short survival in colorectal cancer. *Gastroenterology,* 106**,** 42-8.

HAMPEL, H. 2009. Genetic testing for hereditary colorectal cancer. *Surg Oncol Clin N Am,* 18**,** 687-703.

HAWKINS, N.J., TOMLINSON, I., MEAGHER, A. & WARD, R.L. 2001. Microsatellite-stable diploid carcinoma: a biologically distinct and aggressive subset of sporadic colorectal cancer. *Br J Cancer,* 84**,** 232-6.

HEDLEY, D.W., FRIEDLANDER, M.L., TAYLOR, I.W., RUGG, C.A. & MUSGROVE, E.A. 1983. Method for analysis of cellular DNA content of paraffin-embedded pathological material using flow cytometry. *J Histochem Cytochem,* 31**,** 1333-5.

HEIMANN, T.M., MILLER, F., MARTINELLI, G., MESTER, J., KURTZ, R.J., SZPORN, A. & FASY, T. 1990. Significance of DNA content abnormalities in small rectal cancers. *Am J Surg,* 159**,** 199-202; discussion 202-3.

HERRMANN, M.G., DURTSCHI, J.D., BROMLEY, L.K., WITTWER, C.T. & VOELKERDING, K.V. 2006. Amplicon DNA Melting Analysis for Mutation Scanning and Genotyping: Cross-Platform Comparison of Instruments and Dyes. *Clin Chem,* 52**,** 494-503.

HIGUCHI, R., DOLLINGER, G., WALSH, P.S. & GRIFFITH, R. 1992. Simultaneous amplification and detection of specific DNA sequences. *Biotechnology (N Y),* 10**,** 413-7.

HINRICHS, A.S., KAROLCHIK, D., BAERTSCH, R., BARBER, G.P., BEJERANO, G., CLAWSON, H., DIEKHANS, M., FUREY, T.S., HARTE, R.A., HSU, F., HILLMAN-JACKSON, J., KUHN, R.M., PEDERSEN, J.S., POHL, A., RANEY, B.J., ROSENBLOOM, K.R., SIEPEL, A., SMITH, K.E., SUGNET, C.W., SULTAN-QURRAIE, A., THOMAS, D.J., TRUMBOWER, H., WEBER, R.J., WEIRAUCH, M., ZWEIG, A.S., HAUSSLER, D. & KENT, W.J. 2006. The UCSC Genome Browser Database: update 2006. *Nucleic Acids Res,* 34**,** D590-D598.

HOLCH, J.W., DEMMER, M., LAMERSDORF, C., MICHL, M., SCHULZ, C., VON EINEM, J.C., MODEST, D.P. & HEINEMANN, V. 2017. Pattern and Dynamics of Distant Metastases in Metastatic Colorectal Cancer. *Visc Med,* 33**,** 70-75.

HOLLSTEIN, M., SIDRANSKY, D., VOGELSTEIN, B. & HARRIS, C.C. 1991. p53 mutations in human cancers. *Science,* 253**,** 49-53.

HORBINSKI, C., NIKIFOROVA, M.N., HOBBS, J., BORTOLUZZI, S., CIEPLY, K., DACIC, S. & HAMILTON, R.L. 2012. The importance of 10q status in an outcomes-based comparison between 1p/19q fluorescence in situ hybridization and polymerase chain reaction-based microsatellite loss of heterozygosity analysis of oligodendrogliomas. *J Neuropathol Exp Neurol,* 71**,** 73-82.

HSIANG, J.C., BAI, W. & LAL, D. 2013. Symptom presentations and other characteristics of colorectal cancer patients and the diagnostic performance of the Auckland Regional Grading Criteria for Suspected Colorectal Cancer in the South Auckland population. *N Z Med J,* 126**,** 95-107.

HUEBNER, M., WOLFF, B.G., SMYRK, T.C., AAKRE, J. & LARSON, D.W. 2012. Partial pathologic response and nodal status as most significant prognostic factors for advanced rectal cancer treated with preoperative chemoradiotherapy. *World J Surg,* 36**,** 675-83.

HUTCHINS, G., SOUTHWARD, K., HANDLEY, K., MAGILL, L., BEAUMONT, C., STAHLSCHMIDT, J., RICHMAN, S., CHAMBERS, P., SEYMOUR, M., KERR, D., GRAY, R. & QUIRKE, P. 2011. Value of mismatch repair, KRAS, and BRAF mutations in predicting recurrence and benefits from chemotherapy in colorectal cancer. *J Clin Oncol,* 29**,** 1261-70.

IBRAHEM, S. (2012) Interactions of oncogenic pathways in colorectal cancer. University of Nottingham.

IBRAHEM, S., SETH, R., O'SULLIVAN, B., FADHIL, W., TANIERE, P. & ILYAS, M. 2010. Comparative analysis of pyrosequencing and QMC-PCR in conjunction with high resolution melting for KRAS/BRAF mutation detection. *Int J Exp Pathol,* 91**,** 500-5.

ILLEI, P.B., BELCHIS, D., TSENG, L.H., NGUYEN, D., DE MARCHI, F., HALEY, L., RIEL, S., BEIERL, K., ZHENG, G., BRAHMER, J.R., ASKIN, F.B., GOCKE, C.D., ESHLEMAN, J.R., FORDE, P.M. & LIN, M.T. 2017. Clinical mutational profiling of 1006 lung cancers by next generation sequencing. *Oncotarget,* 8**,** 96684-96696.

ILYAS, M., HAO, X.P., WILKINSON, K., TOMLINSON, I.P., ABBASI, A.M., FORBES, A., BODMER, W.F. & TALBOT, I.C. 1998. Loss of Bcl-2 expression correlates with tumour recurrence in colorectal cancer. *Gut,* 43**,** 383-7.

ILYAS, M., STRAUB, J., TOMLINSON, I.P. & BODMER, W.F. 1999. Genetic pathways in colorectal and other cancers. *Eur J Cancer,* 35**,** 1986-2002.

ISCAN, Y., KARIP, B., ONUR, E., OZBAY, N., TEZER, S. & MEMISOGLU, K. 2016. Sister Mary Joseph nodule in colorectal cancer. *Ulus Cerrahi Derg,* 32**,** 295-297.

ITALIANO, A., HOSTEIN, I., SOUBEYRAN, I., FABAS, T., BENCHIMOL, D., EVRARD, S., GUGENHEIM, J., BECOUARN, Y., BRUNET, R., FONCK, M., FRANCOIS, E., SAINT-PAUL, M.C. & PEDEUTOUR, F. 2010. KRAS and BRAF mutational status in

primary colorectal tumors and related metastatic sites: biological and clinical implications. *Ann Surg Oncol*, 17**,** 1429-34.

JAEGER, E., WEBB, E., HOWARTH, K., CARVAJAL-CARMONA, L., ROWAN, A., BRODERICK, P., WALTHER, A., SPAIN, S., PITTMAN, A., KEMP, Z., SULLIVAN, K., HEINIMANN, K., LUBBE, S., DOMINGO, E., BARCLAY, E., MARTIN, L., GORMAN, M., CHANDLER, I., VIJAYAKRISHNAN, J., WOOD, W., PAPAEMMANUIL, E., PENEGAR, S., QURESHI, M., FARRINGTON, S., TENESA, A., CAZIER, J.B., KERR, D., GRAY, R., PETO, J., DUNLOP, M., CAMPBELL, H., THOMAS, H., HOULSTON, R. & TOMLINSON, I. 2008. Common genetic variants at the CRAC1 (HMPS) locus on chromosome 15q13.3 influence colorectal cancer risk. *Nat Genet*, 40**,** 26-8.

JAKOBSEN, A., ANDERSEN, F., FISCHER, A., JENSEN, L.H., JORGENSEN, J.C., LARSEN, O., LINDEBJERG, J., PLOEN, J., RAFAELSEN, S.R. & VILANDT, J. 2015. Neoadjuvant chemotherapy in locally advanced colon cancer. A phase II trial. *Acta Oncol*, 54**,** 1747-53.

JANAVICIUS, R., MATIUKAITE, D., JAKUBAUSKAS, A. & GRISKEVICIUS, L. 2010. Microsatellite instability detection by high-resolution melting analysis. *Clin Chem*, 56**,** 1750-7.

JANKU, F., LEE, J.J., TSIMBERIDOU, A.M., HONG, D.S., NAING, A., FALCHOOK, G.S., FU, S., LUTHRA, R., GARRIDO-LAGUNA, I. & KURZROCK, R. 2011. PIK3CA mutations frequently coexist with RAS and BRAF mutations in patients with advanced cancers. *PLoS One*, 6**,** e22769.

JANNE, P.A., BORRAS, A.M., KUANG, Y., ROGERS, A.M., JOSHI, V.A., LIYANAGE, H., LINDEMAN, N., LEE, J.C., HALMOS, B., MAHER, E.A., DISTEL, R.J., MEYERSON, M. & JOHNSON, B.E. 2006. A Rapid and Sensitive Enzymatic Method for Epidermal Growth Factor Receptor Mutation Screening. *Clin Cancer Res*, 12**,** 751-758.

JANSSEN, A., KOPS, G.J. & MEDEMA, R.H. 2009. Elevating the frequency of chromosome mis-segregation as a strategy to kill tumor cells. *Proc Natl Acad Sci U S A*, 106**,** 19108-13.

JASPERSON, K.W., TUOHY, T.M., NEKLASON, D.W. & BURT, R.W. 2010. Hereditary and familial colon cancer. *Gastroenterology*, 138**,** 2044-58.

JASS, J.R. 2007. Classification of colorectal cancer based on correlation of clinical, morphological and molecular features. *Histopathology*, 50**,** 113-30.

JONES, S., CHEN, W.D., PARMIGIANI, G., DIEHL, F., BEERENWINKEL, N., ANTAL, T., TRAULSEN, A., NOWAK, M.A., SIEGEL, C., VELCULESCU, V.E., KINZLER, K.W., VOGELSTEIN, B., WILLIS, J. & MARKOWITZ, S.D. 2008. Comparative lesion sequencing provides insights into tumor evolution. *Proc Natl Acad Sci U S A*, 105**,** 4283-8.

KAKAR, S., DENG, G., SAHAI, V., MATSUZAKI, K., TANAKA, H., MIURA, S. & KIM, Y.S. 2008. Clinicopathologic characteristics, CpG island methylator phenotype, and BRAF mutations in microsatellite-stable colorectal cancers without chromosomal instability. *Arch Pathol Lab Med*, 132**,** 958-64.

KANG, N., WANG, Y., GUO, S., OU, Y., WANG, G., CHEN, J., LI, D. & ZHAN, Q. 2018. Mutant TP53 G245C and R273H promote cellular malignancy in esophageal squamous cell carcinoma. *BMC Cell Biol,* 19**,** 16.

KARRAN, P. 1995. Appropriate partners make good matches. *Science,* 268**,** 1857-8.

KASTRINOS, F. & SYNGAL, S. 2011. Inherited colorectal cancer syndromes. *Cancer J,* 17**,** 405-15.

KAYE, P.V., HAIDER, S.A., JAMES, P.D., SOOMRO, I., CATTON, J., PARSONS, S.L., RAGUNATH, K. & ILYAS, M. 2010. Novel staining pattern of p53 in Barrett's dysplasia--the absent pattern. *Histopathology,* 57**,** 933-5.

KENNEDY, R.D. & D'ANDREA, A.D. 2006. DNA repair pathways in clinical practice: lessons from pediatric cancer susceptibility syndromes. *J Clin Oncol,* 24**,** 3799-808.

KENT, W.J. 2002. BLAT--the BLAST-like alignment tool. *Genome Res,* 12**,** 656-64.

KHINE, K., SMITH, D.R. & GOH, H.S. 1994. High frequency of allelic deletion on chromosome 17p in advanced colorectal cancer. *Cancer,* 73**,** 28-35.

KIM, G.P., COLANGELO, L.H., WIEAND, H.S., PAIK, S., KIRSCH, I.R., WOLMARK, N. & ALLEGRA, C.J. 2007. Prognostic and predictive roles of high-degree microsatellite instability in colon cancer: a National Cancer Institute-National Surgical Adjuvant Breast and Bowel Project Collaborative Study. *J Clin Oncol,* 25**,** 767-72.

KIMURA, O., SUGAMURA, K., KIJIMA, T., MAKINO, M., SHIRAI, H., TATEBE, S., ITO, H. & KAIBARA, N. 1996. Flow cytometric examination of p53 protein in primary tumors and metastases to the liver and lymph nodes of colorectal cancer. *Dis Colon Rectum,* 39**,** 1428-33.

KITTS. A & SHERRY. S (2002) The Single Nucleotide Polymorphism Database (dbSNP) of Nucleotide Sequence Variation. IN J. McEntyre & J. Ostell (Eds.) *NCBI Handbook.* Bethesda (MD), National Center for Biotechnology Information (US).

KLARSKOV, L., LADELUND, S., HOLCK, S., ROENLUND, K., LINDEBJERG, J., ELEBRO, J., HALVARSSON, B., VON SALOME, J., BERNSTEIN, I. & NILBERT, M. 2010. Interobserver variability in the evaluation of mismatch repair protein immunostaining. *Hum Pathol,* 41**,** 1387-96.

KNIJN, N., MEKENKAMP, L.J., KLOMP, M., VINK-BORGER, M.E., TOL, J., TEERENSTRA, S., MEIJER, J.W., TEBAR, M., RIEMERSMA, S., VAN KRIEKEN, J.H., PUNT, C.J. & NAGTEGAAL, I.D. 2011. KRAS mutation analysis: a comparison between primary tumours and matched liver metastases in 305 colorectal cancer patients. *Br J Cancer,* 104**,** 1020-6.

KOBEL, M., REUSS, A., BOIS, A., KOMMOSS, S., KOMMOSS, F., GAO, D., KALLOGER, S.E., HUNTSMAN, D.G. & GILKS, C.B. 2010. The biological and clinical value of p53 expression in pelvic high-grade serous carcinomas. *J Pathol,* 222**,** 191-8.

KOREN-MICHOWITZ, M., SHIMONI, A., VIVANTE, A., TRAKHTENBROT, L., RECHAVI, G., AMARIGLIO, N., LOEWENTHAL, R., NAGLER, A. & COHEN, Y. 2008. A new MALDI-TOF-based assay for monitoring JAK2 V617F mutation level in

patients undergoing allogeneic stem cell transplantation (allo SCT) for classic myeloproliferative disorders (MPD). *Leuk Res,* 32**,** 421-7.

KORESSAAR, T. & REMM, M. 2007. Enhancements and modifications of primer design program Primer3. *Bioinformatics,* 23**,** 1289-91.

KOURI, M., LAASONEN, A., MECKLIN, J.P., JARVINEN, H., FRANSSILA, K. & PYRHONEN, S. 1990. Diploid predominance in hereditary nonpolyposis colorectal carcinoma evaluated by flow cytometry. *Cancer,* 65**,** 1825-9.

KROL, L.C., T HART, N.A., METHORST, N., KNOL, A.J., PRINSEN, C. & BOERS, J.E. 2012. Concordance in KRAS and BRAF mutations in endoscopic biopsy samples and resection specimens of colorectal adenocarcinoma. *Eur J Cancer,* 48**,** 1108-15.

KRYPUY, M., AHMED, A., ETEMADMOGHADAM, D., HYLAND, S., AUSTRALIAN OVARIAN CANCER STUDY, G., DEFAZIO, A., FOX, S., BRENTON, J., BOWTELL, D. & DOBROVIC, A. 2007. High resolution melting for mutation scanning of TP53 exons 5-8. *BMC Cancer,* 7**,** 168.

KU, B.M., HEO, M.H., KIM, J.H., CHO, B.C., CHO, E.K., MIN, Y.J., LEE, K.H., SUN, J.M., LEE, S.H., AHN, J.S., PARK, K., KIM, T.J., LEE, H.Y., KIM, H., LEE, K.J. & AHN, M.J. 2018. Molecular Screening of Small Biopsy Samples Using Next-Generation Sequencing in Korean Patients with Advanced Non-small Cell Lung Cancer: Korean Lung Cancer Consortium (KLCC-13-01). *J Pathol Transl Med,* 52**,** 148-156.

LABIANCA, R., NORDLINGER, B., BERETTA, G.D., MOSCONI, S., MANDALA, M., CERVANTES, A. & ARNOLD, D. 2013. Early colon cancer: ESMO Clinical Practice Guidelines for diagnosis, treatment and follow-up. *Ann Oncol,* 24 Suppl 6**,** vi64-72.

LADAS, I., YU, F., LEONG, K.W., FITARELLI-KIEHL, M., SONG, C., ASHTAPUTRE, R., KULKE, M., MAMON, H. & MAKRIGIORGOS, G.M. 2018. Enhanced detection of microsatellite instability using pre-PCR elimination of wild-type DNA homo-polymers in tissue and liquid biopsies. *Nucleic Acids Res,* 46**,** e74.

LANE, D.P. 1992. Cancer. p53, guardian of the genome. *Nature,* 358**,** 15-6.

LANGEROD, A., ZHAO, H., BORGAN, O., NESLAND, J.M., BUKHOLM, I.R., IKDAHL, T., KARESEN, R., BORRESEN-DALE, A.L. & JEFFREY, S.S. 2007. TP53 mutation status and gene expression profiles are powerful prognostic markers of breast cancer. *Breast Cancer Res,* 9**,** R30.

LARKI, P., GHARIB, E., YAGHOOB TALEGHANI, M., KHORSHIDI, F., NAZEMALHOSSEINI-MOJARAD, E. & ASADZADEH AGHDAEI, H. 2017. Coexistence of KRAS and BRAF Mutations in Colorectal Cancer: A Case Report Supporting The Concept of Tumoral Heterogeneity. *Cell J,* 19**,** 113-117.

LAY, M.J. & WITTWER, C.T. 1997. Real-time fluorescence genotyping of factor V Leiden during rapid-cycle PCR. *Clin Chem,* 43**,** 2262-7.

LEE, J.W., SOUNG, Y.H., KIM, S.Y., NAM, H.K., PARK, W.S., NAM, S.W., KIM, M.S., SUN, D.I., LEE, Y.S., JANG, J.J., LEE, J.Y., YOO, N.J. & LEE, S.H. 2005. Somatic mutations of EGFR gene in squamous cell carcinoma of the head and neck. *Clin Cancer Res,* 11**,** 2879-82.

LEVITT, N.C. & HICKSON, I.D. 2002. Caretaker tumour suppressor genes that defend genome integrity. *Trends Mol Med,* 8**,** 179-86.

LI, J., WANG, L., MAMON, H., KULKE, M.H., BERBECO, R. & MAKRIGIORGOS, G.M. 2008. Replacing PCR with COLD-PCR enriches variant DNA sequences and redefines the sensitivity of genetic testing. *Nat Med,* 14**,** 579-584.

LIÈVRE A, B.J., LE CORRE D, BOIGE V, LANDI B, EMILE JF, CÔTÉ JF, TOMASIC G, PENNA C, DUCREUX M, ROUGIER P, PENAULT-LLORCA F, LAURENT-PUIG P. 2006. KRAS mutation status is predictive of response to cetuximab therapy in colorectal cancer. *Cancer Res. ,* 15**,** 3992-5.

LIEW, M., PRYOR, R., PALAIS, R., MEADOWS, C., ERALI, M., LYON, E. & WITTWER, C. 2004. Genotyping of single-nucleotide polymorphisms by high-resolution melting of small amplicons. *Clin Chem,* 50**,** 1156-64.

LINNEBACHER, M., OSTWALD, C., KOCZAN, D., SALEM, T., SCHNEIDER, B., KROHN, M., ERNST, M. & PRALL, F. 2013. Single nucleotide polymorphism array analysis of microsatellite-stable, diploid/near-diploid colorectal carcinomas without the CpG island methylator phenotype. *Oncol Lett,* 5**,** 173-178.

LINNEKAMP, J.F., HOOFF, S.R.V., PRASETYANTI, P.R., KANDIMALLA, R., BUIKHUISEN, J.Y., FESSLER, E., RAMESH, P., LEE, K., BOCHOVE, G.G.W., DE JONG, J.H., CAMERON, K., LEERSUM, R.V., RODERMOND, H.M., FRANITZA, M., NURNBERG, P., MANGIAPANE, L.R., WANG, X., CLEVERS, H., VERMEULEN, L., STASSI, G. & MEDEMA, J.P. 2018. Consensus molecular subtypes of colorectal cancer are recapitulated in in vitro and in vivo models. *Cell Death Differ,* 25**,** 616-633.

LIU, Y., CHEN, C., XU, Z., SCUOPPO, C., RILLAHAN, C.D., GAO, J., SPITZER, B., BOSBACH, B., KASTENHUBER, E.R., BASLAN, T., ACKERMANN, S., CHENG, L., WANG, Q., NIU, T., SCHULTZ, N., LEVINE, R.L., MILLS, A.A. & LOWE, S.W. 2016. Deletions linked to TP53 loss drive cancer through p53-independent mechanisms. *Nature,* 531**,** 471-475.

LOCKER, G.Y., HAMILTON, S., HARRIS, J., JESSUP, J.M., KEMENY, N., MACDONALD, J.S., SOMERFIELD, M.R., HAYES, D.F. & BAST, R.C., JR. 2006. ASCO 2006 update of recommendations for the use of tumor markers in gastrointestinal cancer. *J Clin Oncol,* 24**,** 5313-27.

LONNING, P.E., KNAPPSKOG, S., STAALESEN, V., CHRISANTHAR, R. & LILLEHAUG, J.R. 2007. Breast cancer prognostication and prediction in the postgenomic era. *Ann Oncol,* 18**,** 1293-306.

LOTHE, R.A. 1997. Microsatellite instability in human solid tumors. *Mol Med Today,* 3**,** 61-8.

LOUPAKIS, F., RUZZO, A., CREMOLINI, C., VINCENZI, B., SALVATORE, L., SANTINI, D., MASI, G., STASI, I., CANESTRARI, E., RULLI, E., FLORIANI, I., BENCARDINO, K., GALLUCCIO, N., CATALANO, V., TONINI, G., MAGNANI, M., FONTANINI, G., BASOLO, F., FALCONE, A. & GRAZIANO, F. 2009. KRAS codon 61, 146 and BRAF mutations predict resistance to cetuximab plus irinotecan in KRAS codon 12 and 13 wild-type metastatic colorectal cancer. *Br J Cancer*.

LYNCH, H.T. & DE LA CHAPELLE, A. 2003. Hereditary colorectal cancer. *N Engl J Med,* 348**,** 919-32.

MARCHETTI, A., MARTELLA, C., FELICIONI, L., BARASSI, F., SALVATORE, S., CHELLA, A., CAMPLESE, P.P., IARUSSI, T., MUCILLI, F., MEZZETTI, A., CUCCURULLO, F., SACCO, R. & BUTTITTA, F. 2005. EGFR mutations in non-small-cell lung cancer: analysis of a large series of cases and development of a rapid and sensitive method for diagnostic screening with potential implications on pharmacologic treatment. *J Clin Oncol,* 23**,** 857-65.

MARGRAF, R.L., MAO, R., HIGHSMITH, W.E., HOLTEGAARD, L.M. & WITTWER, C.T. 2006. Mutation Scanning of the RET Protooncogene Using High-Resolution Melting Analysis. *Clin Chem,* 52**,** 138-141.

MARLEY, A.R. & NAN, H. 2016. Epidemiology of colorectal cancer. *Int J Mol Epidemiol Genet,* 7**,** 105-114.

MEI, R., GALIPEAU, P.C., PRASS, C., BERNO, A., GHANDOUR, G., PATIL, N., WOLFF, R.K., CHEE, M.S., REID, B.J. & LOCKHART, D.J. 2000. Genome-wide detection of allelic imbalance using human SNPs and high-density DNA arrays. *Genome Res,* 10**,** 1126-37.

MICHELASSI, F., EWING, C., MONTAG, A., VANNUCCI, L., SEGALIN, A., PANOZZO, M., BIBBO, M., DYTCH, H. & CHIECO-BIANCHI, P. 1992. Prognostic significance of ploidy determination in rectal cancer. *Hepatogastroenterology,* 39**,** 222-5.

MIDGLEY, R. & KERR, D.J. 2005. Adjuvant chemotherapy for stage II colorectal cancer: the time is right! *Nat Clin Pract Oncol,* 2**,** 364-9.

MIDGLEY, R.S., MCCONKEY, C.C., JOHNSTONE, E.C., DUNN, J.A., SMITH, J.L., GRUMETT, S.A., JULIER, P., IVESON, C., YANAGISAWA, Y., WARREN, B., LANGMAN, M.J. & KERR, D.J. 2010. Phase III randomized trial assessing rofecoxib in the adjuvant setting of colorectal cancer: final results of the VICTOR trial. *J Clin Oncol,* 28**,** 4575-80.

MIDTHUN, L., SHAHEEN, S., DEISCH, J., SENTHIL, M., TSAI, J. & HSUEH, C.T. 2019. Concomitant KRAS and BRAF mutations in colorectal cancer. J Gastrointest Oncol.

MOIEL, D. & THOMPSON, J. 2011. Early detection of colon cancer-the kaiser permanente northwest 30-year history: how do we measure success? Is it the test, the number of tests, the stage, or the percentage of screen-detected patients? *Perm J,* 15**,** 30-8.

MORENO, C.C., MITTAL, P.K., DIXON, W.T., KITAJIMA, H.D., KANG, J., SMALL, W.C., OSHINSKI, J., VOTAW, J.R., SULLIVAN, P.S., STALEY, C.A., CARDONA, K., RUTHERFORD, R., HAWK, N.N. & KANG, J. 2016. Colorectal Cancer Initial Diagnosis: Screening Colonoscopy, Diagnostic Colonoscopy, or Emergent Surgery, and Tumor Stage and Size at Initial Presentation. *Clin. Colorectal Cancer Clinical Colorectal Cancer,* 15**,** 67-73.

MORIKAWA, T., KUCHIBA, A., LIAO, X., IMAMURA, Y., YAMAUCHI, M., QIAN, Z.R., NISHIHARA, R., SATO, K., MEYERHARDT, J.A., FUCHS, C.S. & OGINO, S. 2011. Tumor TP53 expression status, body mass index and prognosis in colorectal cancer. *Int J Cancer*.

MORRIN, M., KELLY, M., BARRETT, N. & DELANEY, P. 1994. Mutations of Ki-ras and p53 genes in colorectal cancer and their prognostic significance. *Gut,* 35**,** 1627-31.

MORRIS, E., QUIRKE, P., THOMAS, J.D., FAIRLEY, L., COTTIER, B. & FORMAN, D. 2008. Unacceptable variation in abdominoperineal excision rates for rectal cancer: time to intervene? *Gut,* 57**,** 1690-7.

MORRIS, E.J., MAUGHAN, N.J., FORMAN, D. & QUIRKE, P. 2007. Who to treat with adjuvant therapy in Dukes B/stage II colorectal cancer? The need for high quality pathology. *Gut,* 56**,** 1419-25.

MORRISON, T.B., WEIS, J.J. & WITTWER, C.T. 1998. Quantification of low-copy transcripts by continuous SYBR Green I monitoring during amplification. *Biotechniques,* 24**,** 954-8, 960, 962.

MUKHERJI, A., RATHI, A.K., SHARMA, K., KUMAR, V., SINGH, K. & BAHADUR, A.K. 2011. A study on presentation and behavior of colo-rectal carcinoma in young Indian patients. *Trop Gastroenterol,* 32**,** 122-7.

MURNYAK, B. & HORTOBAGYI, T. 2016. Immunohistochemical correlates of TP53 somatic mutations in cancer. *Oncotarget,* 7**,** 64910-64920.

MUZNY, D.M., BAINBRIDGE, M.N., CHANG, K., DINH, H.H., DRUMMOND, J.A., FOWLER, G., KOVAR, C.L., LEWIS, L.R., MORGAN, M.B., NEWSHAM, I.F., REID, J.G. & SANTIBANEZ, J. 2012. Cancer-Genome-Atlas-Network; Comprehensive molecular characterization of human colon and rectal cancer. *Nature,* 487**,** 330-7.

NASER, W.M., SHAWARBY, M.A., AL-TAMIMI, D.M., SETH, A., AL-QUORAIN, A., NEMER, A.M. & ALBAGHA, O.M. 2014. Novel KRAS gene mutations in sporadic colorectal cancer. *PLoS One,* 9**,** e113350.

NATIONAL GENETICS REFERENCE LABORATORY MANCHESTER, 2005. *SNPCheck*. [online] Update Date: 26 September 2013 Available at:<https://secure.ngrl.org.uk/SNPCheck/snpcheck.htm>[Accessed 10 October 2008].

NCCN, 2017. *Clinical practices in oncology (National Comprehensive Cancer Network guidelines), colon cancer*. [online] Update Date: 13 March 2017 Available at:<https://www.nccn.org/professionals/physician_gls/default.aspx>[Accessed 13 March 2019].

NEEDLEMAN, S.B. & WUNSCH, C.D. 1970. A general method applicable to the search for similarities in the amino acid sequence of two proteins. *J Mol Biol,* 48**,** 443-53.

NENUTIL, R., SMARDOVA, J., PAVLOVA, S., HANZELKOVA, Z., MULLER, P., FABIAN, P., HRSTKA, R., JANOTOVA, P., RADINA, M., LANE, D.P., COATES, P.J. & VOJTESEK, B. 2005. Discriminating functional and non-functional p53 in human tumours by p53 and MDM2 immunohistochemistry. *J Pathol,* 207**,** 251-9.

NICE, 2011. *Colorectal cancer: diagnosis and management (2011 updated 2014) NICE guideline CG131*. [online] Update Date: Available at:<https://www.nice.org.uk/guidance/CG131>[Accessed 11 March 2019].

NICE, 2017a. *Cetuximab and panitumumab for previously untreated metastatic colorectal cancer: Technology appraisal guidance [TA439]*. [online] Update Date: 29 March 2017 Available at:<https://www.nice.org.uk/guidance/TA439>[Accessed 11 March 2019].

NICE, 2017b. *Diagnostics guidance [DG27]; Molecular testing strategies for Lynch syndrome in people with colorectal cancer*. [online] Update Date: Available at:<https://www.nice.org.uk/guidance/dg27/chapter/1-Recommendations>[Accessed 11 March 2019].

NOMOTO, K., TSUTA, K., TAKANO, T., FUKUI, T., FUKUI, T., YOKOZAWA, K., SAKAMOTO, H., YOSHIDA, T., MAESHIMA, A.M., SHIBATA, T., FURUTA, K., OHE, Y. & MATSUNO, Y. 2006. Detection of EGFR mutations in archived cytologic specimens of non-small cell lung cancer using high-resolution melting analysis. *Am J Clin Pathol,* 126**,** 608-15.

ODEN-GANGLOFF, A., DI FIORE, F., BIBEAU, F., LAMY, A., BOUGEARD, G., CHARBONNIER, F., BLANCHARD, F., TOUGERON, D., YCHOU, M., BOISSIERE, F., LE PESSOT, F., SABOURIN, J.C., TUECH, J.J., MICHEL, P. & FREBOURG, T. 2009. TP53 mutations predict disease control in metastatic colorectal cancer treated with cetuximab-based chemotherapy. *Br J Cancer,* 100**,** 1330-5.

OHHARA, Y., FUKUDA, N., TAKEUCHI, S., HONMA, R., SHIMIZU, Y., KINOSHITA, I. & DOSAKA-AKITA, H. 2016. Role of targeted therapy in metastatic colorectal cancer. *World J Gastrointest Oncol,* 8**,** 642-55.

ORMEROD, M.G., TRIBUKAIT, B. & GIARETTI, W. 1998. Consensus report of the task force on standardisation of DNA flow cytometry in clinical pathology. DNA Flow Cytometry Task Force of the European Society for Analytical Cellular Pathology. *Anal Cell Pathol,* 17**,** 103-10.

OSTWALD, C., LINNEBACHER, M., WEIRICH, V. & PRALL, F. 2009. Chromosomally and microsatellite stable colorectal carcinomas without the CpG island methylator phenotype in a molecular classification. *Int J Oncol,* 35**,** 321-7.

OWCZARZY, R., TATAUROV, A.V., WU, Y., MANTHEY, J.A., MCQUISTEN, K.A., ALMABRAZI, H.G., PEDERSEN, K.F., LIN, Y., GARRETSON, J., MCENTAGGART, N.O., SAILOR, C.A., DAWSON, R.B. & PEEK, A.S. 2008. IDT SciTools: a suite for analysis and design of nucleic acid oligomers. *Nucleic Acids Res,* 36**,** W163-9.

PACKHAM, D., WARD, R.L., AP LIN, V., HAWKINS, N.J. & HITCHINS, M.P. 2009. Implementation of novel pyrosequencing assays to screen for common mutations of BRAF and KRAS in a cohort of sporadic colorectal cancers. *Diagn Mol Pathol,* 18**,** 62-71.

PALLES, C., CAZIER, J.B., HOWARTH, K.M., DOMINGO, E., JONES, A.M., BRODERICK, P., KEMP, Z., SPAIN, S.L., ALMEIDA, E.G., SALGUERO, I., SHERBORNE, A., CHUBB, D., CARVAJAL-CARMONA, L.G., MA, Y., KAUR, K., DOBBINS, S., BARCLAY, E., GORMAN, M., MARTIN, L., KOVAC, M.B., HUMPHRAY, S., THOMAS, H.J., MAHER, E., EVANS, G., LUCASSEN, A., CUMMINGS, C., STEVENS, M., WALKER, L., HALLIDAY, D., ARMSTRONG, R., PATERSON, J., HODGSON, S., HOMFRAY, T., SIDE, L., IZATT, L., DONALDSON, A., TOMKINS, S., MORRISON, P., GOODMAN, S., BREWER, C., HENDERSON, A., DAVIDSON, R., MURDAY, V., COOK, J., HAITES, N., BISHOP, T., SHERIDAN, E., GREEN, A., MARKS, C., CARPENTER, S., BROUGHTON, M., GREENHALGE, L., SURI, M., DONNELLY, P.C., BELL, J., BENTLEY, D., MCVEAN, G., RATCLIFFE, P., TAYLOR, J., WILKIE, A., BROXHOLME, J., BUCK, D., CORNALL, R., GREGORY, L., KNIGHT, J., LUNTER, G., TOMLINSON, I., BUCK, D.L., KINGSBURY, Z., MCVEAN, G.L., DONNELLY, P., GROCOCK, R., HATTON, E., HOLMES, C.C., HUGHES, L., HUMBURG, P., KANAPIN, A., MURRAY, L.,

RIMMER, A., PETRIDIS, C., ROYLANCE, R., SAWYER, E.J., KERR, D.J., CLARK, S., GRIMES, J., KEARSEY, S.E. & HOULSTON, R.S. 2012. Germline mutations affecting the proofreading domains of POLE and POLD1 predispose to colorectal adenomas and carcinomas. *Nat Genet*.

PELTOMAKI, P. 2003. Role of DNA mismatch repair defects in the pathogenesis of human cancer. *J Clin Oncol,* 21**,** 1174-9.

PERUCHO, M. 1999. Correspondence re: C.R. Boland et al., A National Cancer Institute workshop on microsatellite instability for cancer detection and familial predisposition: development of international criteria for the determination of microsatellite instability in colorectal cancer. Cancer Res., 58: 5248-5257, 1998. *Cancer Res,* 59**,** 249-56.

PETERS, U., JIAO, S., SCHUMACHER, F.R., HUTTER, C.M., ARAGAKI, A.K., BARON, J.A., BERNDT, S.I., BEZIEAU, S., BRENNER, H., BUTTERBACH, K., CAAN, B.J., CAMPBELL, P.T., CARLSON, C.S., CASEY, G., CHAN, A.T., CHANG-CLAUDE, J., CHANOCK, S.J., CHEN, L.S., COETZEE, G.A., COETZEE, S.G., CONTI, D.V., CURTIS, K.R., DUGGAN, D., EDWARDS, T., FUCHS, C.S., GALLINGER, S., GIOVANNUCCI, E.L., GOGARTEN, S.M., GRUBER, S.B., HAILE, R.W., HARRISON, T.A., HAYES, R.B., HENDERSON, B.E., HOFFMEISTER, M., HOPPER, J.L., HUDSON, T.J., HUNTER, D.J., JACKSON, R.D., JEE, S.H., JENKINS, M.A., JIA, W.H., KOLONEL, L.N., KOOPERBERG, C., KURY, S., LACROIX, A.Z., LAURIE, C.C., LAURIE, C.A., LE MARCHAND, L., LEMIRE, M., LEVINE, D., LINDOR, N.M., LIU, Y., MA, J., MAKAR, K.W., MATSUO, K., NEWCOMB, P.A., POTTER, J.D., PRENTICE, R.L., QU, C., ROHAN, T., ROSSE, S.A., SCHOEN, R.E., SEMINARA, D., SHRUBSOLE, M., SHU, X.O., SLATTERY, M.L., TAVERNA, D., THIBODEAU, S.N., ULRICH, C.M., WHITE, E., XIANG, Y., ZANKE, B.W., ZENG, Y.X., ZHANG, B., ZHENG, W. & HSU, L. 2013. Identification of Genetic Susceptibility Loci for Colorectal Tumors in a Genome-Wide Meta-analysis. *Gastroenterology,* 144**,** 799-807 e24.

PEYRET, N., SENEVIRATNE, P.A., ALLAWI, H.T. & SANTALUCIA, J., JR. 1999. Nearest-neighbor thermodynamics and NMR of DNA sequences with internal A.A, C.C, G.G, and T.T mismatches. *Biochemistry,* 38**,** 3468-77.

PICHLER, M., BALIC, M., STADELMEYER, E., AUSCH, C., WILD, M., GUELLY, C., BAUERNHOFER, T., SAMONIGG, H., HOEFLER, G. & DANDACHI, N. 2009. Evaluation of high-resolution melting analysis as a diagnostic tool to detect the BRAF V600E mutation in colorectal tumors. *J Mol Diagn,* 11**,** 140-7.

PINO, M.S. & CHUNG, D.C. 2010. The chromosomal instability pathway in colon cancer. *Gastroenterology,* 138**,** 2059-72.

POSTON, G.J., TAIT, D., O'CONNELL, S., BENNETT, A. & BERENDSE, S. 2012. Diagnosis and management of colorectal cancer: summary of NICE guidance. *BMJ,* 343**,** d6751.

PRATAP SINGH, A., KUMAR, A., DHAR, A., AGARWAL, S. & BHIMANIYA, S. 2018. Advanced colorectal carcinoma with testicular metastasis in an adolescent: a case report. *J Med Case Rep,* 12**,** 304.

PRITCHARD, C.C. & GRADY, W.M. 2011. Colorectal cancer molecular biology moves into clinical practice. *Gut,* 60**,** 116-29.

PRUITT, K., BROWN, G., TATUSOVA, T. & MAGLOTT, D. (2002) The Reference Sequence (RefSeq) Database. IN J. McEntyre & J. Ostell (Eds.) *The NCBI Handbook.* Bethesda (MD), National Center for Biotechnology Information (US).

QUIRKE, P., FOZARD, J.B., DIXON, M.F., DYSON, J.E., GILES, G.R. & BIRD, C.C. 1986. DNA aneuploidy in colorectal adenomas. *Br J Cancer,* 53**,** 477-81.

RAJAGOPALAN, H., JALLEPALLI, P.V., RAGO, C., VELCULESCU, V.E., KINZLER, K.W., VOGELSTEIN, B. & LENGAUER, C. 2004. Inactivation of hCDC4 can cause chromosomal instability. *Nature,* 428**,** 77-81.

REED, G.H., KENT, J.O. & WITTWER, C.T. 2007. High-resolution DNA melting analysis for simple and efficient molecular diagnostics. *Pharmacogenomics,* 8**,** 597-608.

REED, G.H. & WITTWER, C.T. 2004. Sensitivity and specificity of single-nucleotide polymorphism scanning by high-resolution melting analysis. *Clin Chem,* 50**,** 1748-54.

REMVIKOS, Y., TOMINAGA, O., HAMMEL, P., LAURENT-PUIG, P., SALMON, R.J., DUTRILLAUX, B. & THOMAS, G. 1992. Increased p53 protein content of colorectal tumours correlates with poor survival. *Br J Cancer,* 66**,** 758-64.

RIBIC, C.M., SARGENT, D.J., MOORE, M.J., THIBODEAU, S.N., FRENCH, A.J., GOLDBERG, R.M., HAMILTON, S.R., LAURENT-PUIG, P., GRYFE, R., SHEPHERD, L.E., TU, D., REDSTON, M. & GALLINGER, S. 2003. Tumor microsatellite-instability status as a predictor of benefit from fluorouracil-based adjuvant chemotherapy for colon cancer. *N Engl J Med,* 349**,** 247-57.

RIRIE, K.M., RASMUSSEN, R.P. & WITTWER, C.T. 1997. Product differentiation by analysis of DNA melting curves during the polymerase chain reaction. *Anal Biochem,* 245**,** 154-60.

ROSSETTI, S., CONSUGAR, M.B., CHAPMAN, A.B., TORRES, V.E., GUAY-WOODFORD, L.M., GRANTHAM, J.J., BENNETT, W.M., MEYERS, C.M., WALKER, D.L., BAE, K., ZHANG, Q.J., THOMPSON, P.A., MILLER, J.P. & HARRIS, P.C. 2007. Comprehensive molecular diagnostics in autosomal dominant polycystic kidney disease. *J Am Soc Nephrol,* 18**,** 2143-60.

ROTH, A.D., TEJPAR, S., DELORENZI, M., YAN, P., FIOCCA, R., KLINGBIEL, D., DIETRICH, D., BIESMANS, B., BODOKY, G., BARONE, C., ARANDA, E., NORDLINGER, B., CISAR, L., LABIANCA, R., CUNNINGHAM, D., VAN CUTSEM, E. & BOSMAN, F. 2009. Prognostic role of KRAS and BRAF in stage II and III resected colon cancer: results of the translational study on the PETACC-3, EORTC 40993, SAKK 60-00 trial. *J Clin Oncol,* 28**,** 466-74.

RYLAND, G.L., DOYLE, M.A., GOODE, D., BOYLE, S.E., CHOONG, D.Y., ROWLEY, S.M., LI, J., BOWTELL, D.D., TOTHILL, R.W., CAMPBELL, I.G. & GORRINGE, K.L. 2015. Loss of heterozygosity: what is it good for? *BMC Med Genomics,* 8**,** 45.

SANTINI, D., LOUPAKIS, F., VINCENZI, B., FLORIANI, I., STASI, I., CANESTRARI, E., RULLI, E., MALTESE, P.E., ANDREONI, F., MASI, G., GRAZIANO, F., BALDI, G.G., SALVATORE, L., RUSSO, A., PERRONE, G., TOMMASINO, M.R., MAGNANI, M., FALCONE, A., TONINI, G. & RUZZO, A. 2008. High concordance of

KRAS status between primary colorectal tumors and related metastatic sites: implications for clinical practice. *Oncologist,* 13**,** 1270-5.

SARGENT, D.J., MARSONI, S., MONGES, G., THIBODEAU, S.N., LABIANCA, R., HAMILTON, S.R., FRENCH, A.J., KABAT, B., FOSTER, N.R., TORRI, V., RIBIC, C., GROTHEY, A., MOORE, M., ZANIBONI, A., SEITZ, J.F., SINICROPE, F. & GALLINGER, S. 2010. Defective mismatch repair as a predictive marker for lack of efficacy of fluorouracil-based adjuvant therapy in colon cancer. *J Clin Oncol,* 28**,** 3219-26.

SARTORE-BIANCHI, A., MARTINI, M., MOLINARI, F., VERONESE, S., NICHELATTI, M., ARTALE, S., DI NICOLANTONIO, F., SALETTI, P., DE DOSSO, S., MAZZUCCHELLI, L., FRATTINI, M., SIENA, S. & BARDELLI, A. 2009. PIK3CA mutations in colorectal cancer are associated with clinical resistance to EGFR-targeted monoclonal antibodies. *Cancer Res,* 69**,** 1851-7.

SCHWARTZ, J.L. 1998. Alterations in chromosome structure and variations in the inherent radiation sensitivity of human cells. *Radiat Res,* 149**,** 319-24.

SCHWARTZ, J.L., MURNANE, J. & WEICHSELBAUM, R.R. 1999. The contribution of DNA ploidy to radiation sensitivity in human tumour cell lines. *Br J Cancer,* 79**,** 744-7.

SETH, R., CROOK, S., IBRAHEM, S., FADHIL, W., JACKSON, D. & ILYAS, M. 2009a. Concomitant mutations and splice variants in KRAS and BRAF demonstrate complex perturbation of the Ras/Raf signalling pathway in advanced colorectal cancer. *Gut,* 58**,** 1234-41.

SETH, R., KEELEY, J., ABU-ALI, G., CROOK, S., JACKSON, D. & ILYAS, M. 2009b. The putative tumour modifier gene ATP5A1 is not mutated in human colorectal cancer cell lines but expression levels correlate with TP53 mutations and chromosomal instability. *J Clin Pathol,* 62**,** 598-603.

SHERRY, S.T., WARD, M. & SIROTKIN, K. 1999. dbSNP-database for single nucleotide polymorphisms and other classes of minor genetic variation. *Genome Res,* 9**,** 677-9.

SHIA, J. 2008. Immunohistochemistry versus microsatellite instability testing for screening colorectal cancer patients at risk for hereditary nonpolyposis colorectal cancer syndrome. Part I. The utility of immunohistochemistry. *J Mol Diagn,* 10**,** 293-300.

SHIA, J., STADLER, Z., WEISER, M.R., RENTZ, M., GONEN, M., TANG, L.H., VAKIANI, E., KATABI, N., XIONG, X., MARKOWITZ, A.J., SHIKE, M., GUILLEM, J. & KLIMSTRA, D.S. 2011. Immunohistochemical staining for DNA mismatch repair proteins in intestinal tract carcinoma: how reliable are biopsy samples? *Am J Surg Pathol,* 35**,** 447-54.

SIEBER, O.M., HEINIMANN, K. & TOMLINSON, I.P. 2003. Genomic instability--the engine of tumorigenesis? *Nat Rev Cancer,* 3**,** 701-8.

SILVER, A., SENGUPTA, N., PROPPER, D., WILSON, P., HAGEMANN, T., PATEL, A., PARKER, A., GHOSH, A., FEAKINS, R., DORUDI, S. & SURAWEERA, N. 2011. A distinct DNA methylation profile associated with microsatellite and chromosomal stable sporadic colorectal cancers. *Int J Cancer,* 130**,** 1082-92.

SINICROPE, F.A., FOSTER, N.R., THIBODEAU, S.N., MARSONI, S., MONGES, G., LABIANCA, R., KIM, G.P., YOTHERS, G.,

ALLEGRA, C., MOORE, M.J., GALLINGER, S. & SARGENT, D.J. 2011. DNA mismatch repair status and colon cancer recurrence and survival in clinical trials of 5-fluorouracil-based adjuvant therapy. *J Natl Cancer Inst,* 103**,** 863-75.

SIPOS, R., SZEKELY, A.J., PALATINSZKY, M., REVESZ, S., MARIALIGETI, K. & NIKOLAUSZ, M. 2007. Effect of primer mismatch, annealing temperature and PCR cycle number on 16S rRNA gene-targetting bacterial community analysis. *FEMS Microbiol Ecol,* 60**,** 341-50.

SJOGREN, S., INGANAS, M., NORBERG, T., LINDGREN, A., NORDGREN, H., HOLMBERG, L. & BERGH, J. 1996. The p53 gene in breast cancer: prognostic value of complementary DNA sequencing versus immunohistochemistry. *J Natl Cancer Inst,* 88**,** 173-82.

STAAF, J., LINDGREN, D., VALLON-CHRISTERSSON, J., ISAKSSON, A., GORANSSON, H., JULIUSSON, G., ROSENQUIST, R., HOGLUND, M., BORG, A. & RINGNER, M. 2008. Segmentation-based detection of allelic imbalance and loss-of-heterozygosity in cancer cells using whole genome SNP arrays. *Genome Biol,* 9**,** R136.

SUAREZ, J., VERA, R., BALEN, E., GOMEZ, M., ARIAS, F., LERA, J.M., HERRERA, J. & ZAZPE, C. 2008. Pathologic response assessed by Mandard grade is a better prognostic factor than down staging for disease-free survival after preoperative radiochemotherapy for advanced rectal cancer. *Colorectal Dis,* 10**,** 563-8.

SUN, X.F., CARSTENSEN, J.M., ZHANG, H., STAL, O., WINGREN, S., HATSCHEK, T. & NORDENSKJOLD, B. 1992. Prognostic significance of cytoplasmic p53 oncoprotein in colorectal adenocarcinoma. *Lancet,* 340**,** 1369-73.

SURAWEERA, N., DUVAL, A., REPERANT, M., VAURY, C., FURLAN, D., LEROY, K., SERUCA, R., IACOPETTA, B. & HAMELIN, R. 2002. Evaluation of tumor microsatellite instability using five quasimonomorphic mononucleotide repeats and pentaplex PCR. *Gastroenterology,* 123**,** 1804-11.

SUSANTI, S., FADHIL, W., EBILI, H.O., ASIRI, A., NESTARENKAITE, A., HADJIMICHAEL, E., HAM-KARIM, H.A., FIELD, J., STAFFORD, K., MATHAROO-BALL, B., HASSALL, J.C., SHARIF, A., ONISCU, A. & ILYAS, M. 2018. N_LyST: a simple and rapid screening test for Lynch syndrome. *J Clin Pathol,* 71**,** 713-720.

TANG, R., HO, Y.S., YOU, Y.T., HSU, K.C., CHEN, J.S., CHANGCHIEN, C.R. & WANG, J.Y. 1995. Prognostic evaluation of DNA flow cytometric and histopathologic parameters of colorectal cancer. *Cancer,* 76**,** 1724-30.

TENESA, A., FARRINGTON, S.M., PRENDERGAST, J.G., PORTEOUS, M.E., WALKER, M., HAQ, N., BARNETSON, R.A., THEODORATOU, E., CETNARSKYJ, R., CARTWRIGHT, N., SEMPLE, C., CLARK, A.J., REID, F.J., SMITH, L.A., KAVOUSSANAKIS, K., KOESSLER, T., PHAROAH, P.D., BUCH, S., SCHAFMAYER, C., TEPEL, J., SCHREIBER, S., VOLZKE, H., SCHMIDT, C.O., HAMPE, J., CHANG-CLAUDE, J., HOFFMEISTER, M., BRENNER, H., WILKENING, S., CANZIAN, F., CAPELLA, G., MORENO, V., DEARY, I.J., STARR, J.M., TOMLINSON, I.P., KEMP, Z., HOWARTH, K., CARVAJAL-CARMONA, L., WEBB, E., BRODERICK, P., VIJAYAKRISHNAN,

J., HOULSTON, R.S., RENNERT, G., BALLINGER, D., ROZEK, L., GRUBER, S.B., MATSUDA, K., KIDOKORO, T., NAKAMURA, Y., ZANKE, B.W., GREENWOOD, C.M., RANGREJ, J., KUSTRA, R., MONTPETIT, A., HUDSON, T.J., GALLINGER, S., CAMPBELL, H. & DUNLOP, M.G. 2008. Genome-wide association scan identifies a colorectal cancer susceptibility locus on 11q23 and replicates risk loci at 8q24 and 18q21. *Nat Genet,* 40**,** 631-7.

THELWELL, N., MILLINGTON, S., SOLINAS, A., BOOTH, J. & BROWN, T. 2000. Mode of action and application of Scorpion primers to mutation detection. *Nucleic Acids Res,* 28**,** 3752-61.

THEODOROPOULOS, G.E., KARAFOKA, E., PAPAILIOU, J.G., STAMOPOULOS, P., ZAMBIRINIS, C.P., BRAMIS, K., PANOUSSOPOULOS, S.G., LEANDROS, E. & BRAMIS, J. 2009. P53 and EGFR expression in colorectal cancer: a reappraisal of 'old' tissue markers in patients with long follow-up. *Anticancer Res,* 29**,** 785-91.

THIBODEAU, S.N., BREN, G. & SCHAID, D. 1993. Microsatellite instability in cancer of the proximal colon. *Science,* 260**,** 816-9.

THOMPSON, M.R., O'LEARY, D.P., FLASHMAN, K., ASIIMWE, A., ELLIS, B.G. & SENAPATI, A. 2017. Clinical assessment to determine the risk of bowel cancer using Symptoms, Age, Mass and Iron deficiency anaemia (SAMI). *Br J Surg,* 104**,** 1393-1404.

TOL, J., DIJKSTRA, J.R., VINK-BORGER, M.E., NAGTEGAAL, I.D., PUNT, C.J., VAN KRIEKEN, J.H. & LIGTENBERG, M.J. 2009a. High sensitivity of both sequencing and real-time PCR analysis of KRAS mutations in colorectal cancer tissue. *J Cell Mol Med*.

TOL, J., DIJKSTRA, J.R., VINK-BORGER, M.E., NAGTEGAAL, I.D., PUNT, C.J., VAN KRIEKEN, J.H. & LIGTENBERG, M.J. 2010. High sensitivity of both sequencing and real-time PCR analysis of KRAS mutations in colorectal cancer tissue. *J Cell Mol Med,* 14**,** 2122-31.

TOL, J., KOOPMAN, M., CATS, A., RODENBURG, C.J., CREEMERS, G.J., SCHRAMA, J.G., ERDKAMP, F.L., VOS, A.H., VAN GROENINGEN, C.J., SINNIGE, H.A., RICHEL, D.J., VOEST, E.E., DIJKSTRA, J.R., VINK-BORGER, M.E., ANTONINI, N.F., MOL, L., VAN KRIEKEN, J.H., DALESIO, O. & PUNT, C.J. 2009b. Chemotherapy, bevacizumab, and cetuximab in metastatic colorectal cancer. *N Engl J Med,* 360**,** 563-72.

TOMLINSON, I., WEBB, E., CARVAJAL-CARMONA, L., BRODERICK, P., KEMP, Z., SPAIN, S., PENEGAR, S., CHANDLER, I., GORMAN, M., WOOD, W., BARCLAY, E., LUBBE, S., MARTIN, L., SELLICK, G., JAEGER, E., HUBNER, R., WILD, R., ROWAN, A., FIELDING, S., HOWARTH, K., SILVER, A., ATKIN, W., MUIR, K., LOGAN, R., KERR, D., JOHNSTONE, E., SIEBER, O., GRAY, R., THOMAS, H., PETO, J., CAZIER, J.B. & HOULSTON, R. 2007. A genome-wide association scan of tag SNPs identifies a susceptibility variant for colorectal cancer at 8q24.21. *Nat Genet,* 39**,** 984-8.

TOMLINSON, I.P., WEBB, E., CARVAJAL-CARMONA, L., BRODERICK, P., HOWARTH, K., PITTMAN, A.M., SPAIN, S., LUBBE, S., WALTHER, A., SULLIVAN, K., JAEGER, E., FIELDING, S., ROWAN, A., VIJAYAKRISHNAN, J., DOMINGO, E., CHANDLER, I., KEMP, Z., QURESHI, M., FARRINGTON, S.M., TENESA, A., PRENDERGAST, J.G., BARNETSON, R.A.,

PENEGAR, S., BARCLAY, E., WOOD, W., MARTIN, L., GORMAN, M., THOMAS, H., PETO, J., BISHOP, D.T., GRAY, R., MAHER, E.R., LUCASSEN, A., KERR, D., EVANS, D.G., SCHAFMAYER, C., BUCH, S., VOLZKE, H., HAMPE, J., SCHREIBER, S., JOHN, U., KOESSLER, T., PHAROAH, P., VAN WEZEL, T., MORREAU, H., WIJNEN, J.T., HOPPER, J.L., SOUTHEY, M.C., GILES, G.G., SEVERI, G., CASTELLVI-BEL, S., RUIZ-PONTE, C., CARRACEDO, A., CASTELLS, A., FORSTI, A., HEMMINKI, K., VODICKA, P., NACCARATI, A., LIPTON, L., HO, J.W., CHENG, K.K., SHAM, P.C., LUK, J., AGUNDEZ, J.A., LADERO, J.M., DE LA HOYA, M., CALDES, T., NIITTYMAKI, I., TUUPANEN, S., KARHU, A., AALTONEN, L., CAZIER, J.B., CAMPBELL, H., DUNLOP, M.G. & HOULSTON, R.S. 2008. A genome-wide association study identifies colorectal cancer susceptibility loci on chromosomes 10p14 and 8q23.3. *Nat Genet,* 40**,** 623-30.

TOMODA, H. & KAKEJI, Y. 1995. Immunohistochemical analysis of p53 in colorectal cancer regarding clinicopathological correlation and prognostic significance. *J Surg Oncol,* 58**,** 125-8.

TORNILLO, L., LUGLI, A., ZLOBEC, I., WILLI, N., GLATZ, K., LEHMANN, F., SPICHTIN, H.P., MAURER, R., STOIOS, D., SAUTER, G. & TERRACCIANO, L. 2007. Prognostic value of cell cycle and apoptosis regulatory proteins in mismatch repair-proficient colorectal cancer: a tissue microarray-based approach. *Am J Clin Pathol,* 127**,** 114-23.

TSAI, H.L., HSIEH, J.S., YU, F.J., WU, D.C., CHEN, F.M., HUANG, C.J., HUANG, Y.S., HUANG, T.J. & WANG, J.Y. 2007. Perforated colonic cancer presenting as intra-abdominal abscess. *Int J Colorectal Dis,* 22**,** 15-9.

TSAO, M.S., SAKURADA, A., CUTZ, J.C., ZHU, C.Q., KAMEL-REID, S., SQUIRE, J., LORIMER, I., ZHANG, T., LIU, N., DANESHMAND, M., MARRANO, P., DA CUNHA SANTOS, G., LAGARDE, A., RICHARDSON, F., SEYMOUR, L., WHITEHEAD, M., DING, K., PATER, J. & SHEPHERD, F.A. 2005. Erlotinib in lung cancer - molecular and clinical predictors of outcome. *N Engl J Med,* 353**,** 133-44.

TSUTSUMI, S., TABE, Y., FUJII, T., YAMAGUCHI, S., SUTO, T., YAJIMA, R., MORITA, H., KATO, T., SHIOYA, M., SAITO, J., ASAO, T., NAKANO, T. & KUWANO, H. 2011. Tumor response and negative distal resection margins of rectal cancer after hyperthermochemoradiation therapy. *Anticancer Res,* 31**,** 3963-7.

TURNER, J.R. 2015. The gastrointestinal tract. In V. Kumar, A.K. Abbas, J.C. Aster & J.A. Perkins (Eds.) *Robbins and Cotran pathologic Basis of Diseases.* 9 ed. Philadelphia PA, Elsevier Saunders. pp.749-820

UNTERGASSER, A., CUTCUTACHE, I., KORESSAAR, T., YE, J., FAIRCLOTH, B.C., REMM, M. & ROZEN, S.G. 2012. Primer3--new capabilities and interfaces. *Nucleic Acids Res,* 40**,** e115.

VAGUNDA, V., SMARDOVA, J., VAGUNDOVA, M., JANDAKOVA, E., ZALOUDIK, J. & KOUKALOVA, H. 2003. Correlations of breast carcinoma biomarkers and p53 tested by FASAY and immunohistochemistry. *Pathol Res Pract,* 199**,** 795-801.

VAN BEERS, E.H., JOOSSE, S.A., LIGTENBERG, M.J., FLES, R., HOGERVORST, F.B., VERHOEF, S. & NEDERLOF, P.M. 2006. A

multiplex PCR predictor for aCGH success of FFPE samples. *Br J Cancer,* 94**,** 333-7.

VAN BEERS, E.H., VAN WELSEM, T., WESSELS, L.F., LI, Y., OLDENBURG, R.A., DEVILEE, P., CORNELISSE, C.J., VERHOEF, S., HOGERVORST, F.B., VAN'T VEER, L.J. & NEDERLOF, P.M. 2005. Comparative genomic hybridization profiles in human BRCA1 and BRCA2 breast tumors highlight differential sets of genomic aberrations. *Cancer Res,* 65**,** 822-7.

VAN CUTSEM, E., KOHNE, C.H., HITRE, E., ZALUSKI, J., CHANG CHIEN, C.R., MAKHSON, A., D'HAENS, G., PINTER, T., LIM, R., BODOKY, G., ROH, J.K., FOLPRECHT, G., RUFF, P., STROH, C., TEJPAR, S., SCHLICHTING, M., NIPPGEN, J. & ROUGIER, P. 2009. Cetuximab and chemotherapy as initial treatment for metastatic colorectal cancer. *N Engl J Med,* 360**,** 1408-17.

VAN DEN BOOM, D. & EHRICH, M. 2007. Discovery and identification of sequence polymorphisms and mutations with MALDI-TOF MS. *Methods Mol Biol,* 366**,** 287-306.

VAN DEN INGH, H.F., GRIFFIOEN, G. & CORNELISSE, C.J. 1985. Flow cytometric detection of aneuploidy in colorectal adenomas. *Cancer Res,* 45**,** 3392-7.

VAN KRIEKEN, J.H., JUNG, A., KIRCHNER, T., CARNEIRO, F., SERUCA, R., BOSMAN, F.T., QUIRKE, P., FLEJOU, J.F., PLATO HANSEN, T., DE HERTOGH, G., JARES, P., LANGNER, C., HOEFLER, G., LIGTENBERG, M., TINIAKOS, D., TEJPAR, S., BEVILACQUA, G. & ENSARI, A. 2008. KRAS mutation testing for predicting response to anti-EGFR therapy for colorectal carcinoma: proposal for an European quality assurance program. *Virchows Arch,* 453**,** 417-31.

VANDERSTEEN, J.G., BAYRAK-TOYDEMIR, P., PALAIS, R.A. & WITTWER, C.T. 2007. Identifying common genetic variants by high-resolution melting. *Clin Chem,* 53**,** 1191-8.

VECCHIO, F.M., VALENTINI, V., MINSKY, B.D., PADULA, G.D., VENKATRAMAN, E.S., BALDUCCI, M., MICCICHE, F., RICCI, R., MORGANTI, A.G., GAMBACORTA, M.A., MAURIZI, F. & COCO, C. 2005. The relationship of pathologic tumor regression grade (TRG) and outcomes after preoperative therapy in rectal cancer. *Int J Radiat Oncol Biol Phys,* 62**,** 752-60.

VICTOR COHEN, J.S.A.J.J.G.B.D.S.H.K.N.A.T.W.H.M.J.G.C. 2006. Evaluation of denaturing high-performance liquid chromatography as a rapid detection method for identification of epidermal growth factor receptor mutations in nonsmall-cell lung cancer. *Cancer,* 107**,** 2858-2865.

WANG, W., KANDIMALLA, R., HUANG, H., ZHU, L., LI, Y., GAO, F., GOEL, A. & WANG, X. 2019. Molecular subtyping of colorectal cancer: Recent progress, new challenges and emerging opportunities. *Semin Cancer Biol,* 55**,** 37-52.

WATERFALL, C.M., EISENTHAL, R. & COBB, B.D. 2002. Kinetic characterisation of primer mismatches in allele-specific PCR: a quantitative assessment. *Biochem Biophys Res Commun,* 299**,** 715-22.

WESSELS, L.F., VAN WELSEM, T., HART, A.A., VAN'T VEER, L.J., REINDERS, M.J. & NEDERLOF, P.M. 2002. Molecular classification of breast carcinomas by comparative genomic hybridization: a specific somatic genetic profile for BRCA1 tumors. *Cancer Res,* 62**,** 7110-7.

WEST, C.M.L. 1994. Predictive Assays in Radiation Therapy. In K.I. Altman & J.T. Lett (Eds.) *Advances in Radiation Biology*. Elsevier. pp.149-180

WHITCOMBE, D., THEAKER, J., GUY, S.P., BROWN, T. & LITTLE, S. 1999. Detection of PCR products using self-probing amplicons and fluorescence. *Nat Biotechnol,* 17**,** 804-7.

WHITEHALL, V., TRAN, K., UMAPATHY, A., GRIEU, F., HEWITT, C., EVANS, T.J., ISMAIL, T., LI, W.Q., COLLINS, P., RAVETTO, P., LEGGETT, B., SALTO-TELLEZ, M., SOONG, R., FOX, S., SCOTT, R.J., DOBROVIC, A. & IACOPETTA, B. 2009. A multicenter blinded study to evaluate KRAS mutation testing methodologies in the clinical setting. *J Mol Diagn,* 11**,** 543-52.

WILLIAMS, A.C., MILLER, J.C., COLLARD, T., BROWNE, S.J., NEWBOLD, R.F. & PARASKEVA, C. 1997. The effect of different TP53 mutations on the chromosomal stability of a human colonic adenoma derived cell line with endogenous wild type TP53 activity, before and after DNA damage. *Genes Chromosomes Cancer*, 20**,** 44-52.

WILLMORE-PAYNE, C., HOLDEN, J.A., TRIPP, S. & LAYFIELD, L.J. 2005. Human malignant melanoma: detection of BRAF- and c-kit-activating mutations by high-resolution amplicon melting analysis. *Human Pathology,* 36**,** 486-493.

WILLMORE, C., HOLDEN, J.A., ZHOU, L., TRIPP, S., WITTWER, C.T. & LAYFIELD, L.J. 2004. Detection of c-kit-activating mutations in gastrointestinal stromal tumors by high-resolution amplicon melting analysis. *Am J Clin Pathol,* 122**,** 206-16.

WITTWER, C.T. 2009. High-resolution DNA melting analysis: advancements and limitations. *Hum Mutat,* 30**,** 857-9.

WITTWER, C.T., HERRMANN, M.G., MOSS, A.A. & RASMUSSEN, R.P. 1997a. Continuous fluorescence monitoring of rapid cycle DNA amplification. *Biotechniques,* 22**,** 130-1, 134-8.

WITTWER, C.T. & KUSUKAWA, N. 2004. Real-time PCR. In H.D. Persing, F.C. Tenover, J. Versalovic, Y.W. Tang, E.R. Unger, D.A. Relman & T.J. White (Eds.) *Diagnostic Molecular Microbiology: Principles and Applications.* Washington, DC, ASM Press. pp.71-84

WITTWER, C.T., RASMUSSEN, R.P. & RIRIE, K.M. 2010. Rapid polymerase chain reaction and melting analysis. In S.A. Bustin (Ed.) *The PCR Revolution: Basic Technologies and Applications.* Cambridge, Cambridge University Press. pp.48-69

WITTWER, C.T., REED, G.H., GUNDRY, C.N., VANDERSTEEN, J.G. & PRYOR, R.J. 2003. High-Resolution Genotyping by Amplicon Melting Analysis Using LCGreen. *Clin Chem,* 49**,** 853-860.

WITTWER, C.T., RIRIE, K.M., ANDREW, R.V., DAVID, D.A., GUNDRY, R.A. & BALIS, U.J. 1997b. The LightCycler: a microvolume multisample fluorimeter with rapid temperature control. *Biotechniques,* 22**,** 176-81.

WOJDACZ, T.K. & DOBROVIC, A. 2007. Methylation-sensitive high resolution melting (MS-HRM): a new approach for sensitive and high-throughput assessment of methylation. *Nucleic Acids Res*.

WORM, J., AGGERHOLM, A. & GULDBERG, P. 2001. In-Tube DNA Methylation Profiling by Fluorescence Melting Curve Analysis. *Clin Chem,* 47**,** 1183-1189.

WRIGHT, D.K. & MANOS, M.M. 1990. Sample preparation from paraffin-embedded tissues. In M.A. Innis, D.H. Gelfont, J.j. Sninky & T.J. White

(Eds.) *PCR Protocols: A guide to methods and applications.* London, Academic Press Limited. pp.153-158

WU, J.H., HONG, P.Y. & LIU, W.T. 2009. Quantitative effects of position and type of single mismatch on single base primer extension. *J Microbiol Methods,* 77**,** 267-75.

YAMAGISHI, H., KURODA, H., IMAI, Y. & HIRAISHI, H. 2016. Molecular pathogenesis of sporadic colorectal cancers. *Chin J Cancer,* 35**,** 4.

YUN, J., RAGO, C., CHEONG, I., PAGLIARINI, R., ANGENENDT, P., RAJAGOPALAN, H., SCHMIDT, K., WILLSON, J.K., MARKOWITZ, S., ZHOU, S., DIAZ, L.A., JR., VELCULESCU, V.E., LENGAUER, C., KINZLER, K.W., VOGELSTEIN, B. & PAPADOPOULOS, N. 2009. Glucose deprivation contributes to the development of KRAS pathway mutations in tumor cells. *Science,* 325**,** 1555-9.

ZAKI, B.I., SURIAWINATA, A.A., EASTMAN, A.R., GARNER, K.M. & BAKHOUM, S.F. 2014. Chromosomal instability portends superior response of rectal adenocarcinoma to chemoradiation therapy. *Cancer,* 120**,** 1733-42.

ZANKE, B.W., GREENWOOD, C.M., RANGREJ, J., KUSTRA, R., TENESA, A., FARRINGTON, S.M., PRENDERGAST, J., OLSCHWANG, S., CHIANG, T., CROWDY, E., FERRETTI, V., LAFLAMME, P., SUNDARARAJAN, S., ROUMY, S., OLIVIER, J.F., ROBIDOUX, F., SLADEK, R., MONTPETIT, A., CAMPBELL, P., BEZIEAU, S., O'SHEA, A.M., ZOGOPOULOS, G., COTTERCHIO, M., NEWCOMB, P., MCLAUGHLIN, J., YOUNGHUSBAND, B., GREEN, R., GREEN, J., PORTEOUS, M.E., CAMPBELL, H., BLANCHE, H., SAHBATOU, M., TUBACHER, E., BONAITI-PELLIE, C., BUECHER, B., RIBOLI, E., KURY, S., CHANOCK, S.J., POTTER, J., THOMAS, G., GALLINGER, S., HUDSON, T.J. & DUNLOP, M.G. 2007. Genome-wide association scan identifies a colorectal cancer susceptibility locus on chromosome 8q24. *Nat Genet,* 39**,** 989-94.

ZHANG, L. 2008. Immunohistochemistry versus microsatellite instability testing for screening colorectal cancer patients at risk for hereditary nonpolyposis colorectal cancer syndrome. Part II. The utility of microsatellite instability testing. *J Mol Diagn,* 10**,** 301-7.

ZHANG, W., MAO, J.H., ZHU, W., JAIN, A.K., LIU, K., BROWN, J.B. & KARPEN, G.H. 2016. Centromere and kinetochore gene misexpression predicts cancer patient survival and response to radiotherapy and chemotherapy. *Nat Commun,* 7**,** 12619.

ZHANG, Z., SCHWARTZ, S., WAGNER, L. & MILLER, W. 2000. A greedy algorithm for aligning DNA sequences. *J Comput Biol,* 7**,** 203-14.

ZHENG, G., TSAI, H., TSENG, L.H., ILLEI, P., GOCKE, C.D., ESHLEMAN, J.R., NETTO, G. & LIN, M.T. 2016. Test Feasibility of Next-Generation Sequencing Assays in Clinical Mutation Detection of Small Biopsy and Fine Needle Aspiration Specimens. *Am J Clin Pathol,* 145**,** 696-702.

ZHOU, G., WANG, J., ZHAO, M., XIE, T.X., TANAKA, N., SANO, D., PATEL, A.A., WARD, A.M., SANDULACHE, V.C., JASSER, S.A., SKINNER, H.D., FITZGERALD, A.L., OSMAN, A.A., WEI, Y., XIA, X., SONGYANG, Z., MILLS, G.B., HUNG, M.C., CAULIN, C.,

LIANG, J. & MYERS, J.N. 2014. Gain-of-function mutant p53 promotes cell growth and cancer cell metabolism via inhibition of AMPK activation. *Mol Cell,* 54**,** 960-74.

ZHOU, L., MYERS, A.N., VANDERSTEEN, J.G., WANG, L. & WITTWER, C.T. 2004. Closed-Tube Genotyping with Unlabeled Oligonucleotide Probes and a Saturating DNA Dye. *Clin Chem,* 50**,** 1328-1335.

ZHOU, L., WANG, L., PALAIS, R., PRYOR, R. & WITTWER, C.T. 2005. High-Resolution DNA Melting Analysis for Simultaneous Mutation Scanning and Genotyping in Solution. *Clin Chem,* 51**,** 1770-1777.

ZUKER, M. 2003. Mfold web server for nucleic acid folding and hybridization prediction. *Nucleic Acids Res,* 31**,** 3406-15.